CONFIDENTIAL

Processed Pulmonary Homografts in the Right Ventricle Outflow Tract: An Experimental Study in the Juvenile Ovine Model

JOHANNES JACOBUS VAN DEN HEEVER

Dissertation submitted in fulfilment of the requirements of the degree
PHILOSOPHIAE DOCTOR IN CARDIOTHORACIC SURGERY
(Ph.D.)

Promotor: Prof FE Smit
Co-promotor: Prof PM Dohmen

Department of Cardiothoracic Surgery
Faculty of Health Sciences
University of the Free State
Bloemfontein, South Africa

Acknowledgements

*All glory be to the **Trinity God** alone, for giving me the ability and opportunity to conduct this research study and complete the dissertation*

I would also like to thank the following people for their contributions towards successfully completing the study:

My promotors, Prof Francis Smit and Prof Pascal Dohmen (Germany) for their input, guidance and support during the study;

Drs Johan Jordaan and Johan Honing for their assistance with the surgical procedures;

Dr Angélique Lewies for her invaluable support and many hours of hard work in compiling the dissertation;

Miss Hanlie Grobler from the electron microscope centre at the UFS for preparing all the SEM and TEM samples for evaluation;

Prof Jackie Goedhals and her team for preparation of all the histology samples;

Mr Victor Mokoena and his fellow perfusion technologists for assistance with CPB in theatre;

Mr Seb Lamprecht and personnel for assistance and taking care of experimental animals;

Mr Rudolph Pretorius and Mr Marius van Jaarsveld for performing all the echocardiographic sonars;

Miss Prennie Marimuthu (Vet nurse) for theatre assistance and animal health care;

Me Yvonne Visagie and her colleagues for all the calcium analyses;

Prof Leon Neethling, friend and mentor, for his advice;

My mother and parents-in-law for their continuous prayers and support;

A special word of thank you and gratitude to my wife Coretha and children Elzanne & Christian, Hannes & Mariska and Iselle for their motivation, prayers, understanding, believing in me and supporting me all the way in reaching the pinnacle of my academic career!

"In Christ lie hidden all the treasures of wisdom and knowledge"

~Colossians 2:3

DECLARATION

I, Johannes Jacobus van den Heever, do hereby declare that this dissertation,

PROCESSED PULMONARY HOMOGRAFTS IN THE RIGHT VENTRICLE OUTFLOW TRACT: AN EXPERIMENTAL STUDY IN THE JUVENILE OVINE MODEL,

submitted to the University of the Free State for the degree of ***Philosophiae Doctor*** **in Cardiothoracic Surgery**, is my own, independent work, and that it has not been submitted to any institution by me or any other person in fulfilment of the requirements for the attainment of any qualification.

Principal investigator:

Signed:  Date: 28 February 2020

Johannes Jacobus van den Heever

Table of contents

List of figures

Chapter 4 – Manuscript 2

Chapter 5 – Manuscript 3

List of tables

Chapter 5 – Manuscript 3

Chapter 6 – Conclusions

List of abbreviations and acronyms

CI	Confidence interval
CPB	Cardiopulmonary bypass
DALYs	Disability adjusted life years
DAPI	4′,6-diamidino-2-phenylindole
DSC	Differential scanning calorimetry
DMSO	Dimethylsulfoxide
DNA	Deoxyribonucleic acid
DOA	Doexycholic acid
ECM	Extracellular matrix
EDTA	Ethylenediaminetetraacetic acid
ER	Endoplasmic reticulum
GA	Glutaraldehyde
GAG	Glycosaminoglycan
GBD	Global Burden of Disease
HLA	Human leukocyte antigen
H&E	Hematoxylin and eosin
HVD	Heart valve disease
KW	Kruskal-Wallis
PEG	Polyethylene glycol
PBS	Phosphate buffered saline
PG	Propylene glycol
PMNs	Polymorphonuclear leukocytes
PR	Pulmonary regurgitation
RNA	Ribonucleic acid
RV	Right ventricular
RVOT	Right ventricular outflow tract
SDS	Sodium dodecyl sulphate
SEM	Scanning electron microscopy
TEM	Transmission electron microscopy

TS	Tensile strength
YM	Young’s modulus

Abstract

The availability of pulmonary homografts with improved biomechanical properties, tissue stability, reduced calcification and improved durability for right ventricular outflow tract (RVOT) reconstruction is desired. In paediatric patients, a valve with growth potential will be advantageous. Extending the post-mortem ischaemic time will enlarge the donor pool. Cryopreservation of homografts remains the gold standard, but it damages the extracellular matrix (ECM) and reduces the cellularity, contributing to early valve degeneration. Decellularization of homografts might reduce immunogenicity, promote recellularization and tissue remodeling, maintain mechanical stability and improve clinical outcomes. The decellularization process should not compromise the durability and strength of the homograft, and alternative stabilization of the scaffold might be required. The current study evaluated the effect of the further processing of pulmonary homografts, following a 48 h cold ischaemic post-mortem harvesting time, on the structural integrity and function when implanted in the RVOT position in the juvenile ovine model.

Sheep pulmonary homografts (n = 30) were subjected to 48 h cold ischaemia to simulate the clinical homograft donor circumstances, and equally divided into three groups. Homografts in group 1 were cryopreserved, decellularized in group 2 and decellularized, GA-fixed and detoxified in group 3. Decellularization consists of a multi-detergent and enzymatic protocol with numerous washout steps, and additional fixation and detoxification were done with EnCap technology. The study was divided into three parts. In study 1, the histological (DAPI, H&E, von Kossa, Modified von Gieson, SEM, TEM) and mechanical (TS and YM) properties of the processed homografts (n = 15, 5 per group) were compared. Study 2 involved implantation of cryopreserved and decellularized pulmonary homografts (n = 5 per group) in the RVOT of juvenile sheep for 180 days, monitored with echocardiography and compared on histology, mechanical properties and calcification after explantation. Study 3 involved the same parameters, however, decellularized and decellularized plus EnCap treated homografts (n = 5 per group) were implanted and compared.

Cryopreserved homografts demonstrated collapsed and disrupted/fractured collagen with cells and cellular remnants. Homografts in the decellularized group were acellular with large interfibrillar spaces and a loosely arranged collagen network, while decellularized plus EnCap treated homograft were acellular with a compacted collagen network. Decellularization did not reduce tensile strength and tissue stiffness, but EnCap treatment did increase tissue stiffness. Implanted cryopreserved homografts demonstrated significant regurgitation due to leaflet thickening and retraction, loss of interstitial cells, calcification and increased tissue stiffness. Decellularized homografts showed increased annulus diameter with trivial regurgitation, excellent haemodynamics, remained soft and pliable, recellularized extensively with young fibroblasts exhibiting rough endoplasmic reticulum, and mitigated calcification. Decellularized and EnCap treated homografts became rigid and stenotic, showed poor haemodynamic characteristics, development of bacterial endocarditis and premature death, no leaflet recellularization, and fibrous encapsulation.

Cryopreserved homografts remain the valve of choice for RVOT reconstruction surgery, however, cryopreservation causes cell death and collagen disruption, and loss of cellularity and calcification during implantation, which will result in early valve degeneration. Our proprietary decellularization protocol proved to be effective for complete decellularization of pulmonary homografts with a post-mortem ischaemic time of 48 h, while maintaining a well-organized collagen matrix and tissue strength and stiffness. Implanted decellularized homografts repopulated extensively without signs of inflammation, maintained structural integrity and strength, calcification was mitigated, and the potential for remodeling and growth in size with somatic growth was observed. Additional fixation of the decellularized homograft scaffold will be counterproductive in growing individuals, and should only be performed on adult size homografts where valve growth is not required. GA-fixation restricts valve repopulation with host cells and tissue remodeling, and defies the purposes and advantages of decellularization. Additional fixation may not be necessary when using decellularization methods that achieve complete acellularity without altering the ECM structure and mechanical properties of homografts.

Successful decellularization of donor homograft heart valves and other collagenous tissues holds exciting new prospects and possibilities for tissue processing, and can open a new era in supply of substitution valves and tissues with improved properties and advantages to medical patients in South Africa.

Keywords (10)

Cryopreservation, pulmonary homografts, ischaemic time, valve degeneration, decellularization, recellularization, tissue remodeling, calcification, right ventricular outflow tract, tissue stabilization

Chapter 1 - Introduction

1.1 Background and problem identification

Heart valve disease (HVD) can cause conditions such as regurgitation and stenosis, which can lead to heart failure, sudden cardiac arrest and death. According to the 2017 *Global Burden of Disease* (GBD) report, calcific aortic disease accounted for the loss of 1.5 million disability-adjusted life years (DALYs), while mitral valve disease accounted for 1.1 million DALYs lost, accounting for 0.12 % of total DALYs lost from all diseases in 2017 (Kyu et al., 2018; Yadgir et al., 2018). Pulmonary valve stenosis, characterised by the obstruction in blood flow from the right ventricle to the pulmonary arteries, is a common congenital heart defect that occurs in 6 to 8 of every 10, 000 live births (Idrizi et al., 2015). Compared to coronary heart disease the prevalence of HVD is low; however, the impact that HVD has on the healthcare systems is disproportionately large due to the long-term follow-up, significant examination and treatment costs associated with HVD (Coffey et al., 2016). Surgical intervention is necessary to either repair or replace leaking or stenotic valves. In cardiac surgery, the replacement of patients' diseased heart valves with either mechanical or biological valve prostheses remains the main option of treatment for end-stage HVD. However, mechanical substitutes have limitations, including; 1) the need for lifelong anticoagulation, 2) long-term complications, and 3) the inability to grow in size (Steinhoff et al., 2000; Harris et al., 2015).

Gordon Murray was the first to report on the clinical use of a fresh aortic valve homograft, harvested from a cadaver, in 1956. This homograft was implanted in the descending thoracic aorta to help alleviate the consequences of native aortic valve insufficiency, with partially successful haemodynamic results (Murray, 1956). Although these valves were a significant advancement at the time, long-term outcomes differed substantially between patients and many valves eventually failed because of progressive fibrosis and calcification. The failure of these valve homografts was especially the case with infants and young child recipients, where the ideal would be a valve that can grow in size and repair itself (Hopkins et al., 2009). Availability, optimal storage methods, reliable transportation and the risk of transmission of infectious diseases remain limiting factors in the use of homograft valves.

Combined with the rapid progress in the development and manufacturing of artificial prosthetic valves, this resulted in a decline in the use of homograft valves despite its recognised advantages. Cryopreservation techniques for the long-term storage of human valve allografts were introduced in 1976, and made it possible for allografts to be procured, reliably sterilized and made available in adequate numbers for clinical use (Angell et al., 1976). Cryopreservation as a storage method was further developed in the 1980s and, together with improved organ and tissue donation programs, resulted in increased availability and usage of homografts worldwide (Gulbins et al., 2003).

Most tissue banks accept 12-24 hours of post-mortem warm ischaemic time and/or 48 hours of post-mortem cold ischaemic time in their protocols, and previous studies by our research group has confirmed that increasing the post-mortem harvesting time of homografts beyond 24 h prior to cryopreservation could increase the potential donor pool and address homograft shortages (Appendix A, co-authored publications (Smit et al., 2015) and (Bester et al., 2018)). The study by Smit et al., (2015) showed that the increase in ischaemic harvesting time (time between death and harvesting of the heart valve) of ovine pulmonary homografts from 24 h to 48 h and even 72 h prior to cryopreservation did not affect the tissue strength of the pulmonary homografts. On hematoxylin and eosin (H&E) staining, the extracellular matrix (ECM) was shown to be intact. When these homografts were implanted in the right ventricular outflow tract (RVOT) of juvenile sheep, good haemodynamic function and normal valve function could be observed during a 150-day follow-up period. In the study by Bester et al., (2018), ovine pulmonary homografts were harvested after a 48 h post-mortem period prior to being cryopreserved. The post-mortem time of 48 h was chosen to stimulate a reasonable window of opportunity for obtaining donor consent in human cadaveric donor programs in South Africa (mean = 33h) (Botes et al., 2012). These homografts were then implanted for up to 180 days in the RVOT position of juvenile sheep. The extended post-mortem harvesting time did not negatively affect the long-term performance of the transplanted valves, however, transmission electron microscopy demonstrated that cryopreservation did damage the collagen scaffold (Bester et al., 2018). When a post-mortem harvesting time of $\geq$ 24 h is used, the cells remaining in and on the homograft would be mainly non-viable (Smit et al., 2015), which could lead to unwanted immune reactions in the recipients and premature conduit failure. The cellular debris

that results from apoptotic and necrotic cells present on the homograft after processing and storage leads to calcification and chronic inflammation, which promotes valve failure (Hopkins et al., 2009).

Cryopreserved pulmonary homografts remain the gold standard for RVOT reconstruction procedures (Romeo et al., 2018) and the replacement of the native pulmonary valve in Ross procedures (Hechadi et al., 2013). Research into alternative processing methods of these homografts is driven by the significant incidence of valve degeneration and failure, especially in children and young adults (Selamet Tierney et al., 2005) and their limited availability in paediatric sizes (Goffin et al., 2000). Good clinical results have been reported, despite a lack of treatment of recipients of homografts with immunosuppressive drugs; however, the early failure of these valves does occur through suspected immune reactions (Welters et al., 2002; Baskett et al., 2003).

More recently, different processing techniques including the decellularization of homograft heart valves were developed, improving the usage, durability and long-term performance of these valves through reduced immunogenicity (Cebotari et al., 2011). Decellularization removes all of the host cells and nuclear material from homograft valves and should leave behind only the intact extracellular matrix and associated proteins. CryoValve® SG (CryoLife, Inc, Kennesaw, GA, USA) pulmonary human heart valves are decellularized homografts that are used clinically for RVOT reconstruction. Results compare favourably with cryopreserved homografts (Burch et al., 2010), however, better haemodynamics were observed in the CryoValve® SG group due to the decreased antigenicity (Brown et al., 2010). A wide variety of decellularization protocols have been proposed by numerous institutions, all claiming to have good results. The majority of these protocols use a combination of non-ionic detergents (TritonX-100), ionic detergents (sodium dodecyl sulphate (SDS), deoxycholic acid (DOA)), enzymes (Trypsin, DNAse, RNAse), antibiotics, chelating agents (ethylenediaminetetraacetic acid (EDTA)) and mechanical agitation (stirring, shaking, sonication) (Dohmen and Konertz, 2009). Compared to exonuclease, the use of endonuclease, such as Benzonase, that cleave nucleotides mid-sequence is more effective in fragmenting DNA in preparation for its removal (Crapo et al., 2011; Dijkman et al., 2012). A novel decellularization and sterilization method that is based on a multi-detergent approach, and

makes uses of SDS, DOA and TritonX-100, was previously developed by our research group and used for the decellularization of bovine pericardium. Synergism was observed when using the combination of these detergents, with complete decellularization and intact collagen and elastin (Laker et al., 2020).

Converse and colleagues demonstrated that decellularization does not reduce the cross-linking of collagen as determined by differential scanning calorimetry, but does reduce the glycosaminoglycan (GAG) content with resultant increased extensibility and changes in relaxation behaviour of the pulmonary valve leaflets (Converse et al., 2012). Removal of cellular components from implants might limit the immunological response from the recipient, but tissue strength has to be maintained (Erdbrugger et al., 2006). Therefore, additional fixation and stabilization of the collagen scaffold following decellularization might be required. Xenograft heart valves like commercial porcine valves are tanned with glutaraldehyde (GA) to increase tissue strength and minimize immunological reactions caused by cellular components, but they tend to calcify severely (Manji et al., 2015). Furthermore, the toxicity associated with free aldehyde groups that remain after GA-fixation hinders the endothelialization of the donor homograft with host cells and is associated with inflammatory cytokine release from activated macrophages (Umashankar et al., 2012). The additional treatment of GA-fixed homografts with agents such as polyethyleneglycol (PEG) or propylene glycol (PG) can address this issue, as these agents react with free aldehyde groups of GA, inactivates and masks platelet receptor sites and mitigate calcification (Jeong et al., 2013). EnCap technology describes the fixation of biological tissue with GA and the subsequent treatment of the GA-fixated tissue with a high concentration liquid polyol like PG or glycerol to mitigate calcification of tissue (Seifter and Frater, 1995).

The current study was therefore undertaken to evaluate the effect of the further processing of pulmonary homografts, following a 48 h cold ischaemic post-mortem harvesting time, on the structural integrity and function when implanted in the RVOT position of the juvenile ovine model. The study evaluated whether the processing with a novel decellularization and sterilization method, with proven synergy (Laker et al., 2020), combined with the use of Benzonase will obtain an acellular homograft with maintained structural integrity and restricted

calcification when implanted in the RVOT position of juvenile sheep. In addition, the effect of additional GA-fixation, including a detoxification process (EnCap technology) on the structural integrity and calcification of the decellularized homografts was also investigated. These processes were compared to conventional cryopreservation of pulmonary homografts following a 48 h ischaemic post-mortem harvesting time.

1.2 Aims and objectives

The aim of this study was to compare the clinical performance of differently processed pulmonary homografts in the Right Ventricle Outflow Tract (RVOT) of juvenile sheep, following a post-mortem cold ischaemic harvesting time of 48 hours.

The objectives of this study were:

i. To evaluate the baseline morphological differences and mechanical properties of cryopreserved, decellularized, and decellularized, GA-fixed and detoxified sheep pulmonary homografts following a post-mortem cold ischaemic harvesting time of 48 h **(Chapter 3).**
ii. To implant the cryopreserved, decellularized, and decellularized, GA-fixed and detoxified sheep pulmonary homografts in the RVOT position of juvenile sheep and monitor the clinical performance of the homografts with echocardiography over a study period of 180 days **(Chapter 4 and 5).**
iii. To evaluate the gross macroscopic appearance, structural integrity and histology of explanted cryopreserved, decellularized, and decellularized, GA-fixed and detoxified sheep pulmonary homografts **(Chapter 4 and 5).**
iv. To evaluate the calcification of explanted cryopreserved, decellularized, and decellularized, GA-fixed and detoxified sheep pulmonary homografts **(Chapter 4 and 5).**
v. To evaluate and compare the mechanical properties of cryopreserved, decellularized, and decellularized, GA-fixed and detoxified sheep pulmonary homografts before and after implantation in the RVOT position of juvenile sheep **(Chapter 3, 4 and 5).**

1.3 Structure of the thesis

This thesis is compiled in publishable manuscript-format according to the guidelines set by the University of the Free State, and is comprised of six chapters and appendices which (excluding the current chapter) are summarised as follows:

- **Chapter 2: Literature overview**

This chapter consists of an in-depth review of the relevant literature on pulmonary homografts and processing methods used for homografts and other aspects relevant to this study.

- **Chapter 3: Comparison of the impact of cryopreservation, decellularization and decellularization, glutaraldehyde-fixation and detoxification as processing techniques on the strength and structure of juvenile ovine pulmonary homografts.**

This chapter consists of a manuscript describing the baseline morphological differences and mechanical properties of cryopreserved, decellularized, and decellularized, GA-fixed and detoxified sheep pulmonary homografts following a post-mortem cold ischaemic harvesting time of 48 h.

- **Chapter 4: Comparison of function and structural integrity of cryopreserved pulmonary homografts versus decellularized pulmonary homografts after 180 days implantation in the juvenile ovine model**

This chapter consists of a manuscript describing the clinical performance of cryopreserved compared to decellularized pulmonary homografts, following a post-mortem cold ischaemic harvesting time of 48 h, in the RVOT position of juvenile sheep with a post-implantation follow-up time of 180 days. At the end of the study period, the valves were explanted and compared histologically and also based on mechanical strength and calcium content.

- **Chapter 5: Comparison of function and structural integrity of decellularized pulmonary homografts versus decellularized, glutaraldehyde-fixed and detoxified homografts after 180 days implantation in the juvenile ovine model.**

This chapter consists of a manuscript describing the clinical performance of decellularized and decellularized, GA-fixed and detoxified pulmonary homografts, following a post-mortem cold ischaemic harvesting time of 48 h, in the RVOT position of juvenile sheep with a post-implantation follow-up time of 180 days. At the end of the study period, the valves were explanted and compared histologically and also based on mechanical strength and calcium content.

- **Chapter 6: Summary, conclusion and future recommendations**

This chapter describes the conclusions drawn from this study. The limitations of the study are discussed, and recommendations for future studies are made.

- **Appendices**

Additional co-authored articles, which share points of contact with this study but do not form part of the thesis, are presented in Appendix A. Animal Ethics Approval is given in Appendix B.

1.4 References

The references used in this section are included in the final reference list at the end of this thesis. However, the references used in each manuscript are given at the end of each manuscript. The Harvard reference style is used throughout the thesis.

Chapter 2 - Literature review

2.1 Introduction to the heart valves and heart valve disease

The human heart contains four valves. The tricuspid valve controls blood flow to the right ventricle and the mitral valve controls the blood flow to the left ventricle. The pulmonary and aortic valves control the blood flow out of the ventricles to the lungs and body, respectively. In a sequence of opening and closing as the heart contracts and relaxes, blood is moved uni-directionally in a forward direction and prevented from flowing backward. The mitral and tricuspid valve leaflets are anchored into place on the papillary muscles by chordae tendineae, which are strands of mostly collagen and elastin, preventing the valve leaflets from opening in the wrong direction and into the atria (Ho, 2002; Dahou et al., 2019). The aortic and pulmonary valves are both tri-leaflet valves consisting of three semilunar leaflets without any additional anchoring and rely on their tissue structure to withstand the pressures exerted by blood flow (Fitzgerald and Lim, 2011; Ayoub et al., 2016) (Figure 2.1).

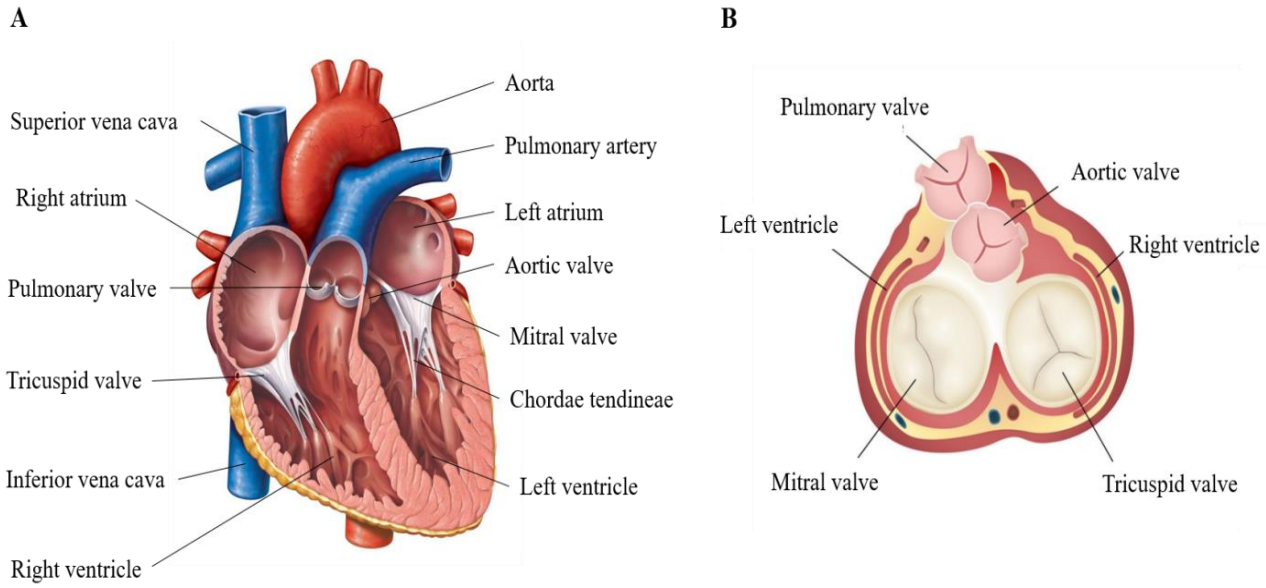

Figure 2.1: Schematic diagram of the gross anatomy of the heart **(A)** and the heart valves **(B)**. (Adapted from Dahou et al., (2019)).

Heart valves can get damaged or diseased, and become stenotic (restricting the one-way flow of blood) or start regurgitating (allowing blood to flow backward), requiring surgical repair or replacement.

Diseased valves can either be surgically repaired by several different available techniques, including the implantation of a supporting ring into the valve annulus (Karas et al., 2007), or by replacing the valve with an artificial mechanical valve, a bioprosthetic valve from xenogeneic origin (Lever, 2005) or a human allograft valve from a tissue donor (Lisy et al., 2017).

The pulmonary valve is the least likely of the heart valves to be affected by acquired disease; therefore, most disorders associated with this valve are congenital (Fitzgerald and Lim, 2011). Pulmonary valve stenosis, characterised by the obstruction in blood flow from the right ventricle to the pulmonary arteries, is a common congenital heart defect that occurs in 6 to 8 of every 10, 000 live births (Idrizi et al., 2015). Patients with congenital heart disease involving a right ventricular outflow tract (RVOT) obstruction or insufficiency requires reconstruction of the RVOT (Gerestein et al., 2001). A method for reconstruction was described by Ross and Somerville in 1966 and involves the insertion of a homograft conduit between the right ventricle and the pulmonary artery (Ross and Somerville, 1966). Although retrospective studies indicated that this procedure has promising outcomes in terms of long-term survival (Gerestein et al., 2001; Brown et al., 2005), stenosis or insufficiency might develop, which causes elevated right heart pressures and progressive heart failure. Therefore, re-interventions and replacements of the homografts may be necessary (Kaza et al., 2009).

Aortic valve disease is one of the leading causes of cardiovascular mortality (Krishnamurthy et al., 2017). Compared to right ventricular outflow conduit exchange, there is a higher risk of repeat aortic valve replacement in children when using homografts for aortic valve replacement (Gulbins et al., 2003). The pulmonary valve is used in the Ross procedure, where a patient's pulmonary valve is used as an aortic valve substitute, followed by the implantation of a homograft in the pulmonary position (Ross, 1991). This procedure is especially advantageous in paediatric patients, where aortic homograft degeneration occurs rapidly compared to in older patients, and who benefit from the increase in autograft diameter with somatic growth (Etnel et al., 2018).

2.2 Pulmonary heart valves: Structure, composition and function

2.2.1 Structure

The structure of the pulmonary and aortic valve appears similar with semilunar-shaped valve leaflets, but the pulmonary valve does not have a ring-like annulus consisting of tough, fibrous tissue. The leaflets are distally attached to the pulmonary trunk at the sinotubular junction and proximally to the infundibular muscle at the ventriculoarterial junction, anatomically forming the valve annulus (Saremi et al., 2014).

The leaflets are attached to one another and the annulus at the commissures. The annulus maintains the proper shape of the valve. The free edge of each leaflet is called the lunule and is thickened where it makes contact with the free edge of the adjacent leaflet. The angulated apex of each leaflet's free edge has another thickening called the nodule, and the leaflets bulge inferiorly into the outflow tract of the right ventricle (Figure 2.2).

The wall of the pulmonary trunk directly adjacent to the three leaflets is slightly dilated, forming a space between the trunk wall and the leaflets called the pulmonary sinus or sinus of Valsalva (Sundjaja and Bordonin, 2019). The sinotubular junction separates the pulmonary sinuses from the tubular component of the pulmonary trunk.

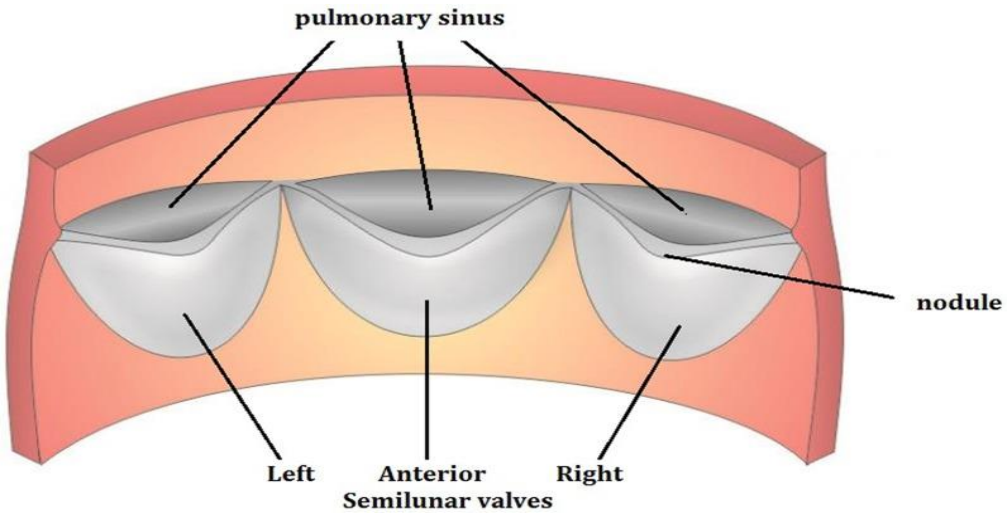

Figure 2.2: Posterior view of the structure of the pulmonary valve. (With permission from Shen et al., (2018)).

2.2.2 Pulmonary valve composition

Pulmonary valve leaflets comprise three distinct tissue layers, namely the ventricularis (facing the right ventricle), spongiosa (middle valve layer) and fibrosa (facing the pulmonary artery), and each layer is enriched in a different extracellular matrix (ECM) component. The ventricularis and fibrosa layers are covered by endothelial cells, forming a cell monolayer that protects the valve (Stephens et al., 2012b). Structural elements within these three layers are arranged in a very systematic orientation, leading to mechanical and physical leaflet properties that differ significantly when measured in different directions (anisotropic). Several structural features enable the leaflets to be extremely soft and pliable when unloaded, and inextensible when high transvalvular pressure is applied when the valve is fully closed (Ibrahim et al., 2017) (Table 2.1).

Table 2.1: Key elements of the heart valve leaflet. (Adapted from Ibrahim et al., (2017)).

Element	Layer	Function
Collagen	Fibrosa and spongiosa	Contributes to tensile and mechanical strength, for example, provides stiffness required for adjustment during diastole
Elastin	Ventricularis	Provide strength and flexibility, allowing valve recoil in systole and valve extension in diastole
Glycosaminoglycans	Spongiosa	Absorbs shock, accommodates shear forces in leaflet layers
Valvular interstitial cells	Fibrosa, Spongiosa, Ventricularis	Matrix synthesis, remodeling
Valvular endothelial cells	Outer surface of leaflets	Create a non-thrombogenic interface, control behaviour of valvular interstitial cells (permeability and crosstalk with paracrine signals)

The fibrosa is mostly composed of large amounts of collagen fibers, organized into large bundles and is predominantly aligned along the circumferential direction of the leaflets. This alignment of the fibers makes the leaflets much stiffer along their circumferential than their radial direction. The fibers are surrounded by glycosaminoglycans (GAG) and proteoglycans, as well as a network of elastic fibers, helping to maintain the microstructure of the valve leaflet during systole. This collagen layer also has a visibly corrugated appearance with many folds on the surface of the leaflets when they are not under tension (Combs and Yutzey, 2009).

The ventricularis layer of the leaflets faces the inflow of the valve (right ventricle). The ventricularis still contains significant amounts of collagen but is largely composed of radially aligned elastic fibers. The collagen fibers are more loosely aligned and are not orientated in any specific direction, making the ventricularis layer more flexible than the fibrosa. The elastin protein in the elastic fibers can stretch out when stressed; however, when the stress is released it returns to its original shape (diastole) (Schoen, 2008).

The spongiosa layer is located between the fibrosa and ventricularis layers of the leaflet. It is primarily composed of water, GAGs and proteoglycans, but also contains loosely arranged collagen and elastin fibers, which connect the fibrosa and ventricularis (Misfeld and Sievers, 2007) (Figure 2.3).

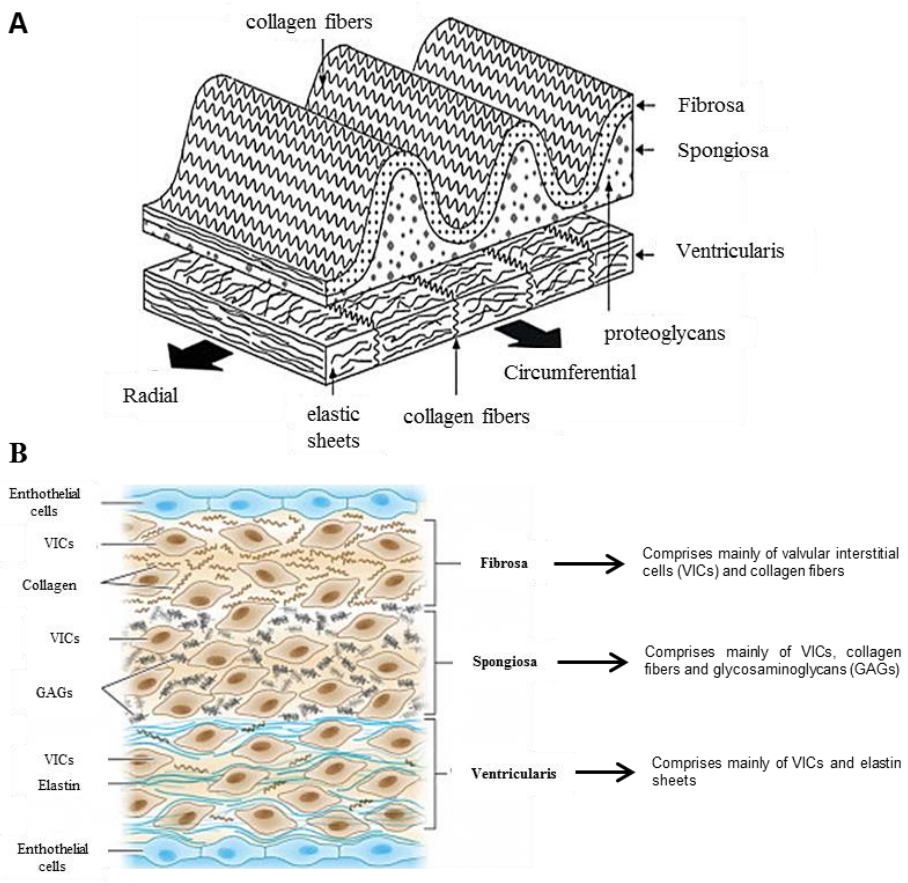

Figure 2.3: **Schematic diagram of trilaminar leaflet structure of semilunar valves**, showing the fibrosa, spongiosa and ventricularis layers, with macroscopic visible corrugations of the fibrosa layer **(A)** and the composition of the different layers of the leaflet **(B)**. (Adapted from Korossis, (2018) and Aikawa and Schoen, (2014)).

The different layers of a leaflet can vary in thickness from the attachment area around the base of the leaflet (valve annulus level) to the free edge and coaptation area between leaflets. The fibrosa is the thickest of the three layers at the basal attachment area, becoming thinner and is gradually overtaken by the spongiosa, which is the main component of both semilunar and atrioventricular leaflets at their free edges. Venules and arterioles are also found in the thicker basal regions of leaflets, where they facilitate supplementary oxygen and nutrient transport in regions where normal diffusion is inadequate to nourish and sustain cells (Korossis, 2018).

2.2.3 Pulmonary valve function

When the right ventricle muscle contracts during systole, the pulmonary valve is pushed open by the increased blood pressure. The valve functions as a unidirectional valve, allowing deoxygenated blood to flow out of the heart and into the pulmonary artery to the lungs to be oxygenated. When the pressure inside the heart drops, the leaflets close and prevents the blood from flowing back into the heart. During systole, the pulmonary sinuses prevent the leaflets from flattening against the walls of the sinuses or pulmonary trunk, as this will restrict the valve to close adequately during diastole (Stephens et al., 2012a; Sundjaja and Bordonin, 2019).

With an abundance of collagen fibers, the fibrosa layer is the primary structural and major load-bearing layer of the pulmonary leaflet, offering the mechanical integrity of the leaflet (Korossis et al., 2005). The collagen aligns in a certain way during the backflow of diastole and allows the valve leaflet to elongate as it closes. This alignment of the collagen fibers in the fibrosa gives the closed valve enough strength to withstand the backward flow of the blood in the pulmonary artery, prevent any regurgitation and ensure optimal coaptation during closure (Schoen, 1997; Schoen, 1999).

As the leaflets stretch in diastole to completely close the valve, the elastin in the ventricularis layer also extends to enlarge the coaptation area of the leaflets and ensure effective valve closure. When the ventricle contracts during systole and the pressure from the backflow are released, the elastin recoils, causing the leaflets to fold up and open the valve to allow blood to flow into the pulmonary artery (Ayoub et al., 2016).

Shear stresses are caused by the differential movements of the fibrosa and ventricularis layers of the leaflet, and the shock of the valve closure. The spongiosa layer helps to lubricate these movements as the hydrophilic GAGs and proteoglycans absorb water and swell to form a deformable gel, providing a natural shock-absorption mechanism along the coaptation region of the leaflets, while also helping to align the collagen during valve movement (Korossis, 2018).

2.3 Homograft valves

Ross and Barratt-Boyes introduced the use of homograft valves into clinical practice in 1962 (Barratt-Boyes, 1965; Ross, 1965). These valves had superior performance compared to the mechanical valves that were available at the time. Besides mechanical heart valves, these homografts were the only successful biological heart valve prosthesis at the time. The advantages of these homograft valves include a low rate of thromboembolic events and, therefore, no need for anticoagulation therapy, also these valves had superior haemodynamic properties compared to the mechanical valves of the time (Gulbins et al., 2003). Initially, fresh homografts were used, but their availability was very unpredictable, and new methods of processing and storage had to be devised.

2.3.1 Ischaemic harvesting time for homografts

When human heart valves (homografts) are donated for transplantation, the hearts must be procured, transported and processed before they are stored. The warm ischaemic period begins at the time of cessation of blood flow and ends at organ recovery or when the body is refrigerated and is a very important factor in the ultimate viability of tissues. As the warm ischaemia lengthens, metabolic alterations occur, including the accumulation of toxic cell products, ion shifts, cell membrane depolarization, and eventual cell death (Dawson and Brockbank, 1997). Minimal irreversible cellular injury occurs in valves exposed to 12 h or less of warm ischaemia (Crescenzo et al., 1993), and longer ischaemic times may provide the ideal conditions for opportunistic organisms to proliferate in the tissue with a resultant increase in cellular damage.

Cold ischaemia begins at refrigeration (4^{o}C) of the body, and ideally, the heart should be procured within 12-24 h after death. This reduction in tissue temperature is the simplest way to slow down the rate of tissue deterioration, whereby aerobic glycolysis, ATP consumption, and

degradative enzyme activity are limited. Once a heart is procured, it is rinsed, placed in cold 4ºC physiological solution and transported. Reducing the tissue temperature aids in slowing down the metabolic activity and functions of valvular cells, and deterioration of the tissue (Dawson and Brockbank, 1997).

Gall and co-workers strongly advocated the harvesting of homografts either from beating heart transplant donors or within 24 h after death from non-beating donors to ensure maximum viability of homografts at the time of implantation. Arguing that viability is one of the factors that will influence the durability of a homograft, as determined by the freedom from structural deterioration (Gall et al., 1998).

Over the years, many have disputed the importance of tissue viability, because of no substantial evidence that viable cells do persist, produce collagen and repair the damaged extracellular matrix of the valve. Viable cells, if present, might merely be an indication of optimal standards of collection, processing and tissue preservation prior to implantation. Smit and co-workers showed that when extending the cold ischaemic time to 48 h before harvesting pulmonary homografts, no differences in tissue strength and extracellular matrix appearance were demonstrated. Furthermore, no differences in inflammatory reactions and haemodynamic performance occurred when implanted in a juvenile sheep model (Smit et al., 2015). A retrospective clinical study in Norway found that extending the ischaemic time in non-beating-heart donors to 48 h has no negative effects on the homograft when compared to an ischaemic time of less than 24 h and that the reintervention rate in patients with homografts with >24 h ischaemic times was lower (Axelsson and Malm, 2018).

2.3.2 Fresh storage of homografts

Until the late 1970s, homografts were freshly stored in a storage medium with an antibiotic cocktail for 6-8 weeks at 4˚C in a refrigerator, after which valves had to be discarded if not used (Gall et al., 1995). The nutrient medium enhanced the viability of the fibroblasts in the allograft, but the viability and elastic properties slowly declined during cold storage, which restricted the storage time and limited the availability of homografts significantly.

Parker and co-workers stored valves in glycerol, however, it also led to a decrease in viability and changes in the histological appearance of the cusp tissue and subsequent decrease in elasticity. Complete sterilization could also not be achieved, and an additional sterilization treatment with antibiotics was required. Storage in glycerol did offer an alternative method for cold storage in a nutrient medium, however, it did not provide any additional practical advantages, and new and improved storage methods had to be found (Parker et al., 1978).

2.3.3 Cryopreservation of homografts

Cryopreservation techniques as an alternative storage method for human valve allografts were developed in 1976 (Angell et al., 1976), and brought about a whole new revolution in tissue banking. Although somewhat expensive, it became the method of storage used by most tissue banks worldwide for homograft heart valves. This storage method allowed storage of valves for up to 5-10 years, thus creating a bank of available valve sizes. Decontamination of valves was done with an antibiotic cocktail, and cocktails used were and still are diverse in terms of the number, combination, and concentrations of antibiotics used by different banks. Incubation temperatures and duration also differ significantly between tissue banks (Heng et al., 2013).

The addition of glycerol and later dimethylsulfoxide (DMSO) as a cryoprotectant to the storage medium, led to valves being frozen at a controlled rate of -1˚C/min to -80˚C and stored in the vapour phase of liquid nitrogen. Initially, it appeared like the ECM was kept relatively intact and cell viability maintained when using this method. However, later research studies suggested that structural damage to the collagen and elastic fibers of the ECM might occur (Wollmann et al., 2011). Bester and co-workers found that the process of cryopreservation causes more damage to the ECM than extending the post-mortem harvesting time of homografts. Cryopreservation led to the collagen of homografts becoming fractured (Bester et al., 2018). Significant reduction in cell viability following long-term storage in liquid nitrogen has also been reported, but this is largely attributed to the freezing and storage protocols used (Boroumand et al., 2018), and not the duration of storage (Heng et al., 2013).

Earlier it was believed that the presence of living endothelial and fibroblast cells in freshly stored or cryopreserved homograft valves were advantageous in the remodeling and regeneration

potential of the extracellular matrix. Contrary to this belief, it is now widely considered that these cells are instead recognized by the recipient as foreign material, which induces an inflammatory response or an immune-mediated rejection of the implant (Mariani et al., 2019).

These living cells and cellular remnants are highly immunogenic and have been associated with fibrosis, structural deterioration and ultimate failure in a significant proportion of transplanted homografts (Dohmen and Konertz, 2009). Many attempts have been made to modify homograft tissue to minimize or avoid the immune response of the recipient to the antigenic or pro-inflammatory triggers, without much success. Glutaraldehyde (GA) is widely used in bioprosthetic valves, especially for xenografts, for cross-linking and stabilization of connective tissue and minimizing host immune reactions. Viability of tissue is detrimental to graft durability, and fixation of the tissue does render the tissue nonviable. GA is toxic, prevents repopulation of the extracellular matrix with host endothelial or interstitial cells and leads to structural deterioration, calcification and inevitable valve failure (Umashankar et al., 2012; Manji et al., 2015).

2.4 Tissue engineering

With the worldwide shortage in the availability of transplantable biological material ranging from structural tissues (skin, cartilage, and bone) to complex organs (heart, liver, kidneys and pancreas), the concept of tissue engineering of such tissues has gained increased attention of researchers. In principle, it involves the reconstitution of biological or artificial 3D scaffolds of the tissue or organ to be replaced, which are then seeded with autologous cells from the recipient either *in vitro* or *in vivo* (Steinhoff et al., 2000). Tissue engineering involving cardiac tissue has mainly focused on aortic and pulmonary valves, blood vessels and the myocardium (Mendelson and Schoen, 2006). While current devices used in heart valve replacement surgery has its own limitations such as anticoagulation control (mechanical valves) and calcification and structural deterioration of tissue and bioprosthetic valves, the advantages of tissue-engineered valves could include non-thrombogenicity, resistance to infection, cellular viability and reduced calcification (Mendelson and Schoen, 2006).

Scaffolds used in tissue engineering could either be synthetic (composite biodegradable polymers) or biological (collagen, elastin, fibrin, glycoproteins), and from either animal (xenograft) or human (homograft) origin (Lam and Wu, 2012). Artificial or synthetic scaffolds are commonly used as a structure to support cell cultures, and for the control of cell growth in the repair of impaired tissues or organs. The scaffold only acts as a temporary support during cell regeneration and is required to gradually biodegrade during or after the healing process, whereafter new tissue with the desired shape and properties is produced. Once the scaffold has degraded, it needs to be removed from the body to mitigate the possible side effects of such foreign materials if it remains in the body (Eltom et al., 2019).

Biological materials mainly consist of a collagen structure combined with a complex extracellular matrix, consisting of proteoglycans, glycoproteins, elastin, metalloproteins with tissue cells and interstitial fluid embedded in it (Mendoza-Novelo and Cauich-Rodriguez, 2011).

2.4.1 Decellularization

In recent years, the decellularization or removal of endothelial and fibroblast cells and nuclear material from biological materials has gained much interest. The decellularization process creates a biological scaffold with largely decreased immunogenicity/antigenicity and reduced risk of calcification (van Steenberghe et al., 2018). Decellularization can be achieved by using a combination of chemical and enzymatic compounds together with physical/mechanical agitation to destroy the cell membranes and remove all the nuclear material, cell debris and residual chemicals, leaving behind an acellular extracellular matrix (ECM) with a retained three-dimensional architecture (Mendoza-Novelo and Cauich-Rodriguez, 2011). Such a scaffold will then serve as a template for cellular attachment and can potentially be repopulated by pre-seeded or endogenous circulating cells while retaining many of the mechanical and structural properties of native tissue (Figure 2.4) (Bourgine et al., 2013). All chemicals have to be removed from the tissue after treatment, as they could be toxic to the host cells following implantation of the scaffold, and residual enzymes can potentially invoke an adverse immune response by the recipient (Gilbert et al., 2006).

Minimum criteria to define adequate decellularization of tissues have only very recently been established. Three quantifiable standards are currently accepted, namely: (1) < 50 ng double-stranded DNA per milligram ECM dry weight, (2) < 200 base pair DNA fragment length, and (3) the lack of visible nuclear material following staining with 4′,6-diamidino-2-phenylindole (DAPI) or hematoxylin and eosin (H&E) (Crapo et al., 2011). Any decellularized tissue(s) should meet one or more of these criteria; otherwise, the decellularization protocol will be deemed ineffective. Ineffective decellularization can trigger the immune response of the recipient with resultant ingrowth of macrophages into the tissue and inhibition of the effective remodeling of the graft (Keane et al., 2012). Different decellularization methods will often negatively affect the structure and protein composition of the tissue, and differ in the effectiveness of removing cellular and nuclear material, lipids and carbohydrates (VeDepo et al., 2017).

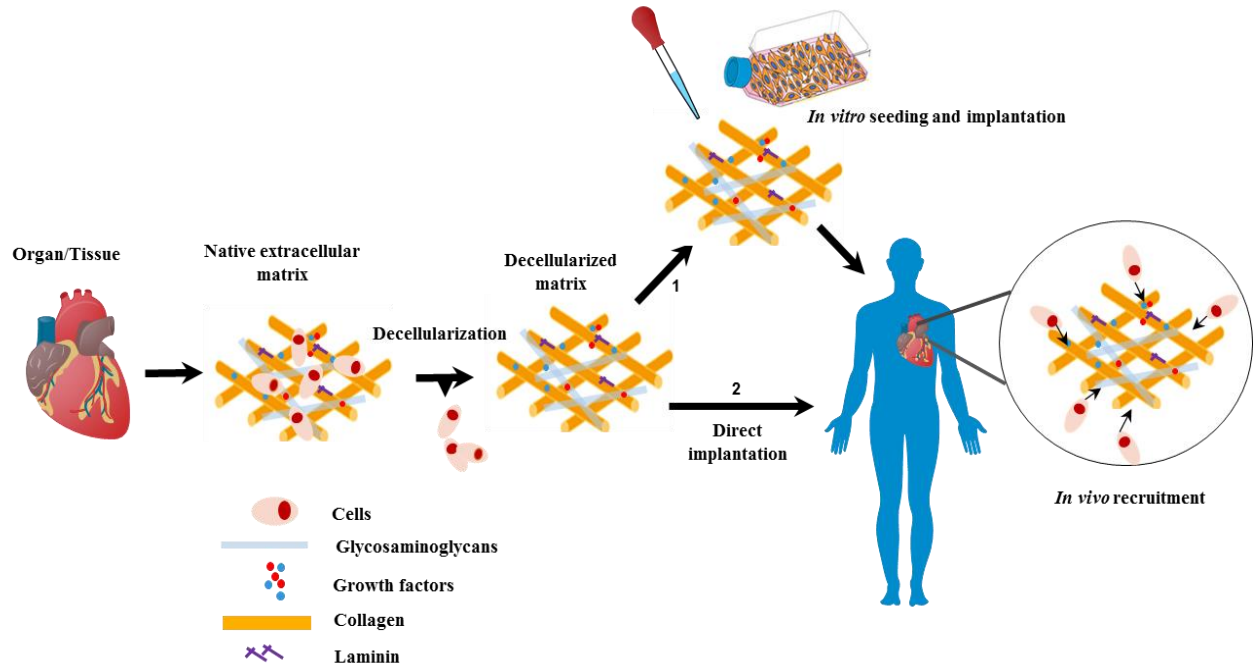

Figure 2.4: Schematic representation of the decellularization and recellularization of tissue. Removal of cells and nuclear material from the native extracellular matrix (ECM) leads to a decellularized but intact ECM that should retain growth factors, collagen, laminin, glycosaminoglycans and other factors that promote the recellularization of the scaffold. Recellularization can occur through (1) the *in vitro* seeding with the recipients own cells followed by the implantation of the scaffold into the recipient or (2) the direct implantation of the scaffold into the recipient followed by the *in vivo* recruitment of host cells. (Adapted from Bourgine et al., (2013)).

The use of a hypotonic solution, followed by a hypertonic solution can induce osmotic shock, resulting in cell lysis. However, using this method as the sole method for decellularization is not recommended, as it is not effective in removing cell remnants (Meyer et al., 2006; Somers et al., 2012). Additional chemical and/or enzymatic treatments can be employed. Enzymatic treatments involve the cleavage of peptide bonds with trypsin, or the hydrolysis of bonds of the RNA or DNA chains with nucleases (RNase or DNase) (VeDepo et al., 2017). Compared to detergents, trypsin is more disruptive to ECM proteins such as collagen; however, it is better in preserving GAG content (Crapo et al., 2011). Endonuclease, such as Benzonase, cleave nucleotides mid-sequence and is more effective than exonuclease in fragmenting DNA in preparation for its removal (Crapo et al., 2011; Dijkman et al., 2012).

A wide variety of chemical treatments have been investigated, and a combination of some of them seems appropriate, especially for heart valve tissue. A non-ionic detergent like TritonX-100 is very effective in disrupting the lipid-lipid and lipid-protein interactions, without affecting the protein-protein interactions. Ionic detergents like sodium dodecyl sulphate (SDS) and sodium deoxycholate (DOA) solubilizes cytoplasmic and nuclear cellular membranes, thus helping to remove nuclear remnants and cytoplasmic proteins from the ECM. It can, however, also denature proteins, thereby disrupting native tissue structure, remove GAGs and damage collagen, and great attention has to be given to the concentrations eventually used (Gilbert et al., 2006; Crapo et al., 2011; VeDepo et al., 2017).

Detergent and enzymatic methods are the most widely used methods for decellularization. However, there is a risk of damage to proteins of the ECM and possible toxicity of the chemicals. Physical methods that can be used for the decellularization of heart valves include the use of freeze-thaw or high hydrostatic pressure (Gilpin and Yang, 2017). These methods maintain the ECM proteins and mechanical properties; however, remnant DNA may remain (Xing et al., 2015). Early conduit degeneration is caused by calcification due to the presence of phospholipids. Alcohols such as methanol and ethanol are more effective in removing lipids than lipase (Flynn, 2010; Brown et al., 2011). Several decellularization techniques can be combined to complement one another to retain the desired characteristics of the decellularized tissue. A multi-detergent approach making use of SDS, DOA and TritonX-100 was previously developed

by our research group and was used for the decellularization of bovine pericardium. Synergism was observed when using the combination of these detergents, with complete decellularization and intact collagen and elastin (Laker et al., 2020).

2.4.2 Decellularization protocols designed for heart valves

Wilson and co-workers decellularized canine arteries in a multistep detergent extraction process using hypotonic and hypertonic solutions and digestion with a nuclease enzyme, with the implants showing no inflammation but minimal recellularization after six months (Wilson et al., 1995). Bader and co-workers introduced a single-step detergent-based method for decellularization of porcine aortic valves (Bader et al., 1998). The presence of cell remnants could still not be excluded; however, a confluent layer of endothelial cells was reported following cell seeding after three days in static *in vitro* conditions. Korossis and co-workers also introduced a single-step detergent treatment using 0.03 % or 0.1 %, w/v SDS in a hypotonic or isotonic buffer, concluding that SDS and hypotonic buffer delivered complete acellularity (Korossis et al., 2002). The use of TritonX-100 and SDS were compared, and cusps were almost free of cells when treated with SDS; however, cells were still present after treatment with TritonX-100 (Naso and Gandaglia, 2018).

Rieder and co-workers decellularized porcine aortic and pulmonary roots with either trypsin, SDS, or a new method using 0.25 % tert-octylphenyl-polyoxyethylene in combination with DOA, followed by RNA and DNA digestion. The decellularization procedures with trypsin and SDS were effective in cell removal and susceptible to recellularization with human cells, however, the porcine matrix treated with 0.25 % tert-octylphenyl-polyoxyethylene/sodium-deoxycholate followed by nuclease digestion presented an excellent scaffold for recellularization with human cells (Rieder et al., 2004).

Cebotari and co-workers decellularized human heart valves with a protocol based on digestion with trypsin, demonstrating a reduction in DNA of more than 98 % and a well maintained three-dimensional network of collagen fibers in the leaflets (Cebotari et al., 2002). Using a similar trypsin-based decellularization protocol, Steinhoff and co-workers also reported almost complete

removal of cells, but signs of inflammatory reactions leading to calcifications were observed after three months implantation in a sheep model (Steinhoff et al., 2000).

The effects of decellularization with 1 % DOA, 1 % SDS, or 0.05 % trypsin/0.02 % EDTA on the cusps, wall and myocardial ring of pulmonary valves were compared. Cusps were completely decellularized with all three methods, while only DOA and SDS were able to completely remove all cells from the valve wall and ring of the myocardium, with superior preservation of ECM proteins and the morphological integrity. Enzyme treatment resulted in the destruction of the basement membrane. Decellularization of pulmonary homografts with detergents like DOA and SDS instead of enzymes better preserve the morphological and biomechanical properties of the scaffold (Tudorache et al., 2007).

Buratto and co-workers reported on their investigations using the detergent taurodeoxycholate as a potential agent for the decellularization of heart valves. Porcine aortic roots were decellularized using TritonX-100 and taurodeoxycholate, followed by nucleic acid digestion with a non-specific endonuclease (Benzonase). Efficient decellularization was achieved and the valve structure was largely maintained, while morphology was mildly altered. Collagen fibers in the fibrosa appeared swollen and laminin immunodetection was reduced. GAGs and elastin distribution were well maintained, and basement membrane components Collagen IV and Fibronectin were largely intact. Transvalvular gradients and regurgitant volumes were, however significantly increased following testing in a pulse duplicator. The study concluded that taurodeoxycholate is a promising detergent for use in heart valve tissue engineering, but that it does influence the hydrodynamic performance of valves negatively (Buratto et al., 2011).

Haupt and co-workers compared three decellularization protocols: 1) Detergents (1 % SDS, 1 % TritonX-100, 1 % DOA) and 0.2 % EDTA with removal of nucleic acids using RNase and DNase; 2) 0.05 % Trypsin and 0.02 % EDTA; 3) Accutase solution followed by an enzymatic step (RNase and DNase) for complete removal of nucleic acids. Incomplete decellularization for the Trypsin/EDTA treatment (group 2), disrupted architecture and degraded ultrastructure in groups 2 and 3, and complete removal of all DNA fragments with intact material architecture for the porcine pulmonary valves in group 1 was observed (Haupt et al., 2018).

Compared to cryopreserved pulmonary homografts, a significant reduction in the immune response and better haemodynamic performance after the clinical use of up to 18 months, was reported for pulmonary homografts decellularized using 1 % DOC or 1 % SDS. However, standardized decellularization in all samples was not achieved with DOC, with residual cell persistence in some treated scaffolds (da Costa et al., 2007).

Various methods that have been used for the decellularization of heart valves are summarized in table 2.2.

Table 2.2: Methods for the decellularization of heart valves. (Adapted from VeDepo et al., (2017) and Gilpin and Yang, (2017)).

Category	Method	Mode of Action	Agent/Technique	General effectiveness	General effect on valve ECM
Chemical and enzymatic	Anionic detergent	Solubilize cell and nucleic membranes, tend to denature proteins	SDS or DOA	Lack of visible cell nuclei, ~ 95 % DNA removal	Increased areal strain and peak stretch ratio; decreased flexural stiffness; preservation of GAGs; may disrupt ECM fiber structure
	Non-ionic detergent		TritonX-100	Lack of visible cell nuclei	Increased areal strain and peak stretch ratio; decreased flexural stiffness; loose ECM network; histological reduction of GAG, laminin, fibronectin and collagen
	Enzymatic and chelating agents	Cleaves peptide bonds on the C-side of Arginine and lysine Chelating agents bind metallic ions and disrupt cell adhesion to ECM	Trypsin + EDTA	Incomplete cell removal	Decreased mechanical properties; histological tissue damage and loss of basement membrane; histological reduction of GAG, laminin, fibronectin and collagen
	Osmotic shock	Cell lysis by osmotic shock, disrupt DNA-protein interactions	Hypotonic/hypertonic Tris buffer	Many visible cell remnants	Histological reduction in MHC antigens loss of non-collagen proteins
	Sequential antigen removal	Solubilize lipophilic and hydrophilic proteins	Dithiothreitol, potassium chloride, amidosulfobetaine-14	Lack of visible cell remnants and reduced antigenicity	Preservation of Young's modulus and ultimate strength, preservation of collagen and elastin, decreased GAGs
Sterilization based methods	Glycol radiation	Destabilizes cell membranes, destruction of DNA, causes cell injury through ROS	PEG + gamma irradiation	Lack of visible cell nuclei; > 92 % cusp DNA removal	Preserve leaflet ultrastructure, removal of α-Gal antigen
Mechanical	Supercritical carbon dioxide	Pressure can burst cells, supercritical fluid facilitates chemical exposure and removal of cellular material (ethanol – cell lysis by dehydration, solubilize and removes lipids)	CO_2; ethanol	Lack of visible cell nuclei; 90 % phospholipid removal	Stiffening of tissue, tissue dehydration

Table 2.2: Methods for the decellularization of heart valves (continued).

Category	Method	Mode of Action	Agent/Technique	General effectiveness	General effect on valve ECM
Combinations	Multi-detergent	Solubilize cell and nucleic membranes, tend to denature proteins	TritonX-100 + sodium cholate	~30 % DNA removal	Increased extensibility and decreased stiffness; GAG reduction; preservation of elastin and collagen components
			TritonX-100 + DOA	Lack of visible cell nuclei; 98 % DNA removal	Histologic preservation of structure and ECM components
	Multi-detergent and osmotic shock and alcohol	Solubilize cell and nucleic membranes, tend to denature proteins; Cell lysis by osmotic shock, disrupt DNA-protein interactions; Cell lysis by dehydration, solubilize and removes lipids	Osmotic shock + TritonX-100 + NLS salt + ethanol	Lack of visible cell nuclei; >97 % dsDNA removal	Increased areal strain and peak stretch ratio; decreased stress relaxation; reduced GAG content
	Enzyme and/or detergent and/or osmotic shock combinations	Solubilize cell and nucleic membranes, tend to denature proteins; Cleaves peptide bonds on the C-side of Arginine and lysine; Cell lysis by osmotic shock, disrupt DNA-protein interactions	Trypsin + SDS	Lack of visible cell nuclei; 96 % DNA removal	Reduction of GAG and α-Gal antigen; preservation of mechanical properties
			Trypsin + DOA	Visible cell remnants; 98 % DNA removal	Histologic disruption of ECM components
			Trypsin + osmotic shock + TritonX-100	Lack of visible cells	Misalignment of collagen fibers
			Trypsin + osmotic shock	Visible cell remnants	Histologic loss of collagen; GAG reduction; decreased mechanical strength

ECM: extracellular matrix; SDS: sodium dodecyl sulphate; DOA: sodium deoxycholate GAG: glycosaminoglycan; NLS: *N*-lauroylsarcosine sodium salt; dsDNA: double-stranded DNA; EDTA: ethylenediaminetetraacetic acid; α-Gal: galactose-α(1,2)-galactose; PEG: polyethylene glycol; ROS: Reactive oxygen species; MHC: major histocompatibility complex.

2.4.3 Impact of decellularization on valve tissue properties

Decellularization of valve leaflets with a single-step enzymatic trypsin/EDTA process demonstrated loss of cells and ECM components with an increase in time of exposure to the enzyme. Biomechanical data demonstrated a similar time-dependent loss of tissue integrity and a gradual weakening in mechanical strength. Half the total GAGs as well as the salt- and acid-soluble fraction of collagen were lost after 24 h of incubation (Schenke-Layland et al., 2003). Decellularization with trypsin caused severe ultrastructural damage and alterations to the ECM (Kasimir et al., 2003), while the flexural behaviour of leaflets was negatively affected because of the disruption of the crimping structure of the collagen fibers (Liao et al., 2008).

Single-step usage of TritonX-100 is more effective in removing cell remnants from thicker tissues such as valve conduits, however, it also increases leaflet extensibility (decreased flexural stiffness), leads to a loose collagen network and the reduction of major GAG content, laminin, fibronectin and collagen (Liao et al., 2008).

Using detergents like SDS or DOA alone to achieve decellularization, Korossis et al., (2002) reported full valve competence under physiological pressure of 120mm mercury (Hg) and physiological leaflet kinematics, while another study reported that the collagen architecture of the ECM was well preserved when using a similar SDS method (Erdbrugger et al., 2006). Disruption of the fiber structure of the ECM was reported by Kasimir et al., (2003), as well as a decrease in flexural stiffness (Liao et al., 2008).

The use of multi-detergents (SDS and TritonX-100) for decellularization resulted in an increase in extensibility and a decrease in stiffness of the leaflets (Naso and Gandaglia, 2018), while TritonX-100 combined with DOA produces good preservation of the ECM structure (Kasimir et al., 2003). The combination of multiple detergents can result in an increased loss of ECM proteins (reduction in GAGs) (Naso and Gandaglia, 2018). Previously, a novel method for decellularization and sterilization of bovine pericardium developed by our research group, combined TritonX-100, DOA and SDS for the decellularization of bovine pericardium. Results indicated that successful decellularization was achieved and the collagen and elastin were not affected. However, the GAG content decreased (Laker, 2018).

2.4.4 Factors affecting successful cell repopulation and valve performance

2.4.4.1 Detergent residues in the decellularized scaffold

The anionic detergent SDS is very frequently used in decellularization protocols. Despite numerous reports of being highly effective in achieving cell-free extracellular matrices, conflicting results were reported on the ability of such scaffolds to repopulate. Porcine aortic valve leaflets decellularized using 0.1 % SDS were completely inhibited to reseeding with human endothelial cells *in vitro* (Rieder et al., 2004). However, pulmonary valve leaflets were reseeded *in vitro* with caprine endothelial cells following decellularization with 0.5 % SDS, and *in vitro* cell adhesion and migration of porcine myofibroblasts occurred on porcine aortic valves treated with 0.1 % SDS (Naso and Gandaglia, 2018).

Effective removal of SDS from xenograft scaffolds after decellularization by numerous washing steps, irrespective of the concentration used, appeared to be extremely difficult. Prolonged washing reduced the presence of SDS in the washing solutions, but it remained present and detectable even if concentrations as low as 0.01 % is used. SDS could still be detected even after intense washing (10 steps of 24 hours each), and complete removal of the detergents from the tissue was never achieved (Cebotari et al., 2010). The presence of residual SDS in the ECM and continuous leakage from the scaffold poses potential cytotoxicity of the scaffolds once implanted, impacting negatively on successful cellular repopulation and growth. SDS, DOA and taurodeoxycholic acid are also known to have a significantly degrading effect on elastin, making it more sensitive to the action of metalloproteinases and degradative enzymes and lowering the tensile strength of the fibers (Naso and Gandaglia, 2018).

2.4.4.2 Cellular debris in decellularized scaffolds

It is widely accepted that the process of decellularization, whatever method is used to decellularize tissue, plays an important role in creating a biologically inert matrix. The ECM, however, still has the potential to attract inflammatory mediators and can induce activation of platelets that can lead to the formation of thrombi and stimulate an inflammation reaction (Kasimir et al., 2005), which is especially evident when using xenografts. Xenograft porcine conduits will initiate the sequential deposition of IgG when coming in contact with human plasma, as well as activation of the classical complement pathway, followed by adhesion and

activation of polymorphonuclear leukocytes (PMNs) leading to an immune response (Bastian et al., 2008). The presence of several antigens in xenograft tissue, and in particular alpha-Gal epitope, is responsible for lifelong stimulation of the immune system with the production of anti-alpha-Gal antibodies in humans (Rieben et al., 2000). Besides the alpha-gal antigen, another 31 proteins were identified in bovine pericardium as putative xenogeneic antigens that are capable of eliciting a T cell-dependent antibody response, as revealed by IgG production. Their involvement in immune responses to xenografts after implantation in humans could have implications for the use of bovine pericardium as a biomaterial in bioprostheses and tissue engineering applications, as well as xenotransplantation in general (Griffiths et al., 2008). When xenogeneic tissue gets recognized, the complement cascade is activated, triggering endothelial cell dysfunction, platelet aggregation and vascular thrombosis. If not efficiently removed by the decellularization process, these antigens may remain present on the membrane remnants that are trapped between the ECM fibers, and still cause immune reactions from the implant recipient (Leventhal et al., 1995).

Similarly, the use of fresh and homovital homografts has been associated with the eventual rejection of the conduit by the recipient due to the viable endothelial cells resulting in pronounced humoral and cellular immune responses (Methe et al., 2007). The donor cells that are present in the cryopreserved homografts may also provoke an immune response from the recipient. Cryopreserved homografts that contain donor cells have been shown to express A and B blood group antigens (Feingold et al., 2009), however, the immunological response to mismatched ABO blood group antigens and homograft longevity is still unclear. ABO mismatching has been shown to not influence long-term graft outcomes (Jashari et al., 2004), while a recent study by Dekens et al., (2019) propose that, especially in younger patients, ABO blood group compatibility between the host and donor could assist in improving homograft durability. When using cryopreserved homografts containing donor cells, human leukocyte antigen (HLA) mismatching is also associated with accelerated homograft failure, especially in children (Baskett et al., 2003).

Furthermore, the cells present in the homograft become apoptotic and necrotic after processing and storage, and the cellular debris leads to calcification and chronic inflammation, which

promotes valve failure (Hopkins et al., 2009). Cellular debris that are not successfully removed after the decellularization of homografts could have similar effects. These donor-reactive immune responses associated with fresh and cryopreserved homografts are considered a major contributor to allograft valve failure (Lisy et al., 2017). Therefore, decellularization must ensure the complete removal of donor cells and cell remnants from the homograft to prevent immune responses from the recipient and subsequent conduit failure. A study by Rieder et al., (2005) described that porcine and human pulmonary scaffolds differ in their residual potential to attract monocytic cells when decellularized. The decellularized porcine pulmonary valve is not a completely non-immunogenic scaffold, whereas the decellularization of the human pulmonary heart valve strongly diminished the migration of monocytes towards the valve tissue. These remaining immunological reactions in the decellularized xenografts and a lack thereof in the decellularized homograft tissue might be a result of the alpha-Gal epitope, showing an important difference between xenografts and homografts (Konakci et al., 2005). Furthermore, the complete removal of all nucleic acid residues is important, as it can potentially initiate the calcification process in implanted scaffolds (Naso and Gandaglia, 2018).

2.4.5 Remodeling and Growth Potential of decellularized homografts

Remodeling of scaffolds involves the creation of a cell-free extracellular matrix, followed by its repopulation by host cells *in vivo* without any signs of calcification, while the haemodynamic properties of the valves should be maintained and there is no need for antithrombotic therapy. *In vivo* animal studies using decellularized scaffolds have provided promising results, where the inner surfaces of implanted valves were covered with endothelial cells, interstitial cells were present, the vessel walls showed some detectable monocytes and immature collagen was demonstrated throughout the heart valve following three months of implantation (Erdbrugger et al., 2006).

Complete recellularization of implanted decellularized valve scaffolds has not yet been achieved, with only the walls being repopulated and only endothelial recellularization of the leaflet surface. Despite the reduction in antigenicity, incomplete recellularization of valve leaflets will ultimately lead to similar valve failure because of the inability for repair and remodeling of the valve matrix (VeDepo et al., 2017). Endothelial cells play an important role in valve haemodynamics and to

provide a non-thrombogenic layer over the valve surface, while interstitial cells are crucial for remodeling of the ECM by ensuring tissue durability and growth characteristics (Liu et al., 2007). Recellularization of the decellularized scaffold with both endothelial and interstitial cells to create a tissue-engineered valve that resembles the native valve remains a challenge.

Native valves will physiologically increase in annular size as the individual grows in size. The ideal implanted heart valve or scaffold should have similar growth potential as that of transplanted autologous valves, to allow paediatric patients an extended period free of reoperation. An increase in valve annulus diameter without central regurgitation in implanted valves would indicate growth of the implant in the growing recipient, whereas only stretching of the valve would be evident by a decreasing coaptation area and eventually central leaking of the valve, as revealed by echocardiography (Erdbrugger et al., 2006).

Several animal studies have suggested an increase in valve annulus diameter of implanted decellularized homografts compared to cryopreserved homografts or bovine jugular vein grafts (Dohmen et al., 2006; Navarro et al., 2010), but it has not yet been proven in humans. Although the research group in Hanover, Germany has reported that decellularized fresh allogeneic valves did show the ability to adaptive growth when compared to conventional cryopreserved allografts and glutaraldehyde-fixed bovine jugular vein valves, only the improved freedom from explantation were statistically significant, with comparable incidence of stenosis and regurgitation (Boethig et al., 2019). Da Costa and colleagues also reported comparable excellent clinical and haemodynamic results for cryopreserved and decellularized pulmonary and aortic homografts used for RVOT reconstruction in Ross procedures (da Costa et al., 2018; Etnel et al., 2018), and low incidence of structural valve deterioration and conduit failure in RVOT reconstruction of other congenital abnormalities (da Costa et al., 2017) in young children, but no real growth of the valve annulus was ever observed.

2.4.6 Stabilization of Tissues or Scaffolds

Bioprosthetic heart valves are crosslinked with GA to reduce tissue antigenicity and prevent tissue degradation. GA form stable crosslinks with collagen through a Schiff base reaction of the

aldehyde with an amine group of the hydroxylysine/lysine in collagen (Figure 2.5) (Shah and Vyavahare, 2008).

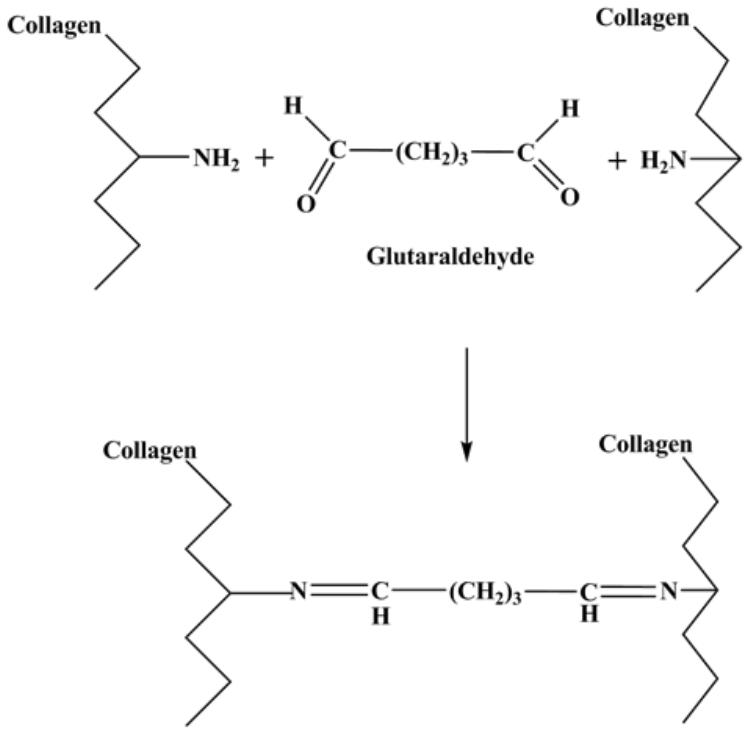

Figure 2.5: Cross-linking of collagen with glutaraldehyde. (Adapted from Jorge-Herrero et al., (2005)).

A disadvantage of GA-fixation is the incomplete stabilization of GAGs (Lovekamp et al., 2006). Similarly to commercially available bioprosthetic valves that are treated with a cross-linking agent/s prior to storage and implantation, decellularized scaffolds can be treated with GA or other cross-linkers before implantation. GA-fixation serves to stabilize the collagen matrix and decrease antigenicity, inhibits autolysis, gives a prolonged shelf-life and allows surgeons to have products of various sizes readily available (Jana et al., 2014). GA-fixation also maintains thromboresistance and antimicrobial sterility, however, results in reduced cellular compatibility because of its toxicity, a reduction in the proliferative capacity of cells following repopulation (Mendoza-Novelo and Cauich-Rodriguez, 2011), and enhanced degradation and calcification of the tissue/scaffold (Jorge-Herrero et al., 2010). Cross-linking of artificial scaffolds also results in a lower porosity and smaller pore size, and a stiffer ECM in biological scaffolds, which has to be countered with additional acidic treatments to allow increased proliferation and migration of cells into the deeper layers (Jana et al., 2014). The free aldehyde groups of GA are associated

with cellular toxicity (Oryan et al., 2018), while conjugated GA may contribute to graft calcification (Lee et al., 2017; Padala, 2018). Washing and detoxifying with solutions that can bind the free aldehyde groups prior to implantation can improve durability and biocompatibility (Strange et al., 2015). Treating the GA-fixated biological tissue with a high concentration liquid polyol like propylene glycol (PG) or glycerol (EnCap technology) mitigates the calcification of the tissue (Seifter and Frater, 1995).

2.5 Clinical experience with decellularized homografts

Due to the shortage of human valves worldwide, using xenografts would be advantageous. However, the use of decellularized xenograft scaffolds in the clinical setting has been far less successful. In paediatric patients, early failure of tissue-engineered porcine heart valve SYNERGRAFTS has prompted the discontinuation of their implantation. These implants elicited a strong inflammatory response, and structural failure or rapid degeneration of the graft occurred within one year of implantation. Furthermore, there were indications of manufacturing problems as indicated by the presence of calcific deposits before implantation and incomplete decellularization (Simon et al., 2003). Decellularized human allografts have proven to be more successful in the clinical application, but some researchers report that there is no clear benefit when compared to cryopreserved valves (VeDepo et al., 2017).

The use of CryoValve® SG (CryoLife, Inc, Kennesaw, GA, USA) decellularized pulmonary human heart valves for RVOT reconstruction compares favourably with cryopreserved homografts (Burch et al., 2010). A retrospective, nonrandomized, multi-centre cohort analysis involving seven implanting institutions in the US compared the use of CryoValve® SG to conventional cryopreserved homografts for patients undergoing Ross procedures and RVOT reconstruction (mean follow-up four years). Acceptable clinical outcomes that compared favourably with conventionally treated homografts were reported; however, better haemodynamic function was observed in CryoValve® SG group (possibly due to decreased antigenicity of these valves) which could improve long-term outcomes (Brown et al., 2010). Also, in patients aged younger than one year, freedom from conduit dysfunction was significantly higher when receiving CryoValve® SG valves compared to standard cryopreserved pulmonary homografts (Bibevski et al., 2017).

Since 2005, a European group led by Haverich has implanted 131 decellularized pulmonary homografts with 100 % freedom from explantation at ten years follow-up, compared to 84.2 % freedom from explantation for cryopreserved homografts and 84.3 % freedom from explantation for GA-fixed bovine jugular vein conduits. Despite a statistically significant improvement in freedom from explantation and a freedom from reintervention rate of 98.3% for decellularized pulmonary homografts, no significant differences in stenosis or regurgitation between cryopreserved and decellularized homografts could be demonstrated (Boethig et al., 2019). Although the reported rate of freedom from infective endocarditis in patients receiving decellularized homografts was 100% (Sarikouch et al., 2016), it has to be emphasized that patients with active infective endocarditis were excluded from receiving decellularized allografts. This could have a major effect on the incidence of reoperations reported in the decellularized homograft group when compared to the cryopreserved homografts and bovine jugular vein groups. The decellularized homografts used by this group provided low gradients in follow-up and exhibited adaptive growth (Cebotari et al., 2011), but there is still no clear evidence of annular growth in the decellularized homografts, and definitive conclusions will require follow-up periods of longer than the current 10 years (Boethig et al., 2019).

In a medium-term follow-up study of decellularized homografts implanted in children below 12 years of age, da Costa and co-workers reported a 90.9% freedom from conduit reintervention at 8 years, actuarial freedom from structural valve deterioration of 64.9% and no incidence of bacterial endocarditis. Some decellularized aortic allografts presented with spotty calcification in the walls, but no or minimal calcific deposits were observed in decellularized pulmonary allografts when compared to cryopreserved homografts (da Costa et al., 2017). In a later propensity-matched study by the same group, they found comparable results regarding actuarial freedom from allograft dysfunction, freedom from allograft reintervention, survival, and event-free survival using cryopreserved and decellularized pulmonary allografts used in RVOT reconstructions in Ross procedures. The decellularization process using 0.1% SDS appears to be beneficial to allograft function from an immunologic standpoint, but may also be associated with detrimental effects such as reduction of beneficial inflammation and impairment of structural integrity, and longer follow-up than 5-8 years will be required (da Costa et al., 2018; Etnel et al., 2018).

Currently, pulmonary autografts are the substitute of choice for aortic valve replacement, especially in paediatric patients and young adults. A group led by da Costa performed the first of its kind procedure by using decellularized aortic homograft replacements. Although early hospital mortality was 7 %, results were encouraging with a reported 100 % freedom from reoperation of the graft at three years (da Costa et al., 2010).

2.6 Study rationale

Acquired and congenital heart valve disease requires surgical replacement or repair of heart valves. Currently, cryopreserved homografts and GA-fixed xenografts are routinely used in valve replacement surgery. The limited availability of cryopreserved homografts can be addressed by extending the post-mortem harvesting time for homografts past 24 h prior to cryopreservation or through the use of GA-fixed xenografts. Cryopreservation alters the ECM of homografts and is associated with calcification of these valves leading to early valve degeneration, especially in paediatric patients. GA-fixation of xenografts aims to mitigate the immunological response from the recipient, however, these immune reactions are not completely diminished and GA promotes calcification and degeneration of valves. Studies on the effect of GA-fixation on homografts are lacking. Decellularization of homografts (and xenografts) provides an alternative processing method for heart valves.

Decellularization of homograft valves can contribute towards lowering the antigenicity associated with host cells and therefore enhance the durability of these valves. However, decellularization of biological tissues can induce some alterations in the mechanical properties and structural composition of the extracellular matrix, associated either with the denaturation of the collagen triple helix or to the loss of macromolecular substances such as glycoproteins and GAGs. Single-step detergent or enzymatic-based decellularization protocols can affect the flexural behaviour of valve leaflets because of the disruption of the crimp structure of collagen. Several decellularization techniques can be combined to complement one another to retain the desired characteristics of the decellularized tissue. Decellularized pulmonary homografts have successfully been used for RVOT reconstruction.

The decellularization of xenografts offers an alternative method as opposed to GA-fixation for lowering the immunological reactions from recipients. However, initial studies with decellularized xenografts showed that valve degeneration occurred. Based on these findings it is necessary to investigate additional fixation of decellularized grafts, especially in a homograft setting. Additional cross-linking of the connective tissue as stabilization can be included in the tissue engineering protocol. Several techniques and chemicals have been proposed by researchers, of which GA has been most widely studied and used. Despite being highly effective in creating additional cross-links, the presence of residual free aldehyde groups remaining in the tissue has been associated with degeneration and calcification of bioprostheses. These free aldehyde groups can be detoxified using PG and propylene oxide following GA tanning of biological tissue (EnCap technology).

The current study was undertaken to investigate the effect of using our proprietary multi-detergent and enzyme-based decellularization technique compared to cryopreservation on the structural integrity and clinical performance of pulmonary homografts, with a post-mortem ischaemic harvesting time of 48 h, in the RVOT of a juvenile ovine model. Additionally, the effect of GA-fixation and detoxification on the decellularized homograft (using EnCap technology) was also investigated.

The aims and objectives of the study are given in chapter 1. The study was divided into three parts:

1. Comparison of the impact of cryopreservation, decellularization and decellularization, glutaraldehyde-fixation and detoxification as processing techniques on the strength and structure of juvenile ovine pulmonary homografts.
2. Comparison of function and structural integrity of cryopreserved pulmonary homografts versus decellularized pulmonary homografts after 180 days implantation in the juvenile ovine model.
3. Comparison of function and structural integrity of decellularized pulmonary homografts versus decellularized, glutaraldehyde-fixed and detoxified pulmonary homografts after 180 days implantation in the juvenile ovine model.

Chapter 3 - Manuscript 1

Comparison of the impact of cryopreservation, decellularization and decellularization, glutaraldehyde-fixation and detoxification as processing techniques on the strength and structure of juvenile ovine pulmonary homografts

[1]van den Heever JJ, [1]Jordaan CJ, [1]Lewies A, [4]Goedhals J, [1]Bester D, [2]Botes L, [1&3]Dohmen PM, [1]Smit FE

Author(s)

1) **Johannes Jacobus van den Heever (corresponding author), Christiaan Johannes Jordaan, Angélique Lewies, Dreyer Bester, Pascal Maria Dohmen, Francis Edwin Smit**
   Department of Cardiothoracic Surgery,
   Faculty of Health Sciences,
   University of the Free State (UFS)
   P.O. Box 339, (Internal Box G32)
   Bloemfontein
   9300
   South Africa
   Tel: +27 51 4053435
   E-mail: vdheeverjj@ufs.ac.za

2) **Lezelle Botes**
   Department of Health Sciences
   Central University of Technology, Free State (CUT)
   Private Bag X20539
   Bloemfontein
   9300
   South Africa

3) **Pascal Maria Dohmen**
   Department of Cardiac Surgery
   Heart Centre Rostock
   University of Rostock
   Rostock
   18107
   Germany

4) **Goedhals J**
   Department of Anatomical Pathology
   Faculty of Health Sciences,
   University of the Free State (UFS)
   P.O. Box 339, (Internal Box G32)
   Bloemfontein
   9300
   South Africa

ABSTRACT

Introduction: Increasing the post-mortem ischaemic harvesting time of pulmonary homografts to 48 h can increase the potential donor pool. Cryopreservation is routinely used for the preservation of these homografts, however, immunogenicity might arise from the presence of donor cells and cellular remnants in the homograft. Decellularization techniques might reduce immunogenicity, but might compromise the strength of the tissue. Additional fixation of decellularized homografts might be necessary to increase homograft durability and strength. This study aimed to evaluate the impact of cryopreservation, decellularization, and decellularization, glutaraldehyde (GA)-fixation and detoxification as processing methods on the strength and structure of juvenile ovine pulmonary homografts.

Method: Pulmonary homografts from juvenile Dorper sheep were subjected to a post-mortem cold ischaemic harvesting time of 48 h, and then either cryopreserved (n = 5), decellularized (n = 5) using a multi-detergent and enzymatic protocol or decellularized, GA-fixed and detoxified with EnCap technology (n = 5). Valve leaflet and wall tissue were evaluated on histological (DAPI, H&E, von Kossa, Modified von Gieson) appearance, scanning (SEM) and transmission (TEM) electron microscopy and mechanical properties [tensile strength (TS) and Young's modulus (YM)].

Results: Sheep homografts were successfully decellularized, as confirmed with DAPI stain, nanodrop readings of below 50 ng/mg and gel electrophoresis with fragmented DNA bands < 200 bp. Histology and TEM demonstrated large interfibrillar spaces in the extracellular matrix of leaflets and walls of decellularized homografts, in contrast with a collapsed collagen network in the cryopreserved group and a compacted and dense collagen network in decellularized plus EnCap treated group. Collagen in the cryopreserved group also appeared disrupted and fractured on TEM, but more uniform in the decellularized and decellularized plus EnCap treated groups. Endothelial coverage was still present in cryopreserved homografts after 48 h ischaemia and absent in the other two groups. Cells and cellular remnants were present in the interstitial layer of the cryopreserved group, but valves in the decellularized and decellularized plus EnCap treated groups were completely acellular on H&E and TEM. Decellularization did not reduce the TS and YM of the leaflet and wall tissue compared to cryopreservation.

Conclusion: Cryopreservation causes collagen breakage and disruption, which can lead to early valve degeneration. The multi-detergent and enzymatic decellularization protocol is effective for the complete decellularization of sheep pulmonary homografts, while maintaining a well-organized collagen matrix and tissue strength and stiffness even without additional GA-fixation. GA-fixation makes the collagen network extremely dense and compacted.

Keywords:

Homografts, ischaemic harvesting, decellularization, cryopreservation, glutaraldehyde-fixation

INTRODUCTION

End-stage heart valve disease mandates the repair or replacement of a patient's diseased heart valve/s with either mechanical or biological valve prostheses. Mechanical prostheses demonstrate superior durability and longevity in patients, however, recipients require lifelong anticoagulation therapy. Bioprosthetic valves, on the other hand, do not require continuous anticoagulation therapy, but has limited durability and requires more frequent reoperation (Diaz et al., 2019). Bioprostheses include glutaraldehyde (GA)-fixed porcine valves or bovine pericardium mounted onto a frame, free xenograft valves or donor homograft valves. Currently, cryopreserved pulmonary homografts remain the valve of choice for replacement of the native pulmonary valve in the Ross procedure (Hechadi et al., 2013), as well as for reconstruction of the right ventricle outflow tract (RVOT) in children with congenital abnormalities (Romeo et al., 2018). Unfortunately, early degeneration of these homografts occur in younger patients (Selamet Tierney et al., 2005) and there is a lack of availability, especially for smaller sized conduits suitable for neonates (Goffin et al., 2000).

Ross, (1965) and Barratt-Boyes et al., (1965) were the first to describe the successful use of “fresh” or homovital homografts in the aortic position and pulmonary homografts for RVOT reconstruction, with acceptable homograft performance. The superior performance and increased long-term durability of cryopreserved allografts with maintained cellular viability, compared to valves stored at 4^{o}C (Angell et al., 1989; O'Brien et al., 1991; O'Brien et al., 1995), unfortunately, led to an internationally accepted guideline that homografts from either beating heart or non-beating heart donors should be harvested and processed within 24 h after death to

retain maximum cell viability. These findings not only restricted the available post-mortem donor pool significantly, but the presence of cellular remnants in the extracellular matrix (ECM) evokes immunological reactions from the recipient, causing tissue degeneration and graft failure (Lopes et al., 2009). However, in contrast, Mitchell et al., (1998) reported the early death and loss of endothelial and interstitial cells in cryopreserved homografts following implantation, arguing that valve durability primarily relies on the retention of structural integrity and preservation of the extracellular matrix instead of cell viability.

Various efforts have been made to address the shortages in homograft availability, and our research group has proven that the post-mortem ischaemic time can be extended safely to around 48 h without affecting valve performance (Smit et al., 2015). Cryopreservation is currently the most frequently used and probably the best method for long-term storage of homografts (Kitagawa et al., 2001). Cryopreservation of homografts does, however, damage the collagen scaffold, irrespective of ischaemic harvesting time (Bester et al., 2018). The effect of cryopreservation on the collagen scaffold might be of greater importance in determining the long-term survival of the homograft, than the impact of extending the post-mortem ischaemic time prior to harvesting. The presence of donor cell antigens in cryopreserved homografts is also associated with adverse immunological response from the recipient, resulting in valve calcification and degeneration (Shaddy and Hawkins, 2002; Baskett et al., 2003; Ryan et al., 2006).

Decellularization processes can remove interstitial and endothelial cellular components from a homograft valve. This process can potentially lead to the creation of a valve with significantly reduced immunogenicity, potential viability and biological activity once implanted, and reduced calcification (Cebotari et al., 2011). CryoValve® SG (CryoLife, Inc, Kennesaw, GA, USA) pulmonary human heart valves were some of the first decellularized homografts to be used clinically for RVOT reconstruction and results compare favourably with cryopreserved homografts (Burch et al., 2010), however, improved haemodynamics was observed in the CryoValve® SG group, possibly due to decreased antigenicity of these valves after four years of implantation (Brown et al., 2010). A European group led by Haverich has implanted 131 decellularized pulmonary homografts since 2005. A ten-year follow-up study found that

decellularized homografts had a 100 % freedom from explantation at ten years follow-up, compared to 84.2 % freedom from explantation for cryopreserved homografts and 84.3 % freedom from explantation for GA-fixed bovine jugular vein conduits. Also, the rate of freedom of infective endocarditis was 100 % in patients receiving decellularized homografts (Sarikouch et al., 2016). Although the decellularized homografts used by this group provided low gradients in follow-up and exhibited adaptive growth (Cebotari et al., 2011), a careful observation of their latest data shows no statistical difference in terms of stenosis and regurgitation when compared to the conventional cryopreserved homografts (Boethig et al., 2019). An early and midterm study by a group led by da Costa reported that decellularized aortic allografts replacements, the first of its kind, had 100 % freedom from reoperation of the graft at three years follow-up. The decellularized aortic valves retained structural integrity, low calcification rates and adequate haemodynamics (da Costa et al., 2010).

Concerns have been raised on maintaining the strength of the conduit once the cellular components are removed (Erdbrugger et al., 2006). Furthermore, using multi-detergent enzyme-based decellularization methods might also decrease flexural stiffness and disrupt the ECM structure (VeDepo et al., 2017), and reduce the glycosaminoglycan (GAG) content (Bourgine et al., 2013) which fills most of the extracellular space and provide mechanical support to the tissue (Korossis et al., 2002). Therefore, the additional fixation and stabilization of the collagen scaffold with GA might be required (Sheehy et al., 2018). Due to the shortages experienced in the supply of cryopreserved homografts for RVOT reconstruction, especially in smaller sizes for young children, valved bovine jugular vein grafts (Contegra^{TM}, Medtronic Inc., Minneapolis, Minnesota, USA) have been introduced as an alternative conduit for the reconstruction of the RVOT. Despite being fixed and stored in GA, these grafts are routinely used with acceptable clinical outcomes (Breymann et al., 2004; Falchetti et al., 2019). However, the free aldehyde groups of GA are associated with cellular toxicity (Oryan et al., 2018), while conjugated GA may contribute to graft calcification (Lee et al., 2017; Padala, 2018). Washing and detoxifying with solutions that can bind the free aldehyde groups prior to implantation can improve durability and biocompatibility (Strange et al., 2015). EnCap technology describes the fixation of biological tissue with GA and the subsequent treatment of the GA-fixated tissue with a high concentration liquid polyol like propylene glycol (PG) or glycerol. The PG binds to the free

aldehyde group of the GA, blocking the free aldehyde group as a potential binding site for calcium and other minerals and thereby mitigating the calcification of the tissue (Seifter and Frater, 1995). In one study evaluating the performance of commercially stent-mounted GA-preserved aortic homografts (not decellularized), it was concluded that better long-term performance of the homograft tissue compared to GA-fixed heterologous biological valves could be expected (Succi et al., 1986), but other studies using GA-fixed decellularized homograft valves are lacking.

The aim of this study was to compare the morphology and mechanical properties of standard cryopreserved pulmonary homografts to decellularized pulmonary homografts and decellularized pulmonary homografts treated with EnCap technology, evaluating the impact of the processing method on ovine homografts harvested after 48 hours cold ischaemia. Our proprietary decellularization protocol with proven synergy was used (Laker et al., 2020).

MATERIALS AND METHODS

Study design

Pulmonary homografts harvested from juvenile Dorper sheep (n = 15), with a post-mortem cold ischaemic harvesting time of 48 h, were divided into three groups: Group 1, cryopreserved (n = 5), Group 2, decellularized (n = 5) and Group 3, decellularized plus EnCap treated (n = 5). Structural integrity and strength of leaflet and wall tissue after processing were evaluated and compared. Strength analysis included tensile strength (TS) and Young's modulus (YM), and morphological evaluation included DAPI staining to confirm decellularization, H&E, von Kossa staining, modified von Gieson staining, scanning electron microscopy (SEM) and transmission electron microscopy (TEM). A schematic representation of the study design is given in Figure 1. The interfaculty Animal Ethics Committee of the University of the Free State (UFS-AED2016/0101) approved the study.

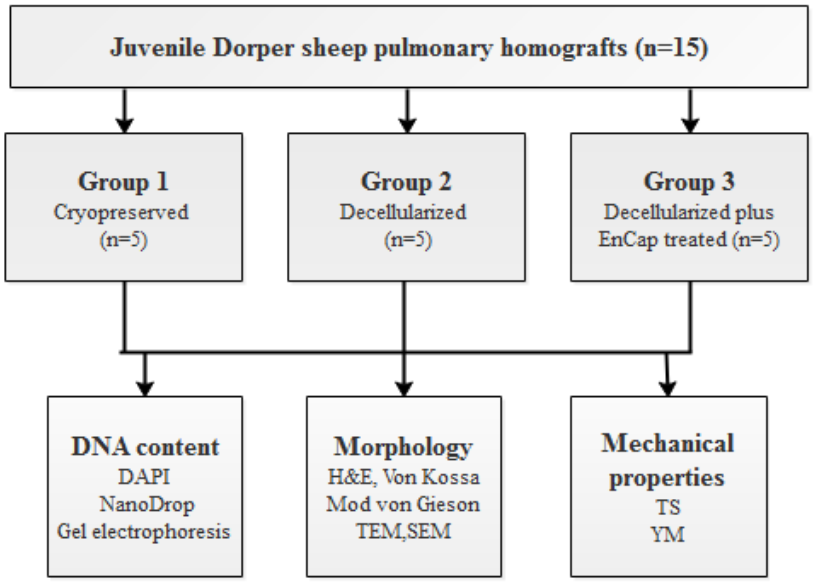

Figure 1: Schematic diagram of the study design.

Preparation of homografts

Heart-lung blocks (n = 15) from freshly slaughtered juvenile Dorper sheep with a bodyweight of 24-30 kg were collected from a local abattoir and subjected to 48 h ischaemia at 4^{o}C before dissection and processing as previously described by Bester et al., (2018). Pulmonary homografts (n = 15) were harvested and washed in copious amounts of cold 4^{o}C Ringers lactate solution (Fresenius Kabi / Intramed, Midrand, SA). Thereafter all homografts were sterilized overnight at 4^{o}C in 100 ml Medium199 (Whitehead Scientific, Johannesburg, SA) and an antibiotic cocktail consisting of 2.5 mg Amphotericin B (Bristol-Myers Squibb, Bedfordview, SA), 50 mg Piperacillin (Brimpharm SA (Pty) Ltd, Cape Town, SA), 50 mg Vancomycin (Gulf Drug Company, Mount Edgecombe, SA) and 25 mg Amikacin sulphate (Bodene (Pty) Ltd, trading as Intramed, Port Elizabeth, SA). Valves in Group 1 (n = 5) were cryopreserved the next day in 100ml M199 + 11ml DMSO (Highveld Biological, Johannesburg, SA) in a Cryoson controlled rate freezer (Consarctic, Schöllkrippen, Germany) at a rate of -1^{o}C/min to -140^{o}C and stored in the vapour phase of liquid nitrogen (LN_2) until evaluation.

Decellularized homografts (Group 2, n = 5) were prepared according to our proprietary protocol (Bester et al., 2017; Laker et al., 2020). Briefly, homografts were subjected to osmotic shock in two changes of hypertonic 5% NaCl-solution and distilled water, repeated changes in a multi-

detergent solution [0,5% SDS (Sigma-Aldrich, Johannesburg, SA), 1% Deoxycholic acid (Sigma-Aldrich, Johannesburg, SA), 1% Triton-X100 (Sigma-Aldrich, Johannesburg, SA)] in PBS, and followed by numerous washings in PBS and half strength antibiotic cocktail as used for sterilization of cryopreserved valves, under constant shaking. These steps were followed by enzymatic treatment with descending concentrations of Benzonase (Thermo Fisher Scientific, Johannesburg, SA) (Dijkman et al., 2012), repeated washing in PBS, delipidation in 70% ethanol and final storage in PBS with antibiotics.

Additionally, decellularized homografts (Group 3, n = 5) were treated with EnCap technology and stored in propylene oxide (Sigma-Aldrich, Johannesburg, SA) (Seifter and Frater, 1995). EnCap technology includes GA-tanning of the collagen scaffold, binding of a polyol namely propylene glycol (Sigma-Aldrich, Johannesburg, SA) to the free aldehyde groups to lower toxicity, reducing the host inflammatory response and mitigate calcification.

All homografts were confirmed to be culture-negative. To confirm the effective decellularization of the homografts in Groups 2 and 3, DNA quantification was done with DAPI staining, gel electrophoresis and nanodrop counts by the Cardiovascular Research Unit, UCT Medical School (Crapo et al., 2011).

Evaluation of processed homografts

Histological analysis

Leaflet and wall tissue samples were collected in 4 % buffered Formalin, embedded in paraffin wax, sectioned and stained according to standard H&E, von Kossa and modified von Gieson staining protocols for histological evaluation (Mepham, 1991).

Pulmonary leaflet and wall tissue samples for scanning and transmission electron microscopy were collected in 3 % GA and processed according to standard protocols for SEM and TEM evaluations (Spurr, 1969). Tissue specimens for SEM were dried using the critical point method (Tousimis critical point dryer, Rockville, Maryland, USA, ethanol dehydration, carbon dioxide drying gas) and sputter-coated with gold (BIO-RAD, Microscience Division Coating System, London, UK; Au/Ar sputter coating @ 50-60 nm). A Shimadzu SSX 550 scanning electron

microscope (Kyoto, Japan, with integral imaging (SDF, TIF and JPG format)) was used to examine and photograph the tissue surface.

Leaflet and wall samples for TEM were fixed in 3 % GA overnight, post fixated in Palade's osmium tetroxide, and dehydrated in a graded acetone series. Dehydrated samples were impregnated/embedded in an epoxy (Spurr, 1969) to facilitate the creation of ultra-thin sections for the TEM evaluation. Ultra-thin sections were cut from the sample imbedded in the epoxy using a Leica ultra-microtome (Leica Ultracut UC7, Vienna, Austria). After sectioning, the samples were stained with uranyl acetate and lead citrate. Sections of the leaflet samples were evaluated by using a Philips (FEI, Netherlands) CM100 transmission electron microscope and photographed using an Olympus Soft Imaging System Megaview III digital camera, with Soft Imaging System digital image analysis and documentation software (Olympus, Tokyo, Japan).

Mechanical properties

Mechanical properties of pulmonary valve leaflet and wall samples were examined using a tensile strength testing apparatus (Lloyds LS100 Plus, IMP, Johannesburg, South Africa), according to the method described by Thubrikar et al., (1983). Tissue samples measured 5 x 10 mm, with leaflets and pulmonary sinus wall samples cut in the circumferential direction. The tissue sample was fixed between clamps at both ends and gradually stretched (0.1 mm/s) by applying constant tension on the two ends, and the data recorded on a personal computer.

Statistical analysis

All values are expressed as median values with corresponding InterQuartile ranges. Statistical analyses were performed using GraphPad Prism version 8.3.1 (GraphPad Software, La Jolla, CA, USA, www.graphpad.com). The overall difference between the groups was assessed using a Kruskal-Wallis (KW) test. Significance was set as $p < 0.05$.

RESULTS

Successful decellularization of both the valve leaflets and pulmonary artery wall tissue in the decellularized (Fig.2C,D) and decellularized plus EnCap treated (Fig.2E,F) groups was achieved and confirmed with DAPI staining.

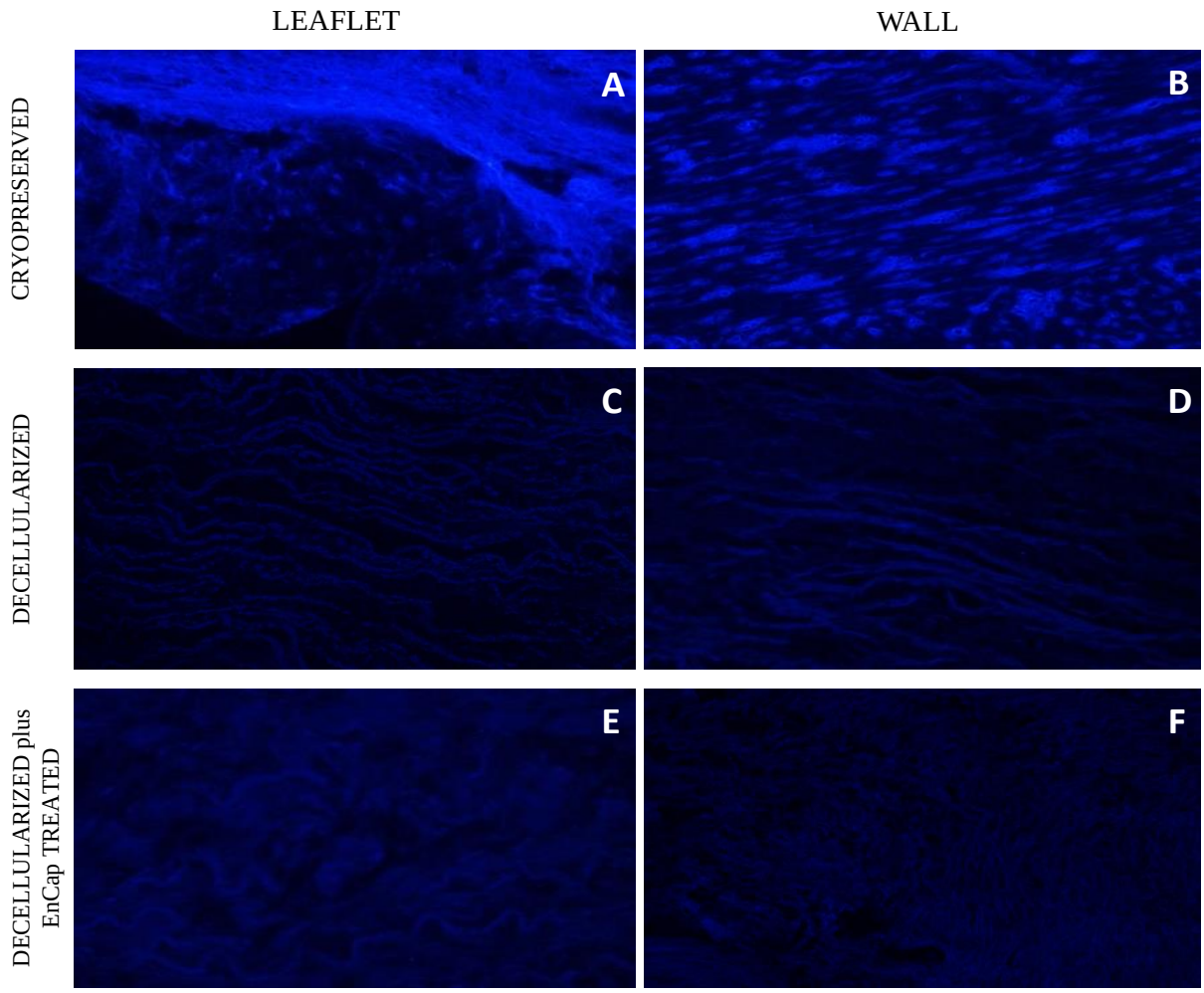

Figure 2: Representative images of DAPI stained sections of cryopreserved (n = 5) **(A,B)**, decellularized (n = 5) **(C,D)** and decellularized plus EnCap treated (n = 5) **(E,F)** leaflet and wall tissue, demonstrating the absence of nuclei and cellular material in the decellularized groups.

Gel electrophoresis (fragmented DNA bands < 200 bp) and nanodrop readings of below 50 ng/mg for the same tissue samples was used to confirm and support the successful decellularization. Nanodrop readings for fresh homograft tissue prior to decellularization was 204.8 ng/mg [200.8-212], and following decellularization no DNA was detectable via Nanodrop. The absence of DNA following decellularization of homograft tissue was also confirmed with gel electrophoresis (Fig.3).

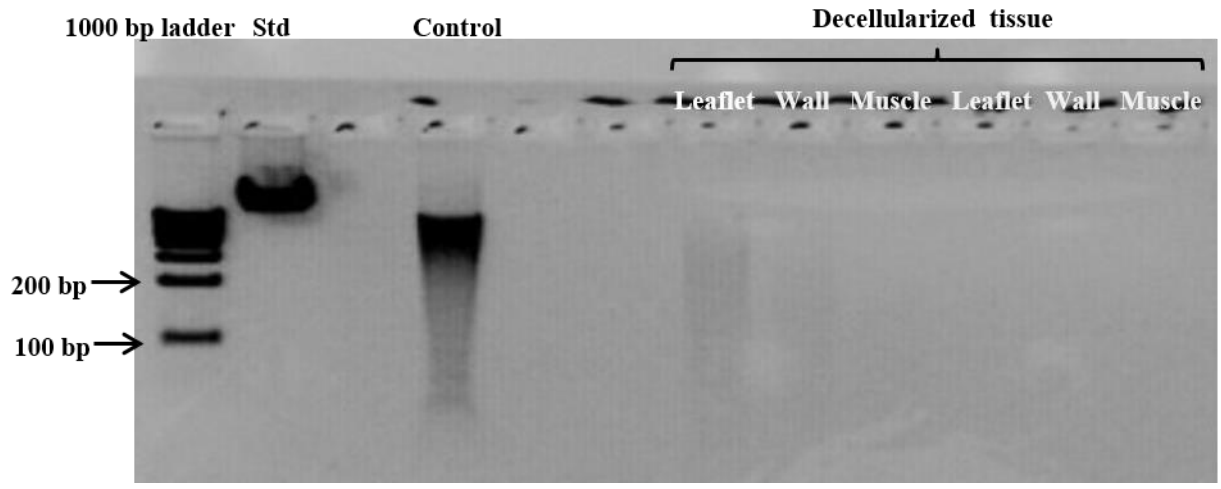

Figure 3: Representative gel electrophoresis image demonstrating the absence of DNA material in leaflet, wall and muscle tissue of homografts after decellularization. [Standard (Std) = Lamba DNA; Control = Fresh homograft tissue].

H&E staining of leaflet samples from cryopreserved homografts after 48 h of ischaemia demonstrated the presence of an endothelial layer and uniform distribution of donor interstitial cells in the extracellular matrix (Fig.4A). Leaflets of valves in the decellularized and decellularized plus EnCap treated groups demonstrated well-preserved collagen matrices without any endothelial or interstitial cells (Fig.4D,G). No calcific deposits were visible in any of the samples on von Kossa staining (Fig.4B,E,H), while large amounts of elastin fibers (black arrows) are clearly demonstrated in the ventricularis region of the leaflets in all three groups on modified von Gieson staining (Fig.4C,F,I). The collagen in the cryopreserved group appeared more collapsed compared to fresh untreated tissue (Bester et al., 2018), more loosely arranged in the decellularized group and more compact and dense in the decellularized plus EnCap treated group.

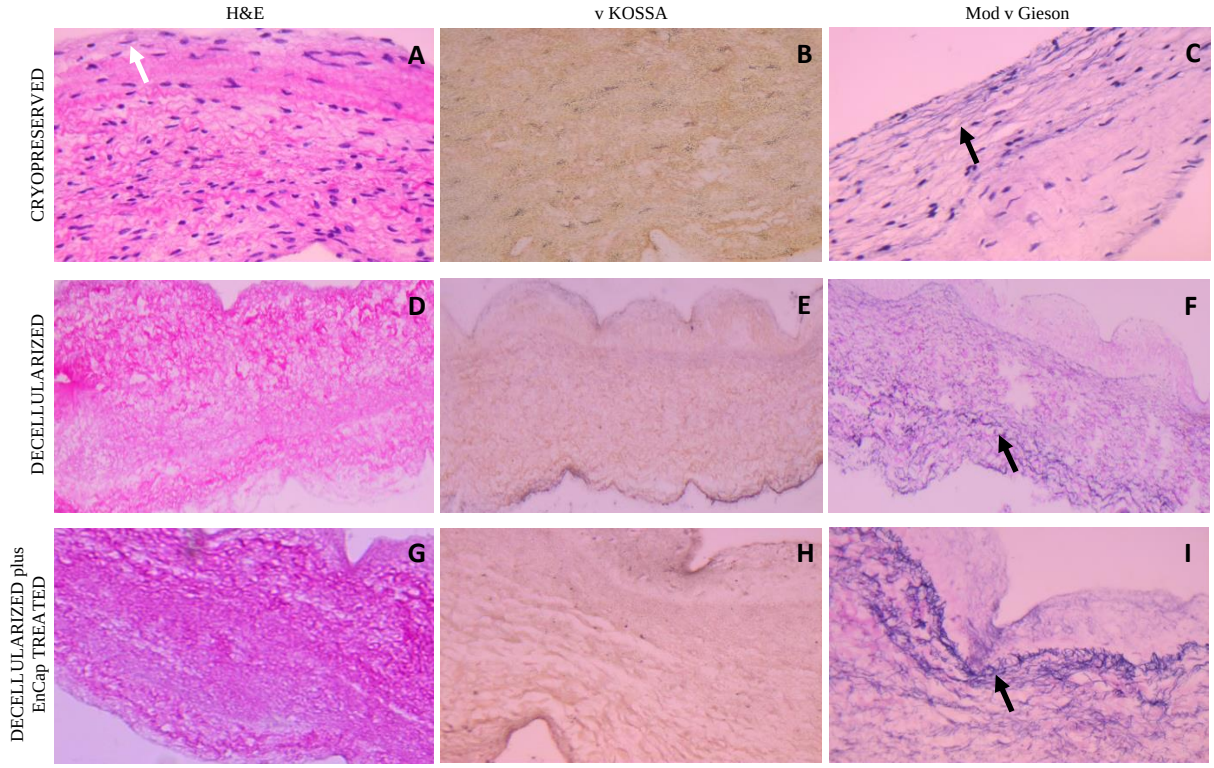

Figure 4: H&E stain of the leaflet samples after 48 h ischaemia demonstrate the presence of endothelial and interstitial cells in the cryopreserved group (n = 5) **(A)**, complete removal of cells in the decellularized group (n = 5) **(D)** and decellularized plus EnCap treated group (n = 5) **(G)**, with well-preserved collagen scaffolds. von Kossa staining showed no calcific deposits in any of the samples **(B,E,H)**, while modified von Gieson stain demonstrated large amounts of elastin fibers (black arrows) in the ventricularis region in all three groups **(C,F,I)**. Collagen in the cryopreserved group appears collapsed, loosely arranged in the decellularized group and dense and compact in the decellularized plus EnCap treated group.

Similar results were demonstrated for the wall tissue as for the leaflets, with an endothelial cell layer (white arrow) and uniform donor interstitial cell distribution in the cryopreserved group (Fig.5A), and no cells present in the decellularized scaffold or decellularized plus EnCap treated group (Fig.5D,G) on H&E staining. No calcific deposits could be demonstrated with von Kossa staining in any of the three groups (Fig.5B,E,H), and dense distribution of elastin fibers (black arrows) were demonstrated in all three groups on Modified von Gieson staining (Fig.5C,F,I). Collagen in the walls of the cryopreserved group is again collapsed, loosely arranged in the decellularized group and dense and compacted in the decellularized plus EnCap treated group.

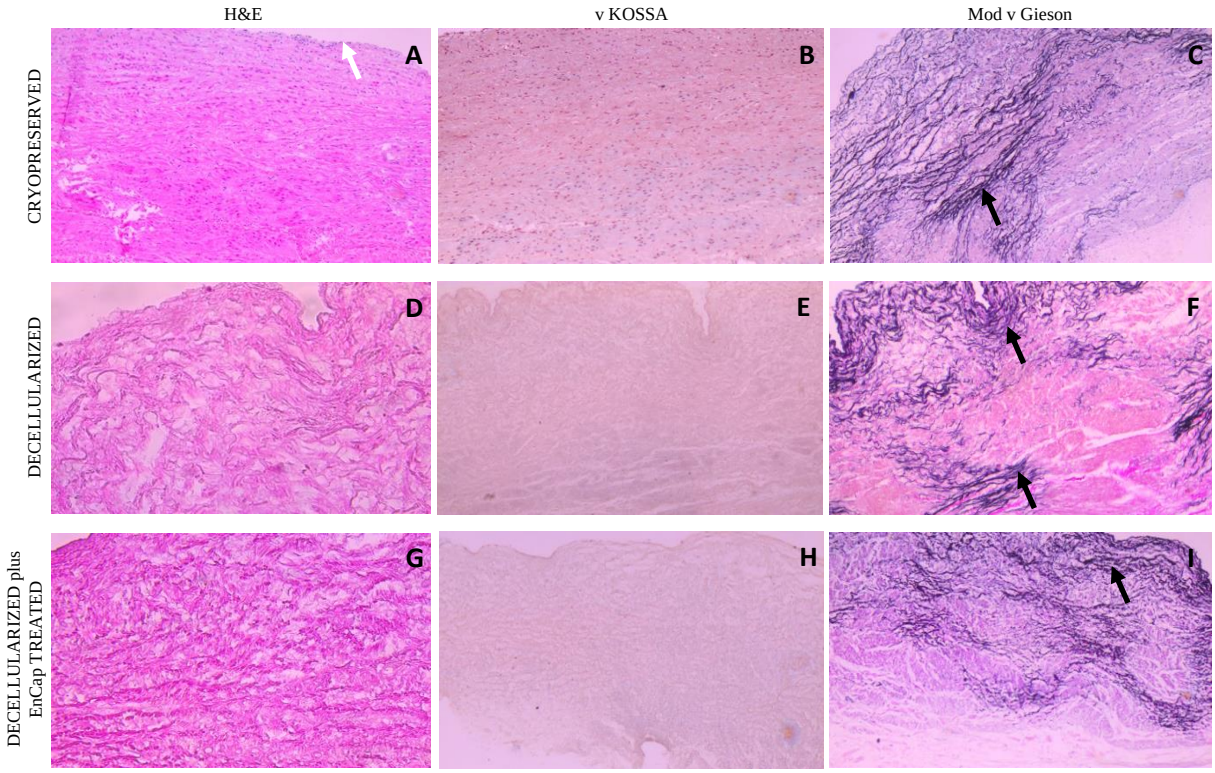

Figure 5: H&E of wall tissue with an endothelial cell layer (white arrow) and uniform distribution of interstitial cells in the cryopreserved group (n = 5) **(A)** and no cells present in the decellularized group (n = 5) (**D)** and decellularized plus EnCap treated group (n = 5) **(G)**. No calcific deposits were demonstrated on von Kossa stain in any of the three groups **(B,E,H)**, and normally distributed elastin fibers (black arrows) were present on Modified von Gieson stain in all three groups **(C,F,I)**. Collagen in the cryopreserved group appears collapsed, loosely arranged in the decellularized group and dense and compact in the decellularized plus EnCap treated group.

SEM demonstrated cell dehiscence, but uniform coverage of leaflets and wall tissue with endothelial cells in the cryopreserved group (Fig.6A,B). Leaflets and walls in both the decellularized (Fig.6C,D) and decellularized plus EnCap treated groups (Fig.6E,F) demonstrated exposed collagen networks without any endothelial cells and only basal membrane remnants (white arrows).

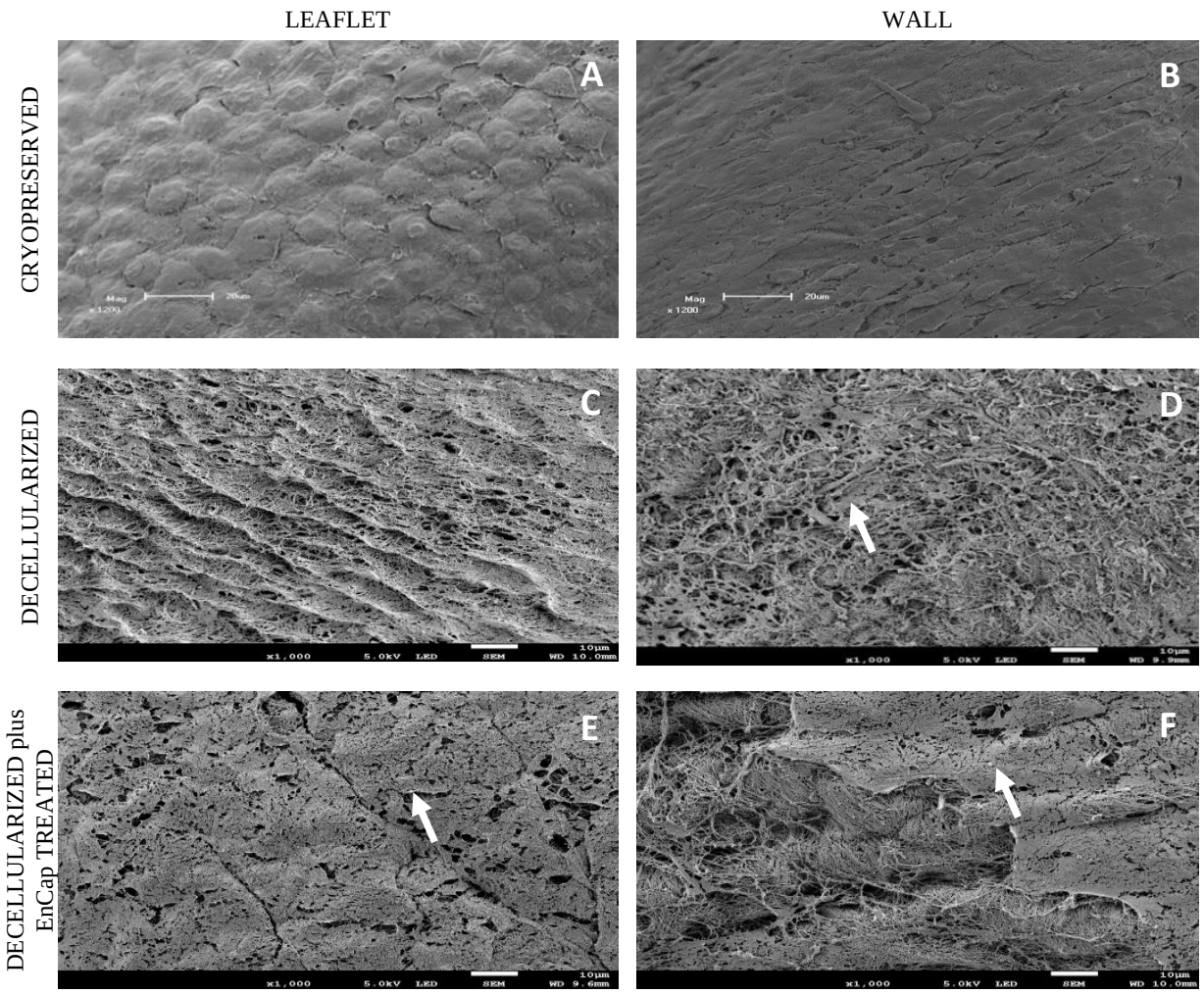

Figure 6: Representative scanning electron microscopy images demonstrating leaflets and wall tissue of cryopreserved homografts (n = 5) with uniform but loose endothelial cell coverage **(A,B)**. Leaflets and walls of the decellularized valves (n = 5) **(C,D)** and decellularized plus EnCap treated valves (n = 5) **(E,F)** displayed exposed collagen networks without any cells and only basal membrane remnants (white arrows).

TEM demonstrated the presence of cells and cellular remnants in the cryopreserved group (Fig.7A,B), and no interstitial cells present in the leaflets and wall tissue in the decellularized group (Fig.7C,D) or decellularized plus EnCap treated group (Fig.7E,F). Collagen bundles appeared more loosely arranged in the decellularized group (Fig.7C,D) and more compressed and dense in the decellularized plus EnCap treated group (Fig.7E,F).

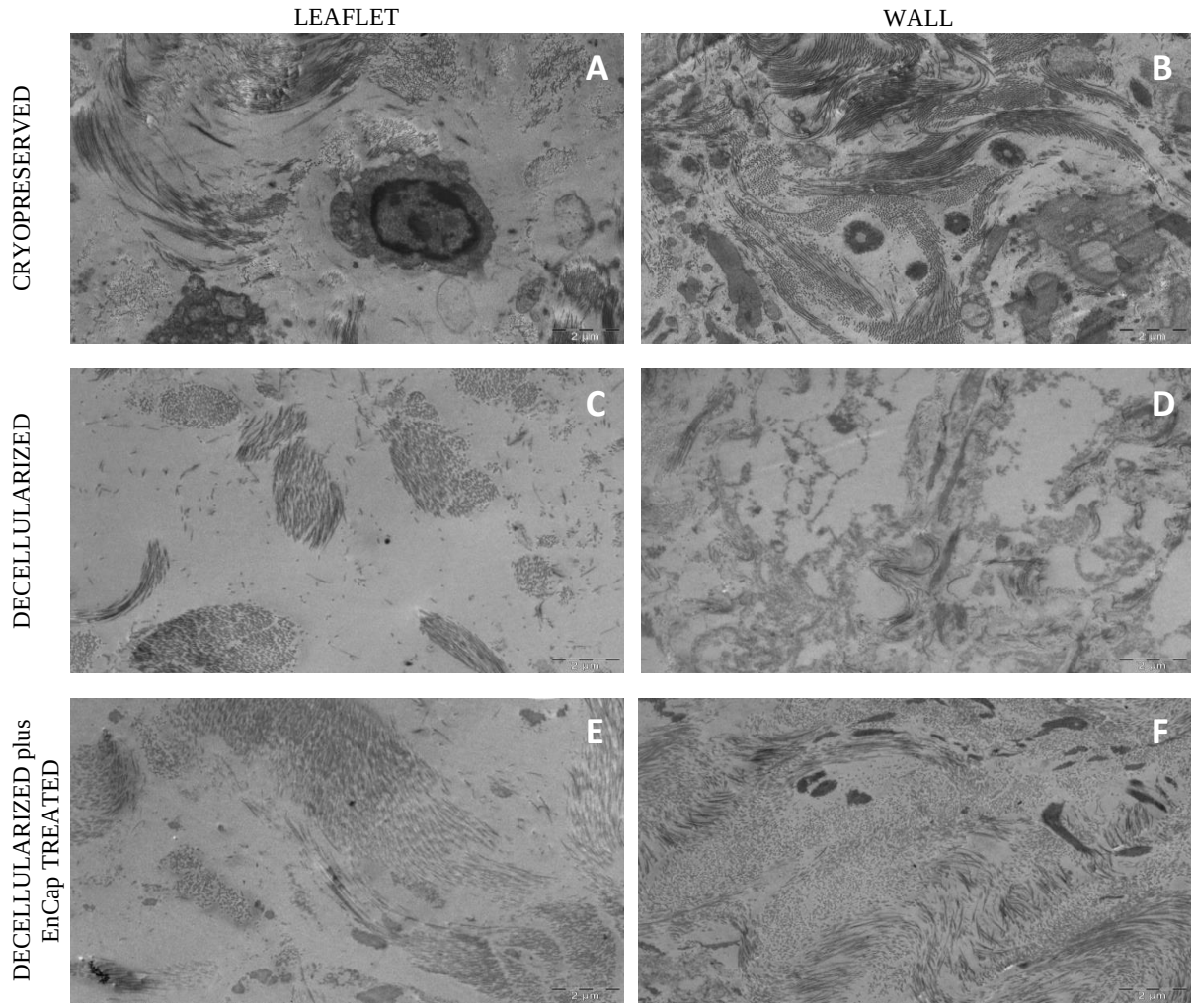

Figure 7: Representative transmission electron microscopy images demonstrating the presence of interstitial cells and cell remnants in leaflets **(A)** and walls **(B)** in the cryopreserved group (n = 5), and no cells in the leaflets or walls of homografts in the decellularized group (n = 5) **(C,D)** and the decellularized plus EnCap treated group (n = 5) **(E,F)**. Collagen bundles appeared loosely arranged in the decellularized group **(C,D)** and more dense in the decellularized plus EnCap treated group **(E,F)**.

The Young's modulus of the decellularized leaflets does suggest more extensible leaflet tissue, but no statistically significant differences in the tensile strength or Young's modulus of the leaflet or wall tissue (Table 3) between the three groups could be demonstrated. The stiffness of the leaflets in the decellularized plus EnCap treated group did increase when compared to that in the other two groups, however, the increase was not significant ($p > 0.05$).

Table 3: Baseline TS and YM of cryopreserved, decellularized unfixed and decellularized plus EnCap treated pulmonary homograft leaflets (n = 5) and wall tissue (n = 5).

Variable		Cryopreserved	Decellularized	Decellularized plus EnCap treated	p-values
Leaflet	TS (MPa)	3.72 [3.12- 5.01]	1.83 [0.01-5.65]	4.96 [4.34-6.76]	0.23
	YM (MPa)	23.34 [14.12-28.87]	22.10 [0.10-55.27]	41.11 [27.76-52.52]	0.40
Wall	TS (MPa)	1.80 [1.35-2.65]	1.89 [1.57-2.38]	1.90 [1.18-2.09]	0.96
	YM (MPa)	1.97 [1.22-3.18]	2.32 [1.82-2.88]	2.21 [1.99-3.58]	0.75

Data presented as median [InterQuartile range], the difference between groups determined with the Kruskal-Wallis (KW) test and significant differences ($p < 0.05$) are indicated with *. [TS = tensile strength; YM = Young's modulus].

DISCUSSION

Histological evaluation of the cryopreserved homografts with H&E demonstrated the presence of an endothelial layer and uniformly distributed interstitial cells, but the collagen scaffold appeared collapsed (Fig.4A and Fig.5A). However, a limitation of H&E staining is the inability to differentiate between morphologically intact cells and non-viable cells (Radosevich et al., 1985; Radosevich et al., 1993). SEM demonstrated a confluent endothelial cell layer on the leaflet and wall tissue of cryopreserved homografts even after 48 hours of ischaemia (Fig.6A,B). These endothelial cells presented with prominent nuclei and collapsed extranuclear areas, indicative of non-viable cells (Bester et al., 2018). Shenke-Layland and co-workers described the presence of limited collagen-containing structures in the ventricularis of cryopreserved valve leaflets after thawing, with significantly altered and deteriorated collagenous and elastic fiber structures as a result of crystal ice formation in the extracellular matrix during cryopreservation (Schenke-Layland et al., 2006). This corresponds with our findings on TEM, where the collagen in the cryopreserved group appeared disrupted and damaged, with interstitial cells and cellular remnants (Fig.7A,B). These cellular remnants that remain in the ECM can activate the immune response from the recipient to the homograft, and together with the damaged and ruptured collagen will result in early valve degradation (Lopes et al., 2009).

Removing all the cellular content and DNA material from a homograft valve through decellularization results in an implant that significantly reduces the immunologic response from the recipient (Bibevski et al., 2017). Decellularized valve leaflets and wall tissue demonstrated complete acellularity with H&E staining (Fig.4D and Fig.5D), however, decellularization of leaflets using sodium dodecyl sulphate (SDS) has been shown to result in a dense extracellular matrix network and small pore sizes, which might make recellularization of the matrix with interstitial cells more difficult (Liao et al., 2008). Our devised decellularization process relies on combining osmotic shock as an initial step to induce cell lysis with detergents (SDS, deoxycholic acid and TritonX-100) and Benzonase, which reduced the concentrations and time of exposure of the tissue to the detergents and the enzyme, thereby reducing the damage to the collagen fibers and extracellular matrix (Zhou et al., 2010; Converse et al., 2012; Somers et al., 2012). Ethanol was used to remove lipids (Flynn, 2010; Brown et al., 2011). The decellularization method used in this study resulted in collagen fibers that were more loosely organised with larger spaces between the fibers (Fig.4D, 5D). SEM confirmed the complete removal of the endothelial cells on the leaflet and wall tissue of the decellularized valves, with only exposed collagen layers and remnants of basal membrane remaining (Fig.6), while TEM also demonstrated the loosely arranged collagen network (Fig.7C,D). The decellularization method proved effective in achieving complete acellularity, and the larger interfibrillar spaces could be very beneficial for *in vivo* recellularization once implanted, while maintaining tissue strength when compared to cryopreservation (Table 3).

Converse and co-workers used a multi-detergent and enzymatic washout decellularization protocol, and differential scanning calorimetry (DSC) showed that this method does not reduce the cross-linking of collagen, and thereby retains the strength of the tissue. However, the decellularization protocol they used did reduce the GAG content, with resultant increased extensibility and changes in the relaxation behaviour of the pulmonary valve leaflets (Converse et al., 2012). The method currently used did lead to a reduction of the GAG content when used for the decellularization of bovine pericardium (Laker et al., 2018). GAG content was not evaluated in the current study and the effect of this decellularization method on the GAG content of pulmonary homografts should be investigated. However, the decellularization process did not significantly affect the stiffness of the homograft leaflet and wall tissue compared to

cryopreserved tissue (Table 3). Although the Young's modulus of decellularized leaflets does suggest more extensible leaflet tissue after decellularization, the lack of significance may be due to the small number of samples tested. The comparable strength and Young's modulus of the decellularized leaflet and wall tissue to that of cryopreserved tissue could be attributed to the dehydration effect of ethanol in the delipidation step.

Due to the concerns that the decellularization process might negatively affect the strength of the scaffold, the additional fixation and stabilization of the decellularized homografts were investigated. Additional fixation and detoxification of the decellularized valves were done using GA as a fixative and PG for detoxifying the GA-fixed homograft (EnCap technology) (Seifter and Frater, 1995). This process resulted in more compacted and dense collagen layers when compared to the leaflet and wall tissue in the cryopreserved and decellularized groups (Fig.4G, Fig.5G, Fig.7E,F), which might make recellularization of the matrix with interstitial cells more difficult (Liao et al., 2008). Additional fixation and detoxification of decellularized homografts using EnCap technology added additional cross-links and increased the Young's modulus of leaflets, although not significantly. GA-fixation has an effect on the hydration properties of fixated tissue, impairing its ability to rehydrate, which is hypothesized to result from the reaction of GA with hydrophilic amine groups in collagen, reducing the tissue's hydrating capacity and increasing stiffness.

CONCLUSION

Confluent layers of endothelial cells were still present on the leaflet and wall tissue of the cryopreserved group even after 48 h cold ischaemia, and our proprietary decellularization protocol proved to be effective in removing all endothelial and interstitial cells from the sheep homografts. The collagen matrix in the cryopreserved group was more collapsed, well organized but loosely arranged with larger interfibrillar spaces in the decellularized group, and much dense and compacted in the decellularized plus EnCap treated group. On ultrastructure, the collagen in the cryopreserved group appeared disrupted and fractured, but intact in the other two groups. Elastin appeared to be well preserved in all three groups after processing, with no visible calcific nodules in any of the groups. Tensile strength was well maintained in decellularized tissue when compared to cryopreserved tissue, but did increase in leaflet tissue after additional EnCap

treatment. The tissue stiffness in the decellularized plus EnCap treated group also increased. Dehydration and fixation during the delipidation phase were most likely responsible for maintaining the tensile strength of the leaflet and wall tissue after decellularization. We conclude that the leaflets and wall tissue of ovine pulmonary homografts remained strong enough after decellularization, and that additional fixation of the decellularized scaffold increased the leaflet stiffness, which will negatively affect the biomechanical behaviour of the homograft.

Limitations of the study

A limitation of this study is the small number of samples used. Tensile strength and Young's modulus data should always be treated with caution, due to the difficulty of getting repeatable results when working with such small tissue samples and low numbers.

Conflict of interest

We certify that all authors named in the manuscript deserve authorship and that all authors have agreed to be listed in the manuscript when submitted to peer review journals. The authors have no conflicts of interest to declare.

Acknowledgments

We want to thank Miss H Grobler from the Centre for Electron Microscopy for the preparation of SEM and TEM samples.

REFERENCES

ANGELL, W. W., OURY, J. H., LAMBERTI, J. J. & KOZIOL, J. 1989. Durability of the viable aortic allograft. *J Thorac Cardiovasc Surg*, 98, 48-55; discussion 55-6.

BARRATT-BOYES, B. G. 1965. Homograft aortic valve replacement. *N Z Med J*, 64, Suppl, 41-3.

BASKETT, R. J., NANTON, M. A., WARREN, A. E. & ROSS, D. B. 2003. Human leukocyte antigen-DR and ABO mismatch are associated with accelerated homograft valve failure in children: implications for therapeutic interventions. *J Thorac Cardiovasc Surg*, 126, 232-9.

BESTER, D., BOTES, L., VAN DEN HEEVER, J. J., KOTZE, H., DOHMEN, P., POMAR, J. L. & SMIT, F. E. 2018. Cadaver donation: structural integrity of pulmonary homografts harvested 48 h post mortem in the juvenile ovine model. *Cell Tissue Bank*, 19, 743-754.

BESTER, D., SMIT, F. E., VAN DEN HEEVER, J. J., BOTES, L. & DOHMEN, P. M. C. E. 2017. *Detoxification and stabilization of implantable or transplantable biological material*. EU. 16792990.0-1455.

BIBEVSKI, S., RUZMETOV, M., FORTUNA, R. S., TURRENTINE, M. W., BROWN, J. W. & OHYE, R. G. 2017. Performance of SynerGraft Decellularized Pulmonary Allografts Compared With Standard Cryopreserved Allografts: Results From Multiinstitutional Data. *Ann Thorac Surg*, 103, 869-874.

BOETHIG, D., HORKE, A., HAZEKAMP, M., MEYNS, B., REGA, F., VAN PUYVELDE, J., HÜBLER, M., SCHMIADY, M., CIUBOTARU, A., STELLIN, G., PADALINO, M., TSANG, V., JASHARI, R., BOBYLEV, D., TUDORACHE, I., CEBOTARI, S., HAVERICH, A. & SARIKOUCH, S. 2019. A European study on decellularized homografts for pulmonary valve replacement: initial results from the prospective ESPOIR Trial and ESPOIR Registry data. *Eur J Cardiothorac Surg*, 56, 503–509. ORIGINAL ARTICLE doi:10.1093/ejcts/ezz054.

BOURGINE, P. E., PIPPENGER, B. E., TODOROV, A., JR., TCHANG, L. & MARTIN, I. 2013. Tissue decellularization by activation of programmed cell death. *Biomaterials*, 34, 6099-108.

BREYMANN, T., BOETHIG, D., GOERG, R. & THIES, W. R. 2004. The Contegra bovine valved jugular vein conduit for pediatric RVOT reconstruction: 4 years experience with 108 patients. *J Card Surg*, 19, 426-31.

BROWN, B. N., FREUND, J. M., HAN, L., RUBIN, J. P., REING, J. E., JEFFRIES, E. M., WOLF, M. T., TOTTEY, S., BARNES, C. A., RATNER, B. D. & BADYLAK, S. F. 2011. Comparison of three methods for the derivation of a biologic scaffold composed of adipose tissue extracellular matrix. *Tissue Engineering, Part C: Methods*, 17, 411-421.

BROWN, J. W., ELKINS, R. C., CLARKE, D. R., TWEDDELL, J. S., HUDDLESTON, C. B., DOTY, J. R., FEHRENBACHER, J. W. & TAKKENBERG, J. J. M. 2010. Performance of the CryoValve SG human decellularized pulmonary valve in 342 patients relative to

the conventional CryoValve at a mean follow-up of four years. *J Thorac Cardiovasc Surg*, 139, 339-348.

BURCH, P. T., KAZA, A. K., LAMBERT, L. M., HOLUBKOV, R., SHADDY, R. E. & HAWKINS, J. A. 2010. Clinical performance of decellularized cryopreserved valved allografts compared with standard allografts in the right ventricular outflow tract. *Ann Thorac Surg*, 90, 1301-5; discussion 1306.

CEBOTARI, S., TUDORACHE, I., CIUBOTARU, A., BOETHIG, D., SARIKOUCH, S., GOERLER, A., LICHTENBERG, A., CHEPTANARU, E., BARNACIUC, S., CAZACU, A., MALIGA, O., REPIN, O., MANIUC, L., BREYMANN, T. & HAVERICH, A. 2011. Use of fresh decellularized allografts for pulmonary valve replacement may reduce the reoperation rate in children and young adults: early report. *Circulation*, 124, S115-23.

CONVERSE, G. L., ARMSTRONG, M., QUINN, R. W., BUSE, E. E., CROMWELL, M. L., MORIARTY, S. J., LOFLAND, G. K., HILBERT, S. L. & HOPKINS, R. A. 2012. Effects of cryopreservation, decellularization and novel extracellular matrix conditioning on the quasi-static and time-dependent properties of the pulmonary valve leaflet. *Acta Biomater*, 8, 2722-9.

CRAPO, P. M., GILBERT, T. W. & BADYLAK, S. F. 2011. An overview of tissue and whole organ decellularization processes. *Biomaterials*, 32, 3233-43.

DA COSTA, F. D. A., COSTA, A. C., PRESTES, R., DOMANSKI, A. C., BALBI, E. M., FERREIRA, A. D. & LOPES, S. V. 2010. The early and midterm function of decellularized aortic valve allografts. *Ann Thorac Surg*, 90, 1854-60.

DIAZ, R., HERNANDEZ-VAQUERO, D., ALVAREZ-CABO, R., AVANZAS, P., SILVA, J., MORIS, C. & PASCUAL, I. 2019. Long-term outcomes of mechanical versus biological aortic valve prosthesis: Systematic review and meta-analysis. *J Thorac Cardiovasc Surg*, 158, 706-714 e18.

DIJKMAN, P. E., DRIESSEN-MOL, A., FRESE, L., HOERSTRUP, S. P. & BAAIJENS, F. P. 2012. Decellularized homologous tissue-engineered heart valves as off-the-shelf alternatives to xeno- and homografts. *Biomaterials*, 33, 4545-54.

ERDBRUGGER, W., KONERTZ, W., DOHMEN, P. M., POSNER, S., ELLERBROK, H., BRODDE, O. E., ROBENEK, H., MODERSOHN, D., PRUSS, A., HOLINSKI, S.,

STEIN-KONERTZ, M. & PAULI, G. 2006. Decellularized xenogenic heart valves reveal remodeling and growth potential in vivo. *Tissue* Eng, 12, 2059-68.

FALCHETTI, A., DEMANET, H., DESSY, H., MELOT, C., PIERRAKOS, C. & WAUTHY, P. 2019. Contegra versus pulmonary homograft for right ventricular outflow tract reconstruction in newborns. *Cardiol Young*, 29, 505-510.

FLYNN, L. E. 2010. The use of decellularized adipose tissue to provide an inductive microenvironment for the adipogenic differentiation of human adipose-derived stem cells. *Biomaterials*, 31, 4715-24.

GOFFIN, Y. A., VAN HOECK, B., JASHARI, R., SOOTS, G. & KALMAR, P. 2000. Banking of cryopreserved heart valves in Europe: assessment of a 10-year operation in the European Homograft Bank (EHB). *J Heart Valve Dis*, 9, 207-14.

HECHADI, J., GERBER, B. L., COCHE, E., MELCHIOR, J., JASHARI, R., GLINEUR, D., NOIRHOMME, P., RUBAY, J., EL KHOURY, G. & DE KERCHOVE, L. 2013. Stentless xenografts as an alternative to pulmonary homografts in the Ross operation. *Eur J Cardiothorac Surg*, 44, e32-9.

KITAGAWA, T., MASUDA, Y., TOMINAGA, T., KANO, M. 2001. Cellular biology of cryopreserved allograft valves. *J Med Invest*, 48, 123-132.

KOROSSIS, S. A., BOOTH, C., WILCOX, H. E., WATTERSON, K. G., KEARNEY, J. N., FISHER, J. & INGHAM, E. 2002. Tissue engineering of cardiac valve prostheses II: biomechanical characterization of decellularized porcine aortic heart valves. *J Heart Valve Dis*, 11, 463-71.

LAKER, L. 2018. *The evaluation of a novel decellularization and sterilization process on bovine pericardial tissue.* Doctor of Philosophy Dissertation, Department of Cardiothoracic Surgery, University of the Free State, Free State, South Africa.

LAKER, L., DOHMEN, P. M. & SMIT, F. E. 2020. Synergy in a detergent combination results in superior decellularized bovine pericardial extracellular matrix scaffolds. *J Biomed Mater Res, Part B: Appl Biomater*. https://doi.org/10.1002/jbm.b.34588.

LEE, C., LIM, H. G., LEE, C. H. & KIM, Y. J. 2017. Effects of glutaraldehyde concentration and fixation time on material characteristics and calcification of bovine pericardium: implications for the optimal method of fixation of autologous pericardium used for cardiovascular surgery. *Interact Cardiovasc Thorac Surg*, 24, 402-406.

LIAO, J., JOYCE, E. M. & SACKS, M. S. 2008. Effects of decellularization on the mechanical and structural properties of the porcine aortic valve leaflet. *Biomaterials*, 29, 1065-74.

LOPES, S. A., COSTA, F. D., PAULA, J. B., DHOMEN, P., PHOL, F., VILANI, R., RODERJAN, J. G. & VIEIRA, E. D. 2009. Decellularized heterografts versus cryopreserved homografts: experimental study in sheep model. *Rev Bras Cir Cardiovasc Surg*, 24(1), 15-22.

MEPHAM, B. L. 1991. *Theory and practice of histological techniques, Third ed*, BANCROFT, J. D. & STEVENS, A.Edinburgh, Churchill Livingstone ISBN:0443035598.

MITCHELL, R. N., JONAS, R. A. & SCHOEN, F. J. 1998. Pathology of explanted cryopreserved allograft heart valves: comparison with aortic valves from orthotopic heart transplants. *J Thorac Cardiovasc Surg*, 115, 118-27.

NIH. 2011. *Guide for the Care and Use of Laboratory Animals, 8th ed.* [Online]. Washington DC: National Academy of Sciences. Available: https://www.ncbi.nlm.nih.gov/pubmed/21595115.

O'BRIEN, M. F., MCGIFFIN, D. C., STAFFORD, E. G., GARDNER, M. A., POHLNER, P. F., MCLACHLAN, G. J., GALL, K., SMITH, S. & MURPHY, E. 1991. Allograft aortic valve replacement: long-term comparative clinical analysis of the viable cryopreserved and antibiotic 4 degrees C stored valves. *J Card Surg*, 6, 534-43.

O'BRIEN, M. F., STAFFORD, E. G., GARDNER, M. A., POHLNER, P. G., TESAR, P. J., COCHRANE, A. D., MAU, T. K., GALL, K. L. & SMITH, S. E. 1995. Allograft aortic valve replacement: long-term follow-up. *Ann Thorac Surg*, 60, S65-70.

ORYAN, A., KAMALI, A., MOSHIRI, A., BAHARVAND, H. & DAEMI, H. 2018. Chemical crosslinking of biopolymeric scaffolds: Current knowledge and future directions of crosslinked engineered bone scaffolds. *Int J Biol Macromol*, 107, 678-688.

PADALA, M. 2018. A heart valve is no stronger than its weakest link: The need to improve durability of pericardial leaflets. *J Thorac Cardiovasc Surg*, 156, 207-208.

RADOSEVICH, J. A., HAINES, G. K., ELSETH, K. M., SHAMBAUGH, G. E., 3RD & MAKER, V. K. 1993. A new method for the detection of viable cells in tissue sections using 3-[4,5-dimethylthiazol-2-yl]-2,5-diphenyltetrazolium bromide (MTT): an application in the assessment of tissue damage by surgical instruments. *Virchows Archiv. B, Cell Pathology including Molecular Pathology*, 63, 345-350.

RADOSEVICH, J. A., MA, Y. X., LEE, I., SALWEN, H. R., GOULD, V. E. & ROSEN, S. T. 1985. Monoclonal antibody 44-3A6 as a probe for a novel antigen found on human lung carcinomas with glandular differentiation. *Cancer Res*, 45, 5808-12.

ROMEO, J. L. R., PAPAGEORGIOU, G., VAN DE WOESTIJNE, P. C., TAKKENBERG, J. J. M., WESTENBERG, L. E. H., VAN BEYNUM, I., BOGERS, A. & MOKHLES, M. M. 2018. Downsized cryopreserved and standard-sized allografts for right ventricular outflow tract reconstruction in children: long-term single-institutional experience. *Interact Cardiovasc Thorac Surg*, 27, 257-263.

ROSS, D. N. 1965. Homograft replacement of the aortic valve. *J Cardiovasc Surg (Torino)*, 5, Suppl, 89-94.

RYAN, W. H., HERBERT, M. A., DEWEY, T. M., AGARWAL, S., RYAN, A. L., PRINCE, S. L. & MACK, M. J. 2006. The occurrence of postoperative pulmonary homograft stenosis in adult patients undergoing the Ross procedure. *J Heart Valve Dis*, 15, 108-13; discussion 113-4.

SARIKOUCH, S., HORKE, A., TUDORACHE, I., BEERBAUM, P., WESTHOFF-BLECK, M., BOETHIG, D., REPIN, O., MANIUC, L., CIUBOTARU, A., HAVERICH, A. & CEBOTARI, S. 2016. Decellularized fresh homografts for pulmonary valve replacement: a decade of clinical experience. *Eur J Cardiothorac Surg*, 50, 281-90.

SCHENKE-LAYLAND, K., MADERSHAHIAN, N., RIEMANN, I., STARCHER, B., HALBHUBER, K. J., KONIG, K. & STOCK, U. A. 2006. Impact of cryopreservation on extracellular matrix structures of heart valve leaflets. *Ann Thorac Surg*, 81, 918-26.

SEIFTER, E. & FRATER, R. W. M. 1995. *Anticalcification treatment for aldehyde-tanned biological tissue*. United States. Albert Einstein College of Medicine of Yeshiva University (Bronx, NY).5476516. http://www.freepatentsonline.com/5476516.html.

SELAMET TIERNEY, E. S., GERSONY, W. M., ALTMANN, K., SOLOWIEJCZYK, D. E., BEVILACQUA, L. M., KHAN, C., KRONGRAD, E., MOSCA, R. S., QUAEGEBEUR, J. M. & APFEL, H. D. 2005. Pulmonary position cryopreserved homografts: durability in pediatric Ross and non-Ross patients. *J Thorac Cardiovasc Surg*, 130, 282-6.

SHADDY, R. E. & HAWKINS, J. A. 2002. Immunology and failure of valved allografts in children. *Ann Thorac Surg*, 74, 1271-5.

SHEEHY, E. J., CUNNIFFE, G. M. & O'BRIEN, F. J. 2018. 5 - Collagen-based biomaterials for tissue regeneration and repair. *In:* BARBOSA, M. A. & MARTINS, M. C. L. (eds.) *Peptides and Proteins as Biomaterials for Tissue Regeneration and Repair*. Woodhead Publishing. https://doi.org/10.1016/B978-0-08-100803-4.00005-X.

SMIT, F. E., BESTER, D., VAN DEN HEEVER, J. J., SCHLEGEL, F., BOTES, L. & DOHMEN, P. M. 2015. Does prolonged post-mortem cold ischaemic harvesting time influence cryopreserved pulmonary homograft tissue integrity? *Cell Tissue Bank*, 16, 531-44.

SOMERS, P., DE SOMER, F., CORNELISSEN, M., THIERENS, H. & VAN NOOTEN, G. 2012. Decellularization of heart valve matrices: search for the ideal balance. *Artif Cells Blood Substit Immobil Biotechnol*, 40, 151-62.

SPURR, A. R. 1969. A low-viscosity epoxy resin embedding medium for electron microscopy. *J Ultrastruct Res*, 26, 31-43.

STRANGE, G., BRIZARD, C., KARL, T. R. & NEETHLING, L. 2015. An evaluation of Admedus' tissue engineering process-treated (ADAPT) bovine pericardium patch (CardioCel) for the repair of cardiac and vascular defects. *Expert Rev Med Devices*, 12, 135-41.

THUBRIKAR, M. J., DECK, J. D., AOUAD, J. & NOLAN, S. P. 1983. Role of mechanical stress in calcification of aortic bioprosthetic valves. *J Thorac Cardiovasc Surg*, 86, 115-25.

VEDEPO, M. C., DETAMORE, M. S., HOPKINS, R. A. & CONVERSE, G. L. 2017. Recellularization of decellularized heart valves: Progress toward the tissue-engineered heart valve. *J Tiss Eng*, 8, 2041731417726327-2041731417726327.

ZHOU, J., FRITZE, O., SCHLEICHER, M., WENDEL, H. P., SCHENKE-LAYLAND, K., HARASZTOSI, C., HU, S. & STOCK, U. A. 2010. Impact of heart valve decellularization on 3-D ultrastructure, immunogenicity and thrombogenicity. *Biomaterials*, 31, 2549-54.

Chapter 4 - Manuscript 2

Comparison of function and structural integrity of cryopreserved pulmonary homografts versus decellularized pulmonary homografts after 180 days implantation in the juvenile ovine model

[1]van den Heever JJ, [1]Jordaan CJ, [1]Lewies A, [1]Bester D, [4]Goedhals J, [2]Botes L, [1&3]Dohmen PM, [1]Smit FE

Author(s)

1) **Johannes Jacobus van den Heever (corresponding author), Christiaan Johannes Jordaan, Angélique Lewies, Dreyer Bester, Pascal Maria Dohmen, Francis Edwin Smit**
   Department of Cardiothoracic Surgery,
   Faculty of Health Sciences,
   University of the Free State (UFS)
   P.O. Box 339, (Internal Box G32)
   Bloemfontein
   9300
   South Africa
   Tel: +27 51 4053435
   E-mail: vdheeverjj@ufs.ac.za

2) **Lezelle Botes**
   Department of Health Sciences
   Central University of Technology, Free State (CUT)
   Private Bag X20539
   Bloemfontein
   9300
   South Africa

3) **Pascal Maria Dohmen**
   Department of Cardiac Surgery
   Heart Centre Rostock
   University of Rostock
   Rostock
   18107
   Germany

4) **Jacqueline Goedhals**
   Department of Anatomical Pathology,
   Faculty of Health Sciences,
   University of the Free State (UFS)
   P.O. Box 339,
   Bloemfontein
   9300
   South Africa

ABSTRACT

Introduction: Cryopreservation is widely used to preserve pulmonary homografts; however, availability and durability remain a big challenge, especially in young children. Increasing the post-mortem ischaemic harvesting time beyond 24 h will lead to an increase in the potential donor pool. However, the cryopreservation process damages the extracellular matrix (ECM), contributing to valve degeneration. Decellularization processes might not only reduce immunogenicity, but an intact ECM will promote host cell infiltration, contributing towards better clinical outcomes. This study compared the performance of cryopreserved versus decellularized pulmonary homografts in the right ventricle outflow tract (RVOT) of a juvenile ovine model.

Method: Pulmonary homografts from juvenile Dorper sheep, subjected to a post-mortem cold ischaemic harvesting time of 48 hours, were cryopreserved (n = 5) or decellularized using a multi-detergent and enzymatic protocol (n = 5) and implanted in the RVOT of juvenile sheep for 180 days. Valve performance was monitored clinically and echocardiographically, and at explantation valve leaflet and wall tissue were evaluated on histological (DAPI, H&E, von Kossa, Modified von Gieson) appearance, scanning (SEM) and transmission (TEM) electron microscopy, mechanical properties [tensile strength (TS) and Young's modulus (YM)] and quantitative calcium content.

Results: Implanted cryopreserved homografts demonstrated an increase in annulus diameter and developed significant 3/5 pulmonary regurgitation (PR), while the annulus diameter of decellularized homografts increased without PR and only trivial regurgitation. On macroscopic evaluation of explanted valves, the cryopreserved leaflets retracted and thickened, accounting for regurgitation. Decellularized valves remained thin and pliable with good leaflet coaptation. For cryopreserved valves, there was a loss of interstitial cells in the leaflet and wall tissue at explantation, while decellularized scaffolds displayed extensive and uniform ingrowth of host fibroblast cells. An intact collagen network could also be observed in the decellularized group. Calcific deposits were visible on von Kossa stain in the leaflets and wall tissue of explanted cryopreserved homografts, but not in decellularized grafts. TEM showed young fibroblasts repopulating leaflets and wall of decellularized scaffolds, with vacuoles and rough endoplasmic

reticulum present in the cytoplasm. YM of cryopreserved and decellularized wall tissue increased significantly from pre-implantation to explantation.

Conclusion: Cryopreserved valves deteriorate over time due to loss of cellularity and calcification. In contrast, decellularized scaffolds demonstrated host cell repopulation, structural maintenance, tissue remodeling and growth potential.

Keywords: Homografts, decellularization, cryopreservation, cell repopulation, remodeling

INTRODUCTION

Cryopreservation can be used for the long-term storage and stabilization of viable cells and tissues for clinical application (Bakhach, 2009), and currently, most tissue banks worldwide employ some form of cryopreservation. Since the 1980s, cryopreserved pulmonary homografts are widely regarded as the conduit of choice for reconstruction of the right ventricle outflow tract (RVOT) in the repair of congenital defects and to replace the native pulmonary valve in Ross procedures in children and young patients (Takkenberg et al., 2002; Jashari et al., 2004; Romeo et al., 2018). Cryopreservation provides the advantage of extended storage time and improved durability of homografts when compared to fresh allografts stored at 4^{o}C in antibiotic solutions (Takkenberg et al., 2002). Event-free survival of cryopreserved homografts in the pulmonary position ranging between 74 % at five years and 53 % at 10 years (Tweddell et al., 2000), and 30 % to 40 % of homografts implanted are still functional after 20 years (Delmo Walter et al., 2012). Unfortunately, small diameter implants result in early dysfunction post-surgery due to stenosis of the RVOT as a result of somatic growth of the patient or calcification of the leaflets or pulmonary walls (Schoen, 2008). Also, concerns have been raised regarding the limited availability of these homografts, especially in paediatric sizes (Goffin et al., 2000) and their early degeneration in young patients (Selamet Tierney et al., 2005).

Studies using the juvenile ovine model showed that increasing the post-mortem ischaemic harvesting time of pulmonary homografts to 48 h prior to cryopreservation, does not influence the long-term valve function (Smit et al., 2015; Bester et al., 2018). The post-mortem time of 48 h was chosen to simulate a reasonable window of opportunity for obtaining donor consent in human cadaveric donor programs in South Africa (mean = 33h) (Botes et al., 2012), thereby

increasing the donor pool and addressing shortages in homograft availability. However, with post-mortem harvesting times exceeding 24 h, the homografts contain non-viable cells (Smit et al., 2015). The cellular debris that results from apoptotic and necrotic cells present on the homograft after processing and storage may lead to calcification and chronic inflammation, which promotes valve failure (Hopkins et al., 2009). Also, the freezing-induced extracellular matrix (ECM) damage caused by ice crystal formation during standardized frozen cryopreservation may contribute towards the degeneration of allograft valves (Lisy et al., 2017).

Decellularization methods can be used to process homografts. The decellularization process will reduce a recipient's immune response to the implant due to the removal of cells (Numata et al., 2004). Decellularization may not only reduce the immunogenicity associated with homografts, but may also contribute towards a reduction in calcification of homografts (da Costa et al., 2010; Lehr et al., 2011) and lead to improved haemodynamics (Brown et al., 2010). The decellularization processes must ensure that adequate biochemical properties (such as an intact ECM) remain and that mechanical tissue stability is not affected (Bourgine et al., 2013). Decellularization might damage the valve tissue less than cryopreservation, which causes disruption of the collagen matrix in the pulmonary homograft (Bester et al., 2018).

The aim of this study was to compare the clinical performance and structural integrity of cryopreserved and decellularized pulmonary homografts following six months implantation in the RVOT of a juvenile ovine model. Homografts in both groups were subjected to a 48 h post-mortem cold ischaemic time, and our proprietary decellularization protocol with proven synergy were used (Laker et al., 2020).

MATERIALS AND METHODS

Study design

The study was a prospective analytical cohort experimental study. The evaluation of baseline data for cryopreserved and decellularized ovine pulmonary homograft tissue has previously been described (Manuscript 1). Pulmonary homografts from juvenile Dorper sheep (n = 10), with a post-mortem cold ischaemic harvesting time of 48 h, were divided into two groups and either cryopreserved (n = 5) or decellularized (n = 5) according to previously described protocols

(Bester et al., 2017; Laker et al., 2020). These homografts were then implanted as interposition grafts into the RVOT of juvenile Dorper sheep (n = 5 per group) for 180 days. Recipient animals were between 3-6 months of age and weighed between 24-32 kg, and each animal received an ear tag with a unique identification number. Recipients were monitored with echocardiography at implantation, and at one, three and six months prior to sacrifice. Following explantation, homografts were evaluated on macroscopic and radiographic appearance. Leaflet and wall tissue integrity were evaluated using strength analysis and morphology. Strength analysis included tensile strength (TS) and Young's modulus (YM), and morphology included H&E, von Kossa staining, modified von Gieson staining, scanning electron microscopy (SEM), transmission electron microscopy (TEM) and quantitative calcium analysis. A schematic representation of the study design is given in Figure 1. The interfaculty Animal Ethics Committee of the University of the Free State (UFS-AED2016/0101) approved the study. All animal experiments and surgical procedures were performed in compliance with the *Guide for the Care and Use of Laboratory Animals* as published by the US National Institutes of Health (NIH, 2011).

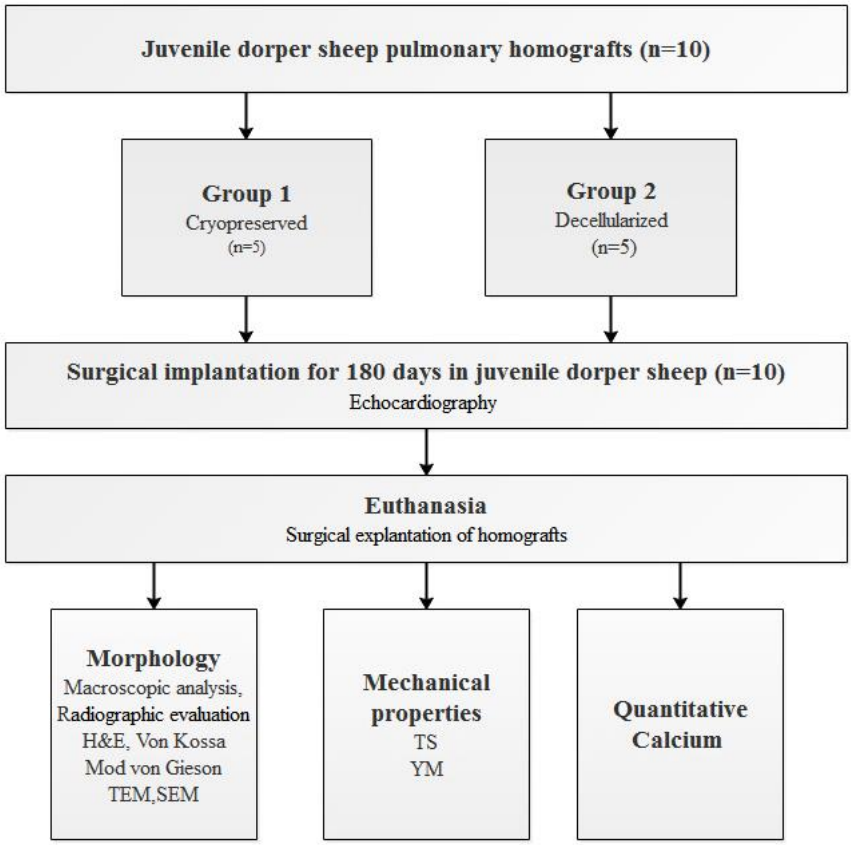

Figure 1: Schematic diagram of the study design.

Preparation of homografts

Heart-lung blocks (n = 10) were harvested from freshly slaughtered juvenile Dorper sheep with body weights of between 24-30 kg and subjected to 48 h ischaemia at 4ºC before dissection and processing per the method described by Bester et al., (2018).

Cryopreserved homografts (Group 1, n = 5) were processed, sterilized in 100 ml Medium 199 (Whitehead Scientific, Johannesburg, SA) and an antibiotic cocktail [2.5 mg Amphotericin B (Bristol-Myers Squibb, Bedfordview, SA), 50 mg Piperacillin (Brimpharm SA (Pty) Ltd, Cape Town, SA), 50 mg Vancomycin (Gulf Drug Company, Mount Edgecombe, SA) and 25 mg Amikacin sulphate (Bodene (Pty) Ltd, trading as Intramed, Port Elizabeth, SA], cryopreserved using DMSO (Highveld Biological, Johannesburg, SA) as cryoprotectant and stored according to a standard protocol previously described (Smit et al., 2015) until implantation.

Decellularized homografts (Group 2, n = 5) were prepared according to our proprietary protocol (Bester et al., 2017; Laker et al., 2020). Homografts were subjected to osmotic shock, repeated changes in a multi-detergent solution [0,5% SDS (Sigma-Aldrich, Johannesburg, SA), 1% Deoxycholic acid (Sigma-Aldrich, Johannesburg, SA), 1% Triton-X100 (Sigma-Aldrich, Johannesburg, SA)] and numerous washings in PBS and half-strength antibiotic cocktail used for cryopreserved homografts, under constant shaking. These steps were followed by enzymatic treatment with descending concentrations of Benzonase (Thermo Fisher Scientific, Johannesburg, SA) (Dijkman et al., 2012), repeated washing in PBS, delipidation in 70% ethanol and final storage in PBS with antibiotics until implantation.

All homografts were confirmed to be culture-negative prior to implantation. To confirm effective decellularization of the homografts in Group 2, DNA quantification was done with DAPI staining, gel electrophoresis and nanodrop counts by the Cardiovascular Research Unit, UCT Medical School (Crapo et al., 2011).

Implantation and clinical performance of homografts

Surgical procedure

Prepared homografts were implanted into ten juvenile Dorper wether sheep (n = 5 per group) with body weights ranging between 24-32 kg. Recipient sheep were anaesthetized, intubated and ventilated. Cardiopulmonary bypass (CPB) was achieved through cannulation of the left carotid artery and right atrium, arterial and central venous lines inserted and the surgical procedure performed on a beating heart. The pulmonary artery was transected, the native pulmonary valve leaflets removed and the pulmonary homograft implanted as an interposition graft (Ali et al., 1995; Flameng et al., 2006,) with end-to-end anastomoses with continuous 4/0 Prolene sutures in the main pulmonary artery. The animal was weaned off CPB, all incisions closed, extubated, chest drain and monitoring lines were removed, before moving the sheep to an overnight facility with a companion sheep. Analgesics and a broad-spectrum antibiotic were administered twice daily for five days post-operatively, and animals were followed for six months until sacrifice and explantation for further analysis of the homografts.

Clinical performance of implanted valves

Implanted homografts were evaluated for changes in annular dimensions, transvalvular gradients, pulmonary valve regurgitation, calcification and possible aneurysm formation over the study period, using echocardiographic data that were recorded immediately after homograft implantation, at 30 and 90 days post-surgery and just before sacrifice (day 180) using a GE Vivid-Q-mobile sonographic machine.

Evaluation of explanted homografts

Gross macroscopic appearance and microscopic analysis

Evaluation of gross macroscopic appearance of valve leaflet and wall tissue was performed immediately after valves were explanted, and photographed. Radiographic pictures of homografts were taken for the detection of calcific nodules before dissection. Leaflet and wall tissue samples were collected in 4 % buffered Formalin, embedded in paraffin wax, sectioned and stained according to standard hematoxylin and eosin (H&E), von Kossa and modified von Gieson staining protocols for histological evaluation (Mepham, 1991). The histology of the explants was compared to that of similarly processed pre-implanted homografts. Cell counts

were performed on H&E images with ImageJ version 1.52t software (National Institute of Health, Bethesda, Maryland, USA, https://imagej.nih.gov/ij/). Leaflet and wall tissue samples for scanning and transmission electron microscopy (SEM and TEM) were collected in 3 % GA and processed according to standard protocols for SEM and TEM evaluations (Spurr, 1969) (detailed method given in manuscript 1).

Calcium quantification

Quantitative calcium analyses were performed by the Eco-Analytica Laboratory, School for Environmental Sciences & Development, Northwest University, Potchefstroom, South Africa. Explanted samples were dried, weighed, hydrolyzed in 1 ml 50 % nitric acid + 50 µl hydrogen peroxide (H_2O_2) / dry sample at 90^oC for 30-40 minutes, the extractable calcium content determined by atomic absorption spectrophotometry (Agilent ICP-MS 7500c, Chemetrix, Midrand, South Africa) and expressed as µg calcium per mg tissue (dry weight).

Mechanical properties

Mechanical properties of explanted pulmonary valve leaflet and wall samples were examined using a tensile strength testing apparatus (Lloyds LS100 Plus, IMP, Johannesburg, South Africa), according to the method described by Thubrikar and co-workers. Tissue samples measured 5 x 10 mm, with leaflets and pulmonary sinus wall samples cut in the circumferential direction. The tissue sample was fixed between clamps at both ends and gradually stretched (0.1 mm/s) by applying constant tension on the two ends, and the data recorded on a personal computer (Thubrikar et al., 1983). The mechanical properties of the explants were compared to that of similarly processed pre-implanted homografts.

Statistical analysis

All values are expressed as median values with corresponding InterQuartile ranges. Statistical analyses were performed using GraphPad Prism version 8.3.1 (GraphPad Software, La Jolla, CA, USA, www.graphpad.com). The percentage change between Day 180 and Day 0 was calculated as (Day 180 – Day 0)/Day 0 * 100. The Wilcoxon Test was used to measure differences between paired groups, and the Mann-Whitney U Test was used to measure differences between unpaired

groups. Confidence intervals (CI) of 95 % of the difference between medians was calculated to test for the significance ($p < 0.05$).

RESULTS

Successful decellularization of both the valve leaflets and pulmonary artery walls was achieved and confirmed with DAPI staining. Additional gel electrophoresis (fragmented DNA bands < 200 bp) and nanodrop readings of below 50ng/mg for the same tissue samples confirmed that the homografts were successfully decellularized (Manuscript 1).

All animals were successfully operated on and survived until the end of the implantation period of 180 days. Echocardiography and doppler images revealed the development of significant homograft regurgitation of ¾ in four of the five animals in the cryopreserved group after 180 days implantation (Fig.2A), and only trivial (1/4) regurgitation in two of the animals in the decellularized group (Fig.2B). No calcification could be identified on echocardiography, and no aneurysm formation was observed in any of the implants in both groups.

CRYOPRESERVED DECELLULARIZED

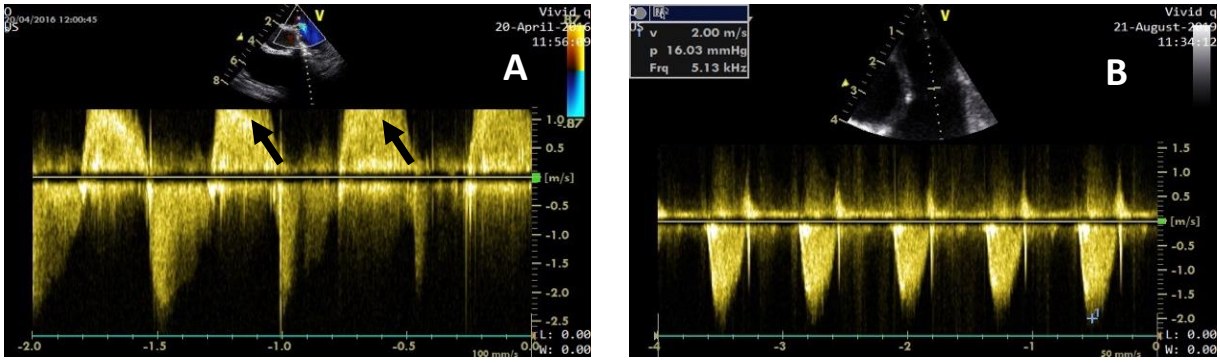

Figure 2: Representative Doppler images of cryopreserved (n = 5) **(A)** and decellularized (n = 5) **(B)** pulmonary homografts after 180 days implantation in sheep. Moderate regurgitation is clearly evident in the cryopreserved group (black arrows).

The increase in the annulus diameter in Group 1 (cryopreserved) from implantation (baseline) till day 180 was not significant, but for the homografts in Group 2 (decellularized) the increase in annulus diameter proved to be significant ($p < 0.05$). The measurement of the median change in annulus diameter over the study period in the two groups using echocardiography showed an

increase in the annulus diameter by 20.0 % in the cryopreserved group and 43.75 % in the decellularized group; however, when comparing the change in annulus diameter between the two groups, the change was not significant (Table 1).

Table 1: Comparison of increase in annular size (mm) between cryopreserved (n = 5) and decellularized (n = 5) pulmonary homografts over the six-month implantation period as measured on echocardiography.

Group	Baseline	180 day explant	95 % CI Baseline vs. day 180 explant	% Change from Baseline	95 % CI Group 1 vs. Group 2
1	14.00 [13.00-15.50]	18.00 [15.50-18.00]	-6.00; 0.00	20.00 [3.57-39.29]	-57.14; 8.57
2	15.00 [14.00-16.50]	23.00 [20.0-23.00]	-9.00; -3.00*	43.75 [24.71-64.29]	

Data presented as median [InterQuartile range], and the 95 % confidence interval (CI) of the control (baseline) and after 180 days of implantation, and the 95 % CI of the difference between the cryopreserved and decellularized groups (*p < 0.05). [Group 1 = Cryopreserved; Group 2 = Decellularized].

The median transvalvular gradient in the cryopreserved group increased over time by 70.0 %, while the median transvalvular gradient in the decellularized group increased by 60.0 %. The increase in the transvalvular gradient did not differ significantly between the two groups (Table 2).

Table 2: Comparison of changes in transvalvular gradients (mm Hg) over time between cryopreserved (n = 5) and decellularized (n = 5) pulmonary homografts, as measured on echocardiography.

Group	Day 0	Day 90	Day 180	PI	95 % CI Baseline vs. day 180 explant	% Change from baseline	95 % CI Group1 vs. Group 2
1	10.00 [6.00-22.00]	10.00 [5.00-14.50]	17.00 [15.50-20.50]	3/4	-10.00; 3.00;	70.00 [-8.50-171.4]	-110.00; 211.10
2	10.00 [7.00-16.50]	8.00 [4.50-10.00]	15.00 [9.00-16.00]	1/4	-9.00; 11.00	60.00 [-42.22-123.3]	

Data presented as median [InterQuartile range], and the 95 % confidence interval (CI) of the control (baseline) and after 180 days of implantation, and the 95 % CI of the difference between the cryopreserved and decellularized groups (*p < 0.05). [PI = Pulmonary Insufficiency; Group 1 = Cryopreserved; Group 2 = Decellularized].

On macroscopic inspection at explantation, leaflets of two of the valves in the cryopreserved group appeared very thin, but with visible nodules of calcification (Fig.3A), while leaflets from

the other valves appeared thickened and retracted (Fig.3B). Leaflets from valves in the decellularized group appeared pristine, very thin and almost translucent (Fig.3C), with only a slight sign of calcific deposit in one leaflet (Fig.3D).

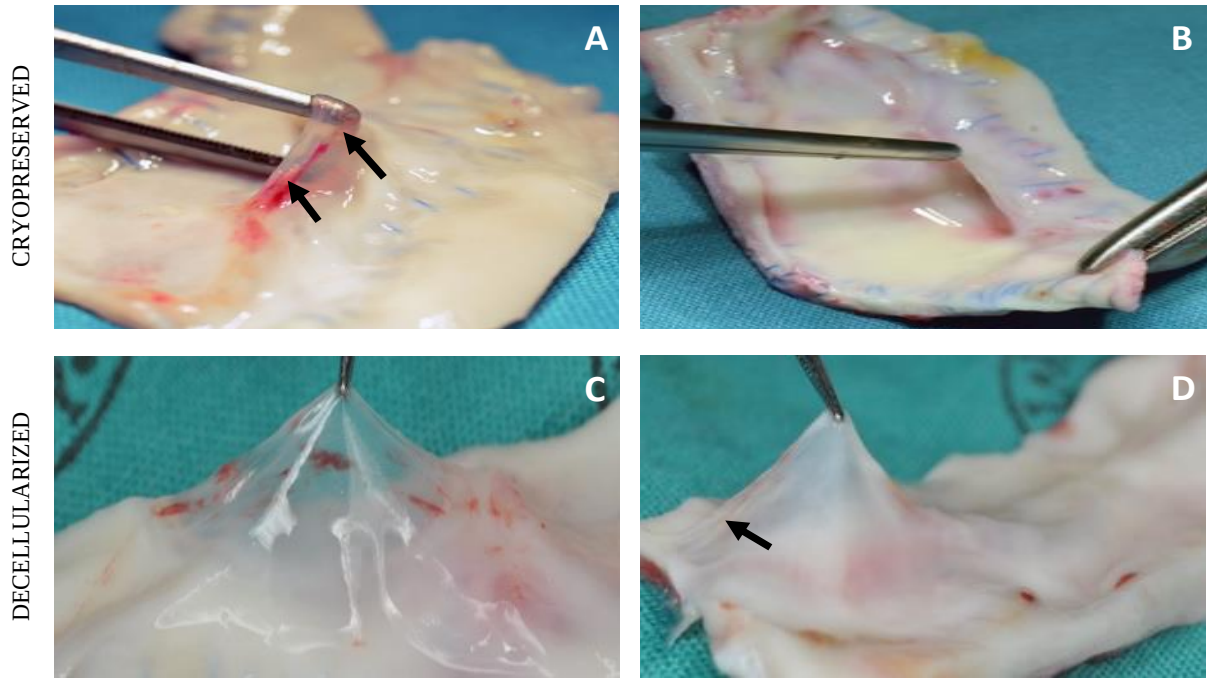

Figure 3: Representative images of gross morphology of cryopreserved (n = 5) **(A,B)** and decellularized (n = 5) **(C,D)** valves at explantation. Leaflets were thin **(A)** and slightly retracted **(B)** with calcific nodules (black arrows) in cryopreserved valves, and thin and translucent **(C,D)** in decellularized scaffolds.

The wall tissue of valves in both the cryopreserved and decellularized groups appeared very soft and pliable without visible signs of calcification or abnormalities (results not shown). Calcific deposits were clearly visible on radiographic evaluation on leaflets from valves in the cryopreserved group (Fig.4A), while valves in the decellularized group demonstrated single calcium deposits (Fig.4B). No calcific nodules were observed in the sinus wall tissue of either of the two groups, but calcification on the suture lines was clearly evident in both groups.

CRYOPRESERVED DECELLULARIZED

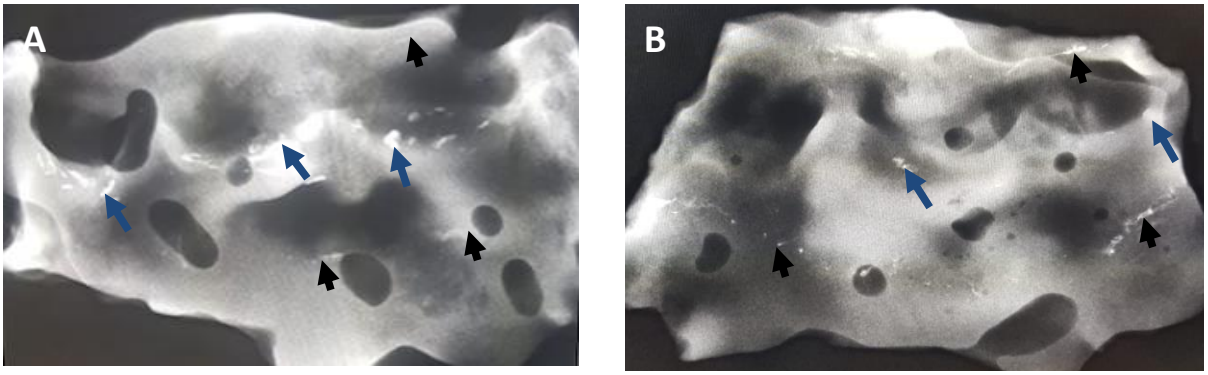

Figure 4: Representative radiographic images of calcific deposits (blue arrows) in valve tissue in the cryopreserved (n = 5) **(A)** and decellularized (n = 5) **(B)** groups. Calcification of the suture lines is clearly distinguishable (black arrows).

H&E staining of explanted valves demonstrated substantial loss of interstitial cells from the spongiosa layer (white arrow) of the leaflets in the cryopreserved group (Fig.5A) and extensive ingrowth and uniform distribution of host cells in the decellularized group (Fig.5D). Collagen appeared collapsed in the cryopreserved group, and well preserved but with larger pores between the fibers in the decellularized group. Calcific deposits (black arrows) were clearly evident on von Kossa stain in the leaflets of the cryopreserved group (Fig.5F), with no visible signs of calcification in the leaflets of the decellularized group (Fig.5H). No clear evidence of the presence of elastin could be demonstrated with modified von Gieson staining in the leaflets of any of the two groups (Fig.5J,L).

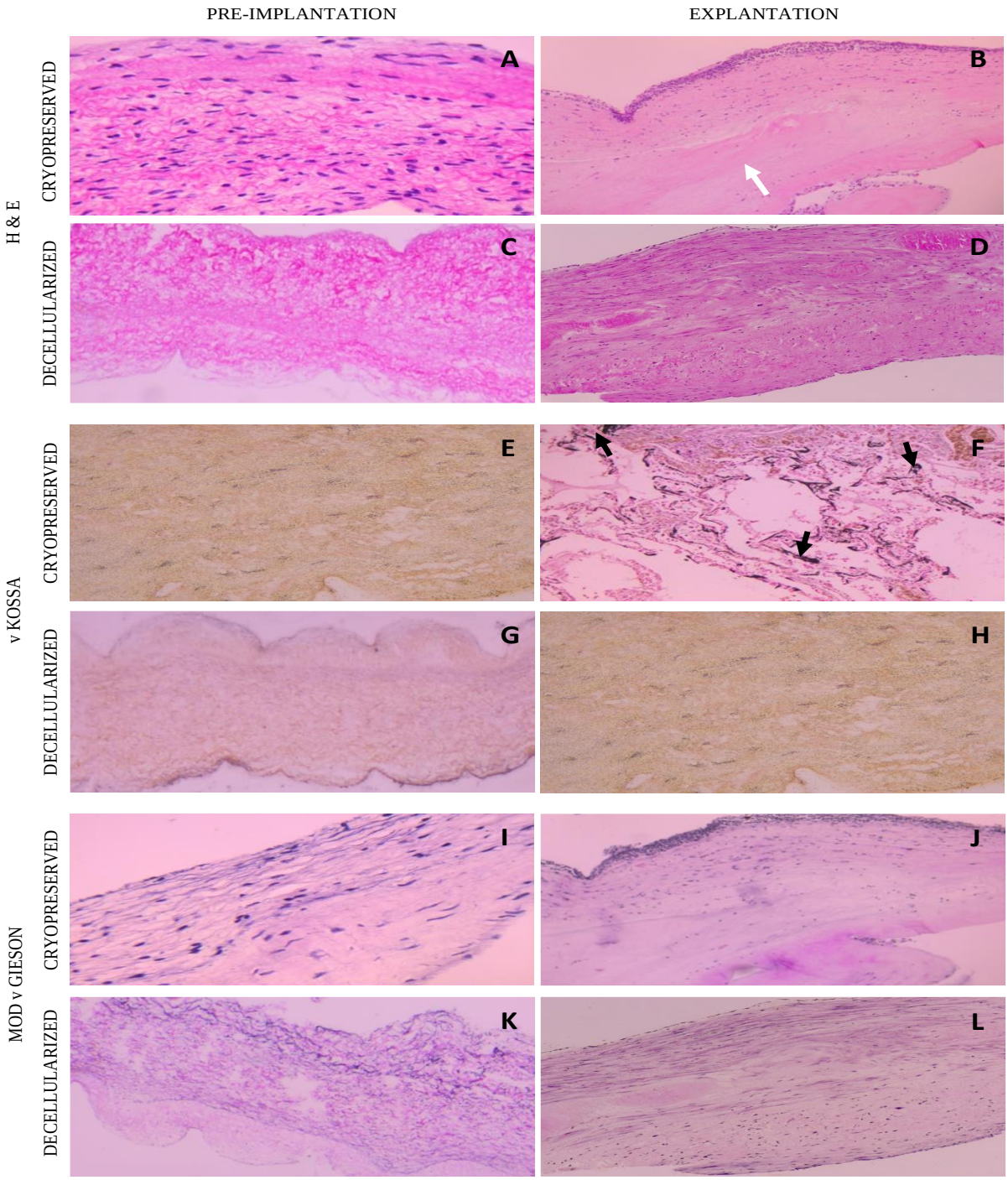

Figure 5: H&E stain of the leaflets of explanted valves demonstrates substantial cell loss in the cryopreserved group **(B)**, and extensive recellularization of host cells into the decellularized scaffold **(D)**. Collagen in the cryopreserved group is more collapsed, and well preserved with large interfibrillar spaces in the decellularized group. von Kossa stain only showed calcification in the cryopreserved group **(F)** and not in the decellularized group **(H)**, and no elastin could be shown with Modified von Gieson staining in any of the two groups **(J,L)** (n = 5).

Similar results were obtained for the wall tissue as for the leaflets, with uneven distribution of cells in the cryopreserved group (Fig.6B) and extensive recellularization in the decellularized scaffold (Fig.6D) on H&E staining. Collagen in the wall tissue appeared collapsed in the cryopreserved group, but well preserved with large pores in the decellularized group. Calcific deposits (black arrows) could only be demonstrated on von Kossa staining in the cryopreserved group (Fig.6F), and elastin fibers were present in both groups on Modified von Gieson staining (Fig.6J,L).

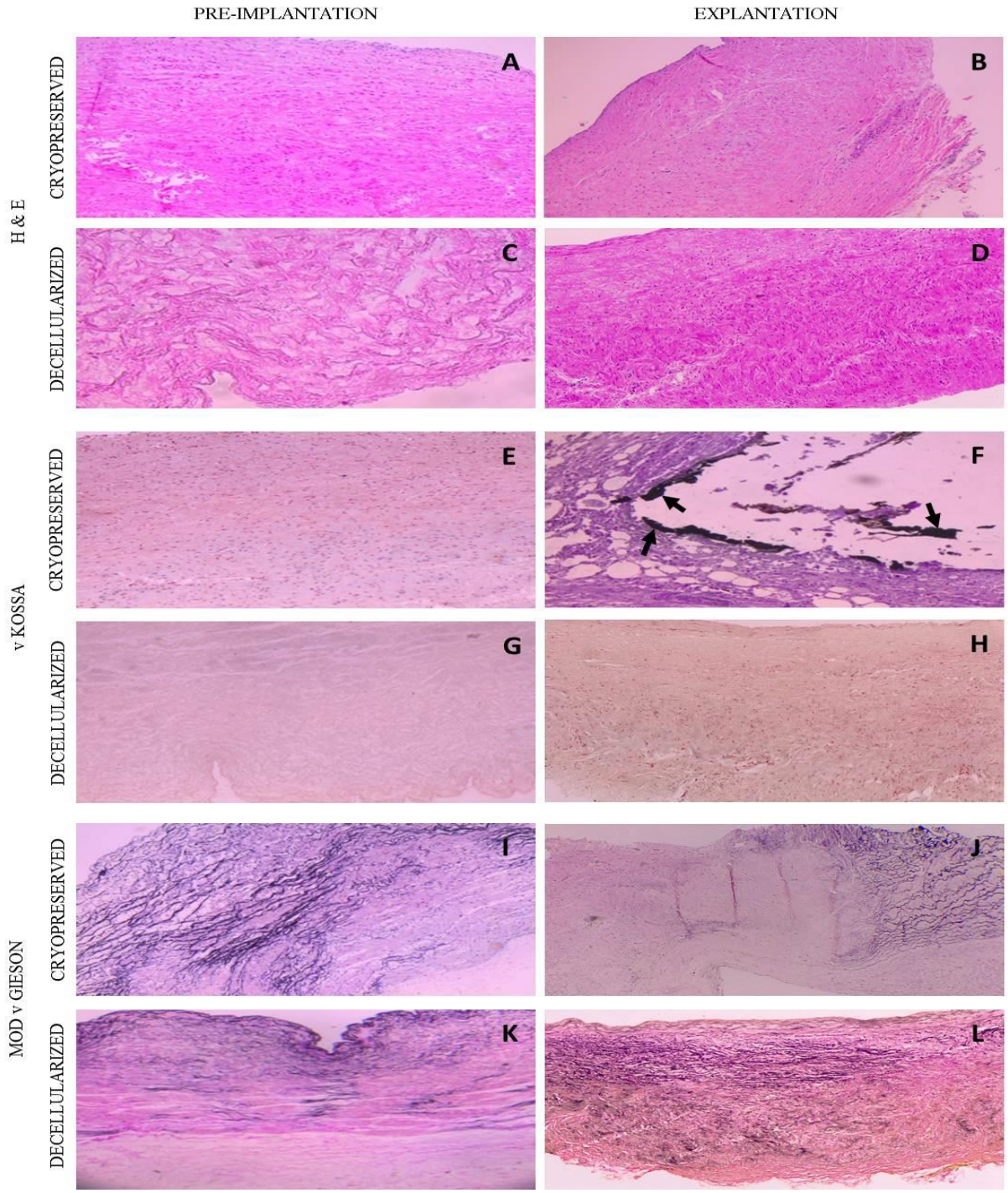

Figure 6: Representative photographs of pulmonary wall tissue, showing uneven distribution and loss of interstitial cells on H&E in the explanted cryopreserved group **(B)**, and extensive recellularization in the decellularized scaffold **(D)**. Collagen in the cryopreserved group appears collapsed, and is well maintained with large interfibrillar spaces in the decellularized group. Calcific deposits (black arrows) were demonstrated on von Kossa stain only in explants in the cryopreserved group **(F)** and not in the decellularized group **(H),** and elastin fibers were present on Modified von Gieson stain in explants in both groups **(J,L)** (n = 5).

H&E images were used to determine cells counts. The cell counts of the cryopreserved homografts decreased significantly ($p < 0.05$) for both leaflet and wall tissue in the explants compared to pre-implanted homografts (Table 3).

Table 3: Cell counts based on H&E images of the leaflets and walls of cryopreserved pulmonary homografts after 48 h ischaemia before implantation (n = 5) and when explanted after 180 days (n = 5).

Variable	Pre-implant	180 day explant	95 % CI Pre-implant vs. explant
Leaflet	456 [299.50-583.50]	95.00 [70.00-119.00]	194.00; 499.00*
Wall	530 [355.50-572.00]	103 [71.00-145.00]	227.00; 478.00*

Data presented as median [InterQuartile range], and the 95 % confidence interval (CI) of the pre-implant and explant at day 180 (*$p < 0.05$).

Decellularized homografts contained no cells at implantation. As indicated by the H&E images (Fig.5D and Fig.6D), the leaflets and wall tissue of the decellularized homografts were repopulated with host cells at explantation. Based on the cell counts, the leaflets and wall tissue of the explanted decellularized homografts contained significantly ($p < 0.05$) more cells than that of the cryopreserved homografts at explantation (Table 4).

Table 4: Comparison of cell counts of the leaflets and walls of explanted cryopreserved (n = 5) and decellularized pulmonary homografts (n = 5) based on H&E images.

Variable	Group 1	Group 2	95 % CI Group 1 vs. Group 2
Leaflet	95.00 [70.00-119.00]	177.00 [157.00-193.50]	-107.00; -22.00*
Wall	103.00 [71.00-145.00]	421.00 [358.00-473.00]	-381.00; -235.00*

Data presented as median [InterQuartile range], and the 95 % confidence interval (CI) of the pre-implant and explant at day 180 (* $p < 0.05$). [Group 1 = Cryopreserved, Group 2 = Decellularized].

SEM demonstrated monolayer endothelial cell coverage of both the leaflets and walls in the cryopreserved group (Fig.7A,B) as well as in the decellularized group (Fig.7C,D), with only limited areas of exposed collagen networks (white arrow) visible.

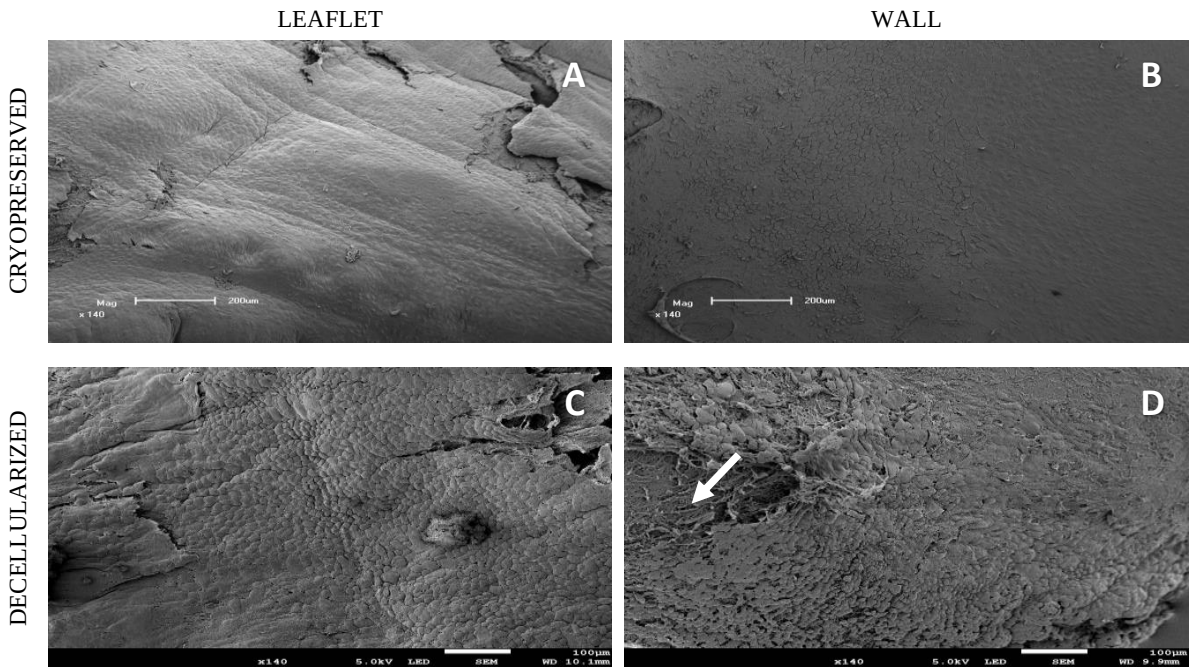

Figure 7: Representative scanning electron microscopy (SEM) images demonstrating a monolayer of endothelial cells covering the leaflets and walls of cryopreserved valve explants (n = 5) **(A,B)** and decellularized valve explants **(C,D)**, with small areas of exposed collagen (white arrow) visible in the walls of the decellularized group (n = 5). (Scale 200 μM **(A,B)** and Scale 100 μM **(C,D)**).

TEM demonstrated the presence of living cells in the leaflets (Fig.8A,C) and walls (Fig.8B,D) of valves in both cryopreserved and decellularized homografts at explantation, with numerous vacuoles or vesicles (black arrows) present in the cytoplasm. However, the number of interstitial cells that repopulated the decellularized scaffold was significantly higher ($p < 0.05$) than those in the cryopreserved tissue (as seen on H&E, Table 4).

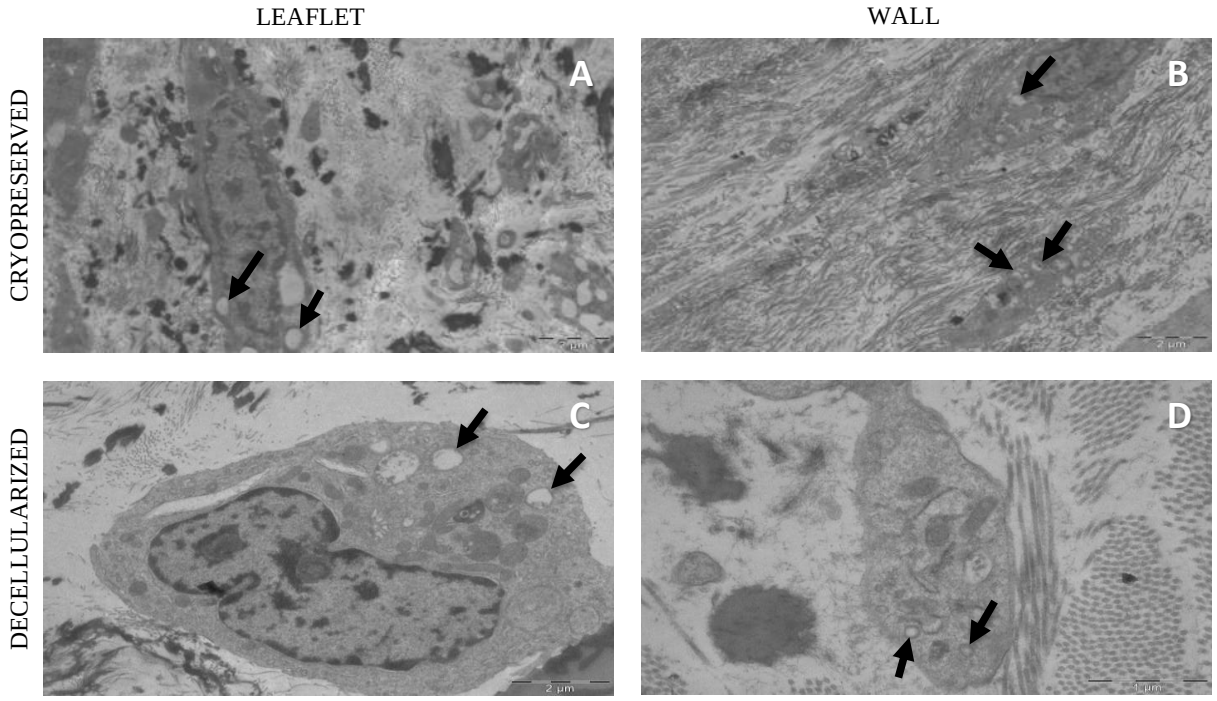

Figure 8: Representative transmission electron microscopy (TEM) images demonstrating the presence of living cells in leaflets and walls of explanted cryopreserved (n = 5) **(A,B)** and decellularized valves (n = 5) **(C,D)**. Numerous vesicles (black arrows) were present in all the cells.

On higher magnification (x 34000), new cells in the leaflets (Fig.9A) and walls (Fig.9B) of the decellularized scaffolds demonstrated the presence of rough endoplasmic reticulum (black arrows), however, no rough ER was visible in the cells in the cryopreserved group.

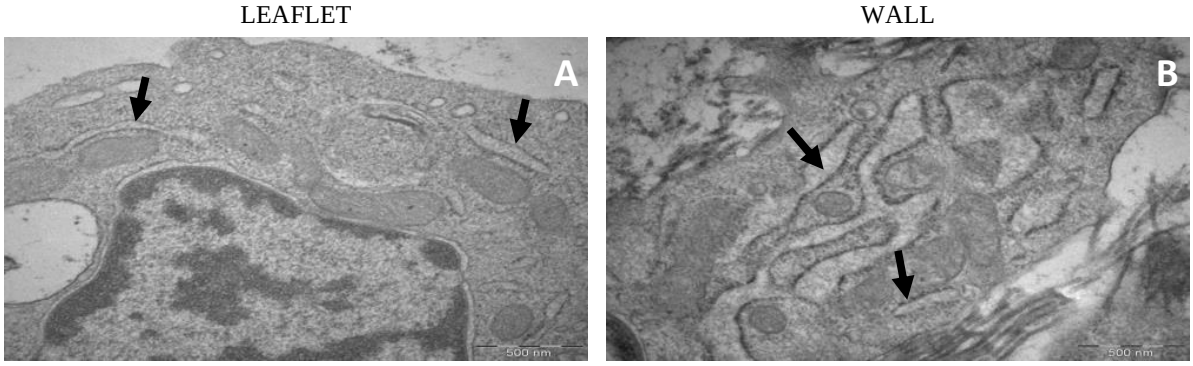

Figure 9: Representative images of repopulated interstitial cells in the leaflet and wall tissue of decellularized scaffolds demonstrate rough endoplasmic reticulum (black arrows), responsible for the production of new collagen (n = 5) **(A,B)**. (x 34000 magnification).

The TS and YM of the explanted cryopreserved homografts leaflets and the TS of the wall tissue did not change compared to the pre-implantation values. However, a significant increase ($p < 0.05$) was observed in the YM of the wall tissue on explantation (Table 5).

Table 5: TS and YM of the leaflets and walls of cryopreserved pulmonary homografts after 48 h ischaemia before implantation (n = 5) and when explanted after 180 days (n = 5).

Variable		Pre-implant	180 day explant	95 % CI Pre-implant vs. explant
Leaflets	TS (MPa)	3.72 [3.12-5.01]	4.67 [2.56-7.17]	-4.59; 3.09
	YM (MPa)	23.34 [14.12-28.87]	23.07 [14.99-38.10]	-29.11; 15.46
Walls	TS (MPa)	1.80 [1.35-2.65]	1.72 [1.37-2.49]	-0.98; 1.01
	YM (MPa)	1.97 [1.22-3.18]	5.15 [3.42-7.54]	-6.09; -0.29*

Data presented as median [InterQuartile range], and the 95 % confidence interval (CI) of the pre-implant and explant at day 180 (*$p < 0.05$). [TS = tensile strength; YM = Young's modulus].

The TS and YM of the explanted decellularized homograft leaflets and walls increased compared to the pre-implantation values. However, the only significant increase ($p < 0.05$) was observed in the YM of the explanted homograft wall tissue (Table 6).

Table 6: TS and YM of leaflets and walls of decellularized pulmonary homografts after 48 h ischaemia before implantation (n = 5) and when explanted after 180 days (n = 5).

Variable		Pre-implant	180 day explant	95 % CI Pre-implant vs. explant
Leaflets	TS (MPa)	1.83 [0.01-5.65]	6.06 [2.18-10.69]	-10.68; 3.12
	YM (MPa)	22.10 [0.10-55-27]	50.73 [21.6-118.1]	-118.00; 33.29
Walls	TS (MPa)	2.39 [1.73-3.71]	7.92 [1.29-12.64]	-1.77; 10.63
	YM (MPa)	2.32 [1.82-2.88]	16.35 [8.67-24.05]	-22.04; -6.095*

Data presented as median [InterQuartile range], and the 95 % confidence interval (CI) of the pre-implant and explant at day 180 (*$p < 0.05$). [TS = tensile strength; YM = Young's modulus].

Calcification was markedly reduced in the decellularized group compared to the cryopreserved group. The amount of calcium in the wall tissue of the cryopreserved group was significantly higher ($p < 0.05$) compared to the decellularized group (Table 7).

Table 7: Comparison of quantitative calcium content (µg calcium per mg tissue) between cryopreserved (n = 5) and decellularized pulmonary homograft (n = 5) leaflet and wall tissue after 180 days implantation.

Variable	Group 1	Group 2	95 % CI Group 1 vs. Group 2
Leaflet	16.00 [13.70-354.10]	2.38 [0.97-41.46]	-42.16 ; 684.0
Wall	769.50 [113.90-1210]	0.49 [0.40-0.82]	39.37 ; 1262*

Data presented as median [InterQuartile range], and the 95 % CI of the difference between the cryopreserved and decellularized groups (*$p < 0.05$). [Group 1 = Cryopreserved; Group 2 = Decellularized].

DISCUSSION

Cryopreserved pulmonary homografts remain the gold standard for RVOT reconstruction and Ross procedures. However, due to their limited availability and durability in especially paediatric patients, alternative processing methods have been investigated. Increasing the post-mortem ischaemic harvesting time for cryopreserved homografts from 24 h to 48 h can increase the potential donor pool for pulmonary homografts (Smit et al., 2015; Bester et al., 2018). The increase in the ischaemic harvesting time yielded good valve performance; however, the homografts contained non-viable cells (Smit et al., 2015). The remaining cellular remnants might lead to immune reactions in recipients and contribute towards premature conduit failure.

Removing all the cellular content and DNA material from a homograft valve through decellularization, results in an implant that significantly reduces the immunologic response from the recipient (Crapo et al., 2011; Bibevski et al., 2017). Our devised decellularization protocol, consisting of a 48 h ischaemic period, antibiotic sterilization, osmotic shock, multi-detergents and Benzonase as enzymatic treatment, proved to be efficient for the decellularization of sheep pulmonary homografts. Decellularization was also confirmed with DAPI and H&E staining, demonstrating that collagen fibers were slightly more loosely organized with larger spaces between the fibers (Manuscript 1). Both cryopreserved homografts and decellularized scaffolds maintained good haemodynamic characteristics and valve function after implantation in a juvenile ovine model, and no calcification or aneurysm formation could be demonstrated on echocardiography. Only three animals displayed transvalvular gradients above 15 mm Hg immediately post-surgery, which all decreased over the study period (Table 2).

Annulus diameter in the cryopreserved and decellularized groups increased over time, but with no significant difference when compared (Table 1). Interstitial cells were progressively lost from the wall tissue and the spongiosa and fibrosa layers of the leaflets in the cryopreserved group after 6 months, and the mild increase in diameter of the cryopreserved homografts could be attributed to annular dilatation rather than annular growth. Cryopreserved pulmonary homografts displayed increased distensibility of up to 30% when compared to aortic homografts (Vesely et al., 2000), which could also result in mild or even moderate annular dilatation without any significant central valve leakage. The growth potential of implanted decellularized valves depend on the recellularization by metabolically active recipient's cells (Sarikouch et al., 2016).
Decellularized homografts in this study were extensively repopulated, which could be an indication of the growth potential of these homografts.

Over time, significant central regurgitation (3/4) was observed with echocardiography in four of the valves from the cryopreserved group (Fig.2A), correlating with the thickening and leaflet retraction as seen on macroscopic evaluation after explantation (Fig.3A,B). Homografts in the decellularized group demonstrated good haemodynamic performance with only trivial (1/4) regurgitation observed in two valves (Fig.2B). This result could indicate that there was potential annulus growth in the decellularized valves and not simply dilatation of the valve annulus with decreased coaptation of the leaflets and resultant central leakage. Erdbrügger and co-workers also reported similar findings of annulus growth with decellularized porcine pulmonary valves used for pulmonary valve replacement (Erdbrugger et al., 2006). Native valves will physiologically increase in annular size as the individual grows, while annular growth of autologous pulmonary valves that were transplanted into the aortic position of young growing children were reported by Elkins et al., (1994). Although decellularized pulmonary homografts will not necessarily behave in a similar manner to pulmonary autografts in the aortic position, the ideal implanted heart valve or scaffold should have similar growth potential as that of transplanted autologous valves, to allow paediatric patients an extended period free from reoperation.

There was no significant difference in the increase in transvalvular gradients between homografts in the cryopreserved or decellularized group. In the clinical setting, gradients frequently develop

over the implanted valve in the first few months following RVOT reconstruction, especially in children (Carr-White et al., 2001). The late increase in gradients in the decellularized group could be as a result of the sheep adding almost half their bodyweight since implantation, resulting in the homograft diameters becoming too small and slightly obstructive. Decellularized valve scaffolds displayed excellent haemodynamic characteristics with transvalvular gradients never rising above 16mm Hg, and only as high as 22mm Hg in the cryopreserved group (Table 2). Brown and co-workers reported similar findings of improved haemodynamic function of decellularized CryoValve® SG homografts (CryoLife, Inc, Kennesaw, GA, USA) compared to cryopreserved homografts in the pulmonary position, possibly due to decreased antigenicity, which could improve long-term outcomes (Brown et al., 2010). Findings by da Costa and co-workers also confirmed that SDS decellularized allografts implanted in the pulmonary position were associated with lower gradients when compared with conventional cryopreserved allografts (da Costa et al., 2014), and decellularized aortic allografts in the aortic position showed good structural integrity, low calcification rates and adequate haemodynamic performance (da Costa et al., 2010).

Explanted leaflet and wall tissue samples in the cryopreserved and decellularized groups demonstrated an endothelial-like multi-layer cell coverage on H&E staining (Fig.5B,D and Fig.6B,D). Interstitial cellularity in the cryopreserved valve leaflets and wall tissue was progressively lost during the implantation period and leaflet cellularity was mainly confined to the leaflet margins. Similar findings were also reported by other authors (Quinn et al., 2011), and the steady decline in the cellularity of cryopreserved allografts will eventually result in a cell-free but structurally intact collagen matrix (Armiger, 1998) which is not cell conductive. Similar to the current study, previous studies in our center confirmed this gradual loss of interstitial cells from implanted cryopreserved homografts (Smit et al., 2015). The decellularized scaffold group demonstrated extensive uniform repopulation with autologous interstitial cells in the leaflet and wall tissue. Similar findings were reported by Dohmen and co-workers in another study on sheep, arguing that matrix repopulation with interstitial cells will create the possibility for interstitial cells to differentiate into myofibroblasts and fibroblasts, which could begin the production of collagen, elastin and other extracellular matrix proteins (Dohmen et al., 2006). Cell counts indicated that both leaflets and walls were not yet completely repopulated when compared

to cryopreserved tissue pre-implantation, and incomplete recellularization of decellularized porcine valves implanted in sheep were also reported by (Dohmen et al., 2003). Recellularization of the decellularized scaffolds with recipient endothelial and interstitial cells can potentially create a valve with viable living tissue that can reduce the inflammatory response to the implant, maintain valve architecture and function, and mitigate calcification. The possible roles of intimal hyperplasia in the leaflets and the adventitial reaction on the conduits in the repopulation of the decellularized homografts can also not be excluded, and a more detailed characterization of the repopulated cells using immunohistochemical investigations will be required.

Furthermore, the results obtained for cardiovascular devices that were tested *in vivo* in animal implants cannot simply be translated to *in vivo* clinical outcomes in the human setting. Despite providing invaluable information in a physiological environment, data from animal implants may not accurately predict device performance in humans due to differences in anatomy and physiology, limited numbers and lack of extended implantation periods (Zhang et al., 2019).

SEM confirmed endothelial cell coverage of leaflet and wall tissue in both groups (Fig.7A,B and Fig.7C,D). However, cells were present on the cryopreserved homograft before implantation (Manuscript 1) and it was not evaluated whether the cells present on the explant were of donor or recipient origin. Re-endothelialization in the decellularized scaffold group, as well as an intact collagen network, could be observed with SEM (Fig.7C,D). Recellularization of the decellularized scaffolds with recipient endothelial and interstitial cells will create valvular tissue with viable cells that can reduce the inflammatory response to the implant, maintain valve architecture and function, and mitigate calcification.

TEM demonstrated interstitial cells with fairly large nuclei, which is characteristic of young fibroblast cells (Dohmen et al., 2006). In the decellularized scaffold group and to a lesser extent in the cryopreserved group, these interstitial cells demonstrated numerous vacuoles (secretory vacuoles) in the cytoplasm (Fig.8), which are the cellular structures from where new pro-collagen is likely to be produced later on for maintenance and remodeling of the tissue. These vacuoles are normally associated with the transport of protein complexes synthetized in the rough endoplasmic reticulum, to the Golgi apparatus (Hodgson et al., 1990). Many of these

vacuoles may contain short collagen fibrils that are embedded in the cytoplasm and then enclosed by the vacuoles, making them more mature and playing an important role in the secretion of procollagen from the cell (Canty and Kadler, 2005). The presence of these collagen-containing vacuoles is a clear indicator of protein synthesis in the cells, and might be an important indicator of young fibroblast cells actively involved in the production of new collagen fibrils and bundles and the remodeling of the implanted scaffold. Although similar findings were reported for the Matrix P and Matrix P Plus valves (decellularized xenograft valve), histological studies revealed poor cell ingrowth and low neovascularization. Conduit stenosis was a common cause of valve failure after <3 years implantation and growth potential of the valve could not be demonstrated following implantation in the human setting (Blum et al., 2018).

The synthesis of proteins to be used for activities within the cells, like cytoplasmic filament formation, begins in the free polyribosomes in the cytoplasm. When these polyribosomes are attached to the endoplasmic reticulum (ER), synthesized proteins travel to the Golgi apparatus and are destined for secretion, lysosomes, plasma, ER or Golgi membranes (Cross & Mercer, 1993). The presence of rough ER in the cytoplasm of repopulated interstitial cells in the leaflet and wall tissue of the decellularized homografts (Fig.9), as observed with TEM, is a clear indication for the maintenance and remodeling potential of the collagen scaffold of the implanted valve, as the rough ER will start to produce new collagen (Dohmen et al., 2006).

The wall tissue of cryopreserved homografts remained mostly soft and pliable at explantation, but the areas where calcific nodules were observed, becoming more rigid and stiff. The calcium content was significantly reduced in the decellularized group compared to the cryopreserved group (Table 7). The decellularization of the homograft valve resulted in a collagen matrix that was still functional and was repopulated by recipient cells, allowing for remodeling of the tissue and mitigating the calcification thereof. Following explantation, very little indication of calcification and no sign of leaflet retraction could be demonstrated in the leaflets or wall tissue of the decellularized group (Fig.3C,D). Calcification of wall and/or leaflet tissue, which could negatively influence valve performance, together with the hydrolysis of the extracellular matrix during storage in PBS at 4^{o}C (Hopkins et al., 2009), was not observed in the decellularized scaffold group.

In this study, leaflets of explanted cryopreserved valves revealed different early signs of long-term valve degeneration, i.e. nodules of calcification and leaflet thickening (Fig.3A,B). In a recent study, Biermann and co-workers also observed leaflet thickening as well as moderate T-cell infiltration, which is responsible for early valve degeneration, in the leaflets of cryopreserved pulmonary valves in a juvenile sheep model (Biermann et al., 2019). Leaflet infiltration with mononuclear cells followed by swelling of the leaflets and loss of cellularity results in the destruction of the leaflets (Legare et al., 2000). However, no signs of inflammatory reaction or infiltration of mononuclear cells were observed on H&E in the current study. Homografts containing viable endothelium and interstitial cells with immunogenic epitopes will elicit an immune response (Jane-Wit et al., 2013). In this study, with a harvesting time in excess of 24 h, endothelial viability is unlikely (Smit et al., 2015), which could account for the lack of an immune response towards the cryopreserved homografts. Calcific deposits were observed in the leaflet and pulmonary wall tissue of explanted cryopreserved homografts (Fig.5F and Fig.6F) following von Kossa staining, while no calcific deposits were observed in the decellularized scaffolds (Fig.5H and Fig.6H). Similarly, da Costa and co-workers also reported no significant calcification of decellularized porcine heterografts up to 150 days of observation in young sheep (da Costa et al., 2004). No mineralization in the cusps or vascular parts of fresh decellularized or decellularized, freeze-dried and rehydrated pulmonary allografts after six months implantation in the RVOT of sheep was also reported by Goecke et al., (2018). In the current study, the formation of calcific deposits observed in the explanted cryopreserved homografts is most probably a result of the loss of cellularity and layered architecture due to cryopreservation, creating non-viable valve tissue that is prone to tissue degeneration (Numata et al., 2004). Our group also previously observed disruption and damage to the collagen scaffold after cryopreservation (Bester et al., 2018). Cryopreservation also leads to interstitial ice formation in conventionally cryopreserved heart valves, which may cause damage to the extracellular matrix and make valves prone to calcification (Brockbank et al., 2000). Altered tissue structure with edema and vacuolization within the leaflet spongiosa and irreversible cell damage of homografts after cryopreservation was previously reported (Fischlein et al., 1994), making the cryopreserved allograft tissue more likely to calcify and degenerate.

No calcific nodules were seen on radiological evaluation in the sinus wall tissue of valves in any of the two groups, but despite mitigating the calcification of leaflets and walls, decellularization could not protect the tissue against calcifications in the suture lines. Calcification of the suture lines is a common finding in sheep RVOT reconstructions, and is most probably as a result of surgical injury to the native tissue, causing inflammatory reactions and tissue calcification (Hopkins et al., 2009).

The strength of neither leaflet or wall tissue in the cryopreserved or decellularized group decreased over time. The increase in stiffness of the wall tissue of the explanted cryopreserved valves, when compared to the pre-implant values (Table 5), are largely attributed to the damage to the collagen scaffold after cryopreservation, resulting in early calcification of the tissue. In a study on aortic valve implants, the increase in local stiffness of aortic valve leaflets was also associated with the formation of calcific nodules, and combined with the disruption of the ECM will lead to further calcification. These calcific nodules will eventually result in localized disturbances in the biomechanical behaviour of the tissue (Gomel et al., 2019). Stiffness of leaflets and wall tissue in the decellularized homografts increased over the implantation period (Table 6), probably as a result of the extensive repopulation of the ECM *in vivo*, filling up the larger interfibrillar spaces that were created during decellularization. Similar findings were reported in a study with decellularized xenograft valves that were implanted into sheep, where the increased stiffness of the valve cusps was attributed to the infiltration of collagen-synthesizing myofibroblast-like cells (Hennessy et al., 2017).

LIMITATIONS OF THE STUDY

A limitation of this study is the small number of juvenile sheep that were investigated. The juvenile ovine model currently represents the best preclinical model to evaluate the potential for differentially processed homograft heart valve calcification in humans. However, the direct translation of the results from this study to human subjects cannot be made based on the ovine model used. A primate model should be used to relate the results from this study directly to humans. Tensile strength and Young's modulus data should always be treated with caution, due to the difficulty of getting repeatable results when working with such small tissue samples and

low numbers. Immunohistochemical investigations of the repopulated interstitial cells to allow more detailed characterization will also be required.

CONCLUSION

Decellularization of homografts, with a post-mortem cold ischaemic harvesting time of 48 h, successfully retained the haemodynamic characteristics and tissue properties of pulmonary valves, while significantly mitigating calcification. Cryopreservation was less successful in protecting the homograft from calcification, and leaflet thickening and retraction resulted in significant valve regurgitation that will ultimately lead to right heart failure. Successful repopulation of the decellularized scaffold with host interstitial cells presenting with rough endoplasmic reticulum, will promote tissue maintenance and remodeling and potentially extend the durability of these implants in young patients. The potential of decellularized homografts to grow in diameter size while maintaining good leaflet coaptation and closure without developing valve regurgitation makes decellularization of pulmonary homografts, even after extended post-mortem ischaemic harvesting times, a promising alternative processing method for these homografts to be used in RVOT reconstruction in the clinical setting. The strength of decellularized tissue did not decrease once implanted in the circulatory system, while the tissue stiffness increased, most likely due to the repopulation of the ECM with host fibroblast cells.

CONFLICT OF INTEREST

We certify that all authors named in the manuscript deserve authorship, and that all authors have agreed to be listed in the manuscript when submitted to peer review journals. The authors have no conflicts of interest to declare.

ACKNOWLEDGEMENTS

We would like to thank Miss H Grobler from the Centre for Electron Microscopy for all the tissue preparation for SEM and TEM, the UFS Experimental Animal Unit for their assistance, Department of Anaesthesiology and all perfusion technologists.

REFERENCES

ALI, M. L., KUMAR, S. P., BJORNSTAD, K. & DURAN, C. M. 1996. The sheep as an animal model for heart valve research. *Cardiovasc Surg*, 4, 543-9.

ARMIGER, L. C. 1998. Postimplantation leaflet cellularity of valve allografts: Are donor cells beneficial or detrimental? *Ann Thorac Surg*, 66(6 Suppl), S233-5.

BAKHACH, J. 2009. The cryopreservation of composite tissues: Principles and recent advancement on cryopreservation of different type of tissues. *Organogenesis*, 5, 119-26.

BESTER, D., BOTES, L., VAN DEN HEEVER, J. J., KOTZE, H., DOHMEN, P., POMAR, J. L. & SMIT, F. E. 2018. Cadaver donation: structural integrity of pulmonary homografts harvested 48 h post mortem in the juvenile ovine model. *Cell Tissue Bank*, 19, 743-754.

BESTER, D., SMIT, F. E., VAN DEN HEEVER, J. J., BOTES, L. & DOHMEN, P. M. C. E. 2017. *Detoxification and stabilization of implantable or transplantable biological material*. EU. 16792990.0-1455.

BIBEVSKI, S., RUZMETOV, M., FORTUNA, R. S., TURRENTINE, M. W., BROWN, J. W. & OHYE, R. G. 2017. Performance of SynerGraft Decellularized Pulmonary Allografts Compared With Standard Cryopreserved Allografts: Results From Multiinstitutional Data. *Ann Thorac Surg*, 103, 869-874.

BIERMANN, A. C., MARZI, J., BRAUCHLE, E., WICHMANN, J. L., ARENDT, C. T., PUNTMANN, V., NAGEL, E., ABDELAZIZ, S., WINTER, A. G., BROCKBANK, K. G. M., LAYLAND, S., SCHENKE-LAYLAND, K. & STOCK, U. A. 2019. Improved long-term durability of allogeneic heart valves in the orthotopic sheep model. *Eur J Cardiothorac Surg*, 55, 484-493.

BLUM, K. M., DREWS, J. D. & BREUER, C. K. 2018. Tissue-Engineered Heart Valves: a Call for Mechanistic Studies. *Tissue Eng, Part B: Rev*, 24(3), 240-253.

BOTES, L., VAN DEN HEEVER, J. J., SMIT, F. E. & NEETHLING, W. M. 2012. Cardiac allografts: a 24-year South African experience. *Cell Tissue Bank*, 13, 139-46.

BOURGINE, P. E., PIPPENGER, B. E., TODOROV, A., JR., TCHANG, L. & MARTIN, I. 2013. Tissue decellularization by activation of programmed cell death. *Biomaterials*, 34, 6099-108.

BROCKBANK, K. G., LIGHTFOOT, F. G., SONG, Y. C. & TAYLOR, M. J. 2000. Interstitial ice formation in cryopreserved homografts: a possible cause of tissue deterioration and calcification in vivo. *J Heart Valve Dis*, 9, 200-6.

BROWN, J. W., ELKINS, R. C., CLARKE, D. R., TWEDDELL, J. S., HUDDLESTON, C. B., DOTY, J. R., FEHRENBACHER, J. W. & TAKKENBERG, J. J. M. 2010. Performance of the CryoValve SG human decellularized pulmonary valve in 342 patients relative to the conventional CryoValve at a mean follow-up of four years. *J Thorac Cardiovasc Surg*, 139, 339-348.

CANTY, E. G. & KADLER, K. E. 2005. Procollagen trafficking, processing and fibrillogenesis. *J Cell Sci*, 118, 1341-53.

CARR-WHITE, G. S., KILNER, P. J., HON, J. K., RUTLEDGE, T., EDWARDS, S., BURMAN, E. D., PENNELL, D. J. & YACOUB, M. H. 2001. Incidence, location, pathology, and significance of pulmonary homograft stenosis after the Ross operation. *Circulation*, 104, I16-20.

CRAPO, P. M., GILBERT, T. W. & BADYLAK, S. F. 2011. An overview of tissue and whole organ decellularization processes. *Biomaterials*, 32, 3233-43.

CROSS, P. C. & MERCER, K. L. 1993. *Cell and Tissue Ultrastructure – a Functional Perspective*, WH Freeman, New York.

DA COSTA, F. D., COSTA, A. C., PRESTES, R., DOMANSKI, A. C., BALBI, E. M., FERREIRA, A. D. & LOPES, S. V. 2010. The early and midterm function of decellularized aortic valve allografts. *Ann Thorac Surg*, 90, 1854-60.

DA COSTA, F. D., TAKKENBERG, J. J., FORNAZARI, D., BALBI FILHO, E. M., COLATUSSO, C., MOKHLES, M. M., DA COSTA, A. B., SAGRADO, A. G., FERREIRA, A. D., FERNANDES, T. & LOPES, S. V. 2014. Long-term results of the Ross operation: an 18-year single institutional experience. *Eur J Cardiothorac Surg*, 46, 415-22; discussion 422.

DA COSTA, F. D. A., DOHMEN, P. M., LOPES, S. V., LACERDA, G., POHL, F., VILANI, R., AFFONSO DA COSTA, M. B., VIEIRA, E. D., YOSCHI, S., KONERTZ, W. & AFFONSO DA COSTA, I. 2004. Comparison of cryopreserved homografts and decellularized porcine heterografts implanted in sheep. *Artif Organs*, 28, 366-70.

DELMO WALTER, E. M., DE BY, T. M., MEYER, R. & HETZER, R. 2012. The future of heart valve banking and of homografts: perspective from the Deutsches Herzzentrum Berlin. *HSR Proc Intensive Care Cardiovasc Anesth*, 4, 97-108.

DIJKMAN, P. E., DRIESSEN-MOL, A., FRESE, L., HOERSTRUP, S. P. & BAAIJENS, F. P. 2012. Decellularized homologous tissue-engineered heart valves as off-the-shelf alternatives to xeno- and homografts. *Biomaterials*, 33, 4545-54.

DOHMEN, P. M., OZAKI, S., NITSCH, R., YPERMAN, J., FLAMENG, W. & KONERTZ, W. 2003. A tissue engineered heart valve implanted in a juvenile sheep model. *Med Sci Monit*, 9(4), 97-104.

DOHMEN, P. M., DA COSTA, F., HOLINSKI, S., LOPES, S. V., YOSHI, S., REICHERT, L. H., VILLANI, R., POSNER, S. & KONERTZ, W. 2006. Is there a possibility for a glutaraldehyde-free porcine heart valve to grow? *Eur Surg Res*, 38, 54-61.

ELKINS, R. C., KNOTT-CRAIG, C. J., WARD, K. E., MCCUE, C. & LANE, M. M. 1994. Pulmonary autograft in children: realized growth potential. *Ann Thorac Surg*, 57, 1387-93; discussion 1393-4.

ERDBRUGGER, W., KONERTZ, W., DOHMEN, P. M., POSNER, S., ELLERBROK, H., BRODDE, O. E., ROBENEK, H., MODERSOHN, D., PRUSS, A., HOLINSKI, S., STEIN-KONERTZ, M. & PAULI, G. 2006. Decellularized xenogenic heart valves reveal remodeling and growth potential in vivo. *Tissue Eng*, 12, 2059-68.

FISCHLEIN, T., SCHUTZ, A., UHLIG, A., FREY, R., KRUPA, W., BABIC, R., THIERY, J. & REICHART, B. 1994. Integrity and viability of homograft valves. *Eur J Cardiothorac Surg*, 8, 425-30.

FLAMENG, W., MEURIS, B., YPERMAN, J., DE VISSCHER, G., HERIJGERS, P. & VERBEKEN, E. 2006. Factors influencing calcification of cardiac bioprostheses in adolescent sheep. *J Thorac Cardiovasc Surg*, 132, 89-98.

GOECKE, T., THEODORIDIS, K., TUDORACHE, I., CIUBOTARU, A., CEBOTARI, S., RAMM, R., HOFFLER, K., SARIKOUCH, S., VASQUEZ RIVERA, A., HAVERICH, A., WOLKERS, W. F. & HILFIKER, A. 2018. In vivo performance of freeze-dried decellularized pulmonary heart valve allo- and xenografts orthotopically implanted into juvenile sheep. *Acta Biomater*, 68, 41-52.

GOFFIN, Y. A., VAN HOECK, B., JASHARI, R., SOOTS, G. & KALMAR, P. 2000. Banking of cryopreserved heart valves in Europe: assessment of a 10-year operation in the European Homograft Bank (EHB). *J Heart Valve* Dis, 9, 207-14.

GOMEL, M. A., LEE, R. & GRANDE-ALLEN, K. J. 2019. Comparing the Role of Mechanical Forces in Vascular and Valvular Calcification Progression. *Front Cardiovasc Med*, 5, 197-197.

HENNESSY, R. S., GO, J. L., HENNESSY, R. R., TEFFT, B. J., JANA, S., STOYLES, N. J., AL-HIJJI, M. A., THADEN, J. J., PISLARU, S. V., SIMARI, R. D., STULAK, J. M., YOUNG, M. D. & LERMAN, A. 2017. Recellularization of a novel off-the-shelf valve following xenogenic implantation into the right ventricular outflow tract. *PloS one,* 12, e0181614-e0181614.

HODGSON, A. N., CROSS, R. H. M. & BERNARD, R. T. F. 1990. *An Illustrated Introduction to the Ultrastructure of Cells*, Butterworths, Durban South Africa.

HOPKINS, R. A., JONES, A. L., WOLFINBARGER, L., MOORE, M. A., BERT, A. A. & LOFLAND, G. K. 2009. Decellularization reduces calcification while improving both durability and 1-year functional results of pulmonary homograft valves in juvenile sheep. *J Thorac Cardiovasc Surg*, 137, 907-13, 913e1-4.

JANE-WIT, D., MANES, T. D., YI, T., QIN, L., CLARK, P., KIRKILES-SMITH, N. C., ABRAHIMI, P., DEVALLIERE, J., MOECKEL, G., KULKARNI, S., TELLIDES, G. & POBER, J. S. 2013. Alloantibody and complement promote T cell-mediated cardiac allograft vasculopathy through noncanonical nuclear factor-kappaB signaling in endothelial cells. *Circulation*, 128, 2504-16.

JASHARI, R., DAENEN, W., MEYNS, B. & VANDERKELEN, A. 2004. Is ABO group incompatibility really the reason of accelerated failure of cryopreserved allografts in very young patients?--Echography assessment of the European Homograft Bank (EHB) cryopreserved allografts used for reconstruction of the right ventricular outflow tract. *Cell Tissue Bank*, 5, 253-9.

LAKER, L., DOHMEN, P. M. & SMIT, F. E. 2020. Synergy in a detergent combination results in superior decellularized bovine pericardial extracellular matrix scaffolds. *J Biomed Mater Res, Part B: Appl Biomater*. https://doi.org/10.1002/jbm.b.34588.

LEGARE, J. F., LEE, T. D., CREASER, K. & ROSS, D. B. 2000. T lymphocytes mediate leaflet destruction and allograft aortic valve failure in rats. *Ann Thorac Surg*, 70(4), 1238-45.

LEHR, E. J., RAYAT, G. R., CHIU, B., CHURCHILL, T., MCGANN, L. E., COE, J. Y. & ROSS, D. B. 2011. Decellularization reduces immunogenicity of sheep pulmonary artery vascular patches. *J Thorac Cardiovasc Surg*, 141, 1056-62.

LISY, M., KALENDER, G., SCHENKE-LAYLAND, K., BROCKBANK, K. G., BIERMANN, A. & STOCK, U. A. 2017. Allograft Heart Valves: Current Aspects and Future Applications. *Biopreserv Biobank*, 15, 148-157.

MEPHAM, B. L. 1991. *Theory and practice of histological techniquea, Third ed*, BANCROFT, J. D. & STEVENS, A. Edinburgh, Churchill Livingstone ISBN:0443035598.

NIH. 2011. *Guide for the Care and Use of Laboratory Animals, 8th ed.* [Online]. Washington DC: National Academy of Sciences. Available: https://www.ncbi.nlm.nih.gov/pubmed/21595115.

NUMATA, S., FUJISATO, T., NIWAYA, K., ISHIBASHI-UEDA, H., NAKATANI, T. & KITAMURA, S. 2004. Immunological and histological evaluation of decellularized allograft in a pig model: comparison with cryopreserved allograft. *J Heart Valve Dis*, 13, 984-90.

QUINN, R. W., HILBERT, S. L., BERT, A. A., DRAKE, B. W., BUSTAMANTE, J. A., FENTON, J. E., MORIARTY, S. J., NEIGHBORS, S. L., LOFLAND, G. K. & HOPKINS, R. A. 2011. Performance and Morphology of Decellularized Pulmonary Valves Implanted in Juvenile Sheep. *Ann Thorac Surg*, 92, 131–7.

ROMEO, J. L. R., PAPAGEORGIOU, G., VAN DE WOESTIJNE, P. C., TAKKENBERG, J. J. M., WESTENBERG, L. E. H., VAN BEYNUM, I., BOGERS, A. & MOKHLES, M. M. 2018. Downsized cryopreserved and standard-sized allografts for right ventricular outflow tract reconstruction in children: long-term single-institutional experience. *Interact Cardiovasc Thorac Surg*, 27, 257-263.

SARIKOUCH, S., HORKE, A., TUDORACHE, I., BEERBAUM, P., WESTHOFF-BLECK, M., BOETHIG, D., REPIN, O., MANIUC, L., CIUBOTARU, A., HAVERICH, A. & CEBOTARI, S. 2016. Decellularized fresh homografts for pulmonary valve replacement: a decade of clinical experience. *Eur J Cardiothorac Surg*, 50, 281-90.

SCHOEN, F. J. 2008. Evolving concepts of cardiac valve dynamics: the continuum of development, functional structure, pathobiology, and tissue engineering. *Circulation*, 118, 1864-80.

SELAMET TIERNEY, E. S., GERSONY, W. M., ALTMANN, K., SOLOWIEJCZYK, D. E., BEVILACQUA, L. M., KHAN, C., KRONGRAD, E., MOSCA, R. S., QUAEGEBEUR, J. M. & APFEL, H. D. 2005. Pulmonary position cryopreserved homografts: durability in pediatric Ross and non-Ross patients. *J Thorac Cardiovasc Surg*, 130, 282-6.

SMIT, F. E., BESTER, D., VAN DEN HEEVER, J. J., SCHLEGEL, F., BOTES, L. & DOHMEN, P. M. 2015. Does prolonged post-mortem cold ischaemic harvesting time influence cryopreserved pulmonary homograft tissue integrity? *Cell Tissue Bank*, 16, 531-44.

SPURR, A. R. 1969. A low-viscosity epoxy resin embedding medium for electron microscopy. *J Ultrastruct Res*, 26, 31-43.

TAKKENBERG, J. J., VAN HERWERDEN, L. A., EIJKEMANS, M. J., BEKKERS, J. A. & BOGERS, A. J. 2002. Evolution of allograft aortic valve replacement over 13 years: results of 275 procedures. *Eur J Cardiothorac Surg*, 21, 683-91; discussion 691.

THUBRIKAR, M. J., DECK, J. D., AOUAD, J. & NOLAN, S. P. 1983. Role of mechanical stress in calcification of aortic bioprosthetic valves. *J Thorac Cardiovasc Surg*, 86, 115-25.

TWEDDELL, J. S., PELECH, A. N., FROMMELT, P. C., MUSSATTO, K. A., WYMAN, J. D., FEDDERLY, R. T., BERGER, S., FROMMELT, M. A., LEWIS, D. A., FRIEDBERG, D. Z., THOMAS, J. P., JR., SACHDEVA, R. & LITWIN, S. B. 2000. Factors affecting longevity of homograft valves used in right ventricular outflow tract reconstruction for congenital heart disease. *Circulation*, 102, III130-5.

VESELY, I., CASAROTTO, D. C. & GEROSA, G. 2000. Mechanics of cryopreserved aortic and pulmonary homografts. *J Heart Valve Dis*, 9(1), 27-37.

ZHANG, B. L., BIANCO, R. W. & SCHOEN, F. J. 2019. Preclinical Assessment of Cardiac Valve Substitutes: Current Status and Considerations for Engineered Tissue Heart Valves. *Front Cardiovasc Med*, 6, 72.

Chapter 5 - Manuscript 3

Comparison of function and structural integrity of decellularized pulmonary homografts versus decellularized, glutaraldehyde-fixed and detoxified pulmonary homografts after 180 days implantation in the juvenile ovine model

[1]van den Heever JJ, [1]Jordaan CJ, [1]Lewies A, [4]Goedhals J, [1]Bester D, [2]Botes L, [1&3]Dohmen PM, [1]Smit FE

Author(s)

5) **Johannes Jacobus van den Heever (corresponding author), Christiaan Johannes Jordaan, Angélique Lewies, Dreyer Bester, Pascal Maria Dohmen, Francis Edwin Smit**
Department of Cardiothoracic Surgery,
Faculty of Health Sciences,
University of the Free State (UFS)
P.O. Box 339, (Internal Box G32)
Bloemfontein
9300
South Africa
Tel: +27 51 4053435
E-mail: vdheeverjj@ufs.ac.za

6) **Lezelle Botes**
Department of Health Sciences
Central University of Technology, Free State (CUT)
Private Bag X20539
Bloemfontein
9300
South Africa

7) **Pascal Maria Dohmen**
Department of Cardiac Surgery
Heart Centre Rostock
University of Rostock
Rostock
18107
Germany

8) **Goedhals J**
Department of Anatomical Pathology
Faculty of Health Sciences,
University of the Free State (UFS)
P.O. Box 339, (Internal Box G32)
Bloemfontein
9300
South Africa

ABSTRACT

Introduction: The decellularization of pulmonary homografts provides an alternative source of conduits for right ventricle tract (RVOT) reconstruction for paediatric patients through reduced immunogenicity. Ideally, decellularization would maintain mechanical tissue stability; however, additional fixation might be needed to stabilize the collagen scaffold. This study investigated the *in vivo* performance of decellularized homografts compared to decellularized, glutaraldehyde (GA)-fixed and detoxified (EnCap treated) homografts in the RVOT in a juvenile ovine model.

Method: Pulmonary homografts from juvenile Dorper sheep were subjected to a 48 h ischaemic period, decellularized (n = 5) using a multi-detergent and enzymatic protocol or decellularized, GA-fixed and detoxified with EnCap technology (n = 5) and implanted in the RVOT of young sheep for 180 days. Valve performance was monitored clinically and echocardiographically, and at explantation valve leaflet and wall tissue were evaluated on histological (DAPI, H&E, von Kossa, Modified von Gieson) appearance, scanning (SEM) and transmission (TEM) electron microscopy, mechanical properties [tensile strength (TS) and Young's modulus (YM)] and quantitative calcium content.

Results: Decellularized homografts showed good haemodynamics and growth potential in young sheep. The decellularized plus EnCap treated homografts displayed poor haemodynamic characteristics and valve function, stenosis and resulted in premature death. Explanted decellularized valves remained thin and pliable with good leaflet coaptation, while the decellularized plus EnCap treated valves were rigid, becoming stenotic and leading to bacterial endocarditis. Uniform endothelialization and recellularization occurred in decellularized homografts and only limited in growth in the walls of decellularized plus EnCap treated homografts. Both processing methods were successful in mitigating calcification. Tensile strength was comparable between the two groups pre-implantation, with increased stiffness of leaflets in the decellularized and EnCap treated group.

Conclusion: Decellularized pulmonary homografts that were subjected to 48 h cold ischaemic time, had good haemodynamic characteristics and tissue properties, limited calcification, recellularization and remodeling potential as well as growth potential. Additional GA-fixation of the decellularized homograft defies the purpose of decellularization, namely mitigating the

immune response, promoting host cell repopulation and tissue remodeling, and may be counterproductive in growing individuals.

Keywords: Homografts, decellularization, glutaraldehyde, fixed, detoxified, calcification

INTRODUCTION

The replacement of a patient's diseased heart valve with either a mechanical or biological valve prostheses remains the treatment option of choice for end-stage valvular disease. However, limitations of mechanical substitutes include the need for lifelong anticoagulation, long-term complications and the inability to grow in size (Tillquist and Maddox, 2011). Cryopreserved pulmonary homografts are still regarded as the gold standard for replacement of the native pulmonary valve in Ross procedures as well as for reconstruction of the right ventricle outflow tract (RVOT) in children with congenital abnormalities. Despite several favourable qualities of cryopreserved pulmonary homografts, their availability remains limited due to donor shortages, especially in paediatric sizes (Yoshikawa et al., 2000), and they have limited durability in young patients (Selamet Tierney et al., 2005). Extending the post-mortem ischaemic harvesting time may be used to address donor shortages (Smit et al., 2015), however, the cellular components remaining on the conduit still poses a risk for immune reactions from recipients and affects long-term valve durability (Shaddy and Hawkins, 2002).

Decellularization of homograft valves created an alternative source of valves that are potentially viable, biologically active and with significantly reduced immunogenicity (Cebotari et al., 2011). Decellularized pulmonary homografts, with a post-mortem ischaemic harvesting time of 48 h, function well haemodynamically, with less damage to the collagen and extensive recellularization compared to cryopreservation (Manuscript 2). Removal of cellular components from implants might limit the immunological response from the recipient; however, tissue strength has to be maintained (Erdbrugger et al., 2006). Decellularization procedures that rely on the use of detergents and enzymes or a combination thereof may alter the extracellular matrix (ECM) components such as collagen and glycosaminoglycans (GAGs) (Bourgine et al., 2013). Damage or reduction of GAG content can lead to increased extensibility and changes in the relaxation behaviour of the pulmonary valve leaflets (Converse et al., 2012). Therefore,

additional fixation and stabilization of the collagen scaffold following a multi-detergent and enzymatic washout decellularization protocol might be required. Tissue-engineered decellularized porcine heart valves, Synergraft (Cryolife Inc., USA), have been previously used for RVOT reconstruction in paediatric patients, and structural failure or rapid degeneration of the graft occurred within one year. Three of four children who received this graft died. Two children died suddenly with degenerated Synergraft valves, six weeks and one year after implantation, respectively. The third child died seven days after implantation due to Synergraft rupture, and the fourth child's graft was replaced prophylactically two days after implantation (Simon et al., 2003). In view of these previously described failures for decellularized xenograft prostheses, it is essential to evaluate decellularization plus glutaraldehyde (GA)-fixation in a homograft setting, as most work using a combination of decellularization and GA-fixation have been done in xenografts (Lim et al., 2015; Park et al., 2017). In one study evaluating the performance of commercially stent-mounted GA-preserved aortic homografts (not decellularized), it was concluded that better long-term performance of the homograft tissue compared to GA-fixed heterologous biological valves could be expected (Succi et al., 1986), but other studies using GA-fixed decellularized homograft valves are lacking.

In an attempt to alleviate the shortages of homograft valves, glutaraldehyde (GA)-fixed bovine jugular vein grafts (Contegra®, Medtronic Inc., Minneapolis, Minnesota, United States of America) are used for RVOT reconstructions in children and neonates (Protopapas and Athanasiou, 2008, Falchetti et al., 2019). GA is a cross-linking fixative that preserves and gives added strength to the graft and is used to make xenografts biologically inert. However, the functional aldehyde groups of GA are toxic for host cells (Oryan et al., 2018), and unconjugated GA may contribute towards the calcification of grafts (Lee et al., 2017; Padala, 2018). Premature graft failure associated with the Contegra® conduits is reported to be due to distal stenosis caused by not only the host immune response and conduit-host size mismatch, but also leaching of the GA (Boudjemline et al., 2003; Holmes et al., 2012). Detoxifying strategies to increase the durability and biocompatibility of GA-fixed tissue relies on wash steps with solutions that bind with and remove the aldehyde groups of any unconjugated GA left after GA-fixation (Strange et al., 2015). EnCap technology describes the fixation of biological tissue with GA and the subsequent treatment of the GA-fixated tissue with a high concentration liquid polyol like

propylene glycol (PG) or glycerol, which mitigates the calcification of the tissue (Seifter and Frater, 1995). Decellularized plus EnCap treated pulmonary homografts have dense and compacted collagen, compared to collapsed collagen in cryopreserved homografts and loosely arranged collagen in decellularized homografts (Manuscript 1).

The aim of this study was to compare the clinical performance and morphology of decellularized pulmonary homografts to that of decellularized, GA-fixed and detoxified (EnCap treated) pulmonary homografts following six months implantation in the RVOT of young sheep. A post-mortem cold ischaemic harvesting time of 48 h was used for homografts in both groups.

MATERIALS AND METHODS

Study design

The study was a prospective analytical cohort experimental study. The evaluation of baseline data for cryopreserved and decellularized ovine pulmonary homograft tissue has previously been described (Manuscript 1). Pulmonary homografts from juvenile Dorper sheep (n = 10) (average annulus diameter 18-19 mm before processing), with a post-mortem cold ischaemic harvesting time of 48 h, were divided into two groups and either decellularized (n = 5) or decellularized, GA-fixed and detoxified (n = 5) using the EnCap process (Bester et al, 2017; Laker et al., 2020). These homografts were then implanted as interposition grafts in the main pulmonary artery (MPA) of juvenile Dorper sheep (n = 5 per group) for 180 days. Recipient animals were between 3-6 months of age and weighed between 24-32 kg, and each animal received an ear tag with a unique identification number. Recipients were monitored with echocardiography at implantation, at three and six months prior to sacrifice. Following explantation, homografts were evaluated on macroscopic appearance and radiographic evaluation (X-rays), while leaflet and wall tissue integrity were evaluated using strength analysis and morphology. Strength analysis included tensile strength (TS) and Young's modulus (YM), and morphology included H&E, von Kossa staining, modified von Gieson staining, scanning electron microscopy (SEM), transmission electron microscopy (TEM) and quantitative calcium analysis. A schematic representation of the study design is given in Figure 1. The interfaculty Animal Ethics Committee of the University of the Free State (UFS-AED2016/0101) approved the project. All animal experiments and surgical

procedures were performed in compliance with the *Guide for the Care and Use of Laboratory Animals* as published by the US National Institutes of Health (NIH, 2011).

Implantation techniques used for the Medtronic Freestyle™ grafts were described as: Root inclusion (RI) technique in five cases (55.6%), Root replacement method (RR) and Sub-coronary method (SC) in two cases each (Butany et al., 2007). Contegra® bovine jugular grafts were also implanted in the MPA with the valve as distal as possible, end-to-side distal anastomoses and PA augmentation with bovine pericardium if required (Schoenhoff et al., 2011).

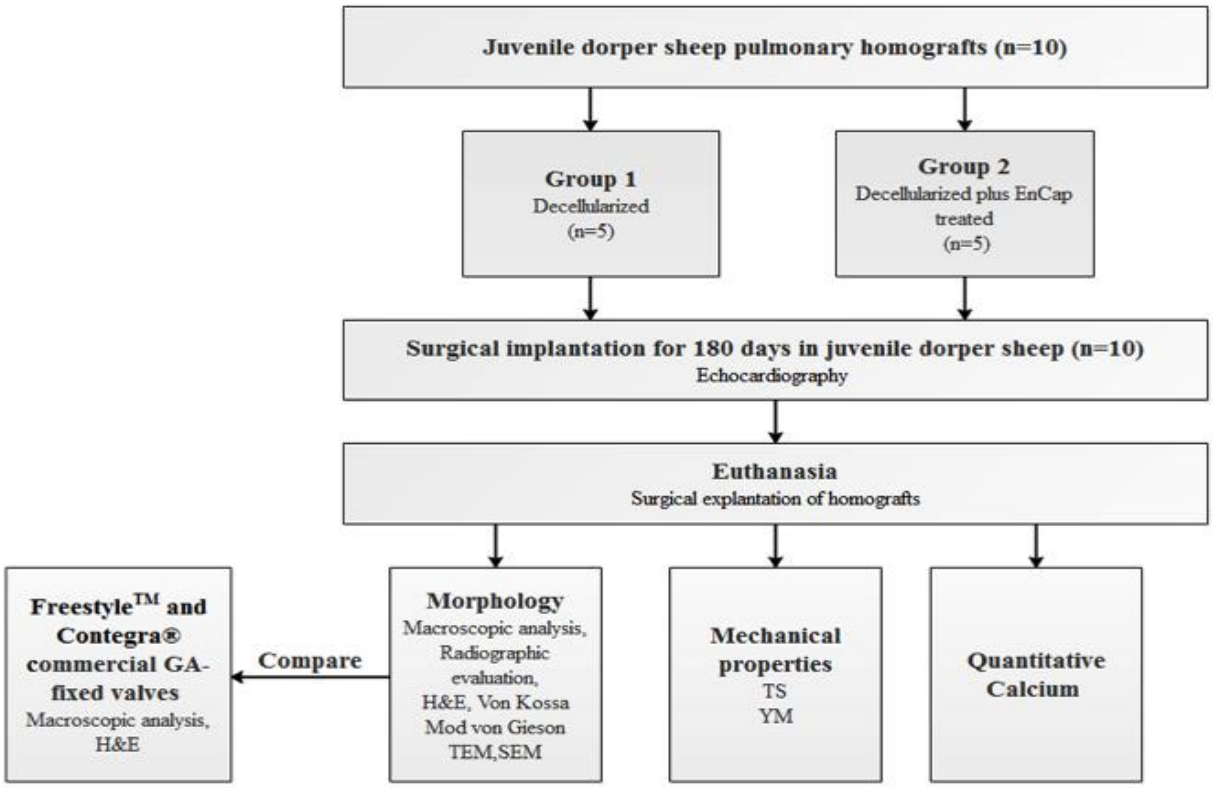

Figure 1: Schematic diagram of the study design.

Preparation of homografts

Heart-lung blocks (n = 10) were harvested from freshly slaughtered juvenile Dorper sheep with body weights of between 24-30 kg, and subjected to 48 h ischaemia at 4ºC before dissection and processing as described by Bester et al., (2018). Decellularized homografts (group 1, n = 5) were prepared according to our proprietary protocol (Bester et al., 2017; Laker et al., 2020). Briefly,

homografts were subjected to osmotic shock, repeated changes in a multi-detergent solution [0,5% SDS (Sigma-Aldrich, Johannesburg, SA), 1% Deoxycholic acid (Sigma-Aldrich, Johannesburg, SA), 1% Triton-X100 (Sigma-Aldrich, Johannesburg, SA)] and numerous washings in PBS and an antibiotic cocktail [1.25 mg Amphotericin B (Bristol-Myers Squibb, Bedfordview, SA), 25 mg Piperacillin (Brimpharm SA (Pty) Ltd, Cape Town, SA), 25 mg Vancomycin (Gulf Drug Company, Mount Edgecombe, SA) and 12.5 mg Amikacin sulphate (Bodene (Pty) Ltd, trading as Intramed, Port Elizabeth, SA)] under constant shaking. These steps were followed by enzymatic treatment with descending concentrations of Benzonase (Thermo Fisher Scientific, Johannesburg, SA) (Dijkman et al., 2012), repeated washing in PBS, delipidation in 70% ethanol and final storage in PBS with antibiotics until implantation. Additionally decellularized homografts (group 2, n = 5) were fixated and detoxified according to an existing protocol used by Glycar South Africa for processing of pericardial tissue, called the EnCap technology, and stored in propylene oxide (Seifter and Frater, 1995). EnCap technology includes tanning of biological tissue in 0.625% GA for 72 h at room temperature immediately after harvesting and cleaning, treatment with a high concentration of Propylene glycol (Sigma-Aldrich, Johannesburg, SA) for 7-14 days at room temperature to remove toxicity, reduce the host inflammatory response and mitigate calcification, and storage in 2% Propylene oxide (Sigma-Aldrich, Johannesburg, SA) at room temperature. This technology was primarily invented as an anti-calcification treatment for biological tissue, and has provided excellent results when used in bovine pericardial patch implants.

All homografts were confirmed culture-negative prior to implantation. To confirm effective decellularization of the homografts, DNA quantification was done with DAPI staining, gel electrophoresis and nanodrop counts by the Cardiovascular Research Unit, UCT Medical School (Crapo et al., 2011).

Implantation and clinical performance of homografts

Surgical procedure

Prepared homografts were implanted into 10 juvenile Dorper wether sheep (n = 5 per group) with body weights ranging between 23-32 kg. Recipient sheep were anaesthetized, intubated and ventilated. Cardiopulmonary bypass (CPB) was achieved through cannulation of the left carotid

artery and right atrium, arterial and central venous lines inserted and the surgical procedure performed on a beating heart. The pulmonary artery was transected, the native pulmonary valve leaflets removed and the pulmonary homograft implanted as an interposition graft (Ali et al., 1995; Flameng et al., 2006) with end-to-end anastomoses with continuous 4/0 Prolene sutures in the main pulmonary artery. The animal was weaned off CPB, all incisions closed, extubated, chest drain and monitoring lines were removed, before moving the sheep to an overnight facility with a companion sheep. Analgesics and a broad-spectrum antibiotic were administered twice daily for five days post-surgery, and animals were followed for six months until sacrifice and explantation for further analysis of the homografts.

Clinical performance of implanted valves

Implanted homografts were evaluated for changes in annular dimensions, transvalvular gradients, pulmonary valve regurgitation, calcification and possible aneurysm formation over the study period, using echocardiographic data that were recorded immediately after homograft implantation, at 30 and 90 days post-surgery and just prior to sacrifice (day 180) using a GE Vivid-Q-mobile sonographic machine.

Evaluation of explanted homografts

Gross macroscopic appearance and microscopic analysis

Evaluation of gross macroscopic appearance of valve leaflet and wall tissue was performed immediately after valves were explanted and photographed. The gross macroscopic appearance of GA-fixed homografts was also compared to that of two other GA-fixed commercially available valve replacement grafts, namely; porcine aortic Freestyle™ and Contegra® bovine jugular vein grafts, both from Medtronic Inc. Leaflet and wall tissue samples were collected in 4 % buffered Formalin, embedded in paraffin wax, sectioned and stained according to standard H&E, von Kossa and modified von Gieson staining protocols for histological evaluation (Mepham, 1991). The histology of the explants was compared to that of similarly processed pre-implanted homografts (baseline, Manuscript 1), and the two commercially available GA-fixed valve replacement grafts. Leaflet and wall tissue samples for SEM and TEM were collected in 3 % GA and processed according to standard protocols for SEM and TEM evaluations (Spurr, 1969) (detailed method given in manuscript 1).

Calcium quantification

Quantitative calcium analyses were performed by the Eco-Analytica Laboratory, School for Environmental Sciences & Development, Northwest University, Potchefstroom, South Africa. Explanted samples were dried, weighed, hydrolyzed in 1 ml 50 % nitric acid + 50 µl hydrogen peroxide (H_2O_2) / dry sample at 90^oC for 30-40 minutes, the extractable calcium content determined by atomic absorption spectrophotometry (Agilent ICP-MS 7500c, Chemetrix, Midrand, South Africa) and expressed as µg calcium per mg tissue (dry weight).

Mechanical properties

Mechanical properties of explanted pulmonary valve leaflet and wall samples were examined using a tensile strength testing apparatus (Lloyds LS100 Plus, IMP, Johannesburg, South Africa), according to the method described by Thubrikar and co-workers. Tissue samples measured 5 x 10 mm, with leaflets and pulmonary sinus wall samples cut in the circumferential direction. The tissue sample was fixed between clamps at both ends and gradually stretched (0.1 mm/s) by applying constant tension on the two ends, and the data recorded on a personal computer (Thubrikar et al., 1983). The mechanical properties of the explants were compared to that of similarly processed pre-implanted homografts (baseline, Manuscript 1).

Statistical analysis

All values are expressed as median values with corresponding InterQuartile ranges. Statistical analyses were performed using GraphPad Prism version 8.3.1 (GraphPad Software, La Jolla, CA, USA, www.graphpad.com). The percentage change between Day 180 and Day 0 was calculated as (Day 180 – Day 0)/Day 0 * 100. The Wilcoxon Test was used to measure differences between paired groups, and the Mann-Whitney U Test was used to measure differences between unpaired groups. Confidence intervals of 95 % of the difference between medians were calculated to test for the significance ($p < 0.05$).

RESULTS

Successful decellularization of both the valve leaflets and pulmonary artery wall tissue in the decellularized and decellularized plus EnCap treated groups was achieved and confirmed with DAPI staining and supported by gel electrophoresis (fragmented DNA bands < 200 bp) and

nanodrop readings of below 50 ng/mg for the same tissue samples (Manuscript 1). Homografts in both groups were of similar size prior to processing. Before implantation, decellularized homografts were soft and pliable and maintained its annular dimensions as before processing. The decellularized and EnCap treated homografts became stiff with rigid conduit tissue and some reduction in annular and tube size post GA-fixation, and increased leaflet stiffness (see manuscript 1).

All animals were successfully operated on, and animals in the decellularized group survived until the end of the implantation period of 180 days. Echocardiography and doppler images revealed no significant regurgitation in pulmonary valves in the decellularized group up to 180 days (Fig 2A). No calcification could be identified on echocardiography, and no aneurysm formation was observed in any of the implants in both groups. However, valves in the decellularized plus EnCap treated group developed high gradients (Fig.2B) as a result of no growth and fixed tube size in the growing sheep. This growth restriction resulted in severe RVOT obstruction, right ventricular (RV) failure with pleural effusion and ascites at post-mortem. Three of the sheep in the GA-fixed group died prematurely (between 3-4 months). Two sheep with moderate RVOT obstruction and RV failure were electively euthanized at four months; therefore the data for the decellularized plus EnCap treated group is only available until three months, when the last echocardiography was done. The median [InterQuartile range] percentage weight increase from implantation to explantation after six months in the decellularized group was 30.61 % [16.55-28.20], and 17.24 % [9.38-23.21] in the decellularized plus EnCap treated group at premature explantation/death. The increase in weight was significant in both groups with 95 % confidence intervals of (-13.00; - 3.00) for the decellularized group and (-7.00; -2.00) for the decellularized plus EnCap treated group respectively.

DECELLULARIZED

DECELLULARIZED plus
EnCap TREATED

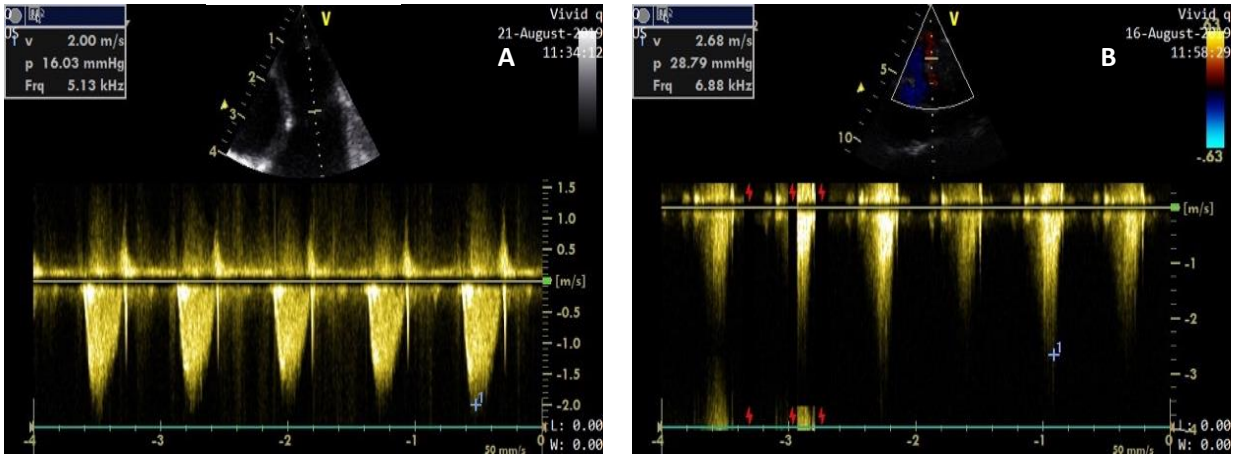

Figure 2: Representative Doppler images of decellularized (n = 5) **(A)** pulmonary homografts after 180 days implantation, and decellularized plus EnCap treated (n = 5) **(B)** pulmonary homografts after 90 days implantation in sheep. Trivial regurgitation is evident in the decellularized group, and unacceptably high transvalvular gradients in the decellularized plus EnCap treated group.

Measurements of the median percentage change in annulus diameter over the study period between the two groups, by means of echocardiography, revealed a significant difference in increase in diameter between decellularized and decellularized plus Encap treated pulmonary homografts. The median annulus diameter (mm) of both the groups increased significantly from baseline until explantation (day 180) for the decellularized group and the final echocardiography at day 90 for the decellularized plus EnCap treated group. A significant increase in median annulus diameter (mm) was also observed for the decellularized group at day 90 (Table 1).

Table 1: Comparison of increase in annular size (mm) between decellularized (n = 5) and decellularized plus EnCap treated (n = 5) homografts as measured on echocardiography over the three and six-month implantation period respectively.

Group	Baseline	90 days	95 % CI Baseline vs. day 90 explant	180 day explant	95 % CI Baseline vs. day 180 explant	% Change from Baseline	95 % CI Group 1 vs. Group 2
1	15.00 [14.00-16.50]	20.00 [18.50-21.00]	-6.00; -2.00*	23.00 [20.00-23.00]	-9.00; -3.00*	43.75 [24.71-64.29]	-50.95; -4.615*
2	14.00 [12.00-15.00]	16.00 [15.00-17.00]	2.00; 4.00*	-	-	14.29 [13.33-25.87]	

Data presented as median [InterQuartile range], and the 95 % confidence interval (CI) of the control (baseline) and after 90 and 180 days of implantation respectively, and the 95 % CI of the difference between the % change from baseline for the decellularized and decellularized plus EnCap treated groups (*$p < 0.05$). [Group 1 = Decellularized ; Group 2 = Decellularized plus EnCap treated].

The median transvalvular gradient in the decellularized group at six months post-implantation was 15 mm Hg (60 % change from baseline). Three months post-implantation the median transvalvular gradient in the decellularized plus EnCap treated group was 43 mm Hg (165 % change from baseline) (Table 2). This change was highly significant and “lethal”. When comparing the transvalvular gradients of the decellularized group at six months to that of the decellularized plus EnCap treated group at three months, the increase in the transvalvular gradient in the decellularized plus EnCap treated group proved significant (95 % CI -39.00 to -15.00).

Table 2: Comparison of changes in transvalvular gradients over time between decellularized (n = 5) and decellularized plus EnCap treated (n = 5) homografts, as measured on echocardiography.

Group	Day 0	Day 30	Day 90	Day 180	95 % CI Baseline vs. explant	% Change from baseline	95 % CI Group1 vs. Group 2
1	10.00 [7.00-16.50]	10.00 [7.50-12.50]	8.00 [4.50-10.00]	15.00 [9.00-16.00]	-9.00; 11.00.	60.00 [-42.22-123.3]	-292,10; 15.00
2	16.00 [12.50-19.00]	35.00 [30.00-48.50]	43.00 [35.50-52.00]	-	-35.00; -16.00*	165.00 [121.00-254.80]	

Data presented as median [InterQuartile range], and the 95 % confidence interval (CI) of the control (baseline) and after 90 or 180 days of implantation respectively, and the 95 % CI of the difference between the % change from baseline for the decellularized and decellularized plus EnCap treated groups (*$p < 0.05$). [Group 1 = Decellularized ; Group 2 = Decellularized plus EnCap treated].

On macroscopic inspection at explantation, leaflets of decellularized homografts appeared thin, translucent and without visible nodules of calcification, and the wall tissue was soft and pliable (Fig.3A,B). Three of the obstructed valves in the decellularized plus EnCap treated group developed bacterial endocarditis, making the valve obstructive and causing destruction of the leaflets (Fig.3D). Leaflets from the other two valves in this group appeared thin and translucent (Fig.3C), with no visible calcific nodules. However, the wall tissue of all the valves in the decellularized and EnCap treated group were rigid, hard and not at all pliable, causing severe progressive stenosis of the valved conduit within 90 days from implantation.

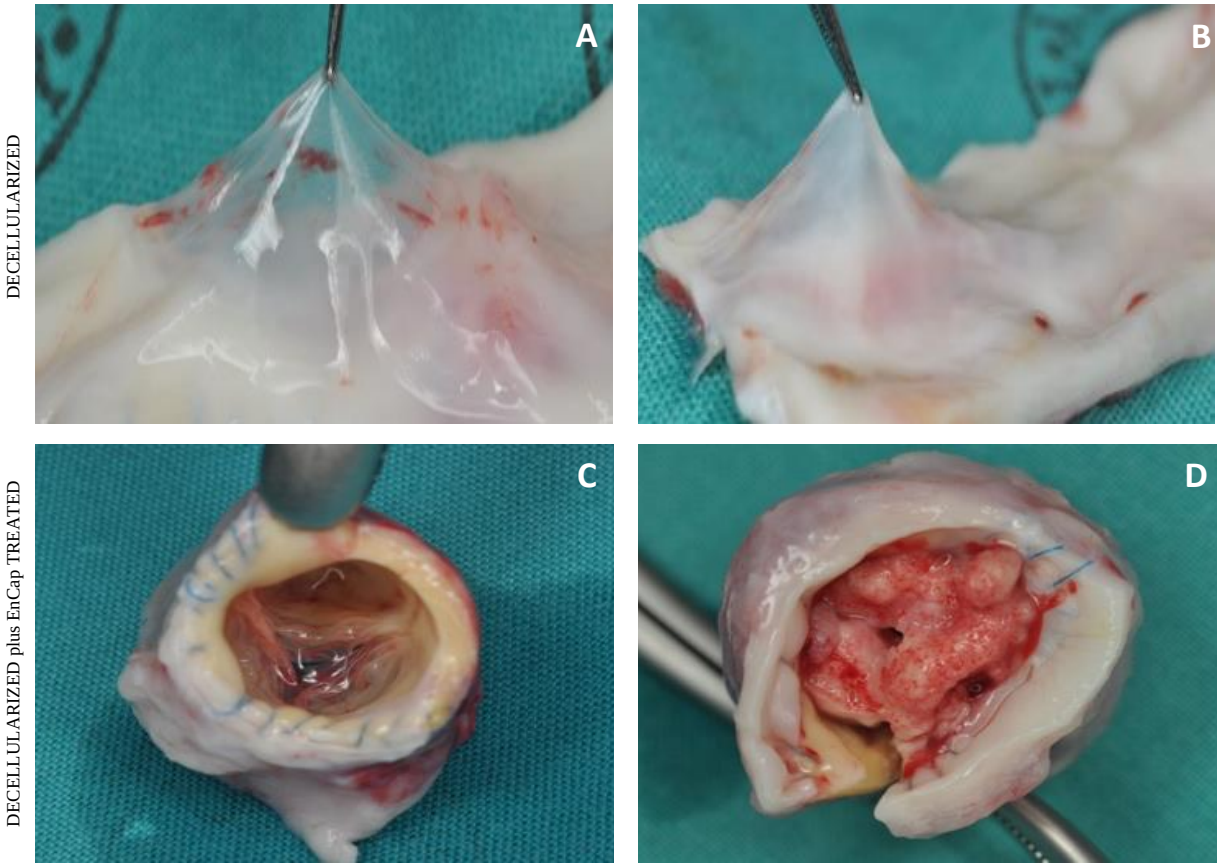

Figure 3: Representative images of gross morphology of decellularized (n = 5) **(A,B)** and decellularized plus EnCap treated (n = 5) **(C,D)** pulmonary homografts at explantation. Leaflets were thin and translucent in decellularized scaffolds. Bacterial endocarditis destroyed leaflets in three valves in the decellularized plus EnCap treated group **(D)**, while leaflets in the remaining two valves in the decellularized plus EnCap treated group appeared thin and translucent **(C)**.

H&E staining of baseline and explanted valves demonstrated intact endothelium and very good ingrowth and uniform distribution of host cells in the leaflets of the decellularized scaffold group (Fig.4A,B). Extensive repopulation occurred, and all cells appeared as fibroblast cells. Importantly, no inflammatory cells or macrophages were observed. No ingrowth of interstitial cells could be identified in leaflets of the decellularized plus EnCap treated group, and a thickened fibrous encapsulation layer containing fibroblast-like cells was present on the ventricularis surface of the leaflets (Fig,4D). The von Kossa stains were negative in all explants, indicating that there was no visible evidence of calcific deposits in the leaflets of the decellularized or decellularized plus EnCap treated groups (Fig.4F,H). No clear evidence of the presence of elastin could be demonstrated with modified von Gieson staining in the leaflets of

any of the two groups (Fig.4J,L). The collagen of the decellularized plus EnCap treated group was dense and compacted pre-implantation. The collagen at explantation remained similar to that before implantation, and this was indicative of a lack of remodeling.

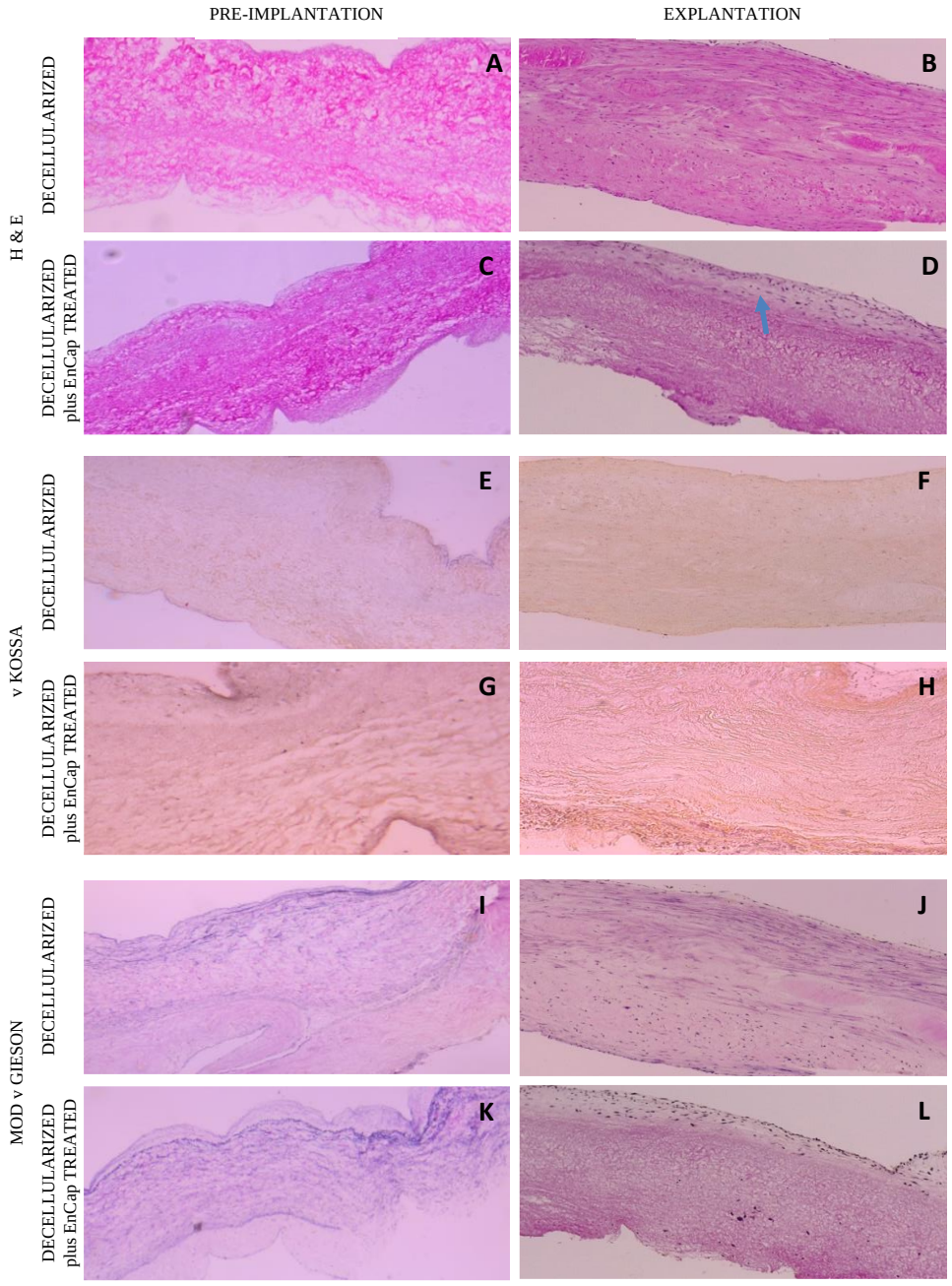

Figure 4: H&E stain of the leaflets clearly demonstrates extensive ingrowth of host cells into the decellularized pulmonary homografts **(B)** and no ingrowth in the decellularized plus EnCap treated group **(D)**. An endothelial layer is present in both groups, and a fibrous encapsulation in the decellularized plus EnCap treated group (blue arrow). von Kossa stain did not demonstrate any calcification in the decellularized **(F)** or decellularized plus EnCap treated group **(H)**, and no elastin could be demonstrated with Modified von Gieson staining in any of the two groups (**J,L)** (n = 5).

For comparison, two other GA-fixed commercially available valve replacement grafts also demonstrated thick fibrous encapsulation (black arrows) and fibrous sheath formation (white arrow) at explantation due to conduit failure (Fig.5).

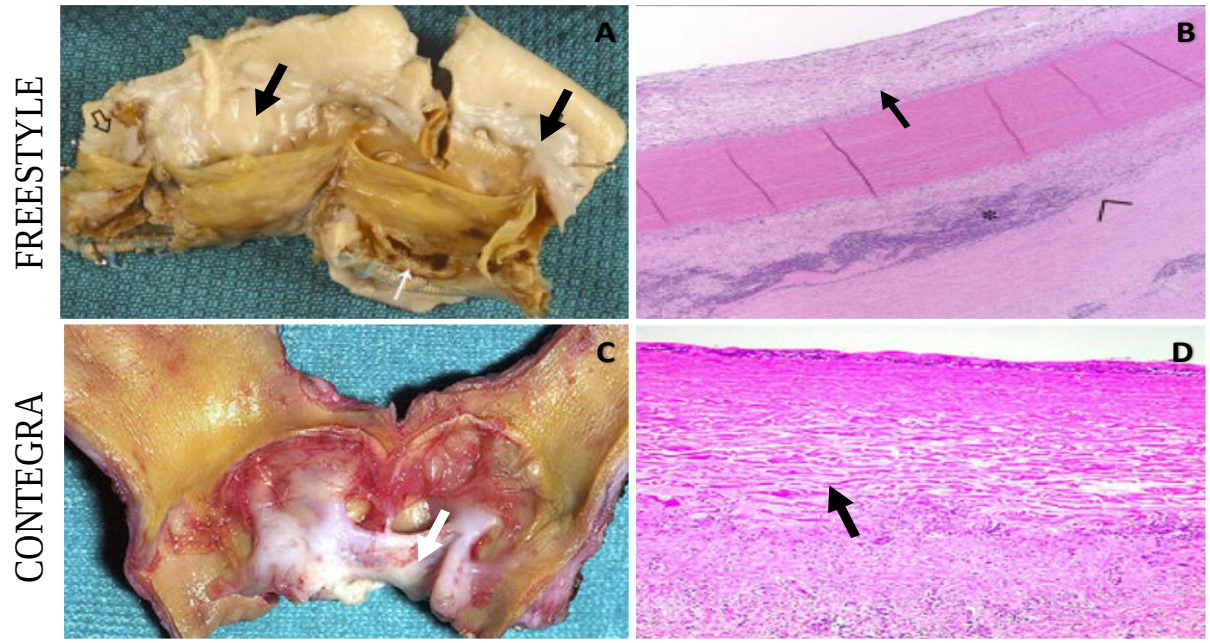

Figure 5: Adapted images of macroscopic evaluation of explanted Aortic Freestyle™ (Medtronic) and Contegra® (Medtronic) conduits showing pannus overgrowth and fibrous sheath formation. Microscopic images of H&E stain of the aortic wall clearly demonstrates thick layer of fibrous encapsulation (pannus) **(B)** and fibrin deposition on the intimal aspect **(D)**. (Adapted from Butany et al., (2007), Schoenhoff et al., (2011)).

The wall tissue demonstrated similar results as for the leaflets, with uniform cell distribution in the ECM of the decellularized scaffold (Fig.6B) and almost no cells in the decellularized plus EnCap treated group (Fig.6D) on H&E staining. An intact endothelial layer was present in both groups, but a fibrous encapsulation containing fibroblast-like cells (blue arrow) was visible in the decellularized plus EnCap treated group. von Kossa staining in the decellularized or decellularized plus EnCap treated group (Fig.6F,H) were negative for calcific deposits in all samples. Elastin fibers (black arrows) were present in both groups on Modified von Gieson staining (Fig.6J,L).

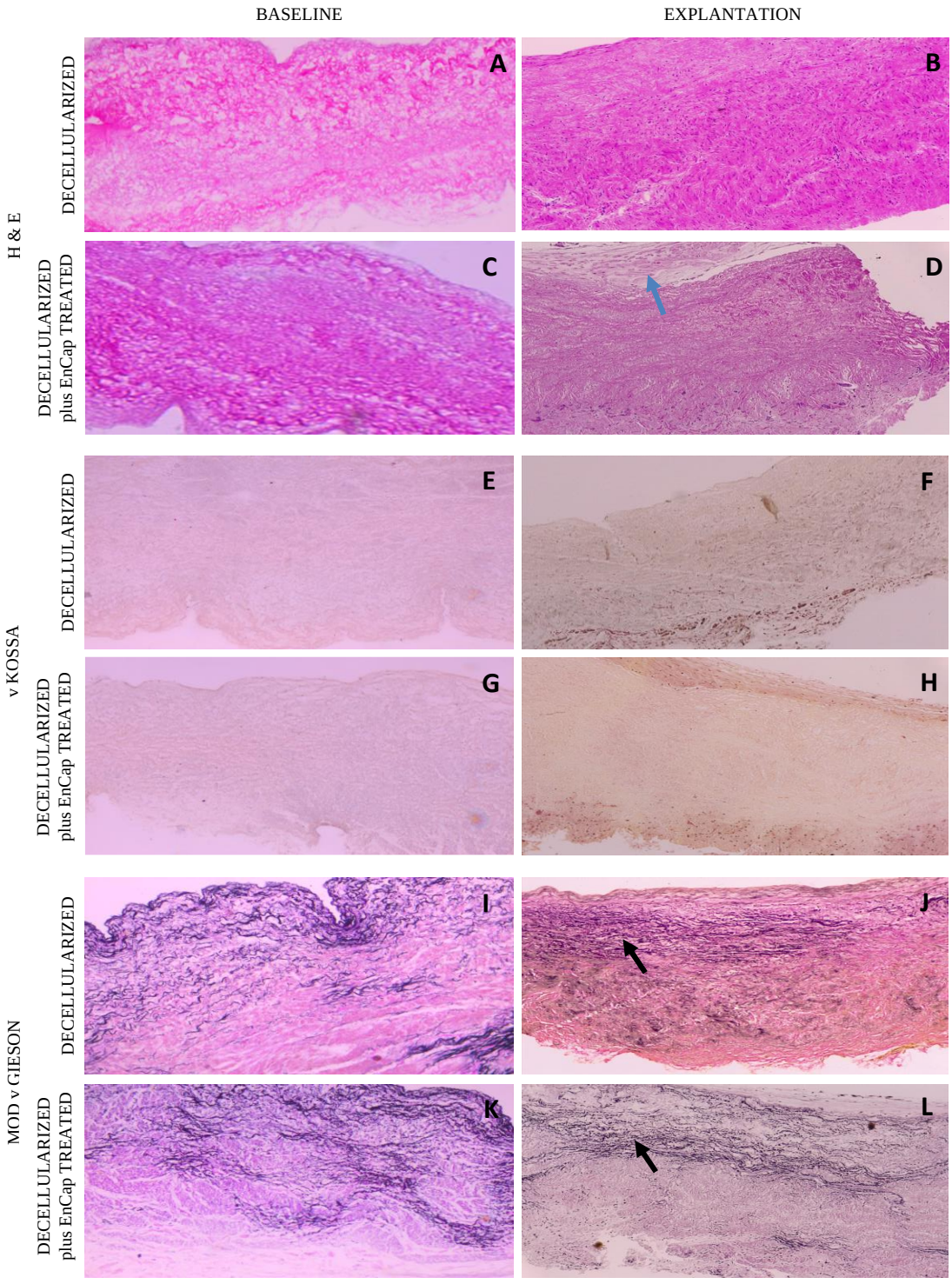

Figure 6: H&E of wall tissue with uniform distribution of fibroblast cells in the decellularized group **(B)** and very limited cell distribution in the decellularized plus EnCap treated group **(D)**. An endothelial layer is present in both groups, and a fibrous encapsulation in the decellularized plus EnCap treated group (blue arrow). No calcific deposits were demonstrated on von Kossa stain in either of the groups **(F,H),** and elastin fibers (black arrows) were present on Modified von Gieson stain in both groups **(J,L)** (n = 5).

SEM demonstrated adequate coverage with endothelial cells of the leaflet and wall tissue in the decellularized group (Fig.7A,B), and a fibrous encapsulation (pannus) with endothelial-like cells in the decellularized plus EnCap treated group (Fig.7C,D).

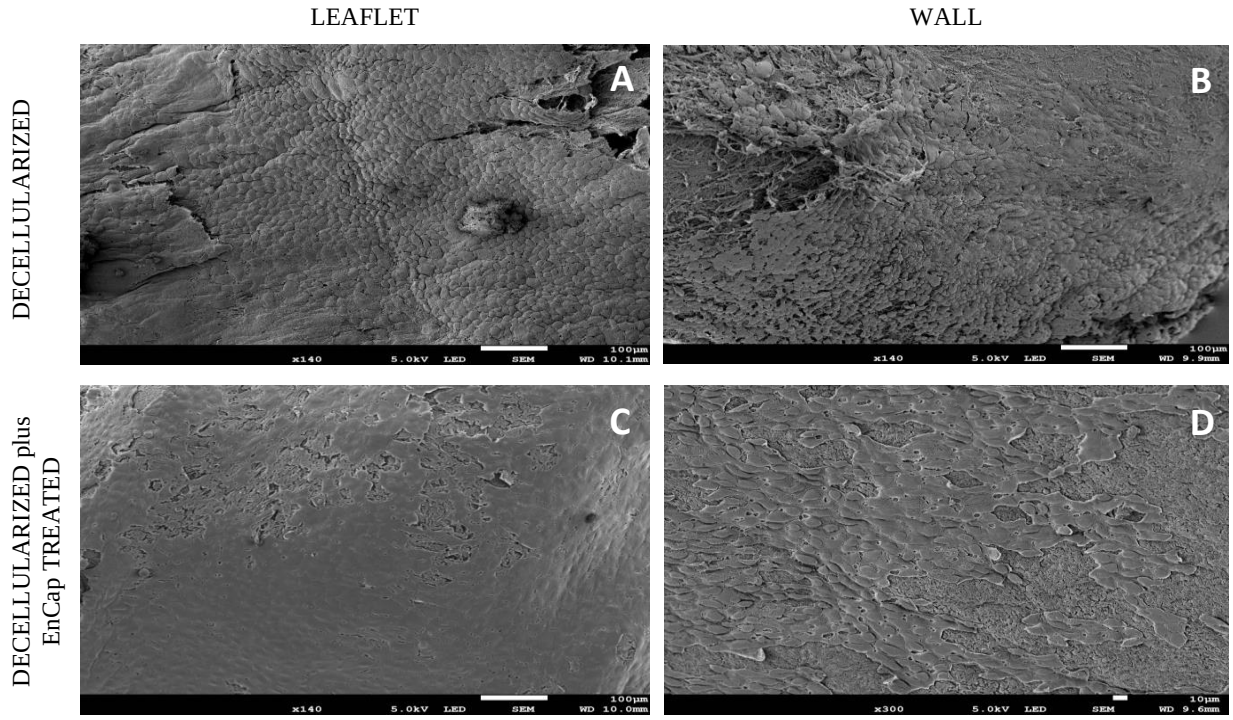

Figure 7: Representative scanning electron microscopy images demonstrating uniform coverage with endothelial cells in the leaflets and walls of decellularized pulmonary homografts (n = 5) **(A,B)**, and a layer of fibrous encapsulation with endothelial-like cells in the decellularized plus EnCap treated pulmonary homografts (n = 5) **(C,D)**. (Scale 100μM **(A,B,C)**, Scale 10 μM **(D)**).

TEM demonstrated the presence of living cells in the leaflets (Fig.8A) and walls (Fig.8B) of valves in the decellularized homograft group. Some cells were also observed in the wall tissue of decellularized plus EnCap treated pulmonary homografts (Fig.8D), but not in the leaflets (Fig.8C). Cells in the leaflets and walls of the decellularized homograft group (Fig.8A,B) had numerous vacuoles or vesicles (black arrows), which are the cellular structures from where new pro-collagen is likely to be produced later for maintenance and remodeling of the tissue.

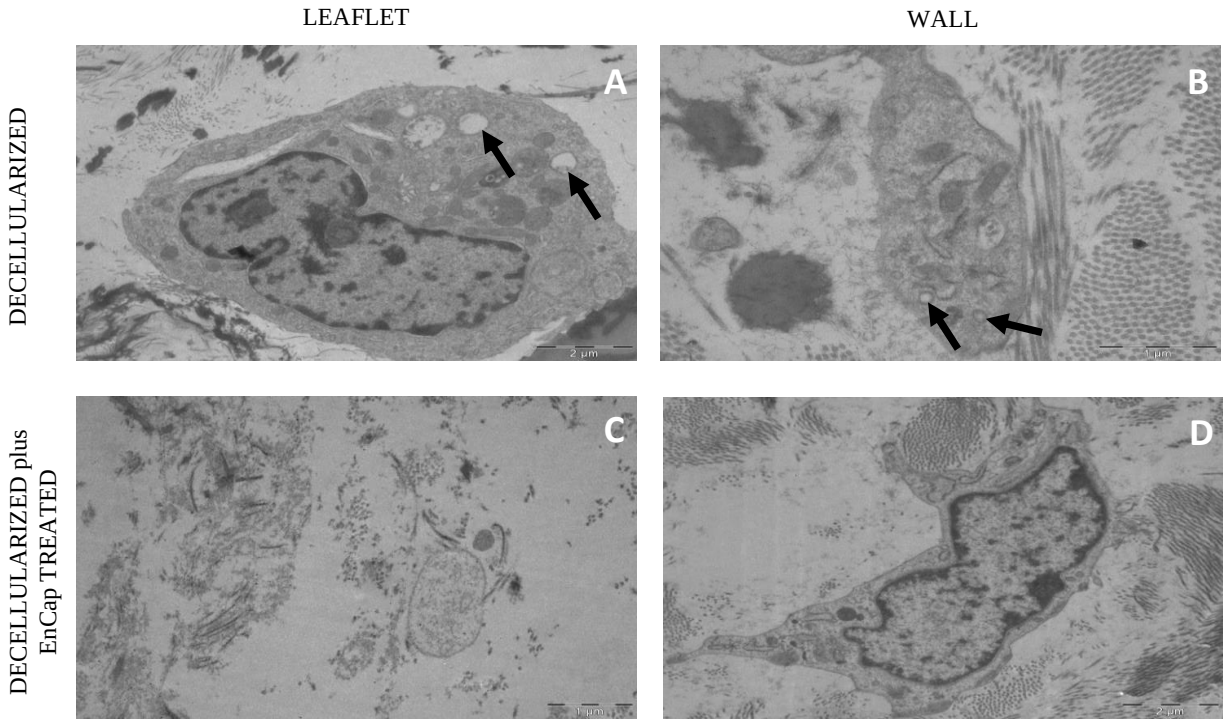

Figure 8: Representative transmission electron microscopy images demonstrating the presence of living cells in leaflets **(A)** and walls **(B)** of pulmonary homografts in the decellularized group, as well as single cells in the walls of the decellularized plus EnCap treated group **(D)**. Numerous vesicles (black arrows) were present in the cells in the leaflets and walls of homografts in the decellularized group **(A,B)**, but not in the leaflets and walls of the decellularized plus EnCap treated group **(C,D) (**n = 5).

On higher magnification (x 34000), new cells in the leaflets (Fig.9A) and walls (Fig.9B) of the decellularized scaffolds demonstrated rough endoplasmic reticulum (black arrows), but this was not observed in the leaflets and walls of pulmonary homografts in the decellularized plus EnCap treated group (Fig.9C,D).

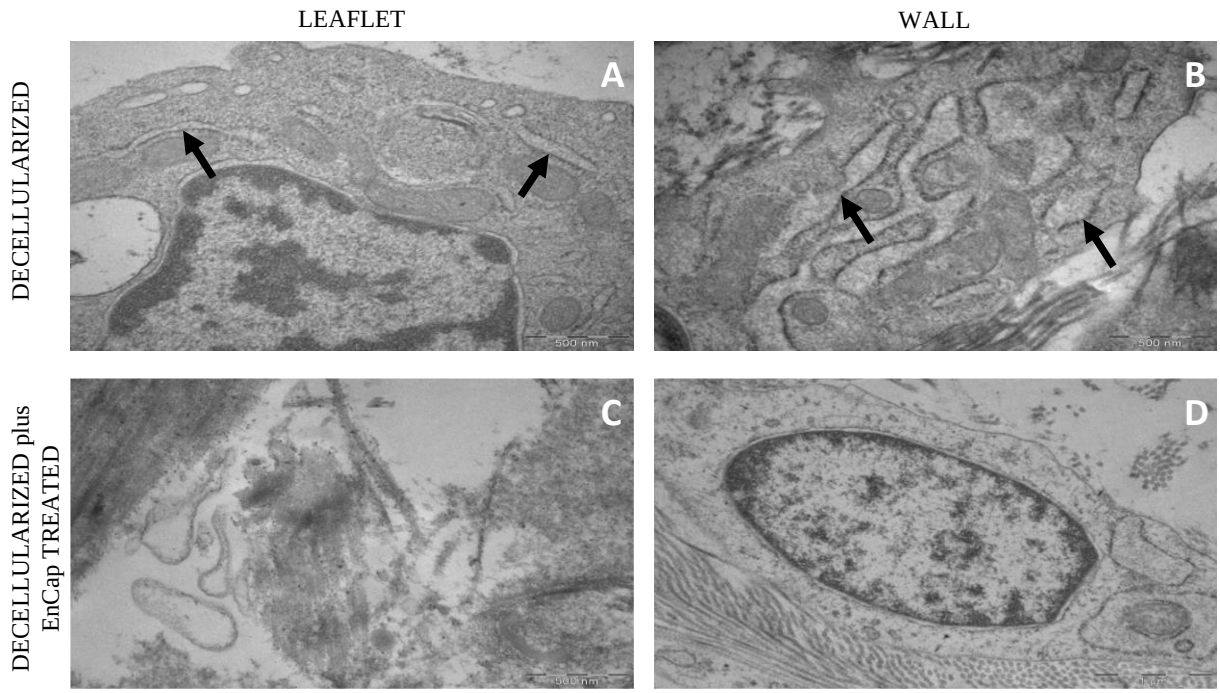

Figure 9: Representative images of leaflet and wall tissue in the unfixed decellularized pulmonary homografts with repopulated interstitial cells demonstrating rough endoplasmic reticulum (black arrows) (n = 5) **(A,B)**, but cells remnants in the leaflets and some living cells in the walls were without rough ER in the decellularized plus EnCap treated group (n = 5) **(C,D)**. (x 34000 magnification).

The mechanical properties (TS and YM) of the explants in the decellularized plus EnCap treated group could not be measured because of valve destruction due to bacterial endocarditis. The leaflets in the decellularized plus EnCap treated group were stiffer and the TS higher compared to the decellularized group prior to implantation, however, there was no significant difference in the TS and YM of the valves and leaflets in the decellularized group compared to the decellularized plus EnCap treated group prior to implantation, (Table 3).

Table 3: TS and YM of baseline decellularized pulmonary homografts (n = 5) and decellularized plus EnCap treated pulmonary homografts after 48 h ischaemia before implantation (n = 5).

Variable		Group 1	Group 2	95 % CI Group 1 vs. Group 2
Leaflets	TS (MPa)	1.83 [0.01-5.65]	4.96 [4.34-6.76]	-6.44; 1.15
	YM (MPa)	22.10 [0.10-55.27]	41.11 [27.76-52.52]	-48.36; 18.31
Walls	TS (MPa)	1.89 [1.57-2.38]	1.90 [1.18-2.09]	-1.14; 0.90
	YM (MPa)	2.32 [1.82-2.88]	2.21 [1.99-3.58]	-1.32; 0.82

Data presented as median [InterQuartile range], and the 95 % confidence interval (CI) of the decellularized and decellularized plus EnCap treated homografts (*$p < 0.05$). [TS = tensile strength; YM = Young's modulus; Group 1 = Decellularized; Group 2 = Decellularized plus EnCap treated].

The TS and YM of the explanted decellularized homografts leaflets and walls increased compared to the baseline (pre-implant) values. However, the only significant increase ($p < 0.05$) was observed in the YM of the wall tissue at explantation (Table 4).

Table 4: TS and YM of leaflets and walls of decellularized pulmonary homografts after 48 h ischaemia before implantation (n = 5) and when explanted after 180 days (n = 5).

Variable		Pre-implant	180 day explant	95 % CI Pre-implant vs. explant
Leaflets	TS (MPa)	1.83 [0.01-5.65]	6.06 [2.18-10.69]	-10.68; 3.12
	YM (MPa)	22.10 [0.10-55-27]	50.73 [21.6-118.1]	-118.00; 33.29
Walls	TS (MPa)	2.39 [1.73-3.71]	7.92 [1.29-12.64]	-1.77; 10.63
	YM (MPa)	2.32 [1.82-2.88]	16.35 [8.67-24.05]	-22.04; -6.095*

Data presented as median [InterQuartile range], and the 95 % confidence interval (CI) of the pre-implant and explant at day 180 (*$p < 0.05$). [TS = tensile strength; YM = Young's modulus].

No statistically significant difference was found between the median calcium content of leaflet or wall tissue of decellularized homografts (after 180 days) when compared to decellularized plus EnCap treated homografts (after 90 days) (Table 6).

Table 5: Comparison of quantitative calcium content (µg calcium per mg tissue) between decellularized (n = 5) and decellularized plus EnCap treated pulmonary homografts (n = 5) leaflet and wall tissue after 90 and 180 days implantation respectively.

Variable	Group 1	Group 2	95 % CI Group 1 vs. Group 2
Leaflet	2.38 [0.97-41.46]	3.44 [1.46-12.80]	-17.76; 58.50
Wall	0.49 [0.40-0.82]	0.95 [0.59-9.56]	-16.73; 0.26

Data presented as median [InterQuartile range], and the 95 % CI of the difference between the decellularized and decellularized plus EnCap treated groups (*p < 0.05). [Group 1 = Decellularized ; Group 2 = Decellularized plus EnCap treated].

Calcification of the suture lines of homografts in the decellularized and decellularized and EnCap treated groups were clearly visible on radiographic evaluation at explantation.

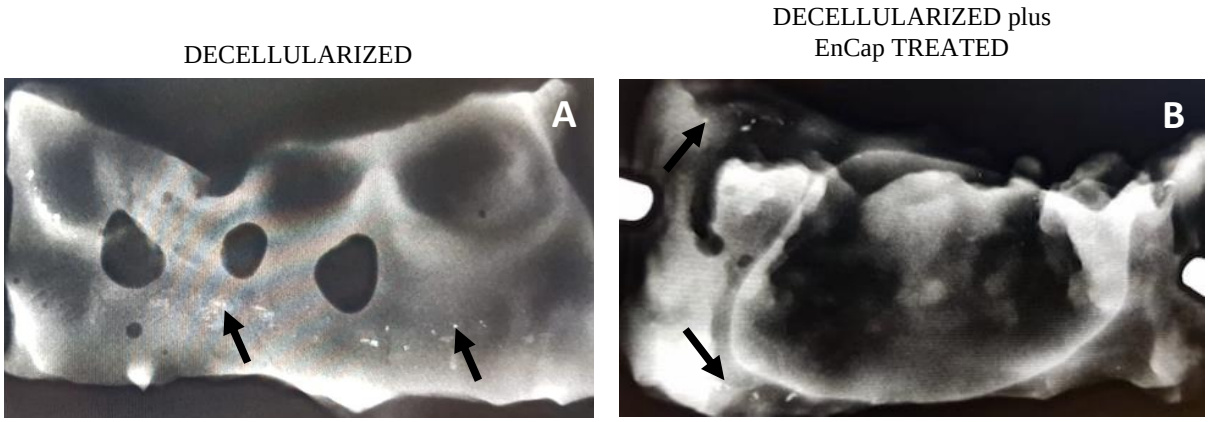

Figure 10: Representative radiographic images of decellularized (n = 5) and decellularized plus EnCap treated (n = 5) pulmonary homografts demonstrating the calcification on the suture lines (black arrows) at explantation.

DISCUSSION

The potential donor pool of pulmonary homografts for the use in RVOT procedures can be increased by extending the post-mortem ischaemic harvesting time to 48 h (Smit et al., 2015). The removal of all the cellular content and DNA material from a homograft valve through decellularization results in an implant that significantly reduces the immunologic response from the recipient, thereby contributing towards long-term durability (Crapo et al., 2011; Bibevski et al., 2017). Our own proprietary protocol effectively decellularized pulmonary homografts from

sheep harvested after 48 h ischaemia at 4◦C (see manuscript 1). The rapid degeneration or structural failure that occurred in tissue-engineered decellularized porcine heart valves (Synergraft, Cryolife Inc., USA) used for the RVOT reconstruction in children (Simon et al., 2003), made it essential to evaluate decellularization plus GA-fixation in a homograft setting. Concerns about the weakening of the ECM through the decellularization protocol prompted the additional GA-fixation and detoxification of the homograft prior to implantation in the juvenile ovine model.

Due to the shortages experienced in the supply of cryopreserved homografts for RVOT reconstruction, especially in smaller sizes for young children, valved bovine jugular vein grafts (Contegra®, Medtronic Inc., Minneapolis, Minnesota, USA) have been created to help alleviate the small supply. These grafts are fixed and stored in GA, and although these conduits are routinely used with good clinical outcomes (Breymann et al., 2004; Falchetti et al., 2019), concerns about the risk of the development of distal stenosis (Boethig et al., 2012) and more recently endocarditis (Ugaki et al., 2015; Mery et al., 2016) have been raised. A study comparing the use of fresh decellularized homografts (6 h warm ischaemic time) to cryopreserved homografts and GA-fixed Contegra® xenografts, reported improved freedom from explantation, lower transvalvular gradients in follow-up and adaptive ability or growth in decellularized homografts compared to conventional cryopreserved homografts and GA-fixed bovine jugular vein valves (Contegra®) (Cebotari et al., 2011).

In the current study, decellularized unfixed homografts (48 h cold ischaemic time) maintained good haemodynamic characteristics and valve function after implantation, with only trivial regurgitation observed in two valves. The decellularization of these valves was also successful in mitigating calcification compared to cryopreservation (Manuscript 2). All five juvenile sheep in the decellularized homograft group had an event-free survival until day 180. The decellularized valves were repopulated with host interstitial cells, with the presence of rough endoplasmic reticulum (Fig.9A,B) and secretory vesicles (Fig.8A,B), the cellular structures responsible for the production of new collagen for tissue maintenance and remodeling. These valves also had an increase in annular diameter, indicating mild dilatation or the possible growth of these valves.

Decellularized plus EnCap treated pulmonary homografts developed high transvalvular gradients that increased over time, but no regurgitation was observed (Fig.2). These results indicate that there were good leaflet coaptation and closure of the valves without central leakage, and that leaflets remained supple and without retraction as with cryopreserved homografts at least up to 90 days. The significant increase in annulus diameter from implantation to echocardiography at 3 months in the decellularized plus EnCap treated group was rather unexpected, as the GA-fixed valves would not have been able to grow in size. Good visualization of the implanted valve was often difficult on trans-thoracic echocardiography, and could have resulted in size measurements made at the level of the native PA proximal to the implanted valve, instead of at the implanted valve annulus, resulting in misjudgement when interpreting the readings. The increase in annulus diameter as measured on echocardiography was significantly higher in the decellularized group compared to the decellularized plus EnCap treated group. This is an indication that the decellularized homografts might display growth potential; however the increased distensibility of the pulmonary homograft tissue could also be responsible for moderate dilatation of the annulus without any valve incompetence.

Three animals who received the decellularized plus EnCap treated homografts died prematurely at between 3-4 months after implantation of the valves. The median peak transvalvular gradient recorded at three-month echocardiography was 43 mm Hg, and vegetations nearly occluded the central openings of all three valves due to bacterial endocarditis (Fig.3D). All freshly harvested homografts initially had a valve diameter of around 18-19 mm, but GA-fixation and detoxification reduced the diameter to 16-17 mm due to tissue crimping and compaction with the formation of the additional cross-links and the larger interfibrillar spaces after decellularization. The valve size was still above the z-score of a 15.3 mm valve for the pulmonary position in a 24 kg patient (derived from a human normogram), and the decision was made to continue with the implants. Although the annular size of the implant did increase on echocardiography measurements, the inability of the conduit tissue distal to the valve to stretch and relax during the cardiac cycle resulted in severe stenosis of the conduit and dilatation of the native pulmonary artery distally to the implant, causing right heart failure and death. Endocarditis usually involves a microbiological inflammation of the endocardial surface, valves or great vessels, in

combination with lesions of these surfaces due to high-velocity and turbulent flow, jet impact and focal increases in the rate of shear stress (Bunag, 2007; Li and Giannakoulas, 2011).

In the remaining valves in this group, the transvalvular gradient also increased significantly to 41 mm Hg and 51 mm Hg respectively, within three months. In consultation with the veterinarian, it was decided to sacrifice the sheep prematurely, as a peak transvalvular gradient of 36-64 mm Hg is considered as moderate stenosis of the pulmonary valve (Baumgartner et al., 2009). No bacterial endocarditis was observed, but the conduits were also stenotic due to rigidity of the pulmonary homograft walls, clearly visible on macroscopic inspection (Fig.3C). Leaflets in these valves were also stiffer compared to cryopreserved and decellularized homografts pre-implantation (Manuscript 1, table 3). In a study comparing fresh decellularized pulmonary homografts with cryopreserved homografts and GA-fixed Contegra® valves, significant gradients were reported for the GA-fixed valves (Cebotari et al., 2011). Also, a significantly higher incidence of bacterial endocarditis was reported when using GA-fixed Contegra® valves compared to using cryopreserved homografts for RVOT construction, especially in children older than three years (Ugaki et al., 2015). These results correlate well with our findings.

At explantation, leaflet and wall samples in the decellularized scaffold group had formed an endothelial layer (Fig.4B and Fig.6B), while even after short implantation of only 3-4 months, the decellularized plus EnCap treated group demonstrated an endothelial-like multi-layer cell coverage that appeared like a fibrous encapsulation on H&E staining (Fig.4,D and Fig.6D). No ingrowth of interstitial cells into the leaflets and very limited ingrowth into the wall tissue was observed for the decellularized plus EnCap treated group (Fig.4D and Fig.6D). When compared to other commercially available valve conduits that are also GA-fixated, like the aortic Freestyle™ and Contegra® bovine jugular vein grafts both from Medtronic Inc, similar pannus overgrowth and fibrous sheath formation (Fig.5B,D) were reported (Butany et al., 2007; Schoenhoff et al., 2011). Pannus formation is common and almost appears to be the rule in GA-fixed valves manufactured from pericardium or valvular tissue and implanted in the sheep model. Stented mitral valve implants using decellularized pericardium and low concentration (0.1%) GA-fixation were however associated with much less pannus formation

when compared to non-decellularized and 0.5% GA-fixated pericardial valve implants in sheep (Collatusso et al., 2019).

Fixation of bioprosthetic implants of xenogeneic origin, such as bovine pericardium, porcine bioprosthesis or valved bovine jugular vein (Contegra®), with GA effectively prevents acute immune responses from the recipient by preventing the immediate recognition of xenoantigens. However, GA-fixation also resulted in a total lack of repopulation of bovine pericardium with recipient interstitial cells and angiogenesis in the rat subcutaneous model (Umashankar et al., 2012), thereby limiting the remodeling potential of the tissue (Liu et al., 2016). This limited repopulation of the homograft leaflet and wall tissue with recipient cells was also the case in our study. SEM of explanted homografts revealed uniformly distributed endothelial cell coverage of leaflet and conduit wall tissue in the decellularized scaffold group, with only small areas of exposed collagen fibers (Fig.7A,B). Leaflets and wall tissue in the decellularized plus EnCap treated group demonstrated fibrous encapsulation of the collagen matrix with a multi-layer of endothelial-like cells (Fig.7C,D). The cytotoxicity of GA to host cells may prevent the spontaneous endothelialization of implanted heart valves, making valves prone to inflammation, thrombogenicity and limited long-term durability (Nina et al., 2005). In the current study, no inflammatory reaction was observed, however significant chronic inflammation was seen in explanted comparable valves such as Freestyle™ valves (Butany et al., 2007), while macrophage and lymphocyte accumulation and giant cell reaction were reported in explanted Contegra® conduits. Focal microcalcifications and partially destructed collagen fibers were also reported for Contegra® conduits (Schoenhoff et al., 2011). Both the Freestyle™ and Contegra® conduits are xenografts, which could account for the observed inflammatory and immunological reactions. Homografts were used in the current study, which could account for the lack of inflammatory reactions. The presence of the inflammatory and immunological reactions in the xenografts and the absence thereof in the homograft tissue might be a result of the alpha-Gal epitope, showing an important difference between xenografts and homografts (Konakci et al., 2005). Only cellular remnants with little content and no living cells could be demonstrated in the leaflets of valves in the decellularized plus EnCap treated group following explantation (Fig.9C). Conduit wall samples in this group demonstrated single, sparsely distributed cells, but without any evidence of rough endoplasmic reticulum (Fig.9D). This observation could be due to the toxicity of the

functional aldehyde groups of GA or the additional fixation step with formaldehyde that forms part of the protocol used by Glycar South Africa for the processing of pericardial tissue, used in this study. However, this needs to be investigated as no cytotoxicity assays were done. The fixation process resulted in more compressed and dense collagen layers when compared to the leaflet and wall tissue in the cryopreserved and decellularized groups (Manuscript 1), which might make recellularization of the matrix with interstitial cells more difficult (Liao et al., 2008).

Tensile strength in both the wall and leaflet tissue and the Young's modulus of the leaflets of the decellularized homograft increased in the explant compared to that of pre-implanted valves (Table 4). Although this increase was not significant, it could be a result of the ingrowth of interstitial cells filling up the larger interfibrillar spaces that were created by the decellularization process. The wall tissue demonstrated a statistically significant increase in YM at explantation. Although strength tests were not performed on leaflet and wall tissue from valves in the decellularized plus EnCap treated group due to valve destruction, the fibrous encapsulation as demonstrated on histology will most certainly cause sharp increases in the tensile strength and stiffness of these tissues. These tissue changes will result in valve conduit stenosis and blood flow obstruction, causing leaflet damage and early valve failure, as observed in the current study.

The decellularization process used in this study proved to be very effective in mitigating the calcification of the implanted homograft tissue (Fig.4F,H and Fig.6F,H). Despite only being implanted for 3-4 months, the decellularized plus GA-fixed homografts showed a slight tendency to calcify more than the decellularized unfixed homografts, but still significantly less than cryopreserved homografts (Manuscript 2). Unconjugated GA may contribute towards the calcification of grafts (Lee et al., 2017), however, in the current study the decellularized, GA-fixated homografts were detoxified using propylene glycol that binds to the aldehyde groups of any unconjugated GA left after GA-fixation (Seifter and Frater, 1995). The slightly higher calcium content in leaflets in the decellularized group (Table 5) can be attributed to; 1) the shorter implantation period of three months for the decellularized plus EnCap treated group, compared to the six months for the decellularized scaffold group, and 2) the intracellular content of the host interstitial cells that repopulated the decellularized valves, compared to no ingrowth of host cells in the leaflets in the decellularized plus EnCap treated group. Despite mitigating the

calcification of leaflets and walls, decellularization and treatment of decellularized GA-fixed homografts with PG could not protect the tissue against calcifications in the suture lines (Fig.10). The calcification was most probably as a result of surgical injury to the native tissue, causing inflammatory reactions and tissue calcification (Hopkins et al., 2009).

LIMITATIONS OF THE STUDY

A limitation of this study is the small number of juvenile sheep that were investigated. The juvenile ovine model currently represents the best pre-clinical model to evaluate the potential for differentially processed homograft heart valve calcification in humans. However, the direct translation of the results from this study to human subjects cannot be made based on the ovine model used. A primate model should be used to relate the results from this study directly to humans. Implantation of larger donor valves to accommodate somatic growth of the patient over time will also be necessary. Tensile strength and Young's modulus data should always be treated with caution, due to the difficulty of getting repeatable results when working with such small tissue samples and low numbers.

CONCLUSION

Decellularization of homografts (48 h cold ischaemic time) maintained good haemodynamic characteristics and tissue properties of the pulmonary valves, limited calcification, and stimulated recellularization and remodeling as well as growth potential. All the sheep in the decellularized homograft group had an event-free survival until day 180. Concerns of the weakening of the ECM through the decellularization protocol prompted the additional GA-fixation and detoxification of the homograft before implantation in the juvenile ovine model. This fixation led to significantly increased transvalvular gradients as well as rigid, non-flexible tissue, and recipient animals developed stenosis and bacterial endocarditis. Sheep in the decellularized plus EnCap treated homograft group either died prematurely or were euthanized before day 180. The decellularization of the homograft tissue proved very successful in mitigating tissue calcification, while the capping of the free aldehydes in the decellularized plus EnCap treated group does not appear to influence the tissue calcification process negatively. More compressed and dense collagen layers were observed on H&E following GA-fixation and the repopulation of the scaffold with host interstitial cells was not successful, with the formation

of a fibrous encapsulation in the explanted valve walls and leaflets. If additional fixation of the scaffold is performed, the conduit should be of adequate size for implantation in an adult patient where valve growth matching the patient's somatic growth, and remodeling is not required. Additional GA-fixation of the decellularized homograft defies the purpose of decellularization, namely mitigating the immune response, promoting host cell repopulation and tissue remodeling, and may be counterproductive in growing individuals.

Conflict of interest

We certify that all authors named in the manuscript deserve authorship, and that all authors have agreed to be listed in the manuscript when submitted to peer review journals. The authors have no conflicts of interest to declare.

Acknowledgements

We would like to thank Miss H Grobler from the Centre for Electron Microscopy for preparation of all the SEM and TEM samples, the UFS Experimental Animal Unit for their assistance, Department of Anaesthesiology and the division of perfusion technology.

REFERENCES

ALI, M. L., KUMAR, S. P., BJORNSTAD, K. & DURAN, C. M. 1996. The sheep as an animal model for heart valve research. *Cardiovasc Surg*, 4, 543-9.

BAUMGARTNER, H., HUNG, J., BERMEJO, J., CHAMBERS, J. B., EVANGELISTA, A., GRIFFIN, B. P., IUNG, B., OTTO, C. M., PELLIKKA, P. A., QUINONES, M., AMERICAN SOCIETY OF, E. & EUROPEAN ASSOCIATION OF, E. 2009. Echocardiographic assessment of valve stenosis: EAE/ASE recommendations for clinical practice. *J Am Soc Echocardiogr*, 22, 1-23; quiz 101-2.

BESTER, D., BOTES, L., VAN DEN HEEVER, J. J., KOTZE, H., DOHMEN, P., POMAR, J. L. & SMIT, F. E. 2018. Cadaver donation: structural integrity of pulmonary homografts harvested 48 h post mortem in the juvenile ovine model. *Cell Tissue Bank*, 19, 743-754.

BESTER, D., SMIT, F. E., VAN DEN HEEVER, J. J., BOTES, L. & DOHMEN, P. M. C. E. 2017. *Detoxification and stabilization of implantable or transplantable biological material*. EU. 16792990.0-1455.

BIBEVSKI, S., RUZMETOV, M., FORTUNA, R. S., TURRENTINE, M. W., BROWN, J. W. & OHYE, R. G. 2017. Performance of SynerGraft Decellularized Pulmonary Allografts Compared With Standard Cryopreserved Allografts: Results From Multiinstitutional Data. *Ann Thorac Surg*, 103, 869-874.

BOETHIG, D., SCHREIBER, C., HAZEKAMP, M., BLANZ, U., PRÊTRE, R., ASFOUR, B., GRECO, R., ALEXI-MESKISHVILI, V., GONÇALVES, A. & BREYMANN, T. 2012. Risk factors for distal Contegra stenosis: results of a prospective European multicentre study. *Thorac Cardiovasc Surg*, 60, 195-204.

BOUDJEMLINE, Y., BEYLER, C., BONNET, D. & SIDI, D. 2003. Surprising outcome similarities between Contegra bovine jugular vein conduit and Shelhigh No-React porcine pulmonary valve conduit: role of immunologic reaction. *Eur J Cardiothorac Surg*, 24, 850-1; author reply 851.

BOURGINE, P. E., PIPPENGER, B. E., TODOROV, A., JR., TCHANG, L. & MARTIN, I. 2013. Tissue decellularization by activation of programmed cell death. *Biomaterials*, 34, 6099-108.

BREYMANN, T., BOETHIG, D., GOERG, R. & THIES, W. R. 2004. The Contegra bovine valved jugular vein conduit for pediatric RVOT reconstruction: 4 years experience with 108 patients. *J Card Surg*, 19, 426-31.

BUNAG, R. 2007. Infective Endocarditis. *In:* ENNA, S. J. & BYLUND, D. B. (eds.) *xPharm: The Comprehensive Pharmacology Reference*. New York: Elsevier. https://doi.org/10.1016/B978-008055232-3.60791-3.

BUTANY, J., ZHOU, T., LEONG, S. W., CUNNINGHAM, K. S., THANGAROOPAN, M., JEGATHEESWARAN, A., FEINDEL, C. & DAVID, T. E. 2007. Inflammation and infection in nine surgically explanted Medtronic Freestyle stentless aortic valves. *Cardiovasc Pathol*, 16, 258-67.

CEBOTARI, S., TUDORACHE, I., CIUBOTARU, A., BOETHIG, D., SARIKOUCH, S., GOERLER, A., LICHTENBERG, A., CHEPTANARU, E., BARNACIUC, S., CAZACU, A., MALIGA, O., REPIN, O., MANIUC, L., BREYMANN, T. & HAVERICH, A. 2011. Use of fresh decellularized allografts for pulmonary valve replacement may reduce the reoperation rate in children and young adults: early report. *Circulation*, 124, S115-23.

COLLATUSSO, C., RODERJAN, J. G., DE NORONHA, L., KLOSOWSKI, A., SUSS, P. H., GUARITA-SOUZA, L. C. & DA COSTA, F. D. A. 2019. Decellularization as a method to reduce calcification in bovine pericardium bioprosthetic valves. *Interact CardioVasc Thorac Surg*, 29, 302–311.

CONVERSE, G. L., ARMSTRONG, M., QUINN, R. W., BUSE, E. E., CROMWELL, M. L., MORIARTY, S. J., LOFLAND, G. K., HILBERT, S. L. & HOPKINS, R. A. 2012. Effects of cryopreservation, decellularization and novel extracellular matrix conditioning on the quasi-static and time-dependent properties of the pulmonary valve leaflet. *Acta Biomater*, 8, 2722-9.

CRAPO, P. M., GILBERT, T. W. & BADYLAK, S. F. 2011. An overview of tissue and whole organ decellularization processes. *Biomaterials*, 32, 3233-43.

DIJKMAN, P. E., DRIESSEN-MOL, A., FRESE, L., HOERSTRUP, S. P. & BAAIJENS, F. P. 2012. Decellularized homologous tissue-engineered heart valves as off-the-shelf alternatives to xeno- and homografts. *Biomaterials*, 33, 4545-54.

ERDBRUGGER, W., KONERTZ, W., DOHMEN, P. M., POSNER, S., ELLERBROK, H., BRODDE, O. E., ROBENEK, H., MODERSOHN, D., PRUSS, A., HOLINSKI, S., STEIN-KONERTZ, M. & PAULI, G. 2006. Decellularized xenogenic heart valves reveal remodeling and growth potential in vivo. *Tissue Eng*, 12, 2059-68.

FALCHETTI, A., DEMANET, H., DESSY, H., MELOT, C., PIERRAKOS, C. & WAUTHY, P. 2019. Contegra versus pulmonary homograft for right ventricular outflow tract reconstruction in newborns. *Cardiol Young*, 29, 505-510.

FLAMENG, W., MEURIS, B., YPERMAN, J., DE VISSCHER, G., HERIJGERS, P. & VERBEKEN, E. 2006. Factors influencing calcification of cardiac bioprostheses in adolescent sheep. *J Thorac Cardiovasc Surg*, 132, 89-98.

HOLMES, A. A., CO, S., HUMAN, D. G., LEBLANC, J. G. & CAMPBELL, A. I. 2012. The Contegra conduit: Late outcomes in right ventricular outflow tract reconstruction. *Ann Pediatr Cardiol*, 5, 27-33.

HOPKINS, R. A., JONES, A. L., WOLFINBARGER, L., MOORE, M. A., BERT, A. A. & LOFLAND, G. K. 2009. Decellularization reduces calcification while improving both durability and 1-year functional results of pulmonary homograft valves in juvenile sheep. *J Thorac Cardiovasc Surg*, 137, 907-13, 913e1-4.

KONAKCI, K. Z., BOHLE, B., BLUMER, R., HOETZENECKER, W., ROTH, G., MOSER, B., BOLTZ-NITULESCU, G., GORLITZER, M., KLEPETKO, W., WOLNER, E. & ANKERSMIT, H. J. 2005. Alpha-Gal on bioprostheses: xenograft immune response in cardiac surgery. *Eur J Clin Invest*, 35, 17-23.

LAKER, L., DOHMEN, P. M. & SMIT, F. E. 2020. Synergy in a detergent combination results in superior decellularized bovine pericardial extracellular matrix scaffolds. *J Biomed Mater Res, Part B: Appl Biomater*. https://doi.org/10.1002/jbm.b.34588.

LEE, C., LIM, H. G., LEE, C. H. & KIM, Y. J. 2017. Effects of glutaraldehyde concentration and fixation time on material characteristics and calcification of bovine pericardium: implications for the optimal method of fixation of autologous pericardium used for cardiovascular surgery. *Interact Cardiovasc Thorac Surg*, 24, 402-406.

LI, W. & GIANNAKOULAS, G. Infective Endocarditis; in GATZOULIS, M. A., WEBB, G.D. & DAUBENEY, E. F. 2011. *Diagnosis and Management of Adult Congenital Heart Disease* (2nd Edition), Elsevier, Philadelphia, USA.

LIAO, J., JOYCE, E. M. & SACKS, M. S. 2008. Effects of decellularization on the mechanical and structural properties of the porcine aortic valve leaflet. *Biomaterials*, 29, 1065-74.

LIM, H. G., KIM, G. B., JEONG, S. & KIM, Y. J. 2015. Development of a next-generation tissue valve using a glutaraldehyde-fixed porcine aortic valve treated with decellularization, alpha-galactosidase, space filler, organic solvent and detoxification. *Eur J Cardiothorac Surg*, 48, 104-13.

LIU, Z. Z., WONG, M. L. & GRIFFITHS, L. G. 2016. Effect of bovine pericardial extracellular matrix scaffold niche on seeded human mesenchymal stem cell function. *Sci Rep*, 6, 37089.

MEPHAM, B. L. 1991. *Theory and practice of histological techniques, Third ed*, BANCROFT, J. D. & STEVENS, A. Edinburgh, Churchill Livingstone ISBN:0443035598.

MERY, C. M., GUZMAN-PRUNEDA, F. A., DE LEON, L. E., ZHANG, W., TERWELP, M. D., BOCCHINI, C. E., ADACHI, I., HEINLE, J. S., MCKENZIE, E. D. & FRASER, C. D., JR. 2016. Risk factors for development of endocarditis and reintervention in patients undergoing right ventricle to pulmonary artery valved conduit placement. *J Thorac Cardiovasc Surg*, 151, 432-9, 441 e1-2.

NIH. 2011. *Guide for the Care and Use of Laboratory Animals, 8th ed.* [Online]. Washington DC: National Academy of Sciences. Available: https://www.ncbi.nlm.nih.gov/pubmed/21595115.

NINA, V. J., POMERANTZEFF, P. M., CASAGRANDE, I. S., CHEUNG, D. T., BRANDAO, C. M. & OLIVEIRA, S. A. 2005. Comparative study of the L-hydro process and glutaraldehyde preservation. *Asian Cardiovasc Thorac Ann*, 13, 203-7.

ORYAN, A., KAMALI, A., MOSHIRI, A., BAHARVAND, H. & DAEMI, H. 2018. Chemical crosslinking of biopolymeric scaffolds: Current knowledge and future directions of crosslinked engineered bone scaffolds. *Int J Biol Macromol*, 107, 678-688.

PADALA, M. 2018. A heart valve is no stronger than its weakest link: The need to improve durability of pericardial leaflets. *J Thorac Cardiovasc Surg*, 156, 207-208.

PARK, C. S., KIM, Y. J., LEE, J. R., LIM, H. G., CHANG, J. E., JEONG, S. & KWON, N. 2017. Anticalcification effect of a combination of decellularization, organic solvents and amino acid detoxification on glutaraldehyde-fixed xenopericardial heart valves in a large-animal long-term circulatory model. *Interact Cardiovasc Thorac Surg*, 25, 391-399.

PROTOPAPAS, A. D. & ATHANASIOU, T. 2008. Contegra conduit for reconstruction of the right ventricular outflow tract: a review of published early and mid-time results. *J Cardiothorac Surg*, 3, 62.

SCHOENHOFF, F. S., LOUP, O., GAHL, B., BANZ, Y., PAVLOVIC, M., PFAMMATTER, J. P., CARREL, T. P. & KADNER, A. 2011. The Contegra bovine jugular vein graft versus the Shelhigh pulmonic porcine graft for reconstruction of the right ventricular outflow tract: a comparative study. *J Thorac Cardiovasc Surg*, 141, 654-61.

SEIFTER, E. & FRATER, R. W. M. 1995. *Anticalcification treatment for aldehyde-tanned biological tissue*. United States. Albert Einstein College of Medicine of Yeshiva University (Bronx, NY).5476516. http://www.freepatentsonline.com/5476516.html.

SELAMET TIERNEY, E. S., GERSONY, W. M., ALTMANN, K., SOLOWIEJCZYK, D. E., BEVILACQUA, L. M., KHAN, C., KRONGRAD, E., MOSCA, R. S., QUAEGEBEUR, J. M. & APFEL, H. D. 2005. Pulmonary position cryopreserved homografts: durability in pediatric Ross and non-Ross patients. *J Thorac Cardiovasc Surg*, 130, 282-6.

SHADDY, R. E. & HAWKINS, J. A. 2002. Immunology and failure of valved allografts in children. *Ann Thorac Surg*, 74, 1271-5.

SIMON, P., KASIMIR, M. T., SEEBACHER, G., WEIGEL, G., ULLRICH, R., SALZER-MUHAR, U., RIEDER, E. & WOLNER, E. 2003. Early failure of the tissue engineered porcine heart valve SYNERGRAFT in pediatric patients. *Eur J Cardiothorac Surg*, 23, 1002-6; discussion 1006.

SMIT, F. E., BESTER, D., VAN DEN HEEVER, J. J., SCHLEGEL, F., BOTES, L. & DOHMEN, P. M. 2015. Does prolonged post-mortem cold ischaemic harvesting time influence cryopreserved pulmonary homograft tissue integrity? *Cell Tissue Bank*, 16, 531-44.

SPURR, A. R. 1969. A low-viscosity epoxy resin embedding medium for electron microscopy. *J Ultrastruct Res*, 26, 31-43.

STRANGE, G., BRIZARD, C., KARL, T. R. & NEETHLING, L. 2015. An evaluation of Admedus' tissue engineering process-treated (ADAPT) bovine pericardium patch (CardioCel) for the repair of cardiac and vascular defects. *Expert Rev Med Devices*, 12, 135-41.

SUCCI, J. E., BUFFOLO, E., SALLES, C. A., CASAGRANDE, I. S. J., NETO, J. V., DE MENDONÇA, J. T., FILHO, R. V., JARAMILLO, I. A. 1986. Valve replacement with aortic glutaraldehyde preserved homografts: a multicenter study. *Rev Bras Cir Cardiovasc Surg*, 1(2), 20-23.

THUBRIKAR, M. J., DECK, J. D., AOUAD, J. & NOLAN, S. P. 1983. Role of mechanical stress in calcification of aortic bioprosthetic valves. *J Thorac Cardiovasc Surg*, 86, 115-25.

TILLQUIST, M. N. & MADDOX, T. M. 2011. Cardiac crossroads: deciding between mechanical or bioprosthetic heart valve replacement. *Patient Prefer Adherence*, 5, 91-9.

UGAKI, S., RUTLEDGE, J., AL AKLABI, M., ROSS, D. B., ADATIA, I. & REBEYKA, I. M. 2015. An increased incidence of conduit endocarditis in patients receiving bovine jugular vein grafts compared to cryopreserved homograft for right ventricular outflow reconstruction. *Ann Thorac Surg*, 99, 140-6.

UMASHANKAR, P. R., MOHANAN, P. V. & KUMARI, T. V. 2012. Glutaraldehyde treatment elicits toxic response compared to decellularization in bovine pericardium. *Toxicol Int*, 19, 51-8.

YOSHIKAWA, Y., KITAMURA, S., TANIGUCHI, S., KAMEDA, Y., NIWAYA, K. & SAKAGUCHI, H. 2000. Pulmonary ventricular outflow reconstruction with a size-reduced cryopreserved pulmonary valve allograft: mid-term follow-up. *Jpn Circ J*, 64, 23-6.

Chapter 6 - Summary, conclusions and future recommendations

The conclusions from each of the three different parts of the study are given below.

Study 1

Comparison of the impact of cryopreservation, decellularization and decellularization, glutaraldehyde-fixation and detoxification as processing techniques on the strength and structure of juvenile ovine pulmonary homografts

Our proprietary decellularization protocol proved to be effective in removing all endothelial and interstitial cells from the sheep homografts, while confluent layers of endothelial cells were still present on the leaflet and wall tissue of the cryopreserved group even after 48 hours cold ischaemia. The collagen matrix in the cryopreserved group was more collapsed, well organized but loosely arranged with larger interfibrillar spaces in the decellularized group, and more dense and compacted in the decellularized plus EnCap treated group. On ultrastructure, the collagen in the cryopreserved group appeared disrupted and fractured, but intact in the other two groups. Elastin appeared to be well preserved in all three groups after processing, with no visible calcific nodules in any of the groups. Tensile strength was well maintained in decellularized tissue when compared to cryopreserved tissue; however, it did increase in leaflet tissue after additional EnCap treatment. The tissue stiffness in the decellularized plus EnCap treated group also increased. Dehydration and fixation during the delipidation phase were most likely responsible for maintaining the tensile strength of the leaflet and wall tissue after decellularization. We conclude that the leaflets and wall tissue of ovine pulmonary homografts remained strong enough after decellularization and that the larger pores in the scaffold, likely due to the removal of GAGs, will assist in the recellularization process. Damaged collagen will lead to earlier valve degeneration in the cryopreserved valves, while the compacted collagen in the decellularized plus EnCap treated tissue will make recellularization more difficult. Additional fixation of the decellularized scaffold increases leaflet stiffness, which will negatively affect the biomechanical behaviour of the homograft.

Study 2

Comparison of function and structural integrity of cryopreserved pulmonary homografts versus decellularized pulmonary homografts after 180 days implantation in the juvenile ovine model

Decellularization of homografts, with a post-mortem cold ischaemic harvesting time of 48 h, successfully retained the haemodynamic characteristics and tissue properties of pulmonary valves, while significantly mitigating calcification. Cryopreservation was less successful in protecting the homograft from calcification, and leaflet thickening and retraction resulted in significant valve regurgitation that will ultimately lead to right heart failure. Successful repopulation of the decellularized scaffold with host interstitial cells presenting with rough endoplasmic reticulum, will promote tissue maintenance and remodeling and potentially extend the durability of these implants in young patients. The potential of decellularized homografts to grow in diameter size while maintaining good leaflet coaptation and closure without developing valve regurgitation makes decellularization of pulmonary homografts, even after extended post-mortem ischaemic harvesting times, a promising alternative processing method for these homografts to be used in RVOT reconstruction in the clinical setting. The strength of decellularized tissue did not decrease once implanted in the circulatory system, while the tissue stiffness increased, most likely due to the repopulation of the ECM with host fibroblast cells.

Study 3

Comparison of function and structural integrity of decellularized pulmonary homografts versus decellularized, glutaraldehyde-fixed and detoxified pulmonary homografts after 180 days implantation in the juvenile ovine model

Decellularized homografts maintained good haemodynamic characteristics and tissue properties of the pulmonary valves, limited calcification, and stimulated recellularization and remodeling as well as growth potential. All the sheep in the decellularized homograft group had an event-free survival until day 180. Concerns of the weakening of the ECM through the decellularization protocol prompted the additional GA-fixation and detoxification of the homograft before implantation in the juvenile ovine model. This fixation led to significantly increased transvalvular gradients as well as rigid, non-flexible tissue, and recipient animals developed stenosis and bacterial endocarditis. Sheep in the decellularized plus EnCap treated

homograft group either died prematurely or were euthanized before day 180. The detoxification method used for the GA-fixed decellularized homografts was successful in mitigating calcification. More compressed and dense collagen layers were observed on H&E following GA-fixation and the repopulation of the scaffold with host interstitial cells was not successful, with the formation of a fibrous encapsulation in the explanted valve walls and leaflets. If additional fixation of the scaffold is performed, the conduit should be of adequate size for implantation in an adult patient where valve growth matching the patient's somatic growth, and remodeling is not required. Additional GA-fixation of the decellularized homograft defies the purpose of decellularization, namely mitigating the immune response, promoting host cell repopulation and tissue remodeling, and may be counterproductive in growing individuals.

Table 6.1: Summary of study results.

Variable	Cryopreserved		Decellularized		Decellularized plus EnCap treated	
Pre-implantation	**Leaflet**	**Pulmonary Wall**	**Leaflet**	**Pulmonary Wall**	**Leaflet**	**Pulmonary Wall**
Clinical Calcification	Y		N		N	
Strength TS (MPa) YM (MPa)	3.72 [3.12- 5.01] 23.34 [14.12-28.87]	1.80 [1.35-2.65] 1.97 [1.22-3.18]	1.83 [0.01-5.65] 22.10 [0.10-55.27]	1.89 [1.57-2.38] 2.32 [1.82-2.88]	4.96 [4.34-6.76] 41.11 [27.76-52.52]	1.90 [1.18-2.09] 2.21 [1.99-3.58]
Morphology **DAPI** Cells	Y	Y	N	N	N	N
H&E Collagen	Collapsed	Collapsed	Interfibrillar spaces	Interfibrillar spaces	Compacted	Compacted
EVG Elastin	Y	Y	Y	Y	Y	Y
VK Calcification	N	N	N	N	N	N
SEM Endothelium	Y	Y	N	N	N	N
TEM Viable fibroblasts	Y	Y	Acellular	Acellular	Acellular	Acellular

Data represented as medians and the corresponding InterQuartile ranges. [Y = Yes; N = No; nd = not done].

Table 6.1: Summary of study results (continued).

Variable	Cryopreserved		Decellularized		Decellularized plus EnCap treated	
Explantation	**Leaflet**	**Pulmonary Wall**	**Leaflet**	**Pulmonary Wall**	**Leaflet**	**Pulmonary Wall**
Clinical						
Handling	Satisfactory	Satisfactory	Satisfactory	Satisfactory	Thin / Destroyed	Rigid
Calcification	Y	Y	N	N	N	N
Aneurysm	N	N	N	N	N	N
Infective Endocarditis	N	N	N	N	Y	Y
Disintegration	N	N	N	N	N	N
Strength						
TS (MPa)	4.67 [2.56-7.17]	1.72 [1.37-2.49]	6.06 [2.18-10.69]	7.92 [1.29-12.64]	nd	nd
YM (MPa)	23.07 [14.99-38.10]	5.15 [3.42-7.54]	50.73 [21.6-118.1]	16.35 [8.67-24.05]	nd	nd
Morphology						
H&E						
Collagen	Collapsed	Collapsed	Normal	Normal	Compacted	Compacted/Rigid
Endothelium	Y	Y	Y	Y	Y	Y
Fibrous encapsulation	N	N	N	N	Y	Y
Cell content /Host cell infiltration	2/10	2/10	4/10	8/10	0/10	1/10
Remodeling	N	N	Y	Y	N	N
EVG						
Elastin	N	Y	N	Y	N	Y
VK						
Calcification	Y	Y	N	N	N	N
SEM						
Re-endothelialization	Y	Y	Y	Y	Y	Y
TEM						
Viable fibroblast-like cells	Y	Y	Y	Y	N	Y

Data represented as medians and the corresponding InterQuartile ranges. [Y = Yes; N = No; nd = not done].

6.1 Summary of key results

6.1.1 Cryopreserved Pulmonary homografts

Pre-implantation Leaflet:

Pliable, confluent endothelium, endothelium coming loose, uniform distribution of interstitial cells, interstitial cells and cellular remnants, collapsed collagen, no calcification, fractured collagen fibers, elastin, adequate strength

Pre-implantation Wall:

Pliable, confluent endothelium, endothelium coming loose, uniform distribution of interstitial cells, interstitial cells and cellular remnants, collapsed collagen, fractured collagen fibers, no calcification, elastin, adequate strength

Explant Leaflet:

Pliable, no aneurysm, no infective endocarditis, no disintegration, no inflammation, re-endothelialized, loss of interstitial cells, collapsed collagen, calcific nodules, ECM calcification, loss of elastin from pre-implantation, no remodelling, thickened and retracted, retained tensile strength, similar stiffness

Explant Wall:

Pliable, no aneurysm, no infective endocarditis, no disintegration, no inflammation, re-endothelialized, loss of interstitial cells, collapsed collagen, calcific nodules, ECM calcification, retained elastin from pre-implantation, no remodeling, calcification of suture lines, retained tensile strength, increased stiffness

6.1.2 Decellularized Pulmonary homografts

Pre-implantation Leaflet:

Pliable, acellular, no endothelial cells, loosely arranged collagen, large interfibrillar spaces, no calcification, elastin, retained strength, retained stiffness

Pre-implantation Wall:

Pliable, acellular, no endothelial cells, loosely arranged collagen, large interfibrillar spaces, no calcification, elastin, retained strength, retained stiffness

Explant Leaflet:

No aneurysm, no infective endocarditis, no disintegration, no inflammation, pliable, good coaptation, thin and translucent, limited calcific nodules, re-endothelialization, loosely arranged collagen, extensive interstitial cell repopulation, living young fibroblasts, vacuoles/vesicles, rough endoplasmic reticulum, potential remodeling, no interstitial calcification, elastin<pre-implant, increased strength, increased stiffness.

Explant Wall:

No aneurysm, no infective endocarditis, no disintegration, no inflammation, pliable, loosely arranged collagen, no visible calcification, re-endothelialization, extensive interstitial cell repopulation, living young fibroblasts, vacuoles/vesicles, rough endoplasmic reticulum, potential remodeling, no interstitial calcification, elastin, increased strength, increased stiffness

6.1.3 Decellularized plus EnCap treated Pulmonary homografts

Pre-implantation Leaflet:

Acellular, no endothelial cells, dense and compacted collagen, no calcification, elastin, basal membrane remnants, retained strength, increased stiffness, limited pliability

Pre-implantation Wall:

Acellular, no endothelial cells, dense and compacted collagen, no calcification, elastin, basal membrane remnants, retained strength, increased stiffness, rigid

Explant Leaflet:

x2: Thin and translucent, compacted collagen, no visible calcification, no aneurysm, no infective endocarditis, no disintegration, fibrous encapsulation, re-endothelialization, no host cell infiltration, no interstitial calcification, no elastin, no rough endoplasmic reticulum, no remodeling

x3: No visible calcification, infective endocarditis, disintegration

Explant Wall:

x2: No visible calcification, no aneurysm, no infective endocarditis, no disintegration, not pliable, fibrous encapsulation, re-endothelialization, limited host cell infiltration, compacted collagen, no interstitial calcification, elastin, no rough endoplasmic reticulum, no remodeling, rigid

x3: No visible calcification, infective endocarditis, rigid

6.2 Conclusions

Donor pulmonary homografts for RVOT reconstruction in young children with congenital abnormalities and in Ross procedures remain the preferred replacement option, as no anticoagulation therapy is required. Donor shortages led to investigations of extending the post-mortem harvesting time to 48 h and proved to be a viable option. Decellularization of such

homografts proved successful, without sacrificing tissue strength and biomechanical properties. Decellularization does create larger interfibrillar spaces, most likely by removing the GAGs from the leaflet and wall tissue, however, this might be advantageous in the repopulation and ingrowth of interstitial cells once implanted. Additional GA-fixation and detoxification of decellularized homografts caused shrinkage, compacted collagen and excessive stiffness of the leaflet and wall tissue, which would be detrimental for optimal valve functioning.

Implanted cryopreserved pulmonary homografts lost interstitial cells that would not be beneficial for tissue remodeling. The presence of cells and cellular remnants in the ECM will make the tissue prone to calcification and degeneration. Leaflet thickening and retraction caused significant regurgitation, resulting in right heart failure over time and will require re-intervention. The tissue handled well and remained pliable, and although calcification was observed in explanted tissue, the tensile strength and stiffness were not negatively affected at explantation.

Decellularized homografts handled well at implantation and had an almost similar appearance to native tissue when explanted. Endothelialization was extensive, and the ingrowth of interstitial cells almost uniform. Less dense collagen matrix with larger pore sizes might allow better and easier recellularization with interstitial cells. Rough endoplasmic reticulum was observed in interstitial cells, indicating the potential for collagen production and tissue regeneration. The potential remodeling will be an important factor in the long-term survival of the homograft, with the possibility of the valve diameter to grow in young patients without creating a leaking valve. Tensile strength and tissue stiffness did increase, however, the tissue was still soft and pliable, and calcification significantly mitigated.

Concern about the strength of the decellularized homograft led to additional GA-fixation and detoxification (EnCap treatment), however, this resulted in compacted collagen and a rigid conduit at explantation. Stenosis of the conduit resulted in a high incidence of bacterial endocarditis, and this processing method should only be considered where somatic growth of the patient will no longer be a factor. Possible toxic effects of GA also resulted in no repopulation of the ECM, which will make tissue remodeling impossible. Formation of a fibrous encapsulation was also observed on the leaflet and wall tissue. Although strength tests were not performed on

leaflet and wall tissue from valves in the decellularized plus EnCap treated group due to valve destruction, the fibrous encapsulation will most certainly cause sharp increases in the tensile strength and stiffness of these tissues.

Although cryopreserved homografts remain a good replacement option for the RVOT in young children, decellularized pulmonary homografts in the sheep model proved an excellent alternative. Strength and biomechanical properties were maintained, calcification was significantly mitigated and recellularization extensive, with good potential tissue remodeling and growth. Additional GA-fixation of the scaffold is unnecessary and seems to defy the purpose of decellularization.

6.3 Limitations and Recommendations

The study was limited by:

(i) Data obtained with the juvenile sheep model cannot be unconditionally translated to human patients.

(ii) Due to the extremely high costs of cardiac surgery procedures, a limited number of animals can be operated, which will affect the statistical calculations of the study.

(iii) The small sample sizes, especially of leaflet tissue, always make TS testing difficult and not so reliable.

Future considerations:

(i) The GAG content following decellularization should be evaluated.

(ii) The duration of implantation should be extended, which might provide more insight into the maintenance of the scaffold, tissue remodeling and valve growth of decellularized homografts in young growing subjects.

(iii) Adaptations to the decellularization protocol regarding chemical concentrations, duration of exposure and washout, and other long-term storage options should be investigated.

(iv) Cell viability testing should be included to evaluate the toxicity of GA-fixation.

(v) The effectiveness of the detoxification method for the removal of free aldehyde groups should be investigated.

(vi) The use of monomeric GA or other fixation options instead of GA solutions should be explored.

(vii) Repeating this study in a primate model to relate the results from this study directly to humans.

Reference list

AIKAWA, E. & SCHOEN, F. J. 2014. Chapter 9 - Calcific and Degenerative Heart Valve Disease. *In*: WILLIS, M. S., HOMEISTER, J. W. & STONE, J. R. (eds.) *Cellular and Molecular Pathobiology of Cardiovascular Disease.* San Diego: Academic Press. https://doi.org/10.1016/B978-0-12-405206-2.00009-0.

ANGELL, J. D., CHRISTOPHER, B. S., HAWTREY, O. & ANGELL, W. M. 1976. A fresh, viable human heart valve bank: sterilization, sterility testing, and cryogenic preservation. *Transplant Proc*, 8(2 Suppl 1), 139–147.

AXELSSON, I. & MALM, T. 2018. Long-Term Outcome of Homograft Implants Related to Donor and Tissue Characteristics. *Ann Thorac Surg*, 106, 165-171.

AYOUB, S., FERRARI, G., GORMAN, R. C., GORMAN, J. H., SCHOEN, F. J. & SACKS, M. S. 2016. Heart Valve Biomechanics and Underlying Mechanobiology. *Compr Physiol*, 6, 1743-1780.

BADER, A., SCHILLING, T., TEEBKEN, O. E., BRANDES, G., HERDEN, T., STEINHOFF, G. & HAVERICH, A. 1998. Tissue engineering of heart valves--human endothelial cell seeding of detergent acellularized porcine valves. *Eur J Cardiothorac Surg*, 14(3), 279-84.

BARRATT-BOYES, B. G. 1965. Homograft aortic valve replacement. *N Z Med J*, 64, Suppl, 41-3.

BASKETT, R. J., NANTON, M. A., WARREN, A. E. & ROSS, D. B. 2003. Human leukocyte antigen-DR and ABO mismatch are associated with accelerated homograft valve failure in children: implications for therapeutic interventions. *J Thorac Cardiovasc Surg*, 126, 232-9.

BASTIAN, F., STELZMULLER, M. E., KRATOCHWILL, K., KASIMIR, M. T., SIMON, P. & WEIGEL, G. 2008. IgG deposition and activation of the classical complement pathway involvement in the activation of human granulocytes by decellularized porcine heart valve tissue. *Biomaterials*, 29, 1824-32.

BESTER, D., BOTES, L., VAN DEN HEEVER, J. J., KOTZE, H., DOHMEN, P., POMAR, J. L. & SMIT, F. E. 2018. Cadaver donation: structural integrity of pulmonary homografts harvested 48 h post mortem in the juvenile ovine model. *Cell Tissue Bank*, 19, 743-754.

BIBEVSKI, S., RUZMETOV, M., FORTUNA, R. S., TURRENTINE, M. W., BROWN, J. W. & OHYE, R. G. 2017. Performance of SynerGraft Decellularized Pulmonary Allografts Compared With Standard Cryopreserved Allografts: Results From Multiinstitutional Data. *Ann Thorac Surg*, 103, 869-874.

BOETHIG, D., HORKE, A., HAZEKAMP, M., MEYNS, B., REGA, F., VAN PUYVELDE, J., HÜBLER, M., SCHMIADY, M., CIUBOTARU, A., STELLIN, G., PADALINO, M., TSANG, V., JASHARI, R., BOBYLEV, D., TUDORACHE, I., CEBOTARI, S., HAVERICH, A. & SARIKOUCH, S. 2019. A European study on decellularized homografts for pulmonary valve replacement: initial results from the prospective ESPOIR Trial and ESPOIR Registry data. *Eur J Cardiothorac Surg*, 56, 503–509. ORIGINAL ARTICLE doi:10.1093/ejcts/ezz054.

BOROUMAND, S., ASADPOUR, S., AKBARZADEH, A., FARIDI-MAJIDI, R. & GHANBARI, H. 2018. Heart valve tissue engineering: an overview of heart valve decellularization processes. *Regen Med*, 13, 41-54.

BOTES, L., VAN DEN HEEVER, J. J., SMIT, F. E. & NEETHLING, W. M. 2012. Cardiac allografts: a 24-year South African experience. *Cell Tissue Bank*, 13, 139-46.

BOURGINE, P. E., PIPPENGER, B. E., TODOROV, A., JR., TCHANG, L. & MARTIN, I. 2013. Tissue decellularization by activation of programmed cell death. *Biomaterials*, 34, 6099-108.

BROWN, B. N., FREUND, J. M., HAN, L., RUBIN, J. P., REING, J. E., JEFFRIES, E. M., WOLF, M. T., TOTTEY, S., BARNES, C. A., RATNER, B. D. & BADYLAK, S. F. 2011. Comparison of three methods for the derivation of a biologic scaffold composed of adipose tissue extracellular matrix. *Tissue Eng, Part C: Methods*, 17, 411-421.

BROWN, J. W., ELKINS, R. C., CLARKE, D. R., TWEDDELL, J. S., HUDDLESTON, C. B., DOTY, J. R., FEHRENBACHER, J. W. & TAKKENBERG, J. J. 2010a. Performance of the CryoValve SG human decellularized pulmonary valve in 342 patients relative to the conventional CryoValve at a mean follow-up of four years. *J Thorac Cardiovasc Surg*, 139, 339-48.

BROWN, J. W., ELKINS, R. C., CLARKE, D. R., TWEDDELL, J. S., HUDDLESTON, C. B., DOTY, J. R., FEHRENBACHER, J. W. & TAKKENBERG, J. J. M. 2010b. Performance of the CryoValve SG human decellularized pulmonary valve in 342 patients relative to

the conventional CryoValve at a mean follow-up of four years. *J Thorac Cardiovasc Surg*, 139, 339-348.

BROWN, J. W., RUZMETOV, M., RODEFELD, M. D., VIJAY, P. & TURRENTINE, M. W. 2005. Right ventricular outflow tract reconstruction with an allograft conduit in non-ross patients: risk factors for allograft dysfunction and failure. *Ann Thorac Surg*, 80, 655-63; discussion 663-4.

BURATTO, E., GASTALDELLO, A., DAL LIN, C., TARZIA, V., NASO, F., BOTTIO, T., GANDAGLIA, A., SPINA, M. & GEROSA, G. 2011. Structural, Morphological and Hydrodynamic Characterisation of Taurodeoxycholate Decellularised Porcine Heart Valves: A Holistic Approach to Heart Valve Tissue Engineering. *Heart, Lung and Circulation*, 20, S229.

BURCH, P. T., KAZA, A. K., LAMBERT, L. M., HOLUBKOV, R., SHADDY, R. E. & HAWKINS, J. A. 2010. Clinical performance of decellularized cryopreserved valved allografts compared with standard allografts in the right ventricular outflow tract. *Ann Thorac Surg*, 90, 1301-5; discussion 1306.

CEBOTARI, S., MERTSCHING, H., KALLENBACH, K., KOSTIN, S., REPIN, O., BATRINAC, A., KLECZKA, C., CIUBOTARU, A. & HAVERICH, A. 2002. Construction of autologous human heart valves based on an acellular allograft matrix. *Circulation*, 106, I63-I68.

CEBOTARI, S., TUDORACHE, I., JAEKEL, T., HILFIKER, A., DORFMAN, S., TERNES, W., HAVERICH, A. & LICHTENBERG, A. 2010. Detergent decellularization of heart valves for tissue engineering: toxicological effects of residual detergents on human endothelial cells. *Artif Organs*, 34(3), 206-10.

CEBOTARI, S., TUDORACHE, I., CIUBOTARU, A., BOETHIG, D., SARIKOUCH, S., GOERLER, A., LICHTENBERG, A., CHEPTANARU, E., BARNACIUC, S., CAZACU, A., MALIGA, O., REPIN, O., MANIUC, L., BREYMANN, T. & HAVERICH, A. 2011. Use of fresh decellularized allografts for pulmonary valve replacement may reduce the reoperation rate in children and young adults: early report. *Circulation*, 124, S115-23.

COFFEY, S., CAIRNS, B. J. & IUNG, B. 2016. The modern epidemiology of heart valve disease. *Heart*, 102, 75-85.

COMBS, M. D. & YUTZEY, K. E. 2009. Heart valve development: regulatory networks in development and disease. *Circ Res*, 105, 408-21.

CONVERSE, G. L., ARMSTRONG, M., QUINN, R. W., BUSE, E. E., CROMWELL, M. L., MORIARTY, S. J., LOFLAND, G. K., HILBERT, S. L. & HOPKINS, R. A. 2012. Effects of cryopreservation, decellularization and novel extracellular matrix conditioning on the quasi-static and time-dependent properties of the pulmonary valve leaflet. *Acta Biomater*, 8, 2722-9.

CRAPO, P. M., GILBERT, T. W. & BADYLAK, S. F. 2011. An overview of tissue and whole organ decellularization processes. *Biomaterials*, 32, 3233-43.

CRESCENZO, D. G., HILBERT, S. L., MESSIER, R. H., JR., DOMKOWSKI, P. W., BARRICK, M. K., LANGE, P. L., FERRANS, V. J., WALLACE, R. B. & HOPKINS, R. A. 1993. Human cryopreserved homografts: electron microscopic analysis of cellular injury. *Ann Thorac Surg*, 55, 25-30; discussion 30-1.

DA COSTA, F. D. A., DOHMEN, P. M., VIEIRA, E., LOPES, S. V., COLLATUSSO, C., PEREIRA, E. W., MATSUDA, C. N. & CAUDURO, S. 2007. Ross Operation with decellularized pulmonary allografts: medium-term results. *Rev Bras Cir Cardiovasc Surg*, 22, 454-62.

DA COSTA, F. D. A., COSTA, A. C., PRESTES, R., DOMANSKI, A. C., BALBI, E. M., FERREIRA, A. D. & LOPES, S. V. 2010. The early and midterm function of decellularized aortic valve allografts. *Ann Thorac Surg*, 90, 1854-60.

DA COSTA, F. D. A., ETNEL, J. R. G., TORRES, R., BALBI FILHO, E. M., TORRES, R., CALIXTO, A. & MULINARI, L. A. 2017. Decellularized Allografts for Right Ventricular Outflow Tract Reconstruction in Children. *World J Pediatr Congenit Heart Surg*, 8(5), 605-612.

DA COSTA, F. D. A., ETNEL, J. R. G., CHARITOS, E. I., SIEVERS, H. H., STIERLE, U., FORNAZARI, D., TAKKENBERG, J. J. M., BOGERS, A. J. J. C. & MOKHLES, M. M. 2018. Decellularized Versus Standard Pulmonary Allografts in the Ross Procedure: Propensity-Matched Analysis. *Ann Thorac Surg*, 105(4), 1205-1213.

DAHOU, A., LEVIN, D., REISMAN, M. & HAHN, R. T. 2019. Anatomy and Physiology of the Tricuspid Valve. *JACC: Cardiovascular Imaging*, 12, 458-468.

DAWSON, P. E. & BROCKBANK, K. G. M. 1997. Human heart cold ischemia and its effect on post-cryopreservation viability of heart valves. *In:* YACOUB, M. H., YANKAH, A. C. & HETZER, R. (eds.) *Cardiac Valve Allografts.* Steinkopff, Heidelberg. https://doi.org/10.1007/978-3-642-59250-8_4.

DEKENS, E., VAN DAMME, E., JASHARI, R., VAN HOECK, B., FRANCOIS, K. & BOVE, T. 2019. Durability of pulmonary homografts for reconstruction of the right ventricular outflow tract: how relevant are donor-related factors? *Interact Cardiovasc Thorac Surg*, 28, 503-509.

DIJKMAN, P. E., DRIESSEN-MOL, A., FRESE, L., HOERSTRUP, S. P. & BAAIJENS, F. P. 2012. Decellularized homologous tissue-engineered heart valves as off-the-shelf alternatives to xeno- and homografts. *Biomaterials*, 33, 4545-54.

DOHMEN, P. M., DA COSTA, F., HOLINSKI, S., LOPES, S. V., YOSHI, S., REICHERT, L. H., VILLANI, R., POSNER, S. & KONERTZ, W. 2006. Is there a possibility for a glutaraldehyde-free porcine heart valve to grow? *Eur Surg Res*, 38, 54-61.

DOHMEN, P. M. & KONERTZ, W. 2009. Tissue-engineered heart valve scaffolds. *Ann Thorac Cardiovasc Surg*, 15, 362-7.

ELTOM, A., ZHONG, G. & MUHAMMAD, A. 2019. Scaffold technques and designs in tissue engineering functions and purposes: A review. *Adv Mater Sci Eng*, 3429527.

ERDBRUGGER, W., KONERTZ, W., DOHMEN, P. M., POSNER, S., ELLERBROK, H., BRODDE, O. E., ROBENEK, H., MODERSOHN, D., PRUSS, A., HOLINSKI, S., STEIN-KONERTZ, M. & PAULI, G. 2006. Decellularized xenogenic heart valves reveal remodeling and growth potential in vivo. *Tissue Eng*, 12, 2059-68.

ETNEL, J. R. G., GRASHUIS, P., HUYGENS, S. A., PEKBAY, B., PAPAGEORGIOU, G., HELBING, W. A., ROOS-HESSELINK, J. W., BOGERS, A., MOKHLES, M. M. & TAKKENBERG, J. J. M. 2018. The Ross Procedure: A Systematic Review, Meta-Analysis, and Microsimulation. *Circ Cardiovasc Qual Outcomes*, 11, e004748.

FEINGOLD, B., WEARDEN, P. D., MORELL, V. O., GALVIS, D. & GALAMBOS, C. 2009. Expression of A and B blood group antigens on cryopreserved homografts. *Ann Thorac Surg*, 87, 211-4.

FITZGERALD, K. P. & LIM, M. J. 2011. The pulmonary valve. *Cardiol Clin*, 29, 223-7.

FLYNN, L. E. 2010. The use of decellularized adipose tissue to provide an inductive microenvironment for the adipogenic differentiation of human adipose-derived stem cells. *Biomaterials*, 31, 4715-24.

GALL, K., SMITH, S., WILLMETTE, C., WONG, M. & O'BRIEN, M. 1995. Allograft heart valve sterilization: a six-year in-depth analysis of a twenty-five-year experience with low-dose antibiotics. *J Thorac Cardiovasc Surg*, 110, 680-7.

GALL, K. L., SMITH, S. E., WILLMETTE, C. A. & O'BRIEN, M. F. 1998. Allograft heart valve viability and valve-processing variables. *Ann Thorac Surg*, 65, 1032-8.

GERESTEIN, C. G., TAKKENBERG, J. J., OEI, F. B., CROMME-DIJKHUIS, A. H., SPITAELS, S. E., VAN HERWERDEN, L. A., STEYERBERG, E. W. & BOGERS, A. J. 2001. Right ventricular outflow tract reconstruction with an allograft conduit. *Ann Thorac Surg*, 71, 911-7; discussion 917-8.

GILBERT, T. W., SELLARO, T. L. & BADYLAK, S. F. 2006. Decellularization of tissues and organs. *Biomaterials*, 27, 3675-83.

GILPIN, A. & YANG, Y. 2017. Decellularization Strategies for Regenerative Medicine: From Processing Techniques to Applications. *Biomed Res Int*, 9831534.

GOFFIN, Y. A., VAN HOECK, B., JASHARI, R., SOOTS, G. & KALMAR, P. 2000. Banking of cryopreserved heart valves in Europe: assessment of a 10-year operation in the European Homograft Bank (EHB). *J Heart Valve Dis*, 9, 207-14.

GRIFFITHS, L. G., CHOE, L. H., REARDON, K. F., DOW, S. W. & CHRISTOPHER ORTON, E. 2008. Immunoproteomic identification of bovine pericardium xenoantigens. *Biomaterials*, 29(26), 3514–3520. doi:10.1016/j.biomaterials.2008.05.006.

GULBINS, H., KREUZER, E. & REICHART, B. 2003. Homografts: a review. *Expert Rev Cardiovasc Ther*, 1, 533-9.

HARRIS, C., CROCE, B. & CAO, C. 2015. Tissue and mechanical heart valves. *Annals of Cardiothoracic Surgery*, 4, 399-399.

HAUPT, J., LUTTER, G., GORB, S. N., SIMIONESCU, D. T., FRANK, D., SEILER, J., PAUR, A. & HABEN, I. 2018. Detergent-based decellularization strategy preserves macro- and microstructure of heart valves. *Interact Cardiovasc Thorac Surg*, 26, 230-236.

HECHADI, J., GERBER, B. L., COCHE, E., MELCHIOR, J., JASHARI, R., GLINEUR, D., NOIRHOMME, P., RUBAY, J., EL KHOURY, G. & DE KERCHOVE, L. 2013. Stentless xenografts as an alternative to pulmonary homografts in the Ross operation. *Eur J Cardiothorac Surg*, 44, e32-9.

HENG, W. L., ALBRECHT, H., CHIAPPINI, P., LIM, Y. P. & MANNING, L. 2013. International heart valve bank survey: a review of processing practices and activity outcomes. *J Transplant*, 2013, 163150.

HO, S. Y. 2002. Anatomy of the mitral valve. *Heart*, 88, Suppl 4, iv5-10.

HOPKINS, R. A., JONES, A. L., WOLFINBARGER, L., MOORE, M. A., BERT, A. A. & LOFLAND, G. K. 2009. Decellularization reduces calcification while improving both durability and 1-year functional results of pulmonary homograft valves in juvenile sheep. *J Thorac Cardiovasc Surg*, 137, 907-13, 913e1-4.

IBRAHIM, D. M., KAKAROUGKAS, A. & ALLAM, N. K. 2017. Recent advances on electrospun scaffolds as matrices for tissue-engineered heart valves. *Materials Today Chemistry*, 5, 11-23.

IDRIZI, S., MILEV, I., ZAFIROVSKA, P., TOSHESKI, G., ZIMBAKOV, Z., AMPOVA-SOKOLOV, V., ANGJUSEVA, T. & MITREV, Z. 2015. Interventional Treatment of Pulmonary Valve Stenosis: A Single Center Experience. *Open Access Maced J Med Sci*, 3, 408-12.

JANA, S., TEFFT, B. J., SPOON, D. B. & SIMARI, R. D. 2014. Scaffolds for tissue engineering of cardiac valves. *Acta Biomater*, 10, 2877-93.

JASHARI, R., DAENEN, W., MEYNS, B. & VANDERKELEN, A. 2004. Is ABO group incompatibility really the reason of accelerated failure of cryopreserved allografts in very young patients?--Echography assessment of the European Homograft Bank (EHB) cryopreserved allografts used for reconstruction of the right ventricular outflow tract. *Cell Tissue Bank*, 5, 253-9.

JEONG, S., YOON, E. J., LIM, H. G., SUNG, S. C. & KIM, Y. J. 2013. The effect of space fillers in the cross-linking processes of bioprosthesis. *Biores Open Access*, 2, 98-106.

JORGE-HERRERO, E., FONSECA, C., BARGE, A. P., TURNAY, J., OLMO, N., FERNANDEZ, P., LIZARBE, M. A. & GARCIA PAEZ, J. M. 2010. Biocompatibility and calcification of bovine pericardium employed for the construction of cardiac

bioprostheses treated with different chemical crosslink methods. *Artif Organs*, 34, E168-76.

JORGE-HERRERO, E., GARCIA PAEZ, J. M. & DEL CASTILLO-OLIVARES RAMOS, J. L. 2005. Tissue heart valve mineralization: Review of calcification mechanisms and strategies for prevention. *J Appl Biomater Biomech*, 3, 67-82.

KARAS, T. Z., REUL, G. J. & COOLEY, D. A. 2007. C-ring mitral annuloplasty: 27-year follow-up. *Tex Heart Inst J*, 34, 102-4.

KASIMIR, M. T., RIEDER, E., SEEBACHER, G., SILBERHUMER, G., WOLNER, E., WEIGEL, G. & SIMON, P. 2003. Comparison of different decellularization procedures of porcine heart valves. *Int J Artif Organs*, 26, 421-7.

KASIMIR, M. T., WEIGEL, G., SHARMA, J., RIEDER, E., SEEBACHER, G., WOLNER, E. & SIMON, P. 2005. The decellularized porcine heart valve matrix in tissue engineering: platelet adhesion and activation. *Thromb Haemost*, 94, 562-7.

KAZA, A. K., LIM, H.-G., DIBARDINO, D. J., BAUTISTA-HERNANDEZ, V., ROBINSON, J., ALLAN, C., LAUSSEN, P., FYNN-THOMPSON, F., BACHA, E., DEL NIDO, P. J., MAYER, J. E., JR. & PIGULA, F. A. 2009. Long-term results of right ventricular outflow tract reconstruction in neonatal cardiac surgery: options and outcomes. *J Thorac Cardiovasc Surg*, 138, 911-916.

KEANE, T. J., LONDONO, R., TURNER, N. J. & BADYLAK, S. F. 2012. Consequences of ineffective decellularization of biologic scaffolds on the host response. *Biomaterials*, 33, 1771-81.

KONAKCI, K. Z., BOHLE, B., BLUMER, R., HOETZENECKER, W., ROTH, G., MOSER, B., BOLTZ-NITULESCU, G., GORLITZER, M., KLEPETKO, W., WOLNER, E. & ANKERSMIT, H. J. 2005. Alpha-Gal on bioprostheses: xenograft immune response in cardiac surgery. *Eur J Clin Invest*, 35, 17-23.

KOROSSIS, S. A., BOOTH, C., WILCOX, H. E., WATTERSON, K. G., KEARNEY, J. N., FISHER, J. & INGHAM, E. 2002. Tissue engineering of cardiac valve prostheses II: biomechanical characterization of decellularized porcine aortic heart valves. *J Heart Valve Dis*, 11, 463-71.

KOROSSIS, S. A., WILCOX, H. E., WATTERSON, K. G., KEARNEY, J. N., INGHAM, E. & FISHER, J. 2005. In-vitro assessment of the functional performance of the decellularized intact porcine aortic root. *J Heart Valve Dis*, 14, 408-21; discussion 422.

KOROSSIS, S. 2018. Structure-Function Relationship of Heart Valves in Health and Disease. *In:* KIRALI, K. (ed.) *Structural Insufficiency Anomalies in Cardiac Valves.* InTech.DOI: 10.5772/intechopen.78280.

KOROSSIS, S. 2018. Structure-Function Relationship of Heart Valves in Health and Disease. *In:* KIRALI, K. (ed.) *Cardiology and Cardiovascular Medicine.* IntechOpen.DOI: 10.5772/intechopen.71281.

KRISHNAMURTHY, V. K., STOUT, A. J., SAPP, M. C., MATUSKA, B., LAUER, M. E. & GRANDE-ALLEN, K. J. 2017. Dysregulation of hyaluronan homeostasis during aortic valve disease. *Matrix Biology : Journal of the International Society for Matrix Biology*, 62, 40-57.

KYU, H. H., ABATE, D., ABATE, K. H., ABAY, S. M., ABBAFATI, C., ABBASI, N., ABBASTABAR, H., ABD-ALLAH, F., ABDELA, J. & ABDELALIM, A. 2018. Global, regional, and national disability-adjusted life-years (DALYs) for 359 diseases and injuries and healthy life expectancy (HALE) for 195 countries and territories, 1990-2017: a systematic analysis for the Global Burden of Disease Study 2017. *Lancet (London, England)*, 392, 1859-1922.

LAKER, L. 2018. *The evaluation of a novel decellularization and sterilization process on bovine pericardial tissue.* Doctor of Philosophy Dissertation, Department of Cardiothoracic Surgery, University of the Free State, Free State, South Africa.

LAKER, L., DOHMEN, P. M. & SMIT, F. E. 2020. Synergy in a detergent combination results in superior decellularized bovine pericardial extracellular matrix scaffolds. *J Biomed Mater Res, Part B: Appl Biomater*. https://doi.org/10.1002/jbm.b.34588.

LAM, M. T. & WU, J. C. 2012. Biomaterial applications in cardiovascular tissue repair and regeneration. *Expert Rev Cardiovasc Ther*, 10, 1039-49.

LEE, C., LIM, H. G., LEE, C. H. & KIM, Y. J. 2017. Effects of glutaraldehyde concentration and fixation time on material characteristics and calcification of bovine pericardium: implications for the optimal method of fixation of autologous pericardium used for cardiovascular surgery. *Interact Cardiovasc Thorac Surg*, 24, 402-406.

LEVENTHAL, J. R., JOHN, R., FRYER, J. P., WITSON, J. C., DERLICH, J. M., REMISZEWSKI, J., DALMASSO, A. P., MATAS, A. J. & BOLMAN, R. M., 3RD 1995. Removal of baboon and human antiporcine IgG and IgM natural antibodies by immunoadsorption. Results of in vitro and in vivo studies. *Transplantation*, 59, 294-300.

LEVER, M. J. 2005. 17 - Cardiovascular assist systems. *In:* HENCH, L. L. & JONES, J. R. (eds.) *Biomaterials, Artificial Organs and Tissue Engineering.* Woodhead Publishing. https://doi.org/10.1533/9781845690861.3.179.

LIAO, J., JOYCE, E. M. & SACKS, M. S. 2008. Effects of decellularization on the mechanical and structural properties of the porcine aortic valve leaflet. *Biomaterials*, 29, 1065-74.

LISY, M., KALENDER, G., SCHENKE-LAYLAND, K., BROCKBANK, K. G., BIERMANN, A. & STOCK, U. A. 2017. Allograft Heart Valves: Current Aspects and Future Applications. *Biopreserv Biobank*, 15, 148-157.

LIU, A. C., JOAG, V. R. & GOTLIEB, A. I. 2007. The emerging role of valve interstitial cell phenotypes in regulating heart valve pathobiology. *Am J Pathol*, 171, 1407-18.

LOVEKAMP, J. J., SIMIONESCU, D. T., MERCURI, J. J., ZUBIATE, B., SACKS, M. S. & VYAVAHARE, N. R. 2006. Stability and function of glycosaminoglycans in porcine bioprosthetic heart valves. *Biomaterials*, 27, 1507-18.

MANJI, R. A., LEE, W. & COOPER, D. K. C. 2015. Xenograft bioprosthetic heart valves: Past, present and future. *Int J Surg*, 23, 280-284.

MARIANI, E., LISIGNOLI, G., BORZI, R. M. & PULSATELLI, L. 2019. Biomaterials: Foreign Bodies or Tuners for the Immune Response? *Int J Mol Sci*, 20, 636.

MENDELSON, K. & SCHOEN, F. J. 2006. Heart valve tissue engineering: concepts, approaches, progress, and challenges. *Ann Biomed Eng*, 34, 1799-819.

MENDOZA-NOVELO, B. & CAUICH-RODRIGUEZ, J. V. 2011. Decellularization, stabilization and functionalization of collagenous tissues used as cardiovascular biomaterials. *In:* PIGNATELLO, R. (ed.) *Biomaterials.* InTechOpen.DOI:10.5772/914

METHE, H., HESS, S. & EDELMAN, E. R. 2007. Endothelial immunogenicity - A matter of matrix microarchitecture. *Thromb Haemost*, 98, 278-82.

MEYER, S. R., CHIU, B., CHURCHILL, T. A., ZHU, L., LAKEY, J. R. & ROSS, D. B. 2006. Comparison of aortic valve allograft decellularization techniques in the rat. *J Biomed Mater Res, Part A*, 79, 254-62.

MISFELD, M. & SIEVERS, H. H. 2007. Heart valve macro- and microstructure. *Philos Trans R Soc Lond B Biol Sci*, 362, 1421-36.

MURRAY, G. 1956. Homologous aortic-valve-segment transplants as surgical treatment for aortic and mitral insufficiency. *Angiology*, 7, 466-71.

NASO, F. & GANDAGLIA, A. 2018. Different approaches to heart valve decellularization: A comprehensive overview of the past 30 years. *Xenotransplantation*, 25, e12354.

NAVARRO, F. B., DA COSTA, F. D. A., MULINARI, L. A., PIMENTEL, G. K., RODERJAN, J. G., VIEIRA, E. D., DE NORONHA, L. & MIYAGUE, N. I. 2010. Evaluation of the biological behaviour of decellularized pulmonary homografts: An experimental sheep model. *Rev Bras Cir Cardiovasc Surg*, 25(3), 377-387.

ORYAN, A., KAMALI, A., MOSHIRI, A., BAHARVAND, H. & DAEMI, H. 2018. Chemical crosslinking of biopolymeric scaffolds: Current knowledge and future directions of crosslinked engineered bone scaffolds. *Int J Biol Macromol*, 107, 678-688.

PADALA, M. 2018. A heart valve is no stronger than its weakest link: The need to improve durability of pericardial leaflets. *J Thorac Cardiovasc Surg*, 156, 207-208.

PARKER, R., RANDEV, R., WAIN, W. H. & ROSS, D. N. 1978. Storage of heart valve allografts in glycerol with subsequent antibiotic sterilisation. *Thorax*, 33, 638-45.

RIEBEN, R., BOVIN, N. V., KORCHAGINA, E. Y., ORIOL, R., NIFANT'EV, N. E., TSVETKOV, D. E., DAHA, M. R., MOHACSI, P. J. & JOZIASSE, D. H. 2000. Xenotransplantation: in vitro analysis of synthetic alpha-galactosyl inhibitors of human anti-Galalpha1->3Gal IgM and IgG antibodies. *Glycobiology*, 10, 141-8.

RIEDER, E., KASIMIR, M. T., SILBERHUMER, G., SEEBACHER, G., WOLNER, E., SIMON, P. & WEIGEL, G. 2004. Decellularization protocols of porcine heart valves differ importantly in efficiency of cell removal and susceptibility of the matrix to recellularization with human vascular cells. *J Thorac Cardiovasc Surg*, 127, 399-405.

RIEDER, E., SEEBACHER, G., KASIMIR, M. T., EICHMAIR, E., WINTER, B., DEKAN, B., WOLNER, E., SIMON, P. & WEIGEL, G. 2005. Tissue engineering of heart valves: decellularized porcine and human valve scaffolds differ importantly in residual potential to attract monocytic cells. *Circulation*, 111, 2792-7.

ROMEO, J. L. R., PAPAGEORGIOU, G., VAN DE WOESTIJNE, P. C., TAKKENBERG, J. J. M., WESTENBERG, L. E. H., VAN BEYNUM, I., BOGERS, A. & MOKHLES, M. M.

2018. Downsized cryopreserved and standard-sized allografts for right ventricular outflow tract reconstruction in children: long-term single-institutional experience. *Interact Cardiovasc Thorac Surg*, 27, 257-263.

ROSS, D. 1991. Replacement of the aortic valve with a pulmonary autograft: the "switch" operation. *Ann Thorac Surg*, 52, 1346-50.

ROSS, D. N. 1965. Homograft replacement of the aortic valve. *J Cardiovasc Surg (Torino)*, 5, Suppl, 89-94.

ROSS, D. N. & SOMERVILLE, J. 1966. Correction of pulmonary atresia with a homograft aortic valve. *Lancet*, 2, 1446-7.

SAREMI, F., GERA, A., HO, S. Y., HIJAZI, Z. M. & SÁNCHEZ-QUINTANA, D. 2014. CT and MR Imaging of the Pulmonary Valve. *RadioGraphics*, 34, 51–71. Published online 10.1148/rg.343135026.

SARIKOUCH, S., HORKE, A., TUDORACHE, I., BEERBAUM, P., WESTHOFF-BLECK, M., BOETHIG, D., REPIN, O., MANIUC, L., CIUBOTARU, A., HAVERICH, A. & CEBOTARI, S. 2016. Decellularized fresh homografts for pulmonary valve replacement: a decade of clinical experience. *Eur J Cardiothorac Surg*, 50, 281-90.

SCHENKE-LAYLAND, K., VASILEVSKI, O., OPITZ, F., KONIG, K., RIEMANN, I., HALBHUBER, K. J., WAHLERS, T. & STOCK, U. A. 2003. Impact of decellularization of xenogeneic tissue on extracellular matrix integrity for tissue engineering of heart valves. *J Struct Biol*, 143, 201-8.

SCHOEN, F. J. 1997. Aortic valve structure-function correlations: role of elastic fibers no longer a stretch of the imagination. *J Heart Valve Dis*, 6, 1-6.

SCHOEN, F. J. 1999. Future directions in tissue heart valves: impact of recent insights from biology and pathology. *J Heart Valve Dis*, 8, 350-8.

SCHOEN, F. J. 2008. Evolving concepts of cardiac valve dynamics: the continuum of development, functional structure, pathobiology, and tissue engineering. *Circulation*, 118, 1864-80.

SEIFTER, E. & FRATER, R. W. M. 1995. *Anticalcification treatment for aldehyde-tanned biological tissue*. United States. Albert Einstein College of Medicine of Yeshiva University (Bronx, NY).5476516. http://www.freepatentsonline.com/5476516.html.

SELAMET TIERNEY, E. S., GERSONY, W. M., ALTMANN, K., SOLOWIEJCZYK, D. E., BEVILACQUA, L. M., KHAN, C., KRONGRAD, E., MOSCA, R. S., QUAEGEBEUR, J. M. & APFEL, H. D. 2005. Pulmonary position cryopreserved homografts: durability in pediatric Ross and non-Ross patients. *J Thorac Cardiovasc Surg*, 130, 282-6.

SHAH, S. R. & VYAVAHARE, N. R. 2008. The effect of glycosaminoglycan stabilization on tissue buckling in bioprosthetic heart valves. *Biomaterials*, 29, 1645-53.

SHEN, X., BAI, L., CAI, L. & CAO, X. 2018. A geometric model for the human pulmonary valve in its fully open case. *PloS one*, 13, e0199390-e0199390.

SIMON, P., KASIMIR, M. T., SEEBACHER, G., WEIGEL, G., ULLRICH, R., SALZER-MUHAR, U., RIEDER, E. & WOLNER, E. 2003. Early failure of the tissue engineered porcine heart valve SYNERGRAFT in pediatric patients. *Eur J Cardiothorac Surg: Official Journal of the European Association for Cardiothoracic Surgery*, 23, 1002-1006.

SMIT, F. E., BESTER, D., VAN DEN HEEVER, J. J., SCHLEGEL, F., BOTES, L. & DOHMEN, P. M. 2015. Does prolonged post-mortem cold ischaemic harvesting time influence cryopreserved pulmonary homograft tissue integrity? *Cell Tissue Bank*, 16, 531-44.

SOMERS, P., DE SOMER, F., CORNELISSEN, M., THIERENS, H. & VAN NOOTEN, G. 2012. Decellularization of heart valve matrices: search for the ideal balance. *Artif Cells Blood Substit Immobil Biotechnol*, 40, 151-62.

STEINHOFF, G., STOCK, U., KARIM, N., MERTSCHING, H., TIMKE, A., MELISS, R. R., PETHIG, K., HAVERICH, A. & BADER, A. 2000. Tissue engineering of pulmonary heart valves on allogenic acellular matrix conduits: in vivo restoration of valve tissue. *Circulation*, 102, III50-5.

STEPHENS, E. H., KEARNEY, D. L. & GRANDE-ALLEN, K. J. 2012a. Insight into pathologic abnormalities in congenital semilunar valve disease based on advances in understanding normal valve microstructure and extracellular matrix. *Cardiovasc Pathol: The Official Journal of the Society for Cardiovascular Pathology*, 21, 46-58.

STEPHENS, E. H., KEARNEY, D. L. & GRANDE-ALLEN, K. J. 2012b. Insight into pathologic abnormalities in congenital semilunar valve disease based on advances in understanding normal valve microstructure and extracellular matrix. *Cardiovasc Pathol*, 21, 46-58.

STRANGE, G., BRIZARD, C., KARL, T. R. & NEETHLING, L. 2015. An evaluation of Admedus' tissue engineering process-treated (ADAPT) bovine pericardium patch (CardioCel) for the repair of cardiac and vascular defects. *Expert Rev Med Devices*, 12, 135-41.

SUNDJAJA, J. H. & BORDONIN, B. 2019. *Anatomy, Thorax, Heart Pulmonic Valve* [Online]. Treasure Island (FL): StatPearls Publishing. Available: https://www.ncbi.nlm.nih.gov/books/NBK547706.

TUDORACHE, I., CEBOTARI, S., STURZ, G., KIRSCH, L., HURSCHLER, C., HILFIKER, A., HAVERICH, A. & LICHTENBERG, A. 2007. Tissue engineering of heart valves: biomechanical and morphological properties of decellularized heart valves. *J Heart Valve Dis*, 16, 567-73; discussion 574.

UMASHANKAR, P. R., MOHANAN, P. V. & KUMARI, T. V. 2012. Glutaraldehyde treatment elicits toxic response compared to decellularization in bovine pericardium. *Toxicol Int*, 19, 51-8.

VAN STEENBERGHE, M., SCHUBERT, T., GERELLI, S., BOUZIN, C., GUIOT, Y., XHEMA, D., BOLLEN, X., ABDELHAMID, K. & GIANELLO, P. 2018. Porcine pulmonary valve decellularization with NaOH-based vs detergent process: preliminary in vitro and in vivo assessments. *J Cardiothorac Surg*, 13, 34.

VEDEPO, M. C., DETAMORE, M. S., HOPKINS, R. A. & CONVERSE, G. L. 2017. Recellularization of decellularized heart valves: Progress toward the tissue-engineered heart valve. *J Tissue Eng*, 8, 2041731417726327.

WELTERS, M. J., OEI, F. B., WITVLIET, M. D., VAESSEN, L. M., CROMME-DIJKHUIS, A. H., BOGERS, A. J., WEIMAR, W. & CLAAS, F. H. 2002. A broad and strong humoral immune response to donor HLA after implantation of cryopreserved human heart valve allografts. *Hum Immunol*, 63, 1019-25.

WILSON, G. J., COURTMAN, D. W., KLEMENT, P., LEE, J. M. & YEGER, H. 1995. Acellular Matrix: A Biomaterials Approach for Coronary Artery Bypass and Heart Valve Replacement. *Ann Thorac Surg*, 60, S353-8.

WOLLMANN, L. C., LAURINDO, C. A., DA COSTA, F. D. A. & MORENO, A. N. 2011. Effects of cryopreservation and/or decellularization on extracellular matrix of porcine valves. *Rev Bras Cir Cardiovasc Surg*, 26, 490-6.

XING, Q., YATES, K., TAHTINEN, M., SHEARIER, E., QIAN, Z. & ZHAO, F. 2015. Decellularization of fibroblast cell sheets for natural extracellular matrix scaffold preparation. *Tissue Eng, Part C: Methods*, 21, 77-87.

YADGIR, S. R., ALAM, T., JOHNSON, C., NAGHAVI, M. & ROTH, G. 2018. Global burden of calcific aortic and degenerative mitral valve diseases: analysis from the global burden of disease 2017 study. *Circulation*, 138, A17238.

Appendix A: Co-authored publications

A1. Smit. F.E., Bester, D., **van den Heever, J.J.,** Schlegel, F., Botes, L. and Dohmen, P.M. 2015. Does prolonged post-mortem cold ischaemic harvesting time influence cryopreserved pulmonary homograft tissue integrity? *Cell Tissue Bank,* 16:531-544.

A2. Bester, D., Botes, L., **van den Heever, J.J.,** Kotze, H., Dohmen, P., Pomar, J.L. and Smit F.E. 2018. Cadaver donation: structural integrity of pulmonary homografts harvested 48 h post mortem in juvenile ovine model. *Cell Tissue Bank,* 19:743-754.

Cell Tissue Bank (2015) 16:531–544
DOI 10.1007/s10561-015-9500-2

ORIGINAL PAPER

Does prolonged post-mortem cold ischemic harvesting time influence cryopreserved pulmonary homograft tissue integrity?

Francis Edwin Smit · Dreyer Bester · Johannes Jacobus van den Heever · Franziska Schlegel · Lezelle Botes · Pascal Maria Dohmen

Received: 28 October 2014 / Accepted: 2 February 2015 / Published online: 8 February 2015

Abstract This study investigated cryopreserved pulmonary homograft (CPA) structural integrity after prolonged cold ischemic harvesting times in a juvenile sheep model. Three groups with different post-mortem cold ischemic harvesting times were studied, i.e. Group 1 (24 h, n = 10); group 2 (48 h, n = 10); group 3 (72 h, n = 10). In each group, 5 CPAs were studied in vitro after cryopreservation and thawing. The other 5 CPAs were implanted in juvenile sheep for a minimum of 180 days. Serology samples were obtained and echocardiography was performed before euthanasia. Hematoxylin and eosin (H&E), scanning electron microscopy (SEM), von Kossa, Picrosirius red, α-actin, immunohistochemistry [von Willebrand factor (vWF), CD4, CD31 and CD34] and calcium content analyses were performed on explanted CPAs. The in vitro and in vivo studies failed to demonstrate any change in tensile strength, Young's Modulus and thermal denaturation (T_d) results between the groups. SEM demonstrated a reduction in endothelial cells (50 % at 24 h, 60.9 % at 48 h and 40.9 % at 72 h), but H&E could not demonstrate autolysis in any CPA in vitro. All cultures were negative. In the explanted groups, IgE, IgM and IgG results were inconclusive. Echocardiography demonstrated normal valve function in all groups. H&E and Picrosirius red staining confirmed tissue integrity. vWF, CD31 and CD34 staining confirmed a monolayer of endothelial cells in all explanted valves. Calcium content of explanted CPA leaflets was similar. This experimental study supports the concept of prolonging the cold ischemic harvesting time of cryopreserved homografts to reduce homograft shortage.

Keywords Cryopreserved homografts · Warm ischemic time · Right ventricular outflow tract reconstruction · Juvenile sheep model

F. E. Smit · D. Bester · J. J. van den Heever · P. M. Dohmen
Department Cardiothoracic Surgery, Faculty of Health Sciences, University of the Free State (UFS), Bloemfontein, South Africa

F. Schlegel · P. M. Dohmen
Department of Cardiac Surgery, Heart Centre Leipzig, University of Leipzig, Leipzig, Saxony, Germany

L. Botes (✉)
Department of Health Sciences, Central University of Technology (CUT), Free State, Private Bag X20539, Bloemfontein, South Africa
e-mail: lbotes@cut.ac.za

Introduction

The gold standard for reconstruction of the right ventricular outflow tract (RVOT) is cryopreserved pulmonary homografts (CPAs). Although Chambers et al. (1997) showed that freedom from reoperation following homograft reconstruction of the RVOT using the Ross procedure to be as high as 80 % at

25 years of follow-up, it is generally agreed that homografts degenerate over time. This degeneration is mostly due to immune responses (Welters et al. 2002; Neumann et al. 2014). Alternatives to homografts are xenogenic heart valves, which are available off-the-shelf. However, these valves are treated with glutaraldehyde and therefore present serious limitations for young patients due to early tissue degeneration and calcification (Holmes et al. 2012; Homann et al. 2000). A further alternative is tissue engineered pulmonary heart valves which show promising results for up to 10 years if the scaffold is a homograft (Dohmen et al. 2011; Cebotari et al. 2011). Since CPA use is limited by donor availability, especially with respect to small valve sizes, investigations are needed to increase the pool of potentially available human heart valves without compromising quality. The international norm for harvesting valves either from heart transplant recipients, beating heart donors or non-beating heart donors, is limited to 24 h post-mortem. The reason for this restraint is that increased homograft durability was demonstrated with retained cellular viability in cryopreserved homografts (Angell et al. 1989; O'Brien et al. 1995). However, Mitchell et al. (1998) argue that most homografts are acellular and that valvular performance is linked to retention of structural integrity of the valve scaffold and not cellular viability.

This study investigated CPA structural integrity after prolonged cold ischemic harvesting times in a juvenile sheep model.

Materials and methods

All animal experiments and surgical procedures were performed in compliance with the *Guide for the Care and Use of Laboratory Animals* as published by the US National Institutes of Health (NIH Publication 85-23, revised 1996). Approval of the study protocol was obtained from the Animal Ethics Committee of the University of the Free State (ETOVS nr. 12/06). A schematic presentation of the study layout is provided in Fig. 1.

Three groups with different post-mortem cold ischemic harvesting times were studied in vitro as well as in vivo, while a fourth group with valves (n = 5) harvested within 6 h post-mortem and non-cryopreserved, were used as control in the in vitro studies: group 1 (24 h, n = 10); group 2 (48 h, n = 10); group 3 (72 h, n = 10). In each of the three groups, 5 CPAs were studied in vitro after processing and thawing to evaluate tissue integrity and impact of processing. The other 5 CPAs from each group were studied in vivo through implantation in juvenile sheep, for a minimum of 180 days (group 1: ñ = 210 days; group 2: ñ = 206 days; group 3: ñ = 188 days), to evaluate valve performance, biological interaction and modes of degeneration. The population median values between the different days of implantation in the three groups proved not to differ significantly ($p > 0.05$) from each other. Wethers of the Dorper strain were used and each carcass and recipient animal received an ear tag with a unique identification number.

Pulmonary valve harvesting and preparation

For the control group, hearts were obtained from a local abattoir directly after slaughtering and transported on ice to the laboratory. The valves were dissected and washed in cold (4 °C) Ringers-lactate (Bodene Pty, Ltd trading as Intramed, Port Elizabeth, SA) and all required samples taken for evaluation. For the other three groups, thirty juvenile sheep were sacrificed by intravenous injection of an overdose of potassium chloride (Adcock Ingram Critical Care, Johannesburg) and pulmonary valve conduits for the preparation of cryopreserved ovine homografts were harvested at 24, 48 and 72 h respectively. Ischemic time was defined as the time between death and harvesting of the heart valve. Ischemic time was composed of a 6 h period of warm ischemia (from death to refrigeration of the cadaver in the mortuary) followed by a longer period of cold ischemia until the heart was removed from the cadaver at the designated times. The carcasses were skinned after euthanasia and the large stomach was removed to limit the effect of the ongoing intestinal fermentation process, which is typical in ruminants and would increase the body temperature and subsequently the rate of autolysis. In group 1 (n = 5) the pulmonary heart valves were removed as a valve conduit and processed after 24 h, in group 2 (n = 5) after 48 h and in group 3 (n = 5) after 72 h. The valves were rinsed, inspected for fenestrations or other abnormalities and the thickness of the myocardium was trimmed to approximately 5 mm. A competency test was performed to evaluate regurgitation control. Each valve was immersed in 100 ml of M199 with

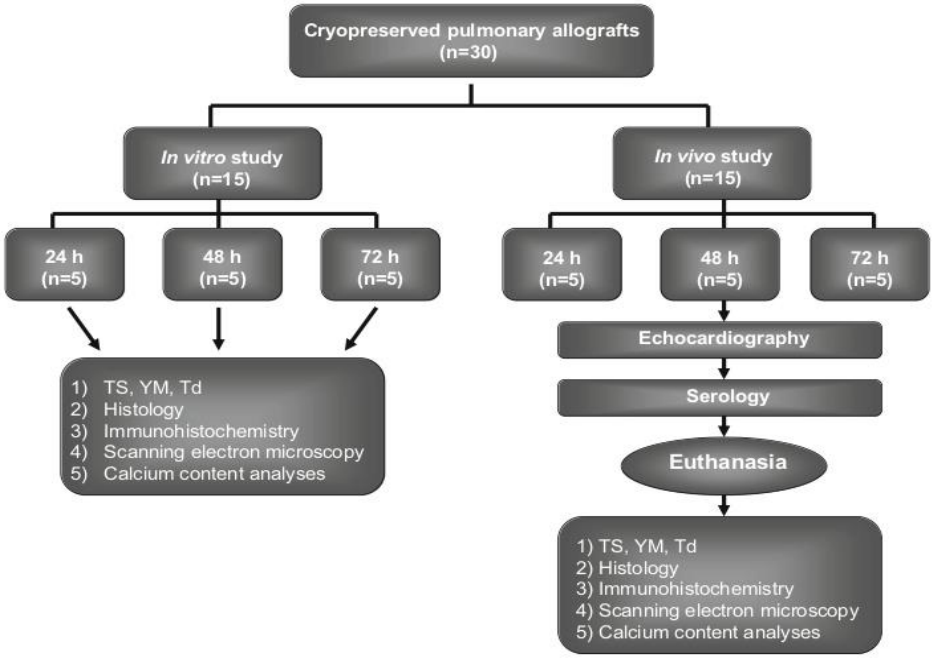

Fig. 1 Outline of the study methodology

Earle's Base (Highveld Biological (Pty) Ltd., Johannesburg, South Africa (SA) containing 2.5 mg Fungizone (Bristol-Meyers Squibb, Johannesburg, SA), 25 mg Amikacin (Fresenius, Bodene (Pty) Limited trading as Intramed, Johannesburg, SA), 50 mg Cefoxitin (Sabax, Johannesburg, SA) and 50 mg Piperacillin (Sabax, Johannesburg, SA) to sterilize for 24 h. Then the pulmonary valves were cryopreserved under sterile conditions using a Cryoson BV-9 Biological Freezer (Consarctic, Schöllkrippen, Germany). Valves were placed in a cryobag containing a solution of 100 ml M199 with 11 ml dimethylsulfoxide (DMSO) and cryopreserved at a rate of approximately −1 °C/min until −140 °C was reached. Quality control for the cryopreservation of the heart valves procured for this study was performed according to ISO 9000 standards.

Cryopreserved valves were stored in the vapor phase of liquid nitrogen (LN_2) for a minimum period of 2 weeks till implantation. At thawing, the cryobags were placed on a shelf at room temperature for ±5 min to eliminate the excessive cold temperature, followed by immersion in a waterbath at 30 °C for another 5–7 min until most of the liquid inside the bag have melted. The bag was then opened sterile and the contents placed gently in two changes of 500 ml of M199 at 4 °C for 10 min each, before implantation.

In vitro study

Biomechanical testing

Biomechanical properties of the tissue samples were examined using a tensile testing apparatus (Lloyds LS100 Plus tensile strength (TS) tester, IMP, Johannesburg, SA). TS and YM were performed on tissue samples fixated with clamps at both ends and gradually stretched (0.1 mm/s) by applying constant tension on the ends (Thubrikar et al. 1983). Both pulmonary valve leaflets and wall samples underwent biomechanical testing.

Determination of Thermal Denaturation Temperature (T_d) is a technique for thermal analysis, performed using differential scanning calorimetry (DSC) (Mettler Toledo, DSC 822e, Microsep, Johannesburg, SA). In DSC, the rate of heat flow to the sample is compared to the rate of heat flow to an inert material, while the materials are heated or cooled concurrently. For proteins, the thermally induced process detectable by DSC is the structural malting

or unfolding of the molecule. The transition of protein from a native to a denatured conformation is accompanied by the rupture of inter- and intra-molecular bonds, and the process has to occur in a cooperative manner to be discerned by DSC (Smith and Judge 1991). This was recorded as T_d for each group (Rüegg et al. 1975).

Microbiological examinations

Blood culture samples were taken intra-cardially from each intact donor heart before harvesting the heart for further dissection of the valves (groups 1–3). These samples were analyzed using standard microbiological techniques for detecting aerobic and anaerobic microbes, as well as for fungi. At cryopreservation, tissue and fluid samples from each valve were also taken for microbiological testing, and compared to the organisms cultured from blood samples taken intra-cardially at harvesting.

Histological evaluation

Specimens, for light microscopy examination, were taken from the middle of the pulmonary leaflet of each CPA as well as the wall of each CPA. These specimens were embedded in paraffin wax and two micrometer thick longitudinal sections were then prepared and routinely processed with H&E, von Kossa and Picrosirius red stainings. Specimen numbers were randomly allocated to each tissue sample, allowing completely blinded evaluation by all the evaluators for histology, immunohistochemistry and scanning electron microscopy (SEM) samples.

Immunohistochemistry

Immunohistochemical staining was performed with anti-von Willebrand factor (vWF) rabbit polyclonal antibody (Abcam, Cambridge, United Kingdom (UK), anti-CD4 rabbit polyclonal antibody (Bioss, Atlanta, United States of America (USA), anti-CD31 mouse monoclonal antibody (Abcam, Cambridge, UK), anti-CD34 goat polyclonal antibody (Santa Cruz Biotechnology Inc, Dallas, Texas, USA) and anti-α-smooth muscle actin rabbit polyclonal antibody (Abcam, Cambridge, UK). Different valvular regions were investigated, due to differing shear stresses at the leaflets compared with the rest of the valves. From each region representative samples were obtained including the inflow and outflow aspects of the valve.

Scanning electron microscopy

All valves were fixed in 2.5 % Glutaraldehyde (Merck, Johannesburg, SA). Valve leaflets were divided into two specimens of approximately 3 × 6 mm. Similar specimen samples were taken from the pulmonary wall, sinus area and pulmonary trunk. Tissue specimens were dried using the critical point method and were metalized using gold.

Evaluations were performed with a Shimadzu SSX 550 scanning electron microscope (Kyoto, Japan). The surface area of each specimen was examined and photographed at either four or five different positions, and all images were then evaluated by three independent evaluators and a score allocated. An average score for each specimen was then calculated. A three category scoring system, adapted from the six categories described by Krs et al. (2006) was used to define endothelial integrity and to evaluate the quality of the extracellular matrix (ECM) surface area. The classification of tissue was based on two key markers, endothelium and basal membrane. Category I; there is a virtual absence of both endothelium and basal membrane and the bare scaffold of the tissue is exposed. Category II; the basal membrane predominantly covers the scaffold and the endothelium is largely missing. Category III; the endothelium is virtually intact.

In vivo study

Echocardiography

Hemodynamic evaluation was performed by one experienced investigator using trans-thoracic echocardiography prior to sacrifice. A Philips Envisor Ultra Sound system (Philips, Johannesburg, SA) was used with a 3.5-MHz probe and all data were recorded. Two-dimensional trans-thoracic echocardiography was performed to evaluate morphological conditions of the valve conduit and leaflets. Additionally, the diameters of the valve annulus, sinotubular junction (ST-junction) and pulmonary artery wall were measured. Pulmonary insufficiency was evaluated semi-quantitatively using pulsed wave, continuous wave and color Doppler flow on the parasternal short axis view. The regurgitation jet across the valve was graded by identification length and

width into the right ventricular outflow tract and mapped as: none/trivial, mild, moderate or severe using standard echocardiography criteria. The mean flow velocities across the implanted valves were obtained by the use of continuous wave Doppler. Each measurement was repeated six times and the mean value over the measurements was calculated. Again animals were only identified by their individual ear tag numbers, allowing blinded evaluation by the sonographer.

Serology samples

Full blood counts were analyzed on a Sysmex XE 2100 (Roche, Johannesburg, SA) according to the TF/DC detection method, hydrodynamic focusing (DC detection), flow cytometry method and a SLS-hemoglobin method. Immunoglobulins (IgG, IgA and IgM) in serum were determined quantitatively by means of immunonephelometry on a Siemens BN ProSpec Nephelometer (Siemens, Johannesburg, SA).

Gross examination

The explanted CPAs were inspected and color photographs were taken before fixation. The leaflets were inspected for fenestrations, retraction, thrombotic material, atheroma and calcification.

Calcium content analysis

Quantitative calcium analyses were performed on samples dried in a temperature controlled Scientific series 100 incubator (Lasec, Johannesburg, SA) at 45 °C for 48 h. Samples were weighed and hydrolyzed in 1 ml 50 % nitric acid and 50 µl hydrogen peroxide. Extractable calcium content was determined by inductively coupled plasma mass spectrometry Agilent ICP-MS 7500c (Chemetrix, Midrand, SA) and expressed as µg calcium per mg dry weight tissue. Only calcium content of the pulmonary leaflet and wall of the control group (<6 h) were determined pre-implantation and used as baseline values, and compared to the explanted tissues of the three ischemic groups.

Statistical analysis

For statistical analysis purposes, the cold ischemic time was described by the time effect and the source of a sample, i.e., whether the sample was sourced from the aortic leaflet or the aortic wall, was described by the source effect. Various measurements (T_d, Calcium, etc.) were analyzed separately using linear models in order to determine whether there were significant time or source effects and whether there was an interaction between time and source. Time and source were treated as simple fixed effects and an interaction effect was also considered. Standard ANOVAs were also done over time and over source to obtain additional clues as to whether either effect was significant. The study was not statistically powered to detect differences due to the cost restraints involved.

Where the interaction effect in the linear model was significant, further investigation was done using ANOVA methods by separating the sources. In a few significant cases (where the time effect was significant for a specific source) the results were investigated even more deeply using Welch Two Sample *t* tests. This involved comparing the three timestamps in pairs. This top-down approach (starting global and drilling down) was followed throughout in order to avoid spurious results and false positives/negatives.

Where the above method was not appropriate, other methods were applied. For example, the sonar data was analyzed using Hotelling's test and the SEM data was analyzed with Pearson's Chi Square test. For Hotelling's test we have to assume multivariate normality as the sample size is too small to conduct tests for this.

Surgical implantation

The juvenile sheep were male with a mean age of 4–6 months and a mean body weight of 34–40 kg. Premedication was administered with 0.175 mg/kg Neurotranq [VirbacRSA (Pty) Ltd, Halfway House, SA] and 0.2 mg/kg Atropine [Bayer (Pty) Ltd, Animal Health Division, Isando, SA] intramuscularly, and anesthesia was induced with 12 mg/kg Bomathal [Merial SA (Pty) Ltd, Halfway House, SA] intravenously. The sheep were intubated, ventilated and positioned in a lateral decubitus position. Arterial cannulation for cardiopulmonary bypass was obtained via the left carotid artery. The stump pressure of the tied-off distal carotid artery was used for invasive arterial pressure measurement. A left mini-thoracotomy was performed and the fourth rib removed. The pulmonary artery was transected and the native

pulmonary valve leaflets were excised. The CPAs, with a diameter of ±16 mm, were implanted as an interposition, with two continuous 4/0 polypropylene suture anastomoses. The sheep was weaned from cardiopulmonary bypass, the mini-thoracotomy was closed in layers and a chest drain was inserted. Systemic pain medication, in the form of 2 mg Morphine sulphate [Bodene (Pty) Ltd, trading as Intramed, Port Elizabeth, SA] intramuscularly twice a day and 5 mg Depomycin [INTERVET SA (Pty) Ltd, Johannesburg, SA] daily as antibiotic, was administered for 5 days post-operatively. Animals were extubated 2–4 h post-operatively. Underwater drains and pressure lines were removed before animals were transferred to an overnight facility.

Results

In vitro study

Biomechanical testing

The following baseline mechanical results were obtained in pulmonary homografts harvested within 6 h after death. These samples were obtained from valves of juvenile sheep from a local abattoir. The mean TS were 1.04 ± 0.36 MPa for the pulmonary wall and 1.24 ± 0.79 MPa for the pulmonary leaflet. The mean TS for the pulmonary wall in the three ischemic groups were as follows: (group 1: 1.03 ± 0.36 MPa; group 2: 0.95 ± 0.22 MPa; group 3: 1.16 ± 0.34 MPa). The mean TS for the pulmonary leaflets in the three ischemic groups were as follows: (group 1: 2.57 ± 1.07 MPa; group 2: 2.93 ± 0.50 MPa; group 3: 3.03 ± 1.02 MPa).

The mean YM baseline value was 2.06 ± 0.77 MPa for the pulmonary wall and 5.68 ± 4.57 MPa for the pulmonary leaflet. The mean YM for the pulmonary wall in the three ischemic groups were as follows: (group 1: 3.21 ± 0.90 MPa; group 2: 3.26 ± 0.93 MPa; group 3: 3.81 ± 1.31 MPa). The mean YM for the pulmonary leaflets in the three ischemic groups were as follows: (group 1: 9.93 ± 2.63 MPa; group 2: 9.25 ± 5.02 MPa; group 3: 10.73 ± 4.33 MPa).

The mean T_d baseline values were 70.57 ± 1.03 °C for the pulmonary wall and 67.16 ± 1.31 °C for the pulmonary leaflets. The mean T_d for the pulmonary wall in the three ischemic groups were as follows: (group 1: 70.57 ± 1.12 °C; group 2: 71.19 ± 1.13 °C; group 3: 72.44 ± 2.85 °C). The mean T_d for the pulmonary leaflets in the three ischemic groups were as follows: (group 1: 70.25 ± 0.76 °C; group 2: 71.25 ± 1.17 °C; group 3: 71.01 ± 0.36 °C).

In vitro evaluation of the TS, YM and T_d temperatures did not reveal any statistically significant differences ($p > 0.05$) between the 24, 48 and 72 h groups.

Microbiological examinations

Microbiological examination detected that the initial microbes present on the CPAs in the different groups were as follows: group 1 (n = 5): no aerobic organisms and 3 positive cultures for anaerobic microorganisms; group 2 (n = 5): 2 positive samples for aerobic organisms and 1 positive sample for anaerobic organism; group 3 (n = 5): 3 samples were positive for aerobic microorganisms and 3 samples were positive for anaerobic microorganisms. The most common microorganisms were gram + bacilli and coagulase negative staphylococci. After 24 h of sterilization in the nutrient antibiotic solution no organisms could be cultured in the pre-cryopreserved specimens. No fungal cultures were positive at any point in time.

Histological evaluation

The histological findings in the control group (harvested <6 h post-mortem) are described as reference.

H&E staining showed endothelial-like cells on the surface of the control valves; however, a confluent layer was not present in all of the specimens. The ECM exhibited a normal configuration with an absence of abnormalities in the collagen and elastin structures, and this was confirmed with Picrosirius red staining. The spindleform-shaped fibroblast-like cells were arranged in a parallel layout; however, the number of cells in some of the samples was limited. Endothelial-like cells were confirmed to be endothelial cells by positive expression of vWF and CD31. Interstitial cells were confirmed to be myofibroblasts since these cells were α-actin positive. No differences between the groups were observed post processing and thawing, compared to the control group.

Scanning electron microscopy

According to the modified Krs et al. (2006) and Smit, PhD, unpublished data, 2011 classification, the

baseline samples of the pulmonary leaflets were all in category III (100 %) and, for the pulmonary wall samples, 86.7 % were in category II and 13.3 % were in category I. In group 1 (24 h), 12.5 % of the pulmonary leaflets fell in category I, 37.5 % in category II and 50 % in category III, while 96 % of the pulmonary wall samples fell in category I and 4 % in category II. In group 2 (48 h), 21.7 % of the pulmonary leaflets fell in category I, 60.9 % in category II and 17.4 % in category III, while 100 % of the pulmonary wall samples fell in category I. In group 3 (72 h), 18.2 % of the pulmonary leaflets fell in category I, 40.9 % in category II and 40.9 % in category III, while 100 % of the pulmonary wall samples fell in category I.

No statistically significant differences ($p > 0.05$) in SEM was found between any of the three ischemic groups.

Calcium content analysis

The mean baseline quantitative calcium content was 1.8 ± 0.09 μg/mg of dry weight for the pulmonary leaflet samples and 0.80 ± 0.06 μg/mg of dry weight for the pulmonary wall samples. Only the baseline values of the control group (<6 h) were determined and compared to the explanted tissues in the three ischemic groups.

In vivo study

Echocardiography

Echocardiographic examinations showed limited morphological calcification. The calcification was in the range of none to mild for the valve leaflets in all the groups. Mild to moderate calcification was observed in the valve annulus and in the pulmonary wall. There were however no differences between the groups.

The mean pressure gradients at the CPAs within the different groups were 12.0 ± 5.6 mmHg in group 1, 10.7 ± 3.6 mmHg in group 2 and 10.5 ± 2.6 mmHg in group 3 respectively. There were no statistically significant differences between the groups (group 1 vs 2, $p = 0.70$; group 1 vs 3, $p = 0.61$; group 2 vs 3, $p = 0.94$). The mean annulus diameter in group 1 was 20.2 ± 2.2 mm, in group 2 it was 20.4 ± 2.6 mm, and in group 3 it was 20.5 ± 1.5 mm. The mean diameter at the ST-junction was 18.4 ± 1.4 mm in group 1, 19.3 ± 1.5 mm in group 2 and 20.1 ± 2.1 mm in group 3. The mean diameter of the pulmonary artery was 20.2 ± 1.5 mm in group 1, 20.5 ± 1.3 mm in group 2 and 20.5 ± 1.4 mm in group 3.

Serology samples

The mean total IgG for group 1 was 7.5 ± 8.9 kU/l, for group 2, 7.3 ± 10.9 kU/l and for group 3, 37.0 ± 31.1 kU/l. The mean IgA and IgM values were below 0.25 g/l for all three groups. There was no obvious trend that would identify a marked immunological process in any specific group.

Gross examination

There was an absence of aneurysm formation, deformations and thrombi in all of the explanted CPAs from the three groups (Fig. 2). The leaflets were pliable without fenestrations in all the samples from the three groups (Fig. 3).

Biomechanical testing

The TS, YM and T_d of the leaflets and wall specimens are summarized in Table 1. No statistically significant differences were found between groups, nor did they differ from the baseline results. Certainly no loss of strength could be demonstrated in any of the groups compared to the baseline values.

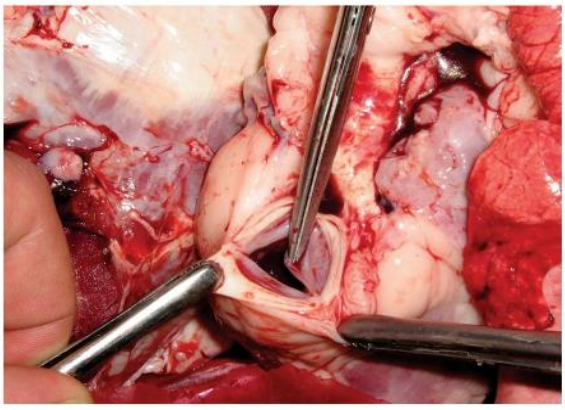

Fig. 2 Explanted cryopreserved pulmonary homograft of group 1 (24 h). Note the pliable leaflet after 150 days of implantation in the juvenile sheep

Histological evaluation

The histological examinations are presented in Fig. 4a–c. In the H&E staining results there was evidence that all samples from group 1 were covered by a monolayer of endothelial-like cells. Acellularity of the ECM in group 1 was between 30 and 90 %. Eighty percent of the CPAs in group 2 were covered by endothelial-like cells. The ECM was completely acellular in 2 samples. The other CPAs in group 2 were between 0 and 90 % acellular. In group 3, all of the CPAs were covered by a monolayer of endothelial-like cells. Acellularity was found in one valve, whereas the other valves were between 20 and 80 % acellular. von Kossa staining detected severe calcification of a leaflet in one of the explanted CPAs from group 3. None of the other explanted CPAs showed calcification of the leaflets. The pulmonary wall of only one of the CPAs from group 1 showed mild calcification. In group 2, there was severe wall calcification in two of the CPAs, moderate calcification in two CPAs and no calcification in one of the CPAs. Moderate calcification was observed in the wall of one of the explanted CPAs from group 3. None of the other explanted CPAs in group 3 exhibited calcification. Picrosirius red staining showed a well preserved ECM in all samples from the three groups. Endothelial–like cells covering the valve surfaces were identified as such since they were vWF, CD31 and CD34 positive. Interstitial cells were α-actin positive, however, since no CD4 positive cells were found, none of the samples showed inflammatory cells within the ECM.

Fig. 3 Inverted cryopreserved pulmonary homograft (24 h) after 150 days implantation

Scanning electron microscopy

After explantation, SEM was able to demonstrate that 88.0 % of the pulmonary leaflets from group 1 fell in category III and 12.0 % fell in category II. In group 2, 62.7 % of the leaflets were classified as category III, 20.0 % as category II and 17.3 % as category I. In group 3, 64.0 % of the leaflets fulfilled the criteria for category III, 12.0 % for category II and 24.0 % for category I.

In group 1, 37.3 % of the CPA pulmonary wall specimens were classified as category III, 37.3 % as category II, and 25.4 % as category I. In group 2, 26.7 % of the pulmonary wall specimens fulfilled the criteria for category III, 37.3 % for category II and 36.0 % for category I. Finally, group 3 had 12.0 % of pulmonary wall specimens in category III, 61.3 % in category II and 26.7 % in category I.

Analysis of the SEM data for both the pulmonary leaflet and wall showed a time-related change over the categories ($p < 0.005$ respectively). Although a gradual deterioration in the endothelial covering of both the pulmonary leaflets and walls in relation to the ischemic time was observed, no differences in structural integrity could be demonstrated.

Calcium content analysis

Mean quantitative calcium content in the pulmonary leaflets was 0.18 ± 0.13 μg/mg dry weight in group 1, 0.30 ± 0.57 μg/mg dry weight in group 2 and 0.05 ± 0.05 μg/mg dry weight in group 3. There is no

Table 1 Cryopreserved pulmonary homograft structural integrity testing

Variable	≤6 h baseline (n = 20)	24 h group (n = 5)	48 h group (n = 5)	72 h group (n = 5)	*p* values
Tensile strength					
Mean	1.24	1.58	1.54	2.18	0.8882*
SD	0.79	0.93	0.19	0.67	
Median	1.01	1.75	1.61	2.40	
Minimum	0.25	0.62	1.29	1.40	
Maximum	3.73	2.72	1.72	3.06	
Young's modulus					
Mean	5.68	6.55	5.94	7.76	0.5820*
SD	4.57	4.71	1.65	2.60	
Median	4.78	7.75	6.14	8.55	
Minimum	0.84	1.42	3.98	4.01	
Maximum	18.42	11.36	8.21	10.57	
Thermal denaturation temperature (T_d)					
Mean	67.16	70.96	68.53	71.99	0.1697*
SD	1.31	1.40	0.36	1.98	
Median	66.68	71.22	68.52	72.36	
Minimum	66.1	68.63	68.03	69.71	
Maximum	69.35	72.11	68.94	74.26	

SD standard deviation, *h* hour

* *p* value for the time effect in a mixed model

difference between calcification in the explanted pulmonary leaflets between the three groups ($p = 0.518$).

For the pulmonary wall the mean quantitative calcium content was 16.12 ± 24.40 μg/mg dry weight in group 1, 84.95 ± 16.07 μg/mg dry weight in group 2 and 68.11 ± 41.64 μg/mg dry weight in group 3. The pulmonary wall calcification does not differ between the groups ($p = 0.218$). Note that only one pulmonary wall had significantly elevated calcium content.

Discussion

The pulmonary homograft remains the gold standard for right ventricle outflow tract (RVOT) reconstruction; its use is however limited by supply. The worldwide practice of limiting homograft harvesting to beating heart donors, or within 24 h post-mortem, may contribute to this shortage. If post-mortem harvesting times can be extended safely, thereby allowing more time to obtain consent or fulfill other legal requirements, cadaver-based donor programs can be expanded or in some cases be re-opened. This depends on whether viability of homografts contributes significantly to attenuate homograft failure as claimed by O'Brien et al. (1991). On the other hand Mitchell et al. (1998) considers all homografts to be eventually acellular and thus non-viable. It is thus possible to view homografts as biological scaffolds.

If all homografts eventually become acellular and function as a biological scaffold, for the purpose of this experimental animal study, it was important to firstly evaluate the impact of extending ischemic harvesting times on the morphology, structural and strength characteristics of homografts, and taking the historical perspectives on homograft biology and degeneration into consideration.

Secondly, valve function and outcomes of the biological interactions post implantation were evaluated in vivo in a standard juvenile ovine model.

Long-term durability of CPAs has previously been correlated with warm- and cold ischemic times. Cell metabolism is unchanged if the cold ischemic time is <24 h and the warm ischemic time is <12 h (Lang et al. 1994; Hu et al. 1989). O'Brien et al. (1991) stated that

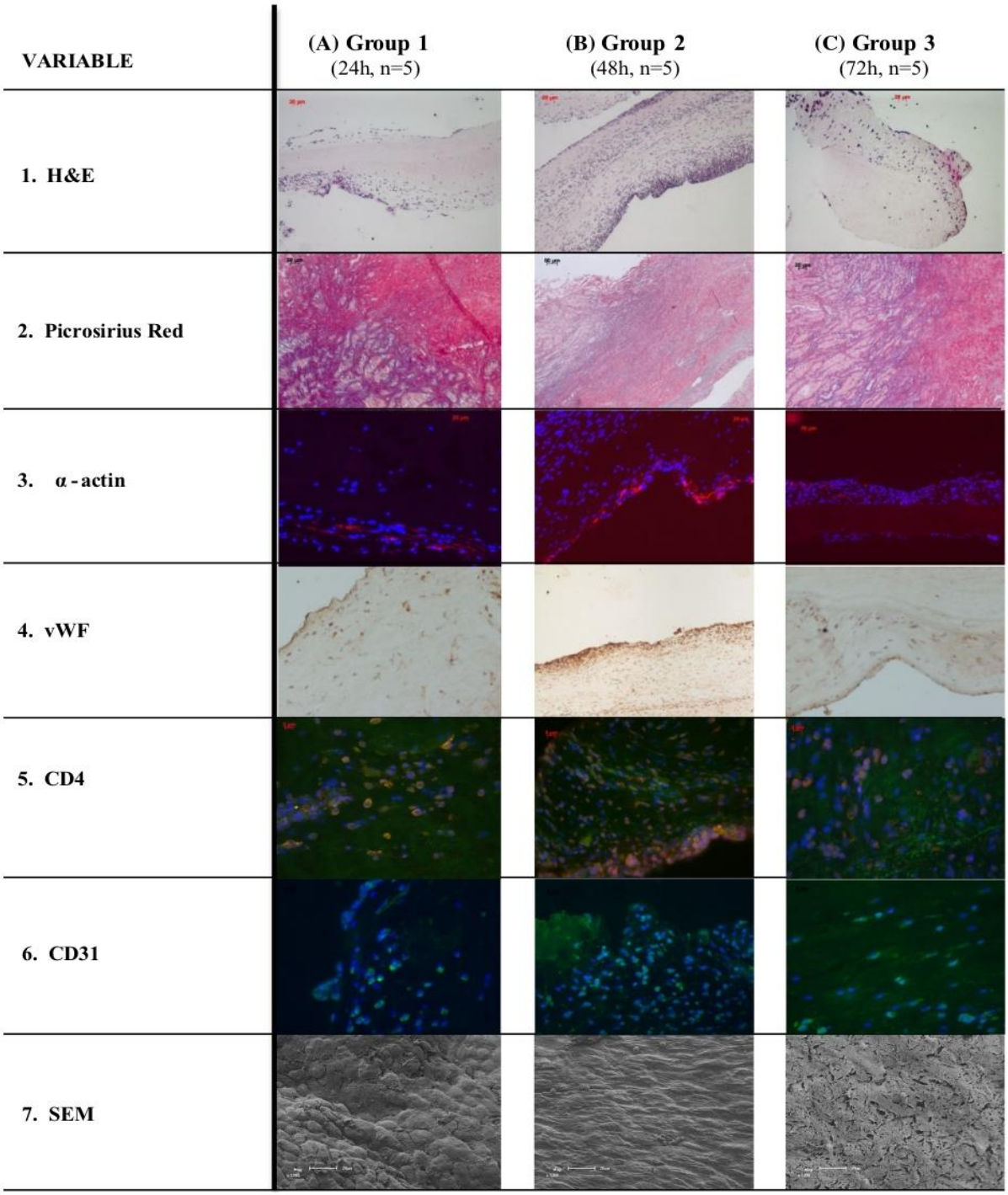

Fig. 4 Histological findings of explanted CPAs. **a** group 1 (24 h), **b** group 2 (48 h), and **c** group 3 (72 h). For each group; 1 H&E staining, 2 Picrosirius red staining, 3 α-actin staining, 4 vWF staining, 5 CD4 staining, 6 CD31 staining and 7 SEM. [*h* hours, *H&E* Hematoxylin and eosin, *vWF* von Willebrand factor, *SEM* scanning electron microscopy]

long-term durability is dependent on the viability of a homograft and therefore the CPA needed to be prepared within 24 h post-mortem. There is, however, no definition of preferred warm and cold ischemic times. In the literature, different homograft banks have customized protocols for processing and cryopreservation of homografts. There are also variations in the ischemic time between harvesting and cryopreservation.

Several studies have addressed homograft viability. Yankah and Hetzer (1987) reported that only 24 % of the endothelial cells survive after 2 h of exposure to room temperature. Crescenzo et al. (1992) noted the relationship between ischemic time and progression of fibroblast cell damage, which is reversible with a warm ischemic time of up to 12 h. However, a warm ischemic time longer than 12 h will lead to apoptosis. Fibroblast response to warm ischemic time is correlated with morphometric measurements (St Louis et al. 1991; Brockbank and Bank 1987).

Significant decreases in freedom of reoperation in the cryopreserved homografts compared to the 4 °C stored homografts were observed in medium term studies. However, in a recent single-center study including 1,022 patients, O'Brien et al. (2001) compared 4 °C stored homografts with viable cryopreserved homografts. In this 29-year follow-up study the viability of homografts progressively reduced, resulting in non-viability after a few days, regardless of whether the homografts were cryopreserved or stored in the refrigerator, and whether they were stored in a balanced salt solution or a nutrient medium. Thus the viable homograft theory did not survive the test of time.

Barrat-Boyes et al. (1987) conducted a long-term follow-up study including 248 patients in which valve incompetence was assessed. Significant freedom of incompetence of antibiotic-sterilized aortic homografts was found in 95 % after 5 years, 78 % after 10 years and 42 % at 14 years. Harvesting time was <24 h in 147 donors, between 24 and 48 h in 88 donors and between 49 and 75 h in 7 donors. Harvesting time was not recorded for 43 of the donors. A multivariate analysis showed that advanced donor valve age ≥55 years (CI 1.12 ± 0.30; $p = 0.0002$), aortic root size >30 mm (CI 1.39 ± 0.41; $p = 0.0007$), and recipient age <15 years (CI 2.03 ± 0.61; $p = 0.0008$) are independent risk factors for homograft incompetence.

Langley et al. (1996) reported, based on a series of 249 patients, a freedom of reoperation of sub-coronary implanted antibiotic sterilized valves with a warm ischemic time of 24 h and cold ischemic time of a maximum of 3 months. The freedom of reoperation of the aortic valve was excellent with 49.7 ± 5.6 % at 20 years follow-up.

The mean warm ischemic time of homografts prepared at the European Homograft Bank is <6 h. However, due to post-mortem delay, the average cold ischemic harvesting time is 24 h, up to a maximum of 36 h (Goffin et al. 1996). The clinical data of these homografts, presented by Meyns et al. (2005) shows that the ischemic time has no statistical influence on the long-term durability of these homografts when implanted into pediatric patients. Only non-anatomic position ($p = 0.001$), smaller graft size ($p < 0.0001$), younger age (on square root scale, $p < 0.0001$) and clamp time ($p = 0.01$) remain as independent risk factors.

On the other hand, Tweddell et al. (2000) investigated the longevity of homografts used to reconstruct the RVOT in 205 patients with congenital heart disease and a mean age of 6.9 ± 7.6 years (range 3 days to 48 years). Freedom from homograft failure was 54 ± 7 % at 10 years follow-up. They found that independent risk factors for homograft failure in a multivariate analysis were younger age ($p < 0.001$), longer warm ischemic time ($p < 0.001$), Z-value <2 ($p = 0.03$), and aortic homograft ($p = 0.04$).

Importantly, Kadoba et al. (1991) performed a study of cryopreserved aortic homografts in a lamb model in which the cold ischemic time was extended up to 48 h. The 48 h group performed as well as the fresh and 24 h groups. The authors concluded that expanding the pool for homografts is feasible by increasing the cold ischemic time. However, no specific tests or histological examinations were performed to systematically evaluate the allograft scaffolds or the quality of the valvular tissue as in the present study.

In the present in vitro study, we could demonstrate the presence of endothelial cells in all groups. However, no pattern was observed between the presence of endothelial cells and cold ischemic harvesting times. These findings suggest that the number of endothelial and interstitial cells present in the 72 h group were comparable with the number of cells in the 24 and 48 h groups. Thus, if the presence of endothelial cells was used to assess suitability, there should be no limitation on increasing the cold ischemic harvesting time. No testing was performed to compare the viability of the different cell types in this study as all samples were harvested after 24 h

ischemic time. This 24 h period was conclusively demonstrated in previous studies to be associated with non-viability (Arminger 1995).

The in vivo part of this study showed that implanted CPAs, from the different cold ischemic harvesting time groups, exhibited intra-luminal coverage with endothelial cells. These endothelial cells are most probably of host origin since, at implantation, most of the endothelial cells were either no longer present or non-viable after at least 24 h post-mortem. However, additional investigation will be required to confirm the origin of these endothelial cells. Gradual loss of endothelial cells with prolonged ischemic times might not be detrimental to the clinical durability of the homograft, as the immune response of the recipient to the implant is severely diminished.

Previous studies have revealed that re-endothelialization is commonly seen in the juvenile sheep model (Dohmen et al. 2006a, b). This can however not be generalized to humans, since this process seems to be more restricted and takes longer in humans (Dohmen et al. 2007; Konertz et al. 2011). Further investigation is needed to better understand the recellularization of decellularized heart valves implanted into patients. The endothelial cells also need to be investigated for their functionality, as they have a major determinant function. Endothelium normally inhibits thrombus formation and leukocyte adhesion, regulates vasomotor function, and inhibits smooth muscle cell proliferation. If there is damage to the endothelium interaction with inflammatory cells and interstitial cells, by expression of vascular adhesion, molecules such as VCAM-1, ICAM-1 and ELAM-1 will change (Ardehali et al. 1995). The intercellular network via macrophages, T-lymphocytes, endothelial cells and smooth muscle cells is generated by a variety of stimulatory cytokines (IL-1, IL-2, IL-6, and tumor necrosis factor-α) and growth factors (PDGF, IGF-1, FGF, HB-EGF, EGF, GM-CSF, and TGF-β) (Duquesnoy and Demetris 1995). Therefore, it is of great interest that autologous endothelial cells overgrow the CPAs to restore the function of the interstitial cells and decrease the activation of the inflammatory cells. On the contrary, it is important to avoid a pseudo-intima formation on the leaflet surface since this will lead to leaflet retraction, resulting in central valve regurgitation (Affonso da Costa et al. 2004). Pseudo-intima formation was not observed in any of the implanted valves in this study.

A well-known disadvantage of viable CPAs in transplant surgery is that donor endothelial and interstitial cells evoke an immune response from the host (Jane-wit et al. 2013). Decellularization of a CPA could attenuate the humoral immune response to donor HLA after implantation of a CPA as was shown by Kneib et al. (2012). Homografts with viable endothelium and interstitial cells have a significantly higher number of immunogenic epitopes, for HLA classes I and II, than the decellularized groups exhibit, and should therefore initiate a more dramatic immune response from the recipient. In this study, with harvesting times in excess of 24 h, endothelial viability is highly unlikely.

On a cellular level there were no differences between the groups with varying cold ischemic times. The extracellular matrix was tested to evaluate if the strength of the scaffold would change by extending the cold ischemic harvesting time. No differences in strength of the valve tissue were detected. Furthermore, there was no increase in tissue denaturation, evaluated by measuring the T_d, in any of the groups. The extracellular matrix was also confirmed to be intact by histological examination. From the in vitro data we are able to conclude that tissue strength is unaltered and therefore extending the cold ischemic harvesting time is possible.

From the in vivo investigations, with a minimum follow-up of 150 days in a juvenile sheep model, hemodynamic data shows no differences between the groups when the cold ischemic time was increased. Furthermore, the histological examinations showed a normal intact extracellular matrix. The immunohistochemistry results in this study did not show any differences in inflammatory reactions when cold ischemic time was increased. An overgrowth of endothelial cells was observed in all groups. Therefore, in this study, there were no contra-indications to extending the cold ischemic harvesting time in order to increase the number of viable homografts.

Limitations

The limitations of this study are that data provided by the juvenile sheep model cannot be unconditionally applied to human patients, since re-endothelialization is more extensive in this model than in humans. Also,

the functionality and viability of the endothelial and interstitial cells were not investigated in this study.

Conclusions

This experimental study supports the concept that, with a limited warm ischemic time, the cold ischemic harvesting time of cryopreserved homografts can be prolonged. This could be a way to reduce homograft shortage since by increasing time limits for harvesting, the opportunities for obtaining consent and facilitating cadaver donor programs are increased. However, long-term clinical hemodynamic evaluation is needed to confirm this approach.

Conflict of interest We certify that all authors named in this manuscript deserve authorship, and that all authors have agreed to be listed and have read and approved the manuscript and its submission to Cell and Tissue Banking. The authors have no conflicts of interest to declare.

References

Angell WW, Oury JH, Lamberti JJ, Koziol J (1989) Durability of the viable aortic homograft. J Thorac Cardiovasc Surg 98:48–55

Ardehali A, Laks H, Drinkwater DC, Ziv E, Drake TA (1995) Vascular cell adhesion molecule-1 is induced on vascular endothelia and medial smooth muscle cells in experimental cardiac homograft vasculopathy. Circulation 92:450–456

Arminger LC (1995) Viability studies of human valves prepared for use as allografts. Ann Thorac Surg 60:S118–S121

Barrat-Boyes BG, Roche AHG, Subramanyan R, Pemberton JR, Whotlock RML (1987) Long-term follow-up of patients with the antibiotic-sterilized aortic homograft valve inserted freehand in the aortic position. Circulation 75:768–777

Brockbank KG, Bank HL (1987) Measurement of post cryopreservation viability. J Card Surg 2:S145–S151

Cebotari S, Tudorache I, Ciubotaru A, Boethig D, Sarikouch S (2011) Use of fresh decellularized homografts for pulmonary valve replacement may reduce the reoperation rate in children and young adults: early report. Circulation 124(11 Suppl):S115–S123

Chambers JC, Somerville J, Stone S, Ross DN (1997) Pulmonary autograft procedure for aortic valve disease: long-term results of the pioneer series. Circulation 96:2206–2214

Crescenzo DG, Hilbert SL, Barrick MK, Corcoran PC, St Louis JD, Messier RH, Ferrans VJ, Wallace RB, Hopkins RA (1992) Donor heart valves: electron microscopic and morphometric assessment of cellular injury induced by warm ischemia. J Thorac Cardiovasc Surg 103:253–257

da Costa FDA, Dohmen PM, Lopes SV, Lacerda G, Pohl F, Vilani R, Da Costa MBA, Vieira ED, Yoschi S, Konertz W, da Costa IA (2004) Comparison of cryopreserved homografts and decellularized porcine heterografts implanted in sheep. Artif Organs 28:366–370

Dohmen PM, da Costa F, Yoshi S, Lopes SV, da Souza FP, Vilani R, Wouk AF, da Costa M, Konertz W (2006a) Histological evaluation of tissue-engineered heart valves implanted in the juvenile sheep model: is there a need for in vitro seeding? J Heart Valve Dis 15:823–829

Dohmen PM, da Costa F, Holinski S, Lopes SV, Yoshi S, Reichert LH, Villani R, Posner S, Konertz W (2006b) Is there a possibility for a glutaraldehyde-free porcine heart valve to grow? Eur Surg Res 38:54–61

Dohmen PM, Lembcke A, Holinski S, Kivelitz D, Braun JP, Pruss A, Konertz W (2007) Mid-term clinical results using a tissue-engineered pulmonary valve to reconstruct the right ventricular outflow tract during the Ross procedure. Ann Thorac Surg 84:729–736

Dohmen PM, Lembcke A, Holinski S, Pruss A, Konertz W (2011) Ten years of clinical results with a tissue-engineered pulmonary valve. Ann Thorac Surg 92:1308–1314

Duquesnoy RJ, Demetris AJ (1995) Immunopathology of cardiac transplant rejection. Curr Opin Cardiol 10:193–206

Goffin Y, Grandmougin D, Van Hoeck B (1996) Banking cryopreserved heart valves in Europe: assessment of a 5-year operation in an international tissue bank in Brussels. Eur J Cardiothorac Surg 10:505–512

Holmes AA, Co S, Human DG, Leblanc JG, Campbell AI (2012) The Contegra conduit: late outcomes in right ventricular outflow tract reconstruction. Ann Pediatr Cardiol 5:27–33

Homann M, Haehnel JC, Mendler N, Paek SU, Holper K, Meisner H, Lange R (2000) Reconstruction of the RVOT with valved biological conduits: 25 years experience with homografts and xenografts. Eur J Cardiothorac Surg 17:624–630

Hu JF, Gilmer L, Hopkins R, Wolfinbarger L Jr (1989) Effects of antibiotics on cellular viability in porcine heart valve tissue. Cardiovasc Res 23:960–964

Jane-wit D, Manes TD, Yi T, Qin L, Clark P, Kirkiles-Smith NC, Abrahimi P, Devalliere J, Moeckel G, Kulkarni S, Tellides G, Pober JS (2013) Alloantibody and complement promote T cell-mediated cardiac homograft vasculopathy through noncanonical nuclear factor-κB signaling in endothelial cells. Circulation 128:2504–2516

Kadoba K, Armiger L, Sawatari K, Jonas RA (1991) Influence of time from donor death to graft harvest on conduit function of cryopreserved aortic homografts in lambs. Circulation 84(Suppl. 5):III100–III111

Kneib C, von Glehn CQ, Costa FD, Costa MT, Susin MF (2012) Evaluation of humoral immune response to donor HLA after implantation of cellularized versus decellularized human heart valve homografts. Tissue Antigens 80:165–174

Konertz W, Angeli E, Tarusinov G, Christ T, Kroll J, Dohmen PM, Krogmann O, Franzbach B, Napoleone CP, Gargiulo G (2011) Right ventricular outflow tract reconstruction with decellularized porcine xenografts in patients with congenital heart disease. J Heart Valve Dis 20:341–347

Krs O, Burkert J, Slízová D, Kobylka P, Spatenka J (2006) Homograft semilunar cardiac valves processing and cryopreservation—morphology in scanning electron microscope. Cell Tissue Bank 7:167–173

Lang SJ, Giordance MS, Cardon-Cardo C, Summers BD, Staino-Cioco L, Hajjar DP (1994) Biochemical and cellular

characterization of cardiac valve tissue after cryopreservation or antibiotic preservation. J Thorac Cardiovasc Surg 108:63–67

Langley SM, Livesey SA, Tsang VT, Barron DJ, Lamb RK, Ross JK, Monro JL (1996) Long-term results of valve replacement using antibiotic-sterilized homografts in the aortic position. Eur J Cardiothorac Surg 10:1097–1106

Meyns B, Jashari R, Gewillig M, Mertens L, Komarek A, Lesaffre E, Budts W, Daenen W (2005) Factors influencing the survival of cryopreserved homografts. The second homograft performs as well as the first. Eur J Cardiothorac Surg 28:211–216

Mitchell RN, Jonas RA, Schoen FJ (1998) Pathology of explanted cryopreserved allograft heart valves: comparison with aortic valves from orthotopic heart transplants. J Thorac Cardiovasc Surg 115:118–127

Neumann A, Sarikouch S, Breymann T, Cebotari S, Boethig D, Horke A, Beerbaum P, Westhoff-Bleck M, Harald B, Ono M, Tudorache I, Haverich A, Beutel G (2014) Early systemic cellular immune response in children and young adults receiving decellularized fresh homografts for pulmonary valve replacement. Tissue Eng Part A 20:1003–1011

O'Brien MF, Harrocks S, Stafford EG, Gardner MA, Pohlner PG, Tesar PJ, Stephens F (2001) The homograft aortic valve: a 29-year, 99.3 % follow-up of 1,022 valve replacements. J Heart Valve Dis 10:334–344

O'Brien MF, McGiffin DC, Stafford EG, Gardner MA, Pohlner PF, McLachlan GJ, Gall K, Smith S, Murphy E (1991) Homograft aortic valve replacement: long-term comparative clinical analysis of the viable cryopreserved and antibiotic 4 degrees C stored valves. J Card Surg 6(Suppl 4):S534–S543

O'Brien MF, Stafford EG, Gardner MA (1995) Homograft aortic valve replacement: long-term follow-up. Ann Thorac Surg 60:S65–S70

Rüegg M, Moor U, Blanc B (1975) Hydration and thermal denaturation of beta-lactoglobulin: a calorimetric study. Biochim Biophys Acta 400:334–342

Smith SH, Judge MD (1991) Relationship between pyridinoline concentration and thermal stability of bovine intramuscular collagen. J Anim Sci 69:1989–1993

St Louis J, Corcoran P, Rajan S, Conte J, Wolfinbarger L, Hu J, Lange PL, Wang YN, Hilbert SL, Analouei A (1991) Effects of warm ischemia following harvesting of homograft cardiac valves. Eur J Cardiothorac Surg 5:458–464

Thubrikar MJ, Deck JD, Aouad J, Nolan SP (1983) Role of mechanical stress in calcification of aortic bioprosthetic valves. J Thorac Cardiovasc Surg 86:115–125

Tweddell JS, Pelech AN, Frommelt PC, Mussatto KA, Wyman JD, Fedderly RT, Berger S, Frommelt MA, Lewis DA, Friedberg DZ, Thomas JP Jr, Sachdeva R, Litwin SB (2000) Factors affecting longevity of homograft valves used in right ventricular outflow tract reconstruction for congenital heart disease. Circulation 102(Suppl. 3):III130–III135

Welters MJ, Oei FB, Witvliet MD, Vaessen LM, Cromme-Dijkhuis AH, Bogers AJ, Weimar W, Claas FH (2002) A broad and strong humoral immune response to donor HLA after implantation of cryopreserved human heart valve homografts. Hum Immunol 63:1019–1025

Yankah AC, Hetzer R (1987) Procurement and viability of cardiac valve homografts. In: Yankah AC (ed) Cardiac valve homografts 1962–1987. Springer, Berlin, pp 23–26

Cell Tissue Bank (2018) 19:743–754
https://doi.org/10.1007/s10561-018-9729-7

Cadaver donation: structural integrity of pulmonary homografts harvested 48 h post mortem in the juvenile ovine model

Dreyer Bester · Lezelle Botes · Johannes Jacobus van den Heever · Harry Kotze · Pascal Dohmen · Jose Luis Pomar · Francis Edwin Smit

Received: 1 February 2018 / Accepted: 5 October 2018 / Published online: 11 October 2018

Abstract Cryopreserved pulmonary homograft (CPH) implantation remains the gold standard for reconstruction of the right ventricular outflow tract (RVOT). Harvesting homografts < 24-h post mortem is the international norm, thereby largely excluding cadaveric donors. This study examines the structural integrity and stability of ovine pulmonary homografts harvested after a 48-h post mortem period, cryopreserved and then implanted for up to 180 days. Fifteen ovine pulmonary homografts were harvested 48-h post mortem and cryopreserved. Five CPH served as a control group (group 1; n = 5). CPH were implanted in the RVOT of juvenile sheep and explanted after 14 days (group 2; n = 5) and 180 days (group 3; n = 5). Leaflet integrity was evaluated by strength analysis, using tensile strength (TS), Young's modulus (YM) and thermal denaturation temperature (T_d), and morphology, including haematoxylin and eosin (H&E), Picrosirius red staining, scanning electron microscopy (SEM), transmission electron microscopy (TEM) and von Kossa stains. Echocardiography confirmed normal function in all implants. In explants, no reduction in TS, YM or T_d could be demonstrated and H&E showed mostly acellular leaflet tissue with no difference on Picrosirius red. TEM demonstrated consistent collagen disruption after cryopreservation in all three groups, with no morphological deterioration during the study period. von Kossa stains showed mild calcification in group 3. No deterioration of structural integrity could be demonstrated using strength or morphological evaluations between the controls and implant groups over the study period. Extending the post mortem harvesting time of homografts beyond 24 h did not appear to negatively affect the long-term performance of such transplanted valves in this study.

Keywords Juvenile ovine model · Homografts · Ischaemic time · Right ventricular outflow tract · Structural integrity

D. Bester · J. J. van den Heever · H. Kotze · P. Dohmen · F. E. Smit
Department of Cardiothoracic Surgery, Faculty of Health Sciences, University of the Free State (UFS), P.O. Box 339, (Internal Box G32), Bloemfontein 9300, South Africa

L. Botes (✉)
Department of Health Sciences, Central University of Technology, Free State (CUT), Private Bag X20539, Bloemfontein 9300, South Africa
e-mail: lbotes@cut.ac.za

P. Dohmen
Department of Cardiac Surgery, Heart Centre Rostock, University of Rostock, 18107 Rostock, Germany

J. L. Pomar
Department of Cardiovascular Surgery, Hospital Clinico de Barcelona, University of Barcelona, Villarroel 170, 08036 Barcelona, Spain

Introduction

Cryopreserved pulmonary homografts remain the gold standard for reconstruction of the RVOT (Hechadi et al. 2013). However, availability has been the Achilles heel of homograft-based surgery, because of donor shortages (Yoshikawa et al. 2000). In 1987, O'Brien et al. (1987a) described the use of viable cryopreserved homografts, which introduced the era of homograft banking. The possibility of delaying homograft degeneration by using viable cryopreserved homografts or homovital homografts (Yacoub et al. 1995) became a well-established concept and homograft banks across the world started using cryopreserved homografts or homovital homografts. Viable cryopreserved homografts are harvested from beating heart donors, and less than 6 h and definitely less than 24 h post mortem in the case of cadaveric donors (O'Brien et al. 1987a). Homovital homografts are untreated homografts harvested under sterile conditions, usually from the recipient at the time of the heart transplantation, and kept in nutrient medium. These homografts are considered viable if implanted within a few days (Yacoub et al. 1995). The post mortem harvesting time of homografts is restricted to a maximum of 24 h by most tissue banks internationally (Dawson and Brockbank 1997). Strict adherence to this criterion reduces the potential homograft pool, as the so-called donor consent window of opportunity is restricted, thereby reducing the potential cadaver donor pool to mainly in-hospital deaths. Potential cadaveric donors who never reach the hospital, for example suicide or traffic deaths, are not recruited either, due to the absence of specific cadaver donor programmes. In South Africa, nearly 70,000 medico-legal autopsies are performed annually. Reactivating cadaver donor programmes has the potential to address general shortages; however, this might require extending the post mortem harvesting time to beyond 24 h. At the Bloemfontein homograft bank, which is largely dependent on cadaver donors, the mean post mortem ischaemic time is 33 h, and it has extended its harvesting times to 48 h with sound results (Botes et al. 2012). Despite detailed studies of homograft viability, endothelial changes (Angell et al. 1989; O'Brien et al. 1995; Yankah and Hetzer 1987) and post mortem cellular changes, the importance of preserved structure and function is still uncertain.

Historically, homografts were harvested from cadavers, and harvesting times varied widely (Botes et al. 2012; O'Brien et al. 1987a). Homografts were stored at 4 °C in an antibiotic solution for up to 90 days (Yacoub and Kittle 1970). Despite O'Brien's claims to the contrary in a medium-term follow-up series (O'Brien et al. 1995, 2001), no difference could be demonstrated between fresh antibiotic homografts, group 1, and viable cryopreserved homografts, groups 2 and 3, in a long-term follow-up series (O'Brien et al. 1987b, 2001). Several other centres have also reported good medium-term results with fresh antibiotic-preserved homografts (Yacoub et al. 1995; Langley et al. 1996).

It is known that humoral and cellular immunological responses to viable endothelium are pronounced (Methe et al. 2007) and that homovital homografts might be rejected (Green et al. 1998). Mitchell et al. (1998) believe that most, if not all, homografts, are eventually essentially dead and acellular and only survive as a scaffold.

The period between harvesting and cryopreservation comprises a culture and a sterilisation phase, which range in length between different tissue banks (between 24 and 75 h) (Langley et al. 1996; Barrett-Boyes 1987). Cryopreservation within 3–4 days is accepted for viable cryopreserved homografts (O'Brien et al. 1987a, b). This means that the actual accepted post mortem ischaemic time before cryopreservation is routinely somewhere between 48 and 96 h. Insisting on a post mortem harvesting time of less than 24 h is therefore questionable from a structural point of view. However, extending homograft harvesting times can increase bacterial exposure, escalating the bio-burden and therefore contributing to graft failure and calcification (Brubaker et al. 2016; Mroz et al. 2008). However, microbiological examinations yielded similar results in the 24 and 48-h post mortem groups harvested from intact sheep carcasses as described by Smit et al. (2015). Furthermore, no fungi were cultured and all samples were free of organisms after 24 h incubation in an antibiotic solution. The Bloemfontein homograft bank has previously indicated that extending the post mortem harvesting time up to 72 h had no deleterious effect on homograft structure and functioning in the juvenile ovine model (Smit et al. 2015).

In this study, cryopreserved homografts that had been harvested 48 h post mortem were implanted in

juvenile ovine models for either 14 or 180 days and, after explantation, compared to non-implanted cryopreserved homografts. The aim of this experimental study was to evaluate the structural stability and integrity of the homografts and to assess modes of failure, if applicable.

Materials and methods

All experiments were performed in accordance with the Principles of Laboratory Animal Care prepared by the National Society of Medical Research, and the Guide for the Care and Use of Laboratory Animals prepared by the Institute of Laboratory Animal Resources and published by the US National Institute of Health 1996 (http://www.nap.edu/catalog/5140.html). Approval of the study protocol was obtained from the Animal Ethics Committee of the University of the Free State (ETOVS Number: UFS–AED2016/0101).

Pulmonary homograft harvesting and preparation

A block removal of all intrathoracic organs as well as the attached liver was performed immediately after slaughtering from fifteen female juvenile Merino sheep [mean age 4.5 months, mean body weight 27.4 ± 1.14 kilograms (kg)]. Each tissue block with remaining blood was lifted from the carcass and sealed in a sterile container without any additives. The tissue blocks were left for 6–8 h at room temperature representing "warm ischaemic time", and then stored at 4 °C for an additional 40 h, representing "cold ischaemic time". At 48 h post mortem the containers were opened and the pulmonary homografts (PH) were dissected from the tissue blocks while being washed in copious amounts of Ringers lactate. The PHs were incubated overnight (mean 20 h) at 4 °C in an antibiotic solution containing 100 ml of Medium199 with Earle's Base (Whitehead Scientific (Pty) Ltd., Brackenfell, South Africa), 2.5 mg Fungizone (Bristol-Meyers Squibb, Johannesburg, South Africa), 25 mg Amikacin (Fresenius, Bodene (Pty) Limited trading as Intramed, Johannesburg, South Africa), 100 mg Vancomycin (Gulf Drug Company (Pty) Ltd, Mount Edgecombe, South Africa) and 50 mg Piperacillin (Sabax, Johannesburg, South Africa) for sterilization. The homografts were then cryopreserved as previously described (Smit et al. 2015) after tissue samples had been obtained for microscopy, microbiological cultures and sensitivity (MC&S).

Five of these homografts served as controls (n = 5) and were not implanted into recipient sheep. The ten remaining pulmonary homografts were implanted into recipient sheep and explanted after 14 days (n = 5) and 180 days (n = 5) respectively in order to evaluate their structural integrity and stability (Fig. 1). Leaflet integrity was evaluated by morphology and strength analysis. Strength analyses included TS, YM and T_d, while morphology included H&E, Picrosirius red staining, SEM, TEM and von Kossa stains. Wethers of the Dorper strain were used as recipient animals, and each recipient received an ear tag with a unique identification number.

Cryopreservation and thawing

Cryopreservation was performed using an automated programmable freezer (Cryoson BV-9 Biological Freezer, Consarctic, Schöllkrippen, Germany). Before cryopreservation 11 ml of dimethyl sulphoxide (DMSO) (Sigma-Aldrich, Midrand, South Africa) was added to 100 ml of M199. Homografts were stored in a double package sachet in a storage vessel in the vapor phase of liquid nitrogen (LN_2) between − 120 and − 160 °C until they were implanted. It was confirmed that all HPs cryopreserved were culture negative on pre-cryopreservation MC&S. Five of these pulmonary homografts were used as controls and the remaining ten homografts were implanted into male juvenile sheep.

Before implantation, homografts were thawed in a water bath at 35–40 °C for 5–7 min until they were about 80% thawed. Both packages were opened aseptically and the homograft was transferred into a bowl with 500 ml cold (4 °C) M199, allowing a 10-min rinse period with gentle shaking to extract most of the DMSO from the homograft tissue. This procedure was repeated in a second bowl of cold M199, and thereafter the homograft was delivered to the surgical team for final trimming and implantation. Another tissue sample was obtained for MC&S at implantation to confirm sterility.

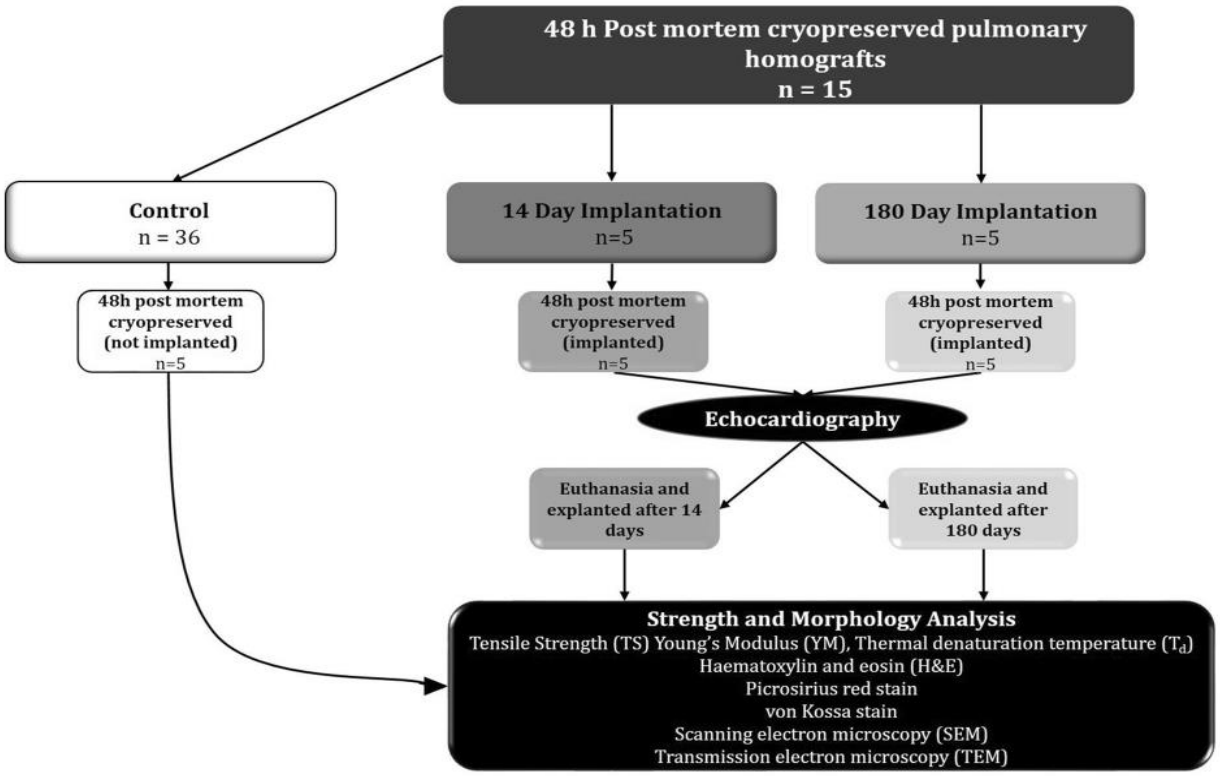

Fig. 1 Study layout

Pulmonary homograft implantation

Recipient sheep (mean age 6.8 months; body weight 40.2 ± 6.38 kg) were premedicated with 0.175 mg/kg Neurotranq (VirbacRSA (Pty) Ltd, Halfway House, South Africa) and 0.2 mg/kg Atropine (Bayer (Pty) Ltd, Animal Health Division, Isando, South Africa) intramuscularly, and anaesthesia was induced intravenously with Bomathal (12 mg/kg IV, Merial SA (Pty) Ltd, Halfway House, Johannesburg, South Africa). After positioning the sheep in a lateral decubitus position they were intubated and ventilated. Cardiopulmonary bypass was obtained by arterial cannulation via the left carotid artery and venous cannulation via the right atrium (Dagum et al. 1999). The stump pressure of the tied-off distal carotid artery was used as an index of invasive arterial pressure. A central line was inserted into the left jugular vein and the surgical procedure was performed on a beating heart.

A mini-thoracotomy was performed on the left side of the sheep and the fourth rib was removed. The pulmonary artery was transected, the native pulmonary valve leaflets resected and the pulmonary homograft was implanted as an RVOT conduit with two continuous 4/0 polypropylene suture anastomoses.

After implantation, the recipient was weaned off cardiopulmonary bypass, the mini-thoracotomy closed in layers and a chest drain was inserted. Systemic pain medication (2 mg Morphine sulphate, Bodene (Pty) Ltd, trading as Intramed, Port Elizabeth, South Africa) was administered intramuscularly twice a day and 5 mg Depomycin (Intervet SA (Pty) Ltd, Johannesburg, South Africa) as antibiotic was administered daily for 5 days post-operatively. Animals were extubated between 2 and 4 h post-operatively. Chest drains were removed before the animals were transferred to an overnight facility with a companion sheep to alleviate stress on the recipient sheep.

Biomechanical testing

The biomechanical properties of the control homograft leaflets and the ten explanted valvular leaflets were examined using a TS testing apparatus (Lloyds LS100 Plus, IMP, Johannesburg, South Africa). Briefly, the pulmonary leaflets were fixed into clamps at both ends and gradually stretched (0.1 mm/s) by applying tension on both ends (Thubrikar et al. 1983). TS and YM were calculated from the stress–strain curves and automatically recorded on the computerised apparatus. The YM was calculated by taking the derivative of the stress–strain curve, where the largest value was chosen before breakage. The TS, measured in Pa, is calculated as the force divided by the cross-sectional area of the leaflet.

In T_d, the rate of heat flow to the sample is compared to the rate of heat flow to an inert material, while the materials are heated or cooled concurrently. For proteins, the thermally induced process detectable by T_d is the structural malting or unfolding of the molecule. The transition of protein from a native to a denatured conformation is accompanied by the rupture of inter- and intra-molecular bonds, and the process has to occur in a cooperative manner to be discerned by T_d (Smith and Judge 1991). This was recorded as T_d for each group (Rüegg et al. 1975). T_d analysis was performed using a differential scanning calorimeter (DSC) (Mettler Toledo, T_d 822e, Microsep, Johannesburg, South Africa). Small samples of the pulmonary leaflets (2–5 mg) were placed in the DSC's hermetically sealed pans and subjected to temperature increasing at a rate of 10 °C/min from 25 to 95 °C. The maximum temperature of protein T_d was electronically recorded for each sample.

Histology

Samples from the middle of each pulmonary homograft leaflet was processed by the Department of Anatomical Pathology of the National Health Laboratory Services in Bloemfontein using standard operative procedures. The specimens were embedded in paraffin wax (Siemens, Johannesburg, South Africa) and two micrometer thick longitudinal sections were prepared and routinely processed for H&E, Picrosirius red and von Kossa staining. The impact of ischaemic time on the structural integrity of pulmonary valvular leaflet tissue was evaluated by performing H&E staining to display cytoplasmic, nuclear, and extracellular matrix features, Picrosirius red staining to study the collagen networks and von Kossa staining to observe the degree of leaflet calcification.

Electron microscopy

Scanning electron microscopy

Each pulmonary homograft tissue sample for SEM was prepared by the Centre for Microscopy at the University of the Free State. All samples were fixed in 2.5% glutaraldehyde (Merck, Johannesburg, South Africa). Homograft leaflets were divided into two specimens of approximately 3 mm × 6 mm. Tissue specimens were dried using the critical point method (Tousimis critical point dryer, Rockville, Maryland, USA, ethanol dehydration, carbon dioxide drying gas) and were metallised using gold (BIO-RAD, Microscience Division Coating System, London, UK; Au/Ar sputter coating @ 50–60 nm). Evaluations were performed with a Shimadzu SSX 550 scanning electron microscope (Kyoto, Japan, with integral imaging (SDF, TIF and JPG format). The surface area of each specimen was examined and photographed in either four or five different positions, and all images were then evaluated by three independent assessors and a score allocated. SEM micrographs were used to assess endothelial integrity and the effect of cryopreservation on endothelium integrity, and to evaluate the quality of the extracellular basal membrane.

Transmission electron microscopy

Pulmonary leaflet samples were fixed in 3.0% glutaraldehyde overnight, post fixated in Palade's osmium tetroxide, and dehydrated in a graded acetone series. Dehydrated samples were impregnated/embedded in an epoxy (Spurr 1969) to facilitate the making of ultra-thin sections for the TEM evaluation. Ultra-thin sections were cut from the sample embedded in the epoxy using an ultra-microtome (Leica Ultracut UC7, Vienna, Austria). After sectioning, the samples were stained with uranyl acetate and lead citrate. Sections of the leaflet samples were evaluated by using a transmission electron microscope (CM100, FEI, Netherlands) and photographed using an Olympus Soft Imaging System Megaview III digital camera

with Soft Imaging System digital image analysis and documentation software (Olympus, Tokyo, Japan).

Echocardiography

The ten implanted pulmonary homografts were explanted after either 14 days (n = 5) or 180 days (n = 5). Before the animal was sacrificed a transthoracic echocardiograph was done using a Philips Envisor Ultra Sound system (Philips, Johannesburg, South Africa) with a 3.5 MHz probe to ensure patency of the implanted homografts. Pulmonary insufficiency was evaluated semi-quantitatively with pulsed wave, continuous wave and colour Doppler flow on the parasternal short-axis view. Each measurement was repeated six times and mean values were calculated. The regurgitation jet across the homograft was graded by identification length and width into the RVOT and mapped as: none/trivial, mild, moderate or severe, using standard echocardiography criteria. The mean flow velocities across the implanted homografts were obtained by the use of continuous wave Doppler. Each measurement was repeated six times and the mean value over the measurements was calculated. Animals were only identified by their individual ear tag numbers, allowing blinded evaluation by the sonographer.

Gross examination

One surgeon and five researchers inspected the explanted homografts visually in a blinded manner. The general appearance of the homograft leaflets was evaluated for fenestrations, retraction, thrombotic material and atheroma or calcification.

Statistical analysis

The unpaired *t* test was used to compare the TS, YM and T_d explant results after 14 days and 180 days to that of the control. The null hypothesis assumes that the population means of the two independent samples are equal. The mean difference (positive or negative) was calculated, as well as a 95% CI for the mean difference (indicating the limits within which the true difference is likely to occur).

Results

Microbiology

All homograft tissue samples were culture negative before cryopreservation as well as before implantation.

Echocardiography

All the homografts functioned normally and no more than mild regurgitation was recorded in any of the homografts. None of the homografts had more than minimal regurgitation or demonstrated a maximum instantaneous gradient of more than 20 mmHg. No leaflet calcification could be demonstrated (Fig. 2).

Gross examination

Blinded visual inspection did not discern differences in the macroscopic appearance of homografts explanted after 14 days and 180 days (Fig. 3).

Biomechanical testing

The strength analysis results are summarised in Table 1. There were no significant differences in TS, YM and T_d between the control and 14-day explanted leaflets. Although TS of the control and the 180-day explanted leaflets did not differ significantly, the trend was towards stronger explanted leaflets, because the value of the lower limit of the 95% CI was much closer to zero than the upper limit. YM of the 180-day explanted leaflets was significantly higher than that of the control leaflets. T_d of control and 180 day explants did not differ significantly. No deterioration of strength could be demonstrated over the study period.

Histology

Figure 4 represents the H&E, Picrosirius red and von Kossa staining of the 48 h control, 14-day and 180-day explants.

The H&E stains show that endothelium covered the leaflets in a monolayer in the control, the 14 days and the 180 days explanted leaflets. Picrosirius red stains for collagen did not differ between the three groups and the von Kossa stains showed no calcification of the

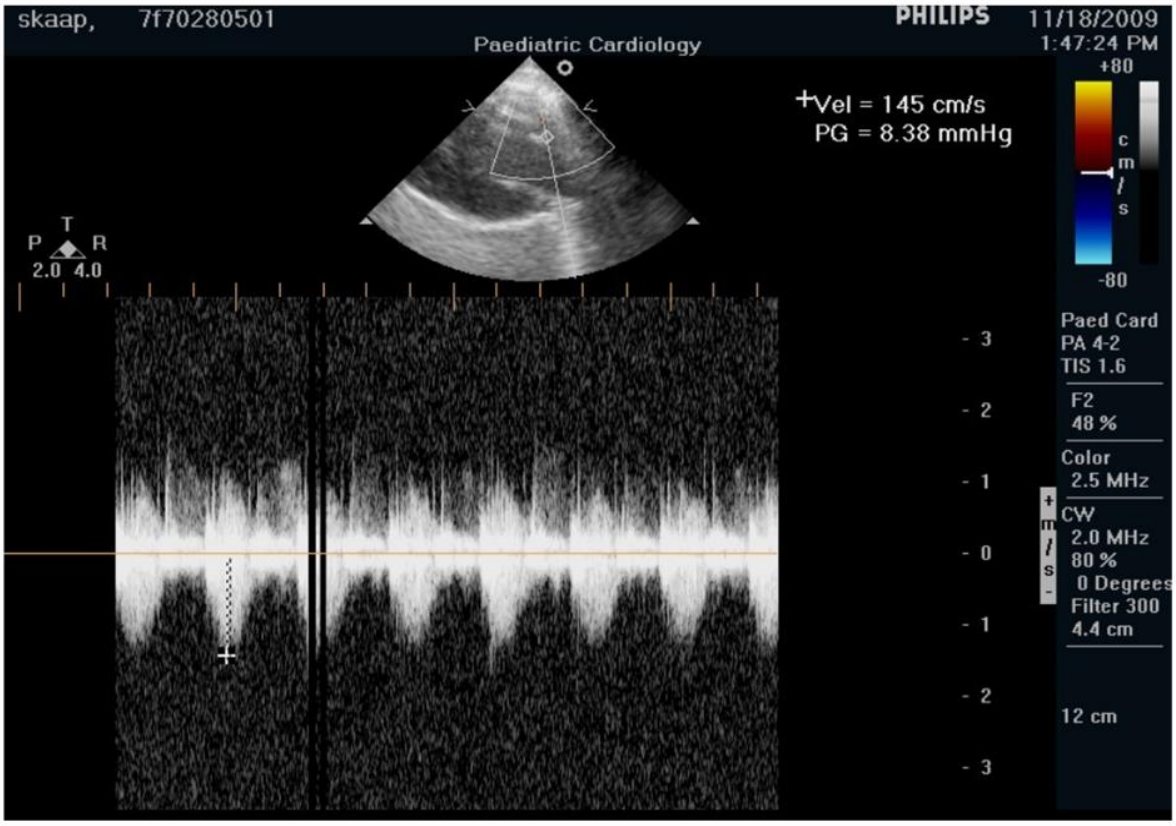

Fig. 2 Transvalvular gradient of a 180-day homograft (Smit 2011)

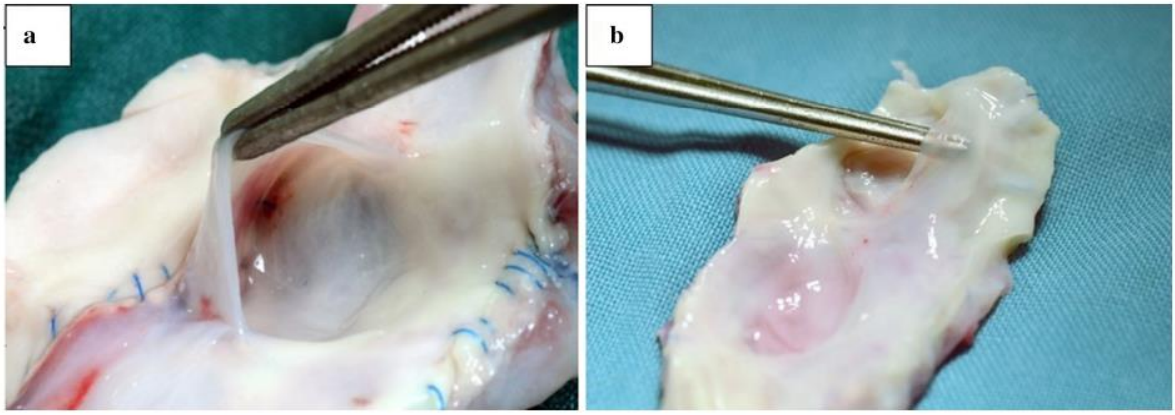

Fig. 3 **a** Macroscopic appearance of 14-day explanted homograft leaflet. **b** Macroscopic appearance of 180-day explanted homograft leaflet

14 days explanted leaflets and only mild calcification of the 180 days explanted leaflets (Fig. 4).

Electron microscopy

SEM confirmed an endothelial layer that was visible in the control, the 14-day and the 180-day explants. SEM

Table 1 TS, YM and T_d of 48 h cryopreserved ovine leaflets before implantation (control, n = 5) and explanted leaflets after 14 days (n = 5) and 180 days (n = 5)

Variable	Mean control	Mean 14 day explant	95% CI control versus 14 day explant	Mean 180-day explant	95% CI control versus 180-day explant
TS	2.461	2.788	− 1.273; 1.927	4.801	− 0.303; 4.983
YM	10.001	11.057	− 7.695; 9.770	25.388	1.819; 28.954*
T_d	70	72	− 0.765; 4.265	70	− 3.785; 4.005

Values are given as a mean and the 95% CI of the difference between the control and 14 and 180 days after implantation ($*p < 0.05$)
TS Tensile strength, *YM* Young's modulus, T_d thermal denaturation temperature

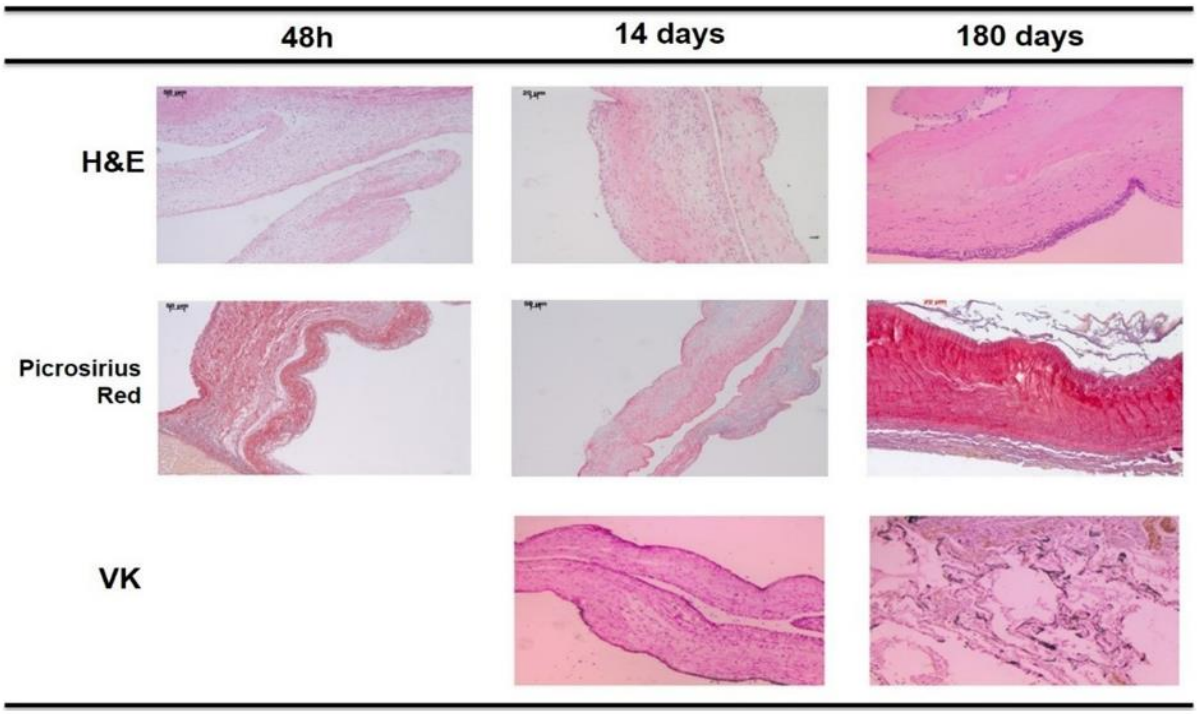

Fig. 4 H&E, Picrosirius red and von Kossa staining of 48 h cryopreserved ovine leaflets before implantation (control, n = 5), and explanted leaflets after 14 days (n = 5) and 180 days (n = 5). *h* Hours, *H&E* Haematoxylin and eosin, *VK* von Kossa

after cryopreservation and at 14 days shows endothelial cells with prominent nuclei, collapsed extranuclear areas and areas of dehiscence from the basal membrane. In contrast, the 180-day samples show a confluent layer of healthy endothelium (Fig. 5). TEM demonstrates consistent collagen disruption after cryopreservation in the control group as well as the 14 days and 180-day explants with no morphological deterioration or changes during the study period (Fig. 5).

Discussion

In an attempt to broaden the scientific basis for extending cadaveric homograft harvesting times, which could attenuate the worldwide shortage of homografts, this study was conducted in the juvenile sheep model. The study focuses on the structural integrity and stability of homografts sterilized and cryopreserved after 48 h post mortem ischaemic time, a time specifically chosen to simulate a reasonable window of opportunity in order to obtain donor

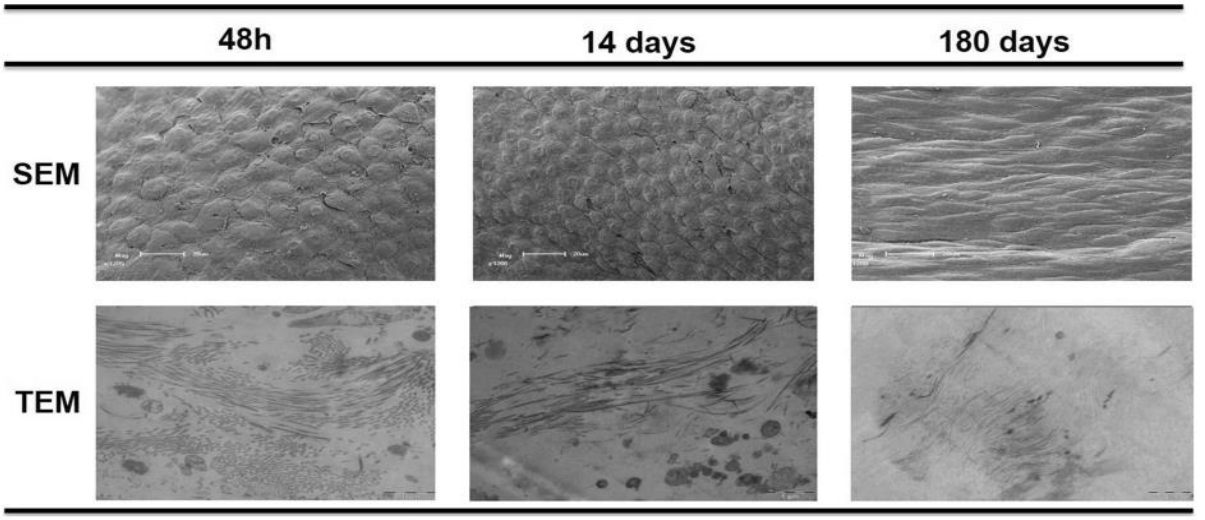

Fig. 5 SEM and TEM of 48 h cryopreserved ovine leaflets before implantation (control, n = 5) and explanted leaflets after 14 days (n = 5) and 180 days (n = 5). *SEM* Scanning electron microscopy, *TEM* transmission electron microscopy, *h* hours

consent in human cadaveric donor programmes in South Africa (mean = 33 h). The ovine model is a widely accepted model for homograft degeneration studies and is well known for its aggressive calcification potential. The ideal is to use primate models for implantation, but this model is very expensive and severely regulated. Although the study revealed excellent results about tissue integrity among the groups, final conclusions and translation to human subjects can only be made once a similar study has been repeated in a primate model.

A limitation of the ovine model is that the fermenting rumen in the large stomach of sheep generates heat post mortem in intact carcasses. In a previous study, the stomach was removed from carcasses otherwise left intact. In that study cultures were obtained from homograft tissue harvested up to 72 h post mortem. The homografts were incubated in Medium199 and antibiotics as described. The homografts were consistently culture negative before cryopreservation and no differences in the outcome at 180 days implantation could be demonstrated between the groups extending harvesting time up to 72 h (Smit et al. 2015). While the organ blocks harvested in this study accurately reflects post mortem ischaemic time as well as confirmed sterility pre-cryopreservation and at implantation (as with human homografts), it does not accurately reflect the effects of temporary bacterial exposure associated with decomposition in human cadavers that might occur before organ explantation and antibiotic incubation.

The 48 h post mortem harvested cryopreserved pulmonary homografts performed well over the study period, maintained its tissue integrity and stability and exhibited no graft failures. This correlates well with findings by researchers in Sweden that transplanted valves in the pulmonary position from non-beating donors with > 24 h ischaemic time and longer times from retrieval to cryopreservation had a lower reintervention rate compared to < 24 h. They concluded that longer ischaemic times of donor valves might even be preferable and does not affect the long-term outcome of transplanted homografts negatively (Axelsson and Malm 2018).

All the homografts functioned well, as assessed by echocardiography before euthanasia, after a minimum post-operative follow-up period of 180 days. None of the homografts showed gradients in excess of 20 mmHg or more than mild pulmonary regurgitation (> 2/4). No calcification could be demonstrated in the leaflets in either the 14 day or 180 day groups, and only mild calcification occurred in the homograft wall, but only in the 180-day group.

Gross macroscopic inspection after euthanasia confirmed the absence of homograft degeneration in both groups. Mild, spotty calcification in the homograft walls occurred in two of the 180-day explant valves.

We speculate that the increase in TS and YM seen in the 180-day explant group compared to both the control and the 14-day explant can be related to pannus or neo–collagen. It is important to note that no deterioration of strength occurred during the study period. It was therefore concluded that strength is maintained in the 48 h post mortem cryopreserved homografts during the study period. T_d values remained constant between the groups and no deterioration could be demonstrated in the 48 h post mortem cryopreserved homografts over the 180-day implantation period.

Histology showed progressive loss of cellularity over the study period, with 180 days explanted homograft leaflets being essentially acellular, as previously described by Mitchell et al. (1998). The 14 days explanted homografts showed mononuclear infiltrates, composed primarily of T-lymphocytes, that were diffuse but not prominent in most valves and which were generally comparable with those seen in the control group. The endothelial cells appeared focally and variably demonstrable in the control group, tattered in the 14 days explant group but "healthy"in the 180 days explants (group 3), because these cells are probably of recipient origin. The Picrosirius red staining confirmed the presence of collagen in all groups and the von Kossa staining showed mild calcification in the 180-day explant group.

SEM studies highlighted the abnormal endothelium after cryopreservation maintained in the 14-day group; however, a pristine endothelial layer was present in the 180 day explants. TEM clearly demonstrated damage to the collagen scaffold caused by cryopreservation, as previously described by Schenke-Layland et al. (2006). This disruption of the collagen matrix was sustained throughout the study period and was similar between all groups.

This study demonstrated severe disruption caused by cryopreservation and this damage remained constant during the study period. The fact that no reorganisation of the collagen scaffold occurred correlates with the progressive acellularity observed in the implanted homograft leaflets over the 180-day study period. In a study that evaluated cryopreservation, ice-free cryopreservation (vitrification) and freeze-drying as preservation methods for decellularized bovine pericardial scaffolds, it was found that cryopreservation resulted in a significant increase in stiffness and tensile strength of the scaffold, which was not observed with the other two preservation methods. Although cryopreservation is the preferred method of preservation for heart valves and other cardiovascular tissues worldwide, it does alter the biomechanical behavior of collagenous tissues (Zouhair et al. 2017).

It is certainly interesting to note that the leaflet strength did not deteriorate over this period, despite confirmed cryopreservation damage to the collagen scaffold as well as progressive acellularity of the leaflets. This acellularity leaves very little hope that damage will be repaired by cells in the leaflet.

The pristine endothelial lining of the 180 day explants is most likely of recipient origin and may perform an important antithrombotic function as well as other anti-inflammatory endothelial functions, which can attenuate thrombotic and inflammatory processes initiated by deterioration and calcification. It is unlikely to contribute to valvular maintenance functions in the absence of valvular interstitial cells.

The damaged, albeit stable, state of the post cryopreservation collagen scaffold, combined with the lack of leaflet cellularity and absence of indications of collagen scaffold repair or new valvular interstitial cells by 180 days, begs the question: How do these cryopreserved homografts retain their strength, as they clearly do in this study, as well as in thousands of homograft recipients over many years?

Study limitations and recommendations

- Direct translation comparison to human subjects cannot be made based on the use of the ovine model.
- To relate the results directly to humans a primate model must be used instead of an ovine model.

Conclusion

Although conditions of human cadaveric tissue donations were not exactly replicated in this study and findings in animal studies can not simply be extrapolated to the human setting, important findings can still be made from the results.

Post mortem harvesting time might be less important in homograft survival than attenuating damage to

the collagen scaffold and providing a scaffold where recipient cells can infiltrate, proliferate and function, thereby maintaining a normal leaflet structure. This remains the goal of tissue-engineered heart valves and valvular conduits.

As cryopreserved homografts still form the backbone of clinical homograft application, prolonging homograft harvesting times to 48 h post mortem in this study was not associated with early graft failure or loss of tissue integrity. Prolonging harvesting time to 48 h post mortem can attenuate homograft donor shortages.

Compliance with ethical standards

Conflict of interest The authors declare that they have no conflicts of interest.

References

Angell WW, Oury JH, Lamberti JJ, Koziol J (1989) Durability of the viable aortic homograft. J Thorac Cardiovasc Surg 98:48–56

Axelsson I, Malm T (2018) Long-term outcome of homograft implants related to donor and tissue characteristics. Ann Thorac Surg 106(1):165–171

Barrett-Boyes B (1987) 25 years clinical experience of homograft surgery—a time for reflection 1962–1987. In: Yankah AC, Hetzer R, Miller DC, Ross DN, Somerville J, Yacoub MH (eds) Cardiac valve allografts. Springer, New York, pp 347–358

Botes L, van den Heever JJ, Smit FE, Neethling WML (2012) Cardiac homografts: a 24-year South African experience. Cell Tissue Bank 13:139–146

Brubaker S, Lotherington K, Zhao J, Hamilton B, Rockl G, Duong A, Garibaldi A, Simunovic N, Alsop D, Dao D, Bessemer R, Ayeni OR (2016) Tissue recovery practices and bioburden: a systematic review. Cell Tissue Bank 17:561–571

Dagum P, Green GR, Timek TA, Daughters GT, Foppiano LE, Tye TL, Bolger AF, Ingels NB, Miller DG (1999) Functional evaluation of the Medtronic stentless porcine xenograft mitral valve in sheep. Circulation 100(19 Suppl. 2):70–77

Dawson PE, Brockbank KGM (1997) Human heart cold ischemia and its effects on post cryopreservation viability of heart valves. In: Yankah AC, Yacoub MH, Hetzer R (eds) Cardiac valve allografts, science and practice. Springer, New York

Green MK, Walsh MD, Dare A, Hogan PG, Zhao XM, Frazer IH, Bansai AS, O'Brien MF (1998) Histologic and immunohistochemical responses after aortic valve allografts in the rat. Ann Thorac Surg 66:S216–S220

Hechadi J, Gerber BL, Coche E, Melchior J, Jashari R, Glineur D, Noirhomme P, Rubay J, El Khoury G, De Kerchove L (2013) Stentless xenografts as an alternative to pulmonary homografts in the Ross operation. Eur J Cardiothorac Surg 44:e32–e39

Institute of Laboratory Animal Research, Commission on Life Sciences, National Research Council. Guide for the Care and Use of Laboratory Animals [online]. http://www.nap.edu/catalog/5140.html. Accessed 20 Jan 2016

Langley SM, Livesey SA, Tsang VT, Barron DJ, Lamb RK, Ross JK, Monro JL (1996) Long-term results of valve replacement using antibiotic-sterilised homografts in the aortic position. Eur J Cardiothorac Surg 10(12):1097–1106

Methe H, Hess S, Edelmann ER (2007) Endothelial immunogenicity—a matter of matrix microarchitecture. Thromb Haemost 98:278–282

Mitchell RN, Jonas RA, Schoen FJ (1998) Pathology of explanted cryopreserved allograft heart valves: comparison with aortic valves from orthotopic heart transplants. J Thorac Cardiovasc Surg 115:118–127

Mroz TE, Joyce MJ, Steinmetz MP, Lieberman IH, Wang JC (2008) Musculoskeletal allograft risks and recalls in the United States. J Am Acad Orthop Surg 16(10):559–565

O'Brien MF, Stafford G, Gardner M, Pohlner P, McGiffin D, Johnston N, Brosnan A, Duffy P (1987a) The viable cryopreserved allograft aortic valve. J Cardiac Surg 2(Suppl 1):153–167

O'Brien MF, Stafford EG, Gardner MAH, Pohlner P, McGiffin D (1987b) A comparison of aortic valve replacement with viable cryopreserved and fresh allograft valves, with a note on chromosomal studies. J Thorac Cardiovasc Surg 94:812–823

O'Brien MF, Stafford GE, Gardner MAH (1995) Allograft aortic valve replacement: long-term follow-up. Ann Thorac Surg 60:S65–S70

O'Brien MF, Harrocks S, Stafford EG, Gardner MAH, Pohlner PG, Tesar PJ, Stephens F (2001) The homograft aortic valve: a 29-year, 99.3% follow up of 1022 valve replacements. J Heart Valve Dis 10(3):334–344

Rüegg M, Moor U, Blanc B (1975) Hydration and thermal denaturation of beta-lactoglobulin. A calorimetric study. Biochim Biophys Acta 400:334–342

Schenke-Layland K, Madershahian N, Riemann I, Starcher B, Halbhuber KJ, König K, Stock UA (2006) Impact of Cryopreservation on extracellular matrix structures of heart valve leaflets. Ann Thorac Surg 81:918–926

Smit F (2011) The effect of pre-harvest ischemic time on valvular homografty performance - an experimental study. PhD. University of the Free State

Smit FE, Bester D, van den Heever JJ, Schlegel F, Botes L, Dohmen PM (2015) Does prolonged post-mortem cold ischemic harvesting time influence cryopreserved pulmonary homograft tissue integrity? Cell Tissue Bank 16(4):531–544

Smith SH, Judge MD (1991) Relationship between pyridinoline concentration and thermal stability of bovine intramuscular collagen. J Anim Sci 69:1989–1993

Spurr AR (1969) A low viscosity epoxy resin embedding medium for electron microscopy. J Ultrastruct Res 26:31–43

Thubrikar MJ, Deck JD, Aouad J, Nolan SP (1983) Role of mechanical stress in calcification of aortic bio prosthetic valves. J Thorac Cardiovasc Surg 86:115–125

Yacoub M, Kittle CF (1970) Sterilization of valve homografts by antibiotic solutions. Circulation 41:SII29–SII31

Yacoub M, Rasmi NRH, Sundt TM, Lund O, Boyland E, Radley-Smith R, Khaghani A, Mitchell A (1995) Fourteen-year experience with homovital homografts for aortic valve replacement. J Thorac Cardiovasc Surg 110:186–194

Yankah AC, Hetzer R (1987) Procurement and viability of cardiac homografts. In: Yankah AC, Hetzer R, Miller C, Ross DN, Somerville J, Yacoub MH (eds) Cardiac valve allografts 1962–1987. Springer, New York, pp 23–26

Yoshikawa Y, Kitamura S, Taniguchi S, Kameda Y, Niwaya K, Sakaguchi H (2000) Pulmonary ventricular outflow reconstruction with a size-reduced cryopreserved pulmonary valve allograft: mid-term follow-up. Jpn Circ J 64:23–26

Zouhair S, Aguiari P, Iop L, Korossis S, Wolkers WF, Gerosa G (2017) Advanced preservation methodologies for decellularized cardiovascular scaffolds. In: 26th Congress of the European association of tissue banks, Treviso, Italy. https://www.eatb.org/images/2017/Final-Program_EATB2017_web.pdf. Accessed Sept 2018

Appendix B: Animal Ethics Approval

UNIVERSITY OF THE FREE STATE
UNIVERSITEIT VAN DIE VRYSTAAT
YUNIVESITHI YA FREISTATA
UFS UV

Internal Post Box / Interne Posbus G40
☎(051) 4052812
Faks / Fax (051) 4444359

E-mail address: StraussHS@ufs.ac.za

Me / Ms H Strauss

2012-06-15

PROF FE SMIT
DEPT OF CARDIOTHORACIC SURGERY
FACULTY OF HEALTH SCIENCES
UFS

Dear Prof Smit

ANIMAL EXPERIMENT NR 08/2012
PROJECT TITLE: "EVALUATION OF DECELLULARIZATION AND ANTICALCIFICATION TREATMENTS ON THE PERFORMANCE OF HOMOGRAFT IMPLANTS IN THE RIGHT VENTRICULAR OUTFLOW TRACT OF THE SHEEP MODEL."

You are hereby kindly informed that the Interfaculty Animal Ethics Committee approved the above study at the meeting held on 14 June 2012.

ANIMAL	*NUMBER*	*EXPIRY DATE*
Dorper Sheep	40 Wether	June 2014
Dorper Sheep	30 Female	June 2014

Kindly take note of the following:

1. *Fully completed and signed applications have to be submitted electronically to StraussHS@ufs.ac.za and a hard copy has to be submitted too.*
2. *A signed progress report with regard to the above study has to be submitted electronically to StraussHS.ufs.ac.za while a hard copy has to be submitted to Ms H Strauss, Room D115, Francois Retief building, Faculty of Health Sciences. A report has to be submitted when animals are physically involved and after completion of the study. Guidelines with regard to progress reports are available from the secretary and on the Faculty intranet.*
3. *Researchers that plan to make use of the Animal Experimentation Unit must request a quotation from the Head, Mr Seb Lamprecht*
4. *Contract research: Fifty (50%) of the quoted amount is payable when you receive the letter of approval.*

Regards

.....
CHAIR:
INTERFACULTY ANIMAL ETHICS COMMITTEE